Organic Carbon Cycling in Marine Sediments and Seabed Seepage Features in Irish Waters

Shane S. O'Reilly, B.Sc.

Thesis submitted for the award of Ph.D.

Under the supervision of Dr. Brian P. Kelleher

2013

School of Chemical Sciences,
Dublin City University

External Supervisors: Dr. Christopher C.R. Allen (Queen's University Belfast),
Prof. Andre J. Simpson (University of Toronto, Scarborough)

Submitted January 2013

Disclaimer

I hereby certify that this material, which I now submit for assessment on the programme of study leading to the award of Ph.D. is entirely my own work, that I have exercised reasonable care to ensure that the work is original, and does not to the best of my knowledge breach any law of copyright, and has not been taken from the work of others save and to the extent that such work has been cited and acknowledged within the text of my work.

Signed: _____

Candidate ID: _____

Date: _____

Abstract

Cycling of organic carbon in marine sediments is of fundamental importance for marine ecosystem function, for marine and atmospheric chemistry, for the petroleum and natural gas industry, and for paleoclimatic and paleoenvironmental studies. While most of this carbon is derived from marine and terrestrial sources, significant improvements in mapping and remote investigation have revealed that seabed fluid flow, principally in the form of thermogenic or microbial methane, is also of fundamental importance. In this thesis, the cycling of organic carbon at a number of sites in Irish waters was conducted, with a focus on recently mapped seabed seepage features. A spatial study of the distribution of lipid biomarkers in surface sediments and water column plankton in the western Irish Sea revealed zonation in diatom, zooplankton and dinoflagellate biomass and detrital input in line with hydrographic zonation and seasonal primary production (Chapter 2). Active gas seepage was recorded from carbonate mounds at the Codling Fault Zone, western Irish Sea as well as extensive eroded nodules, largely covered hard ground pavements, patches of anoxic seabed and extensive fossil tube worms and colonising hydroids. Analysis of retrieved samples has confirmed that these hard grounds are methane-derived authogenic carbonates and that anaerobic oxidation of methane is likely a significant process at this site (Chapter 3). The microbial diversity at a large composite but apparently dormant pockmark in the Malin Sea, NW Ireland was found to be dominated by non-seepage associated microbes and suggests a shift in population structure over a pockmarks lifetime. Bacterial species diversity was low and dominated by *Psychrobacter* and *Sulfitobacter* genera, although downcore microdiversity is apparent and could indicate niche specialisation with depth (Chapter 4). A shallow pockmark field in Dunmanus Bay was found to coincide with regions of acoustic gas signatures in the upper 3 m of seabed. This has been confirmed to be gas, which most likely accumulated below fine-grained impermeable muddy sediment. Numerous lines of evidence suggest that gaseous products, including methane, are produced *in situ* rather than transported from the subsurface, suggesting that the role of microbial activity in pockmark formation in this setting could be underestimated (Chapter 5).

This thesis is dedicated to my parents, Finbarr and Sheila,
and to Declan Gallagher.

Acknowledgements

First and foremost I would like to thank my supervisor and mentor, Dr. Brian Kelleher, for his inspiration and continual commitment, and for opening up a plethora of opportunities and learning experiences thus far. I would like to thank Dr. Christopher Allen for giving me the opportunity to learn invaluable techniques in his group, and for his continuous advice and encouragement. I would like to especially thank Xavier Monteys for his continued guidance and for his considerable contribution to this work. I would like to thank Prof. Andre Simpson and colleagues for their assistance, expertise and contribution in relation to the NMR aspects of this thesis. I would also like to thank my colleagues and friends in Dr. Kelleher's research group: Dr. Michal Szpak for his mentorship and advice; Margaret McCaul for her continual help and assistance; Dr. Kris Hart for the opportunity to work with him in peer-reviewed publications and also for his stimulating opinions; and Brian Murphy for his invaluable assistance and work ethic that contributed to my research while on marine surveys and in the lab. I would like to thank all those I worked with in Dr. Allen's group in QUB, in particular Dr. Paul Flanagan and Dr. Anna Kulakov. I would also like to thank Allessandra Frau, Prassanna Pentlavalli in QUB and Sean Jordan and Sara Sandron in DCU for their contribution to this work, as well as the staff in the DCU School of Chemistry for their support, work ethic and training. I would like to thank Prof. Bill Mahaney the opportunity to work with him in exciting and diverse settings and for opening up considerable publication opportunities. I would also like to thank Dr. Crispin Little (University of Leeds) and Krzysztof Hryniewicz (University of Oslo) for their considerable contribution to Chapter 3.

Finally I would like to especially thank my family – my parents Finbarr and Sheila and my brothers and sisters Fiona, Barry, Daryl and Maria – for their continual support over the past three years. I would like to thank all my friends for sticking by me even during my frequent leaves of absence and absent-mindedness. Finally I would like to thank Dr. Erica G. Tierney (☺). You are the best! I would not have been able, or wanted to do this without you at my side. If we can get through three years with our faces in front of laptop screens and living as hermits, then I think we can get through anything together. Thank you so much for all your support and love.

Contributions

Chapter 2

Cruise preparation and planning was conducted by myself with the consultation of the Marine Institute and Xavier Monteys (Geological Survey of Ireland). The onboard scientific party consisted of Michal T. Szpak, Brian T. Murphy, Sean F. Jordan, Sara Sandron (Dublin City University) and myself. Lipid extraction and fractionation was conducted by an undergraduate research student, Stephen M. Mulligan (Dublin City University), and myself, and lipid analysis, quantification and interpretation was conducted by myself. DNA extraction and qPCR work was performed by Paul V. Flanagan (Queen's University Belfast). DGGE analysis and image analysis was conducted by myself. Mapping of lipid distribution using Ocean Data View was performed by myself.

Chapter 3

Cruise preparation, planning and onboard work was the same as for Chapter 2 above. Lipid extraction, fractionation and analysis were conducted by myself, as was DNA extraction and DGGE analysis. SEM was conducted by myself while SEM-EDS was performed by Nigel Coleman (University of Limerick). Bulk isotope, mineralogy and petrographic analysis was conducted by Krzysztof Hryniewicz (University of Oslo) and Dr. Crispin Little (University of Leeds). Lipid extraction, analysis, quantification and interpretation were conducted by myself. DNA extraction and DGGE analysis was conducted by myself. Maps were constructed in ArcGIS (Ver. 9.0) by myself using bathymetry published under the INFOMAR program.

Chapter 4

Initial survey planning, onboard work and sampling was performed by Michal T. Szpak and Xavier Monteys. DNA extraction, DGGE and DGGE band excision and amplification was conducted by Paul V. Flanagan. Clone library construction, sequence alignment, chimera checking and phylogenetic analysis were conducted by myself. Lipid extraction, fractionation and analysis were conducted by myself.

Chapter 5

Initial preparation for onboard work was conducted by myself, with the consultation of Xavier Monteys and the Marine Institute. Onboard geochemistry was performed by Michal T. Szpak, Brian T. Murphy, Sara Sandron and myself. Sediment core logging and description was conducted by Dr. Nick Owen (Trinity College Dublin). Jennifer Doyle (Marine Institute) and Brian T. Murphy performed sled-towed drop camera operation. Multi-sensor core logging was performed by Dr. Stephen McCarron (NUI, Maynooth) and myself. Data processing and clean-up was conducted by myself with the consultation of Dr. Stephen McCarron and Xavier Monteys. All gas and pore water analysis was performed by myself, except for SO_4^{2-} and Cl^- analysis. Sample preparation and calibrations were prepared by myself and ion chromatograph setup and operation was performed by Sara Sandron. Lipid extraction and analysis was performed by myself, as was DNA extraction, DGGE and DGGE image analysis. HF demineralisation and extraction of bulk sediment for NMR experiments was conducted by myself, with the help of Brian T. Murphy. All NMR experiments, including direct NMR of sediment pore waters, was performed by Prof. Andre Simpson and colleagues (University of Toronto, Scarborough).

Publications and accomplishments

Peer-reviewed publications (6 published, 5 in preparation)

Published

- **O'Reilly, S.S.**, Szpak, M.T., Flanagan, P.V., Monteys, X., Murphy, B.T., Jordan, S.F., Allen, C.C.R., Simpson, A., Mulligan, S.M., Sandron, S., Kelleher, B.P., 2013. Biomarker evidence reveals the effects of hydrography on the sources and fate of marine and terrestril organic matter in the western Irish Sea. Estuarine, Coastal and Shelf Science, accepted manuscript.

This paper is directly associated with Chapter 2 of this thesis.

- **O'Reilly, S.S.**, Hurley, S., Coleman, N., Szpak, M.T., O'Dwyer, T., Kelleher, B.P., 2012. Chemical and physical description of living and non-living maerl rhodoliths from Kingstown Bay, Galway, Ireland. Aquatic Biology 15, 215-214.

My role in this publication was the supervision of lipid extraction and fractionation. I also conducted all GC-MS analysis, analyte identification, quantification and interpretation. Interpretation of the whole dataset and manuscript preparation was conducted by myself.

- Flanagan, P.V., Kelleher, B.P., **O'Reilly, S.S.**, Szpak, M.T., Monteys, X., Kelly, P.P., Kulakova, A.N., Kulakov, L.A., Allen, C.C.R., 2013. A depth-resolved insight into benzoyl CoA reductase and benzoate dioxygenase gene copy numbers within a marine sediment associated with methane seepage. Open Journal of Marine Science 6, 1-9.

DGGE, clone library data and PLFA data presented in Chapter 4 was used for the preparation of this paper.

- Szpak, M.T., Monteys, X., **O'Reilly, S.S.**, Simpson, A.J., Garcia, X., Evans, R.L., Allen, C.C.R., McNally, D.J., Courtier-Murias, D., Kelleher, B.P., 2012. Geophysical and geochemical survey of a large marine pockmark on the Malin Shelf, Ireland. Geochemistry, Geophysics, Geosystems, 13, 1–18.

Chapter 4 is a follow-up study on this paper focusing on the microbiology of the site. My role in this publication was primarily in the in-lab sample processing for NMR and porewater analysis.

- Mahaney, W.C., Hart, K.M., **O'Reilly, S.S.**, Allen, C.C.R., Dohm, J.M., Hancock, R.G.V., Kelleher, B.P., Milner, M.W., 2012. Coleoptera and microbe biomass in Antarctic Dry valley paleosols adjacent to the Inland Ice: Implications for Mars. Planetary and Space Science 60, 386–398.

My role in this publication was primarily in extraction of genomic DNA, PCR-amplification of 16S rRNA bacterial genes, DGGE analysis and interpretation.

- Mahaney, W.C., Hart, K.M., Dohm, J.M., Hancock, R.G.V., Costa, P., **O'Reilly, S.S.**, Kelleher, B.P., Schwartz, S., Lanson, B., 2011. Aluminium extracts in Antarctic paleosols: Proxy data for organic compounds and bacteria and implications for Martian paleosols. Sedimentary Geology 237, 84 -94.

My role in this publication was primarily in extraction of genomic DNA from the paleosol samples and quantification of total DNA yield.

<u>In preparation</u>

- **O'Reilly, S.S.**, Flanagan, P.V., Frau, A., Pentlavalli, P., Kulakova, A.N., Kulakov, L., Monteys, X., Allen, C.C.R., Kelleher, B.P. Bacterial abundance and community diversity of surface sediments in the Western Irish Sea.

This paper is in preparation and planned to be submitted to Geomicrobiology. It is associated with Chapter 2 of this thesis, and comprises a follow-up work investigation of the western Irish Sea gyre and the changes in bacterial abundance and community composition in surface sediments in this region.

- **O'Reilly, S.S.**, Hryniewicz, K., Little, C.T.S., Monteys, X., Szpak, M.T., Croker, P., Allen, C.C.R., Kelleher, B.P. Methane-derived authigenic carbonate mounds at the Codling Fault Zone, western Irish Sea.

This paper is in preparation and planned to be submitted to Marine Geology. This paper is directly associated with Chapter 3 of this thesis.

- **O'Reilly, S.S.,** Mahaney, W.C., Hart, K.M., Allen, C.C.R., Kelleher, B.P. Biomarker evidence for vegetation and environmental change during the Upper Neogene from buried paleosols on Mt. Kenya.

This paper is in preparation and planned to be submitted to the Geological Society of London Journal.

- Szpak MT, Montey X, **O' Reilly SS**, Kelleher BP. Acoustic and geochemical investigation of a shallow pockmark field in Dunmanus Bay, Ireland.

This paper is associated with Chapter 5, whereby this chapter comprises follow-up work from the first investigations of Dunmanus Bay pockmark field. My role in this paper was primarily in in-lab core sectioning, core processing and porewater extraction.

- Mahaney, W.C., Krinsley, D.H., Allen, C.C.R., Milner, M.W., Batchelor, D., LeCompte, M., Kelleher, B.P., **O'Reilly, S.S**. Reassessment of the microbial role of Fe-Mn nodule genesis in Andean paleosol.

This paper is in preparation, and planned to be submitted to Geomicrobiology.

Reports (3)

- **O' Reilly SS**, Szpak MT, Monteys X, Kelleher BP. 2012. INFOMAR onboard geochemical and geomicrobiological sampling protocols. Geological Survey of Ireland Report.
- Monteys X. 2011. INFOMAR ground-truthing program on Porcupine Bank and Dunmanus Bay, Ireland: CE11_017 Cruise Report. Geological Survey of Ireland Report (Chapter Contribution)
- **O' Reilly SS**, Szpak MT, Monteys X, Kelleher BP. 2010. Ground-truthing of gas-related seabed features in the Western Irish Sea: CV10_28 Cruise Report. Geological Survey of Ireland Report.

Conferences and presentations (6 Oral, 9 Posters)

- *Organic carbon cycling in the Irish marine environment and at 'cold seep' sites*. Atlantic Ireland Conference, 11/2012, Burlington Hotel, Dublin (Poster).
- *Seepage and gas features in Dunmanus Bay, Ireland.* 11th International Conference of Gas in Marine Sediments, 09/2012 (Szpak MT, Poster)
- *Acoustic sediment characterisation in near seabed gas environments around the Irish coast*. 11th International Conference of Gas in Marine Sediments, 09/2012 (Monteys X, Poster)
- *Multidisciplinary characterisation of fluid seepage features in Irish waters*. 23rd Annual Meeting of the British Organic Geochemical Society, 07/2012, University of Leeds, UK (Oral).
- *Microbial population diversity at a large pockmark on the Malin Shelf, N.W. Ireland*. 9th Marine Biology Association Postgraduate Conference, 05/2012, University College Cork (Oral).
- *Characterization of microbial diversity and carbon cycling at methane seepage environments in Irish waters*. 9th Marine Biology Association Postgraduate Conference, 05/2012, University College Cork (Poster).
- *Microbial diversity and organic matter cycling in Dunmanus Bay pockmarks*. INFOMAR seminar, 03/2012, Geological Survey of Ireland, Dublin (Oral).
- *Multidisciplinary characterization of seabed fluid flow features in Irish waters*. 55th Irish Geological Research Meeting (IGRM), 02/2012, University College Cork (Poster – Bronze medal award).

- *Multidisciplinary characterization of seabed fluid flow features in Irish waters.* INFOMAR seminar, 11/2011, Marine Institute, Galway (Poster).
- *Multidisciplinary characterization of seabed fluid flow features in Irish waters.* Atlantic Ireland 2011, 10/2011, Burlington Hotel, Dublin (Rapid Oral).
- *Dunmanus, Bay pockmarks.* CE11_017 Survey Workshop, 10/2011, Geological Survey of Ireland, Dublin (Oral).
- *Microbial diversity and organic matter composition of methane-related seepage features in Irish waters.* Tyndall Conference, 09/2011, Dublin Castle (Poster).
- *Microbial diversity and organic matter composition of methane-related seepage features in Irish waters*. 25th International Meeting on Organic Geochemistry (IMOG), 09/2011, Interlaken, Switzerland (Poster).
- *Microbial diversity and organic matter cycling of methane seepage structures in Irish waters.* 6th Conference on Analytical Sciences in Ireland (CASi), 02/2011, The Helix, Dublin City University (Oral).
- *Ground-truthing of gas-related seabed features in the Western Irish Sea (CV10_28)* Geosciences 2010, 11/2010, Dublin Castle (Poster).

Research Surveys (3)

- April 2012 - Shipboard Scientist aboard RV *Celtic Voyager* cruise CV12_07 to the Irish Sea – Amplified growth of SeDiment Waves in the Irish Sea (AmSeDIS). (Funded through the EU EUROFLEETS program)
- May 2011 - Shipboard scientist aboard RV *Celtic Explorer* cruise CE11_017 to Dunmanus Bay and the Porcupine Bank (Funded through the INFOMAR program).
- June 2010 - Shipboard scientist aboard RV *Celtic Voyager* cruise CV10_28 to the Irish Sea (Funded through the INFOMAR program).

Extra curricular modules and training (5)

- February 2012 - Dublin Regional Higher Education authority (DRHEA) Graduate Training Element *Bioinformatics for the Biologist*, National University of Ireland, Maynooth.
- February 2012 - qGIS training workshop offered by the National Centre for Geocomputation, NUIM.
- January 2011 - Dublin Regional Higher Education authority (DRHEA) Graduate Training Element CS551A *Advanced Analytical Techniques*, Dublin City University.
- August 2010 - EUROFLEETS Multidisciplinary Ship-based training course, University College Cork.
- November 2009 - Dublin Regional Higher Education authority (DRHEA) Graduate Training Element CS507A *Multivariate Statistics,* Dublin City University.

List of Tables

List of Figures

Figure 1.6. Early diagenetic geochemical zonation of marine sediments. SMTZ – Sulfate-methane transition zone (after Froelich et al., 1979; Berner, 1981).

Figure 1.7. The universal phylogenetic tree of life as defined by comparative rRNA gene sequencing. The three domains of life – Bacteria, Archaea and Eukarya are shown, along with a number of important representative groups. LUCA – Last universal common ancestor. (taken from Madigan et al., 2012).

Figure 1.8. Marine microbial ecology. (A) [a] Mean annual water depth profiles of crenarchaeota, euryarchaeota and bacteria in the North Pacific. Numbers on x-axis represent percentage of total abundance (using the DAPI nucleic acid stain). [b] Corresponding depth profile of total bacteria, crenarchaeota and euryarchaeota. (Karner et al., 2001); (B) Remotely operated vehicle (ROV) sampling a deep sea bacterial mat, Haakon Mosby Mud Volcano (IFREMER, France); (C) [a] Subseafloor depth profiles of total intact polar lipids (IPLs) from a number of locations and [b] relative contribution of archaeal IPLs to total IPLs (Lipp et al., 2008); (D) Fluorescent in-situ hybridisation identification of an archaea (red)/sulfate-reducing bacteria (green) aggregate apparently mediating anaerobic oxidation of methane (AOM). (Boetius et al., 2000).

Figure 1.9. Marine seabed seepage features. (A) Boomer seismic profile across the Witch's Hole pockmark, North Sea, showing various seismic signals of gas accumulations (Judd and Hovland, 2007). (B) Multibeam echosounder (MBES) bathymetric map showing numerous pockmarks, Witch Ground Basin, North Sea (Judd and Hovland, 2007). (C) Underwater still image of a 3 m diameter unit pockmark in the Central Nile deep sea fan, containing anoxic sediment, authigenic carbonates and vestimentiferan tubeworms. The scale bar represents 1m. (Bayon et al., 2009) (D) Underwater image of methane-derived authigenic carbonate (MDAC) mounds, Black Sea (Reitner et al., 2005) (E) Underwater image of massive MDAC pavement, Central Nile deep sea fan (Bayon et al., 2009). The scale bar represents 1m. (F) Seismic profile showing a mud diapir (highlighted) in the Gulf of Cadiz, associated with Listric faults (Fernandez-Puga et al., 2007).

Figure 1.10. Plot illustrating the range of sizes and depth of pockmarks from 57 published locations globally (after Pilcher et al., 2007). Note the X and Y scales are logarithmic. The large diamond represents so-called 'mega' pockmarks as described by Pilcher et al. (2007). Single points represent the measured value for a single described pockmark or an average value for pockmarks within a field. Error bars represent the range in sizes within a particular pockmark field. The mean diameter and depth is 128 m and 9.5 m, respectively. Source data was obtained from Carvalho 2003; Dimitrov and Woodside 2003; Fader 1991; Games 2001; Hasiotis et al., 2002; Haskell et al., 1997, 1999; Hovland 1982, 1991, 1992, 2003; Hovland et al., 1987; Hovland and Judd 1988; Kelley et al., 1994; Maestro et al., 2002; Mosher et al., 2004; Pickrill 2006; Rise et al., 1999; Schroot and Schuttenhelm, 2003; Söderberg et al., 1992; and Soter 1999.

Figure 1.11. Conceptual model for pockmark formation. Pressure builds up in a shallow porous layer below an impermeable fine-grained sealing layer. This pressure is relieved by seabed doming (first panel). Eventually pore fluid pressure causes the sediment to yield, causing a rapid expulsion and fluidisation of the sediment matrix. Gas, water and sediment are expelled into the water column (second panel). Fine-grained sediments are suspended in the water column and transported by currents, while coarse material may deposit in or near the formed crater (after Hovland and Judd, 1988).

Figure 1.12. Anaerobic oxidation of methane (AOM) via reduction of SO_4^{2-}. This process forms the basis for complex cold seep ecosystems that utilise seeping CH_4 and produced H_2S and hard methane-derived carbonate.

Figure 1.13. Structures of selected major lipid classes utilised as biomarkers to characterise marine organic matter (OM).

Figure 2.1. Map of the Irish Sea and study area location. Sediment boxcore stations are numbered and marked with a black circle. Plankton net tow stations are shown as crosses (T1 and T2). Broken grey lines represent approximate summer hydrographic regions (from Gowen et al., 1995) and black arrows represent the near-bottom residual circulation (from Ramster et al. 1969). SSR – Summer Stratified Region, CMR – Coastal Mixed Region, SMR – Southern Mixed Region.

Figure 2.2. Spatial distribution of bulk physical and chemical parameters in western Irish Sea surface sediments: A. grain size (ϕ); B. sorting; C. sand (%); D. clay (%); E. total organic carbon (TOC; %); and F. total nitrogen (TN; %).

Figure 2.3. Spatial distribution of terrestrial organic matter (TOM) in the study area based on A. Bulk C/N ratio; B. long chain *n*-alkanols (LC_{OH}); C. long chain *n*-alkanes (LC_{HC}); and D. *n*-alkanol carbon preference index (CPI_{OH}).

Figure 2.4. Horizontal boxplot of selected biomarker $\delta^{13}C$ values distinguishing marine and terrestrial organic matter. Each boxplot depicts the range of $\delta^{13}C$ values observed for the analyte at selected stations (n = 4; BC52, BC72, BC78, BC85 for PLFAs and BC55, BC66, BC72 and BC73 for neutral lipids). The black line represents the average $\delta^{13}C$ values.

Figure 2.5. A. total sterol concentration (µg g OC^{-1}); B. $C_{28}\Delta^{5,22}$ (µg g OC^{-1}); C. $C_{27}\Delta^{5,22}$ (% of total sterols); D. $C_{27}\Delta^{5}$ (% of total sterols); E. $C_{30}\Delta^{22}$ (% of total sterols); and F. the ratio of polyunsaturated to branched phospholipid fatty acids (PUFA/brFA). Sterol nomenclature is according to $C_x\Delta^y$, where x refers to the number of carbons and y refers to the position of the unsaturation(s) on the carbon skeleton.

Figure 2.6. Concentrations of major sterol and phospholipid fatty acids in plankton net tow samples from mixed and stratified regions.

Figure 2.7. Hierarchical cluster analysis of multivariate bulk parameter and biomarker data, as shown in Table 2.1, revealing a clear distinction between the dataset that corresponds with the distinct seasonal hydrographic zonation.

Figure 3.1. The Codling Fault Zone mound features (white arrows), sampling stations that recovered hardground material (white crosses), underwater video tracklines (dark grey lines), and representative underwater image stills of exposed carbonates or black reduced sediment (white stars). A. Location of the area of study; B. A 3D Fledermaus image showing the topography of some of the mounds (Data source – Monteys, X.).

Figure 3.2. Underwater towed video (A to F) and grab sampling (G to I) of Codling Fault mound targets. A. Semi-exposed nodules and pavement (P1); B. Semi-exposed hardgrounds (P2); C. Pavement stacking (P3); D. Reduced surface sediment (P4) E. Large exposed hardgounds (P5) F. Exposed colonised and non-colonised hardgrounds

(P6); G. G103, H. G107, I. G109 – a hardground colonised by a *Nemertesia* hydroid (black arrow); Unlabelled scale bars = 25cm; The locations for underwater still images and sampling stations are given in Fig. 3.1 and Table 3.1.

Figure 3.3. Single beam echosounder profile showing topography of one of the Codling Fault mounds and active gas seepage to the water column from close to its apex (black arrows). The broken horizontal lines represent about 10 m water depth. The location of the mound is shown in Fig. 3.1 (inset B). (Data Source – Monteys, X.).

Figure 3.4. A, B. Representative SEM-EDS analyses of the composition of sampled hard grounds (locations given in Fig. 3.1 and Table 3.1). C. SEM micrograph showing carbonate-cemented quartz grain. D. Aragonite crystals and framboidal pyrite. E. Detail of framboidal pyrite close-up.

Figure 3.5. Aragonite cemented allochemic sandstone with bioclasts (G109). All microphotographs from PMO 217.327; A. Low magnification view of petrographic thin section. Note the large contribution of quartz grains in the rock volume. Empty cavities visible in the lover part of the picture are a product of sample preparation. B. Detail showing a possible glaucony granule (black arrow) and a an echinoderm skeletal fragment (grey arrow). C. Detail showing a bivalve fragment, possible an oyster (black arrow) and a red algal fragment (grey arrow). D. Detail showing a balanid barnacle fragment (black arrow) E. Detail showing a gastropod (black arrow) and a possible foraminiferan (grey arrow). F. Same are as in E, but with polarized light. (Data source – Hryniewicz, K.; Little, C.T.S.)

Figure 3.6. X-ray powder diffractogram of sample G109. The blue rhombi represent quartz, red squares represent aragonite and red triangles represent Mg-calcite (Data source – Hryniewicz, K.; Little, C.T.S.).

Figure 3.7. Carbon and oxygen stable isotope data from sample G109. Regression line in red (Data source – Hryniewicz, K.; Little, C.T.S.).

Figure 3.8. Total ion chromatograms of a representative phospholipid fatty acid sample (A) and an alcohol fraction (B) from extracted aragonite-cemented quartz. Major compounds are labeled. Fatty acid nomenclature is according to *X:Y*ω*Z,* where *X* refers to the number of carbon atoms present, *Y* refers to the number of double bonds on the carbon chain and *Z* refers to the position of the first double bond from the

= 1000) to assess confidence intervals. Bootstrap values >50 are reported. This shows distinct clustering of both bacterial populations between the two depths. At 2.1mbsf *Psychrobacter* clones (*n* = 14) are phylogenetically most closely related to *P. nivimaris*, while at 5.9mbsf (*n* = 14) are more diverse and cluster into groups related to *P. celer, P. marincola* and *P. submarinus* (Romanenko et al., 2002). *Sulfitobacter* clones at 2.1mbsf (*n* = 3) are phylogenetically most closely related to *S. pontiacus*, while at 5.9mbsf (*n* = 6) are most related to *S. litoralis*.

Figure 5.1. Bathymetric map of Dunmanus Bay showing the location and outline of Dunmanus Bay pockmark field. Sampling stations for the 2009 and 2011 surveys are shown. Insets: (A) Geographic location of Dunmanus Bay; (B) Sub-bottom pinger profile showing a transect across the Dunmanus Bay pockmark field (yellow dashed line). Acoustic turbidity, providing indirect evidence of gas accumulations, is evident and coincident with the pockmark field.

Figure 5.2. Downcore profiles of physical and chemical parameters from core VC1, sampled from within a pockmark cluster. Blue circles – Lipid and DNA sampling, red circles – pore water NMR sampling, green boxes – sedimentary NMR sampling.

Figure 5.3. Downcore profiles of physical and chemical parameters from core VC2, sampled from acoustically-turbid non-pockmarked sediment within the Dunmanus Bay pockmark field. Blue circles – Lipid and DNA sampling, red circles – pore water NMR sampling, green boxes – sedimentary NMR sampling.

Figure 5.4. Downcore profiles of physical and chemical parameters from core VC3, sampled from representative sandy sediment in Dunmanus Bay. Blue circles – Lipid and DNA sampling, red circles – pore water NMR sampling, green boxes – sedimentary NMR sampling

Figure 5.5. Downcore profiles of total phospholipid fatty acid (PLFA) abundances (A) and relevant PLFA ratios (B to D).

Figure 5.6. Hierarchical cluster analysis of PLFA profiles using the Bray-Curtis similarity matrix.

Figure 5.7. 16S rRNA bacterial denaturing gradient gel electrophoresis (DGGE) profiles and hierarchical cluster analysis.

Figure 5.8. 16S rRNA archaeal denaturing gradient gel electrophoresis profiles of samples from the survey in 2009. Sampling depth for DGGE analysis was 1 mbsf. See Fig. 5.1 for locations. GC14 is the control core, taken from outside the pockmark field.

Figure 5.9. Partial 1D ^{1}H NMR spectra from NaOH extracts. General region assignments correspond to aliphatics (1) - signals from various substituted methylenes, and methanes β to a functionality in hydrocarbons (signals from some amino acid side chains will also resonate here), carbohydrates and amino acids (2) – signals from protons α to O-alkyl functional groups. More specific assignments are protons associated with CH_3 groups in amino acid side chains (3), protons associated with methylene groups in aliphatic compounds (4), protons associated with N-acetyl functional groups in peptidoglycan (5) and protons associated with naturally occurring silicates compounds (*). The grey arrow highlights the resonance peak associated with peptidoglycan.

Figure 5.10. 1D water-suppressed ^{1}H NMR spectra of porewater dissolved organic matter from selected depths in VC1, VC2 and VC3. Specific assignments correspond to leucine (1), ethanol (2), lactic acid (3), acetic acid (4), dimethyl sulphide (5), acetone (6), pyruvate (7), methanol (8) and glycerol (9). Tyrosine, phenylalanine and formate were also identified in the 6.8 to 8.5 ppm region but are not included for clarity.

List of Abbreviations

ANME – ANaerobic MEthanotrophic archaea

AOM – Anaerobic Oxidation of Methane

AT – Acoustic Turbidity

brFA – Branched Fatty Acids

CD – Columnar Disturbances

CFZ – Codling Fault Zone

CMR - Coastal Mixed Region

CPI – Carbon Preference Index

DBPF – Dunmnaus Bay Pockmark Field

DGGE – Denaturing Gradient Gel Electrophoresis

DIC – Dissolved Inorganic Carbon

DMS – Dimethyl Sulfide

DOC – Dissolved Organic Carbon

DOM – Dissolved Organic Matter

ED – Early Diagenesis

EDS – Energy Dispersive Spectroscopy

E_h – Redox Potential

ER – Enhanced Reflector

GC-MS – Gas chromatography mass spectrometry

GC-irMS – Gas chromatography-isotope ratio mass spectrometry

GtC – Gigatonnes Carbon

HMW – High Molecular Weight

INFOMAR – INtegrated mapping FOr the sustainable development of Ireland's MArine Resource

IPL – Intact Polar Lipids

LC_{HC} – Long Chain Odd *n*-alkanes

LC_{OH} – Long Chain Even *n*-alkanols

LMW – Low Molecular Weight

LOI – Loss-On-Ignition

LUCA – Last Universal Common Ancestor

MBSF – Metres Below Seafloor

MDAC – Methane –Derived Authigenic Carbonate

MG – Microbial Gas

MSCL – Multi-sensor core logger

MUFA - Monounsaturated Fatty Acid

NMR – Nuclear Magnetic Resonance

NPP – Net Primary Production

OM - Organic Matter

OC - Organic Carbon

OTU – Operational Taxonomic Unit

pCO_2 – Partial Pressure CO_2

PLFA – Phospholipid Fatty Acids

POC - Particulate Organic Carbon

POM – Particulate Organic Matter

PP – Primary Production

ROV – Remotely Operated Vehicle

RNA – Ribonucleic Acid

SATFA – Saturated Fatty Acid

SEM – Scanning Electron Microscopy

SMR – Southern Mixed Region

SOC – Sedimentary Organic Carbon

SOM – Sedimentary Organic Matter

SRB – Sulfate-Reducing Bacteria

SSR – Summer Stratified Region

SWI – Sediment-Water Interface

TG – Thermogenic Gas

TN - Total Nitrogen

TOC - Total Organic Carbon

TOM – Terrestrial Organic Matter

TLE – Total Lipid Extract

UWTV – Underwater Towed Video

WE – Wax Ester

Table of Contents

Chapter 1

Introduction and Literature Review

1.1. Introduction

The oceans cover 71% of the earth's surface, with about two thirds of the earth's land located in the northern hemisphere. While the ocean seafloor is geologically distinct from the continents, it is intimately linked with terrestrial geological processes. Due to plate tectonics the seafloor is in a perpetual cycle of formation and destruction. Over geological timescales mantle convection causes spreading from the mid ocean ridges towards the continents, the oceanic plate is subducted into the mantle and the continental plate is pushed up to form mountains. The oceans are a natural depository for the dissolved and particulate matter arising from continental weathering, riverine and aeolian transport, and also from marine inputs (Hedges and Keil, 1995; Hedges et al., 1997). Upon input to the oceans dissolved matter is consolidated by biological and geochemical processes and is deposited with particulate matter over geological timescales as marine sediments on the ocean floors. In this way the ocean floor is invaluable for understanding the earth's history and for reconstructing past environmental conditions of continents and oceans (Chester and Jickells, 2012).

In basic terms the ocean's seabed is divided into the continental margins, which are composed of the continental shelf, the slope and the rise, and the vast expanse of the abyssal plains. Marine sediments cover a large fraction of the worlds oceans, and have an average thickness of about 500 m. Nearshore sediments deposited on the shelf are characterised by diverse depositional conditions and typically high accumulation rates (~ mm a^{-1}). Deep-sea sediments cover more than 50% of the earth's surface and are characterised by slow-accumulation rates. Sediments are comprised of an aqueous phase (termed interstitial or pore water), which occupy the pore spaces between sediment particles, and a solid phase. The solid phase can be further sub-divided based on their geological spheres of origin, namely lithogenous, hydrogenous, biogenous and cosmogenous components (Chester and Jickells, 2012). The sedimentary solid phase is not inert but undergoes a range of physical and chemical changes upon deposition until lithification, collectively called diagenesis (Berner, 1980). These changes primarily occur across the pore water phase. Many of the most important diagenetic changes occur during and soon after burial and are usually referred to as early diagenesis (ED).

Improvements in remote seabed mapping technology and remotely operated submersibles over the past few decades have resulted in a distinct shift away from the

aforementioned perception to one of considerable physical and biological diversity. It is now known that the seafloor is characterised by diverse settings such as canyons, cold seeps, deep water coral reefs, mud volcanos, pockmarks, carbonate mounds, ridges and trenches (Jørgensen and Boetius, 2007). Accordingly there are vast regions yet to explore and understand. Much of this diversity has been shown to be associated with marine seabed fluid flow. Sites of active seabed fluid flow, which include hydrothermal vents and cold seeps, have a considerable impact on physical and geological diversity, on the nature and chemical composition of marine and atmospheric systems, and on biological diversity (Judd and Hovland, 2007).

1.2 The marine carbon cycle

Chemical cycling on earth is of vital importance and consists of complex reversible and irreversible fluxes between the geo-, hydro-, atmo- and biosphere. Many chemical cycles are strongly influenced by organisms, particularly plants and microorganisms. These are termed biogeochemical cycles and the major cycles are carbon, nitrogen, oxygen, phosphorus and sulphur (Manahan, 2004). The focus of this review shall be on the carbon cycle, and a schematic outline of the global carbon cycle is given in Fig. 1.1. The earth's natural carbon reservoirs consist of fossil fuels (~ 3700 GtC), vegetation, soil and detritus (~ 2300 GtC), the atmosphere (~ 597 GtC), the surface ocean (~ 900 GtC), the intermediate and deep ocean (~ 37,100 GtC) and surface sediments (~ 150 GtC) (Denman et al., 2007, and references therein). Carbon cycling occurs over very different timescales, whereby biological carbon has a typical half-life of days to tens of years, while geological carbon has a half-life typically in region of millions of years. The 'leak' from the biological to the geological carbon cycle is primarily represented by the burial of organic matter (OM) in sediments and is the source of fossil fuels (Rullkötter, 2006). Only about 1% of the total organic carbon (OC) pool is actively cycled. The largest active reservoir (~ 40 GtC) is dissolved inorganic carbon (DIC) in seawater. Other dynamic pools, which are 1 to 2 orders of magnitude smaller, include atmospheric CO_2, soil humus, terrestrial plant biomass, marine dissolved organic carbon (DOC) and sedimentary organic carbon (SOC) (Hedges and Keil, 1995). It is noteworthy that globally more OC occurs in soil humus (~ 1600 GtC), recently deposited marine sediments (~ 1000 GtC) and dissolved in seawater (~ 700 GtC) than in all land plants (~ 600 GtC) and marine organisms (~ 3

GtC) combined (Hedges et al., 2000). Accordingly, these vast deposits of organic molecules play major roles in global temperature modulation, in weathering processes, in supporting life, and also in composing precursors for coal and petroleum.

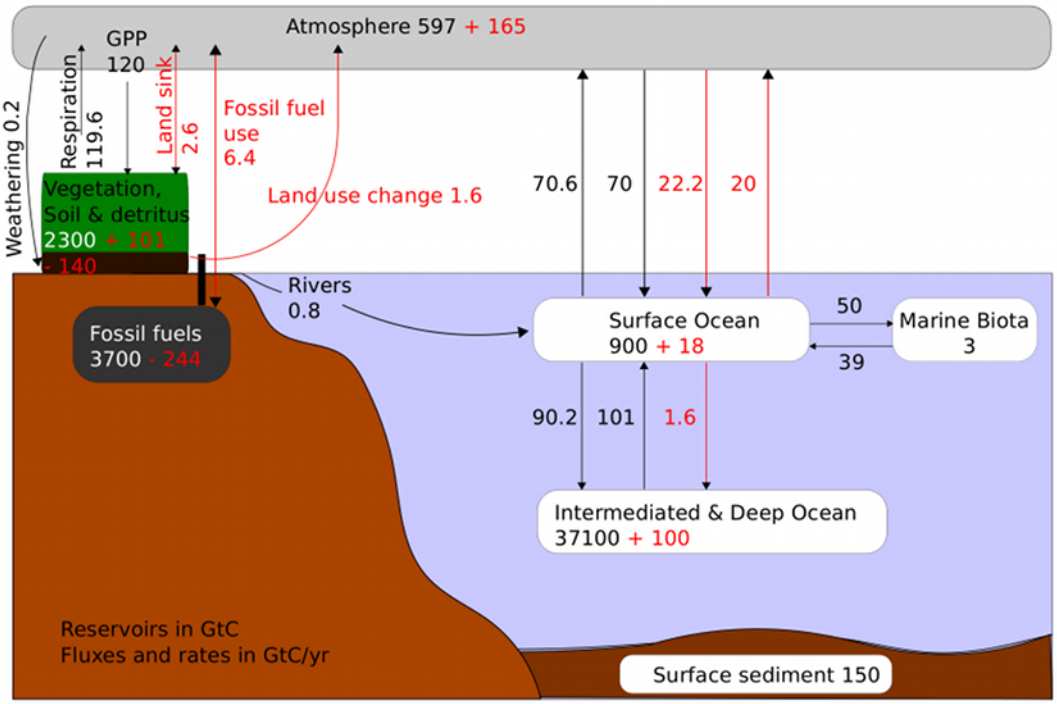

Figure 1.1. The global C cycle for the 1990's, showing annual fluxes in Gt C a^{-1}. Pre-industrial fluxes are shown in black, anthropogenic fluxes are shown in red. GPP is annual gross primary production. (after Denman et al., 2007, and references therein).

CO_2 is removed from the atmosphere via weathering by silicate rocks (0.2 GtC a^{-1}) and also fixed as OC (120 GtC a^{-1}) by plants and microbes, with most of this CO_2 being returned to the atmosphere by respiration (119.6 GtC a^{-1}) (Denman et al., 2007). Continental weathering and biomass degradation delivers 0.8 GtC a^{-1} to the surface oceans via rivers (Hedges and Keil, 1997). Oceanic carbon exists is several forms: DIC (37000 GtC: Falkowski et al., 2000; Sarmiento and Gruber, 2006), DOC (685 GtC: Hansell and Carlson, 1998) and particulate organic carbon (POC, 13 to 23 GtC: Eglinton and Repeta, 2004), with ratios of approximately 2000:38:1 DIC: DOC: POC. CO_2 is exchanged between the atmosphere and the ocean, whereby 70 GtC a^{-1} is transported to the oceans and 70.6 GtC a^{-1} is transported to the atmosphere. This exchange is determined by the partial pressure of CO_2 (pCO_2), which is altered significantly due to factors such as wind speed, precipitation, heat flux, sea ice and the

presence of surfactants. Atmosphere-ocean CO_2 exchange is also altered through what are termed the 'solubility pump', the 'biological pump' (also called the 'organic carbon pump') and the 'carbonate pump'. The solubility pump concerns changes in the solubility of gaseous CO_2, whereby on dissolution CO_2 reacts with water to form HCO_3^- and CO_3^{2-} (making up DIC). A conceptual model for this process is given in Fig. 1.2.

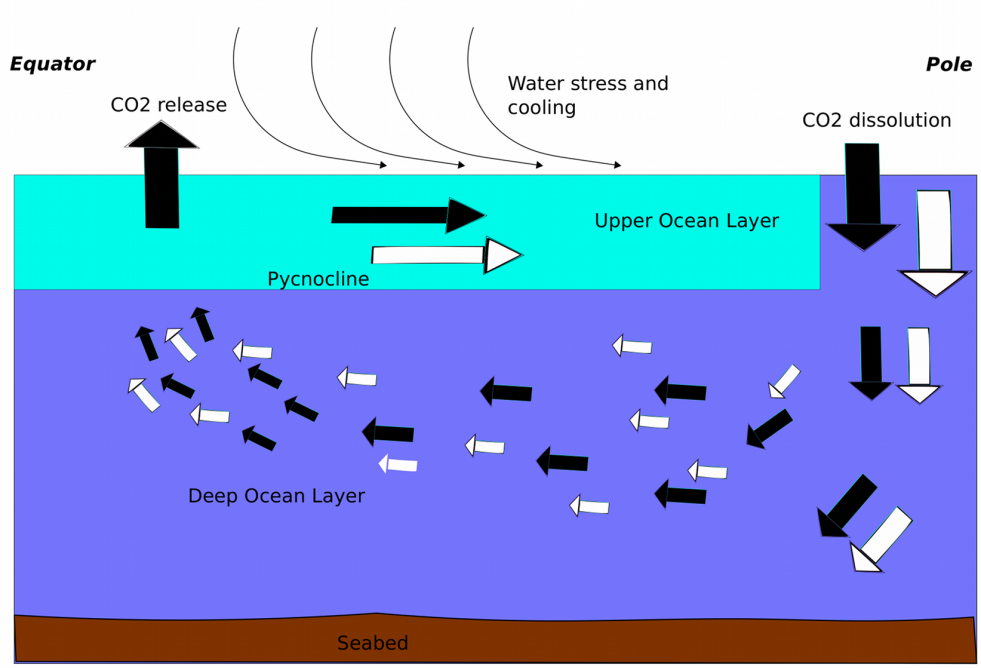

Figure 1.2. Conceptual model of the solubility pump. White and black arrows represent the movement of water and CO_2, respectively. Cooling increases the solubility of CO_2, resulting in a flux from the atmosphere to the surface ocean. At subpolar latitudes water density increases and CO_2-enriched waters sinks rapidly. At depth this CO_2-enriched water moves slowly as it is dispersed throughout the deep ocean. Sinking water masses displace water that is returned to the surface ocean in upwelling regions. As the water warms, pCO_2 increases and escapes from the surface ocean back into the atmosphere. (after Carlson et al., 2001).

The biological pump concerns changes in carbon fixation to POC by phytoplankton via photosynthesis (50 GtC yr^{-1}), at the surface waters (39 GtC yr^{-1}) and export transport to deeper waters, while the $CaCO_3$ pump concerns changes in CO_2 release through formation of planktonic shells ($CaCO_3$) (Volk and Hoffert, 1985). These are illustrated in Fig. 1.3 and 1.4 respectively. DOC is primarily sourced from terrestrial environments via rivers or from marine planktonic water column metabolism, and residence time can vary significantly from days to 10 kyr (Loh et al., 2004).

Mineralisation and remineralisation of OC occurs primarily in the upper 1000 m of the ocean water column (90.2 GtC a^{-1} and 101 Gt a^{-1}), with the remainder of the particle flux entering marine sediments (0.2 GtC a^{-1}). The OC content of sedimentary deposits can range from zero to up to 100% in coals, but is typically less than 2% in freshly deposited marine sediments and averaged over the entire ocean floor is less than 0.25% (Pedersen and Calvert, 1990). A more detailed discussion of the composition and cycling of sedimentary organic matter (SOM) will be given in section 1.2.1.

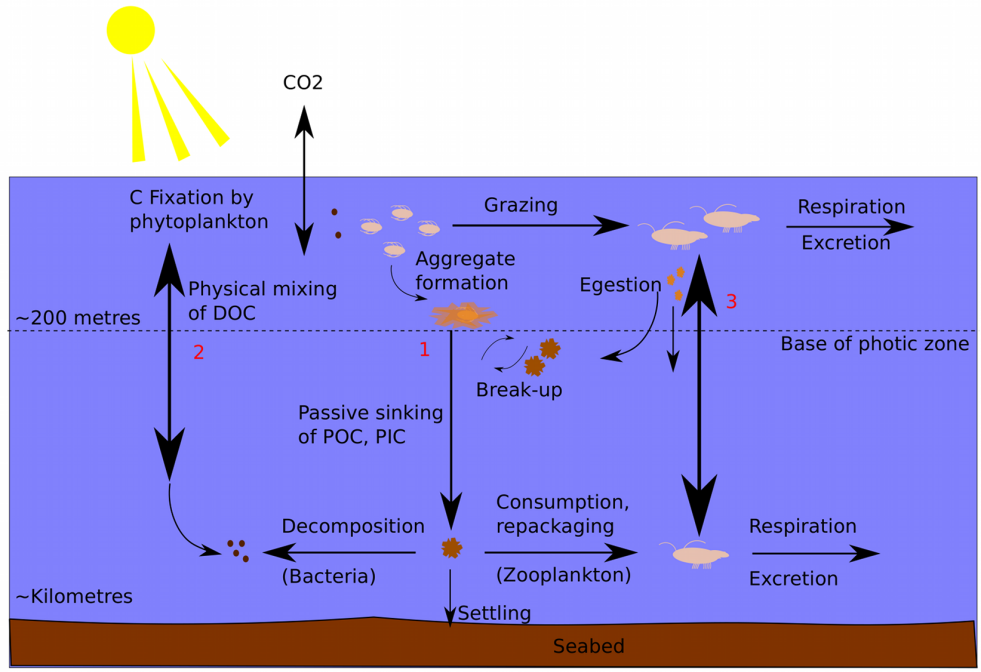

Figure 1.3. Conceptual model of the biological pump. CO_2 is taken up by phytoplankton and organic matter (OM) is produced. As this OM is processed through the marine food web, fecal pellets or aggregates are produced, a portion of which sink as organic (POC) and inorganic (PIC) particulate from surface waters to depth (1). Dissolved organic carbon (DOC) is also produced and removed from surface waters to depth by physical mixing of water (2). DOC and dissolved inorganic carbon (DIC) are also actively transported to depth by vertically migrating organisms such as copepods that feed in surface waters and excrete and respire the consumed OM at depth (3) (taken from Carlson et al., 2001).

The effects of anthropogenic activity on the Earth are illustrated in Fig. 1.1. Red figures and arrows highlight how anthropogenic processes, in particular the burning of fossil fuels such as coal and petroleum, since the industrial revolution (~ 1750), has resulted in enhanced concentrations of atmospheric CO_2, which according to ice core records are the highest in 650 kyr (Petit et al., 1999). Atmospheric CO_2 levels were stable for ~ 10,000 yr pre-1750, at 260-280 ppm, and in about 150 yr had

increased to 380 ppm in 2005 (Forster et al., 2007). While CO_2 is the primary causal factor in current climate change, atmospheric CH_4 is also a significant greenhouse gas, and per mole has a 100 yr global warming potential 25 times greater than CO_2 (Forster et al., 2007). CH_4 atmospheric levels have increased from 770 ppb in 1750 to 1775 ppb in 2005 and is at unprecedented levels over the last 420,000 yr (Petit et al., 1999). This is of particular concern as CH_4 is the most abundant reactive trace gas in the troposphere and has a significant impact on tropospheric and stratospheric chemistry (Wuebbles and Hayhoe, 2002). The primary cause of this increase is agriculture (changing land usage and ruminant animals), waste production and disposal, fossil fuel use and biomass burning, while major natural causes include wetlands, oceans, vegetation and CH_4 hydrates (Denman et al., 2007). However the contribution from from natural sources, in particular from the marine environment, is poorly understood (Knittel and Boetius, 2009). Thus an accurate understanding of global CH_4 compartments, production and fluxes is also vital for understanding and mitigating past, present and future climate change.

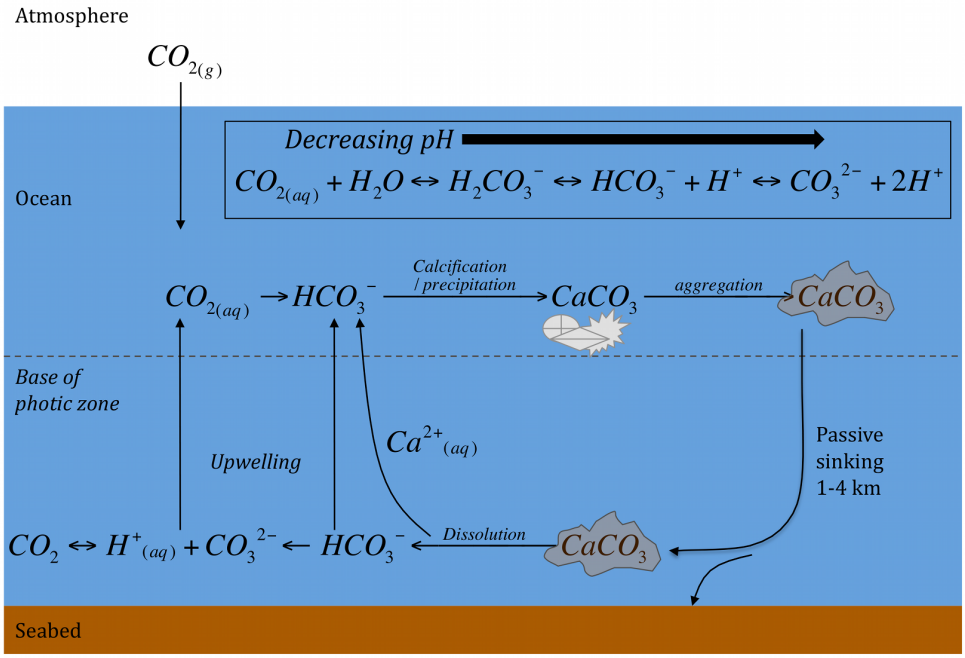

Figure 1.4. Conceptual model of the (simplified) carbonate pump. Certain marine organisms form calcareous skeletal material, a portion of which sinks as $CaCO_3$ aggregates. These aggregates are preserved in shallow ocean sediments or dissolved at greater depths (3000 to 5000 m), thus increasing dissolved inorganic carbon (DIC) concentrations in the deep ocean. The Ca^{2+} and HCO_3^- returns to the surface ocean via upwelling (after Carlson et al., 2001).

As shown in Fig. 1.1, the cycling of OM is a key process in the global carbon cycle. Hedges et al. (2000) describes OM as a "thermodynamic anomaly atop a free-energy precipice that drops off on all sides to dispersed, stable components such as CO_2, H_2O, NO_3^- and PO_4^{3-}". The marine system (~ 44 to 50 GtC a^{-1}) is approximately equal to the terrestrial system (~ 60 GtC a^{-1}) in terms of the addition of new primary production (PP) to the biosphere (Behrenfeld and Falkowski, 1997). PP is the major source of POM in the marine environment, and over 80% of PP occurs in the open ocean settings (Longhurst et al., 1995). The simplest method of describing the composition of marine OM is in elemental form. The Redfield ratio (Redfield et al., 1963) was developed from the relationship between phytoplankton and nutrients available in seawater:

$$C:N:P = 106:16:1$$

Eqn. 1.1

Derived from this Redfield ratio is the generalised molecular formula of phytoplankton OM:

$$106CO_2 + 106H_2O + 16NH_3 + H_3PO_4 \rightarrow (CH_2O)_{106}(NH_3)_{16}H_3PO_4 + 106O_2$$

Eqn. 1.2

However actual elemental composition of marine OM can deviate significantly from the Redfield ratio. Hedges et al. (2002) estimated that the average elemental formula for marine plankton from contrasting marine sites was $C_{106}H_{177}O_{37}N_{17}S_{0.4}$. Parsons et al. (1961) provided one of the early comprehensive studies of the molecular composition of marine biomass, and from a variety of marine algae concluded that protein accounted for an average of 39% of total dry weight, while carbohydrates, lipids, pigments and ash accounted for an average of 23%, 8%, less than 2% and 22%, respectively. Hedges et al. (2002) concluded that marine planktonic OM was composed of on average 65% protein, 19% lipid and 16% carbohydrate.

The total POM reservoir is comparatively small but undergoes rapid mineralisation as a result of grazing by secondary producers (zooplankton and protozoans) (Fig. 1.3). Only about 20% of net primary production (NPP) escapes the photic zone to deeper waters (Harvey, 2006). Sediment trap studies have shown an exponential decrease in POM with depth, whereby as little as 10% of net PP remains

at depths of several hundred metres and less than 1% of net PP remains at depths of 4000 m (Suess, 1980). Thus a tiny fraction of NPP escapes mineralisation to be buried and preserved in the sedimentary record (Rullkötter, 2006). SOM accumulation and preservation shall be discussed in more detail in section 1.2.1.

DOM is one of the largest global active C reservoirs yet one of the least understood. It is known to have a variety of functions from fueling the so-called 'microbial loop', to controlling the marine dynamics of trace metals and radionuclides, to generating gases and nutrients (Ogawa and Tanoue, 2003). Interest in DOM was sparked in the late 1980s when improvements in analytical methodology led to the proposition that previous methods significantly underestimated the reservoir of marine DOM (Suzuki et al., 1985; Sugimura and Suzuki, 1988). Although these initial claims were later retracted, it has nevertheless become apparent, after significant research interest and analytical improvements, that DOM is a hugely important component of the global carbon cycle (Harvey, 2006). DOM is usually operationally defined according to its retention on various filter types, but in reality a size spectrum of DOM exists (Ogawa and Tanoue, 2003). The low-molecular weight (LMW) fraction of DOM (<1 kDa) comprises 65 to 80% of the total, while the high molecular weight (HMW) fraction typically makes up 20 to 35% for >1 kDa and 2 to 7% for >10 kDa. Furthermore it has been shown that HMW DOM is present in greater abundance in surface waters, which suggests that this HMW portion is more reactive and that the LMW fraction comprises the oldest most refractory DOM in the oceans (Ogawa and Tanoue, 2003). Largely for analytical reasons, this LMW portion also remains the most poorly characterised and in total, about three quarters of DOM is uncharacterised at the molecular level (Hedges et al., 2000). C:N values (15:1) and $\delta^{13}C$ analysis of DOM are typically consistent with a marine origin (Ogawa and Tanoue, 2003) but as outlined by McCarthy et al. (1996), ultrafiltered DOM appears to be chemically distinct from fresh phytoplankton, sinking POM or humic substances. Of particular interest are the findings using ^{13}C nuclear magnetic resonance (NMR) characterisation, that ultrafiltered DOM consistently yields high proportions of D-alanine, D-serine, D-glutamic acid and D-aspartic acid compared to the more common L-isomers, which is consistent with the peptidoglycan biopolymer in bacterial cell walls (McCarthy et al., 1998). Thus, it appears that microbes and their remains may be major components of marine DOM pools (Hedges et al., 2000). Recent evidence also indicates that black carbon, a refractory and complex product of

incomplete combustion, is a major component of coastal DOM (Mannino and Harvey, 2004).

Transport of terrestrial material to the marine environment is a major process and thus terrestrial organic matter (TOM) is a major component of the marine carbon cycle. However the fate of TOM in the marine environment is poorly understood (Hedges et al., 1997; Baldock et al., 2004; Benner, 2004). Rivers transport about 1% of terrestrial productivity (~ 60 GtC a^{-1}) to the ocean as POM and DOM (~ 0.15 GtC a^{-1} and ~ 0.25 to 0.36 GtC a^{-1}, respectively). Aoelian transport accounts for less than 0.1 GtC a^{-1} and thus riverine transport of POM and DOM is the major mechanism for transport of terrigenous material to marine sediments (Harvey, 2006). Much of the TOM transported by rivers appears to be sourced from soil, and is primarily composed of highly degraded, recalcitrant and N-poor OM derived from vascular plants (Hedges et al., 1997; Baldock et al., 2004). The composition of soil-derived OM has been reviewed by Derenne and Largeau (2001) and by Kögel-Knabner (2002). Major recalcitrant compound classes include lignins, tannins, suberins and black carbon. More recently it has been proposed that the microbial component of soil OM is much higher than previously thought (Simpson et al., 2007) and hence could be a significant component of TOM being transported to the marine environment. TOM from aoelian transport becomes increasingly important in open ocean settings (Simoneit, 1977; Simoneit et al., 1991).

1.2.1 Sedimentary organic matter: composition, early diagenesis and preservation

A schematic overview of the fate of OM in marine sediments is given in Fig. 1.5. Three distinct processes in the cycling of SOM exist: diagenesis; catagenesis; and metagenesis. As mentioned in section 1.1, diagenesis is the sum total of processes (chemical, physical and biological) that alters the original state of sediments or sedimentary rock (Berner, 1980). This occurs down to about 1000 km, while catagensis and metagenesis occurs down to several kilometres and with an increase in temperature and pressure. These processes result in formation of petroleum and gas reservoirs respectively (Tissot and Welte, 1984). The focus of this review shall be on the processes of ED. SOM is a heterogeneous mixture of particles and molecules having variable physical and chemical properties. Food chain and ED processes alter this general elemental composition of OM considerably, whereby SOM is typically

depleted in oxygen, nitrogen and phosphorus relative to carbon and hydrogen (Rullkötter, 2006). Furthermore diagenetic incorporation of sulfur into SOM results in approximate enrichment of sulfur equal to that of phosphorus (Rullkötter, 2006). Hedges and Oades (1997) summarised the content of coastal SOM as approximately 10 to 15% amino acids, 5 to 10% carbohydrates, 3 to 5% lignin and less than 5% lipids. During sedimentation of decayed organisms, proteins are readily hydrolysed into amino acids and small peptides. However a certain fraction of this nitrogen-bearing OM may be protected against hydrolysis by various protective mechanisms, for example as a bound component of complex recalcitrant OM such as humic substances or kerogen (Rullkötter, 2006). Carbohydrates are typically rapidly hydrolysed to water-soluble pentoses and hexoses, and have a half-life in the sedimentary environment similar to proteins. However, certain complex polysaccharides, such as cellulose and lignin, are recalcitrant and are typically preserved during transport, deposition and sedimentation on the seafloor (Hedges and Oades, 1997). Lipids include a diverse range of compound classes such as aliphatic hydrocarbons, ketones and alcohols, fatty acids, steroids, acylglycerols, phospholipids, terpenoids, carotenoids and vitamins. They are typically more recalcitrant than proteins or sugars, by virtue of their relatively non-polar aliphatic hydrocarbon structures, and are hence preferentially preserved in sediments (Rullkötter, 2006). For this reason lipids have been particularly important as molecular tracers or 'biomarkers' in studes of OC cycling in the marine environment (See section 1.5). About 90% of buried OM is composed of amorphous, insoluble kerogen distributed in shales and other sedimentary rocks (Hedges and Keil, 1995). More recently it has been reported that black carbon can comprise between 10 to 50% of total SOM (Middelburg et al., 1999), although the proportion of black carbon in soils and sediments may be overestimated (Simpson and Hatcher, 2004).

Many of the chemical changes of ED are mediated by degradation of SOM and are driven by redox reactions at the pore water/sediment boundary (Berner, 1980). The boundary layer between the solid and aqueous compartments of marine sediments is a site of intensive chemical, physical and biological processes and reactions (Chester and Jickells, 2012). ED of SOM proceeds along a diagenetic sequence whereby the most energetically favourable electron acceptors are consumed first and succeeded by the next (Froelich et al., 1979). O_2 is considered the primary oxidant and typically results in the mineralisation of the majority of deposited OM:

$$5[(CH_2O)_{106}(NH_3)_{16}(H_3PO_4)] + 690O_2 \rightarrow 530CO_2 + 80HNO_3 + 5H_3PO_4 + 610H_2O$$

Eqn. 1.3

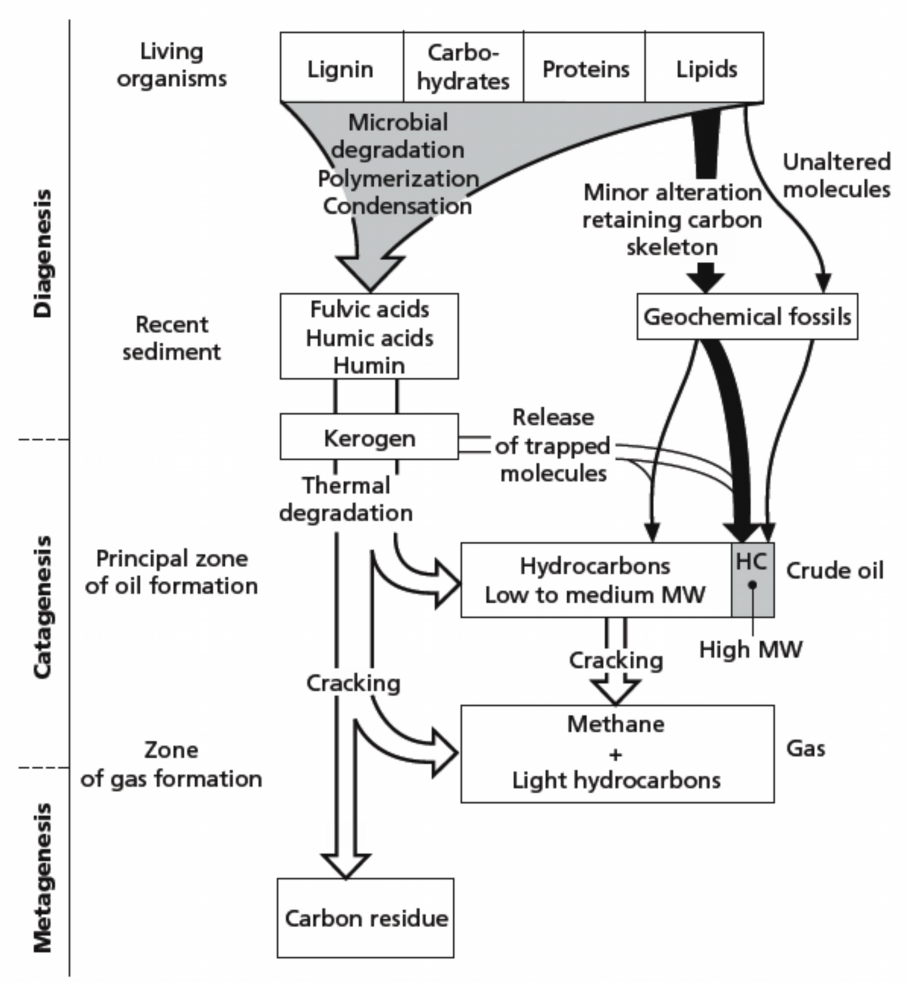

Figure 1.5. Stages in the diagenesis, catagenesis and metagenesis of organic matter in marine sediments (after Tissot and Welte, 1984).

Anaerobic microbial metabolism becomes dominant, only when O_2 reaches low concentration or is completely consumed. Secondary electron acceptors are then utilised in sequence based on their energy yields and typically occurs in the following sequence:

$$NO_3^- \rightarrow MnO_2 \rightarrow Fe_2O_3 \rightarrow SO_4^{2-}$$

Eqn. 1.4

NO_3^- becomes the preferred electron acceptor when O_2 falls to less than 5% and enables denitrification as follows:

$$5[(CH_2O)_{106}(NH_3)_{16}(H_3PO_4)] + 472HNO_3 \rightarrow 276N_2 + 520CO_2 + 5H_3PO_4 + 886H_2O$$

Eqn 1.5

The oxidation of OM by manganese (IV) oxides, iron (III) oxides and SO_4^{2-} can be described as follows:

$$(CH_2O)_{106}(NH_3)_{16}(H_3PO_4) + 236MnO_2 \rightarrow 236Mn^{2+} + 106CO_2 + 8N_2 + H_3PO_4 + 336H_2O$$

Eqn. 1.6

$$(CH_2O)_{106}(NH_3)_{16}(H_3PO_4) + 212Fe_2O_3 + 848H^+$$
$$\rightarrow 424Fe^{2+} + 106CO_2 + 16NH_3 + H_3PO_4 + 530H_2O$$

Eqn. 1.7

$$(CH_2O)_{106}(NH_3)_{16}(H_3PO_4) + 53SO_4^{2-} \rightarrow 106CO_2 + 16NH_3 + 53S^{2-} + H_3PO_4 + 106H_2O$$

Eqn. 1.8

After SO_4^{2-} is consumed and no longer available as an electron acceptor, microbial CH_4 can be formed according to the following equations:

$$CH_3COOH \rightarrow CH_4 + CO_2$$
$$or$$
$$CO_2 + 4H_2 \rightarrow CH_4 + 2H_2O$$

Eqn. 1.9

The aforementioned diaganetic sequence assumes that each reaction is oxidant-limited and thus proceeds sequentially setting up vertical redox zones in the sediment column (Chester and Jickells, 2012). The products of each reaction are thus produced within a specific zone, thereby setting up diffusion gradients from high to low concentrations. Hence the sediment column acts as a sink for certain elements and molecules in the water column but also as a source of other elements and molecules to the water column. This geochemical zonation is illustrated in Fig. 1.6, as well as corresponding sedimentary classification systems proposed by Froelich et al. (1979) and Berner (1981). Most of the CH_4 that is produced in the subsurface normal marine sediments diffuses upwards and is consumed in a zone called the sulfate-methane transition zone

(SMTZ). This is mediated by a procees called the anaerobic oxidation of methane (AOM) and only occurs in sulfate-depleted layers (See section 1.4.2.2 for details.)

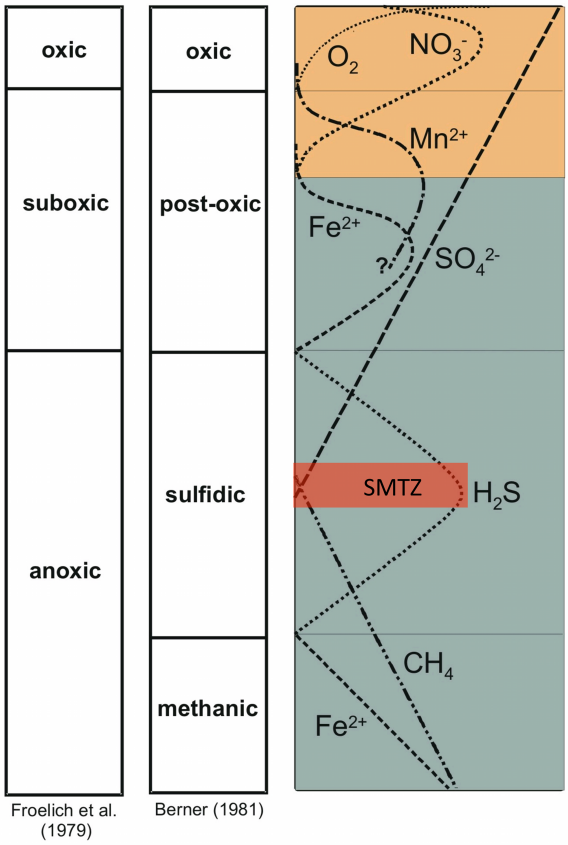

Figure 1.6. Early diagenetic geochemical zonation of marine sediments. SMTZ – Sulfate-methane transition zone (after Froelich et al., 1979; Berner, 1981).

The fossil record provides clear evidence of periods during the Earth's geological history whereby OM accumulation in sediments was favoured. Organic-rich shales, sapropels and other petroleum source rocks are contrasted by sequences of white- or red-coloured sedimentary rocks that are devoid of OM (Rullkötter, 2006). Given the high free energy yield obtained from OM oxidation, it is not surprising that typically less than 1% of organic particulate debris produced in open ocean settings reaches the seafloor. Furthermore less than 1% of this OM escapes the mineralisation in surficial sediments to be preserved in the sedimentary record (Wakeham and Canual, 2006). In coastal and continental shelf settings approximately 40% of this organic detritus may be preserved. Thus one of the major focuses of research in organic matter cycling over the past number of decades, and still in active debate, has been on the major controlling factors governing OM accumulation and preservation in

marine sediments (Hedges and Keil, 1995; Rullkötter, 2006; Lalonde et al., 2012; Eglinton, 2012).

The 'selective preservation' hypothesis proposes that organic compounds and compound classes differ in their potential to be preserved in sediments and to survive ED. Thus SOM is seen as consisting of remnant biosynthetic material that has a higher proportion of recalcitrant material. Water-soluble organic compounds, or macromolecules, which are easily hydrolysed to water-soluble monomers, have a low preservation potential. On the other hand, compounds with a low water-solubility such as lipids and hydrolysis-resistant macromolecules are selectively enriched in SOM. This hypothesis has gained acceptance over others in recent years. However Hedges et al. (2001) used solid-state ^{13}C NMR, to study sediment trap POM and found that there was no significant change in preservation potential between the major compound classes i.e. carbohydrates, amino acids and lipids.

Sediment accumulation rate (SAR) is an important controlling variable on SOM reactivity and preservation. High SAR results in deposited OM being transported more rapidly from the sediment/water interface and thus away from sites of greatest microbial and macrofaunal activity (Hedges and Keil, 1995). High SAR also facilitates in inhibiting the diffusive transport of aqueous electron acceptors, in particular O_2, NO_3 and SO_4^{2-} down into the sediment column. However, while SAR and the percentage of OM preserved is a positive linear relationship, preservation also depends on a variety of additional variables such as dilution effects resulting from changing input of inorganic coarse material (i.e. quartz) (Hedges and Keil, 1995). For example at high deposition rates of about 10 mg cm^{-2} yr^{-1}, the % OM buried plateaus and this effect is most pronounced in coastal and deltaic sediment settings with significant input of inorganic minerals (Rullkötter, 2006). Thus the burial efficiency of OM has been utilised to assess SOM preservation, and is defined as the accumulation rate of OM below surficial sediments divided by the local organic flux to the seafloor. OM burial efficiency ranges from less than 1% in open ocean sediments with low SAR, to up to 80% for some coastal/shelf hot spots of OM burial. OM burial efficiency is generally a linear relationship up to 15 mg cm^{-2} yr^{-1} (Hedges and Keil, 1995). However this approach is limited in the sense that in many circumstances deposited OM is not freshly biosynthesised and has undergone considerable degradation or cycles of resuspension and deposition.

Dissolved water column O_2 is another important parameter mediating the preservation of OM in marine sediments, whereby anoxic bottom waters are known to be characterised by organic-rich sedimentary deposits e.g. the Black Sea (Demaison and Moore, 1980). This is thought to be due to a variety of reasons such as: lower free energy yields from suboxic respiration; the requirement for complex microbial consortia for stepwise OM degradation; the accumulation of toxic by-products e.g. H_2S; reduced sediment mixing and irrigation processes; and the presence of highly insoluble recalcitrant OM that can only be degraded by aerobic oxidative enzymes (Hedges and Keil, 1995, and references therein).

Proponents of the 'primary productivity hypothesis' (Pedersen and Calvert, 1990) contend that changes in primary productivity, brought on by climatic and oceanographic-related changes, best explain the accumulation of OM in Quaternary sediments and Cretacious Black Shales. Upwelling processes transport nutrients from depth and stimulate primary production in the photic zone, and resulting biomass is consumed in the water column with the concurrent depletion of O_2 (Rullkötter, 2006). Recently is has been shown that iron plays a significant role in the preservation of OM in sediments (Lalonde et al., 2012). They demonstrated that between 12.9 and 30.1% of OM in sediments is directly bound by chelation or co-precipitation, to reactive iron phases during ED. On global terms they estimated between 19 and 45 GtC is preserved in marine sediments due to its association with iron. These findings may have a significant impact on our understanding of OM preservation in marine sediments and also in the close coupling of global iron and carbon cycles (Eglinton, 2012).

1.3 Marine sedimentary prokaryotes: the unseen majority

Life was traditionally divided into two domains based on those that had a true nucleus (the eukaryotes) and those that did not (prokaryotes). However Woese and Fox (1977) revolutionised this concept using molecular phylogeny based on the universal and conserved 16S rRNA gene. A third domain, called the archaebacteria, now called archaea, was introduced (Fig. 1.7). Together with bacteria, they now comprise the prokaryotes, although phylogenetically archaea are more closely related to the eukarya than bacteria (DeLong and Pace, 2001). The application of culture-independent nucleic acid based methods (Olsen et al., 1986; Pace 1997; Head et al., 1998; Hugenholtz et al., 1998; DeLong and Pace, 2001) has transformed microbial ecology and in turn our understanding of the limits of the biosphere and the role microbes play in biogeochemical cycling.

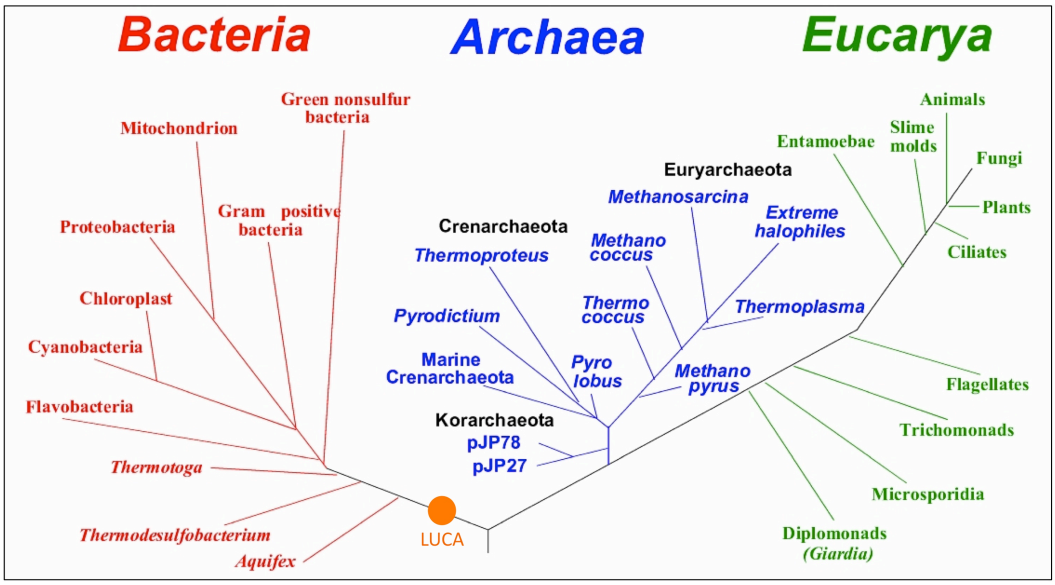

Figure 1.7. The universal phylogenetic tree of life as defined by comparative rRNA gene sequencing. The three domains of life – Bacteria, Archaea and Eukarya are shown, along with a number of important representative groups. LUCA – Last universal common ancestor. (taken from Madigan et al., 2012).

Despite their size, prokaryote biomass is estimated to represent 80 to 100% of the estimated total carbon in all plants, and about 10 times more phosphorus and nitrogen in all plant biomass (Whitman et al., 1998). The cell number and biomass amounts of total prokaryotes in various habitats is given in Table 1.1. After intensive interest over the past few decades (Pomeroy, 1974; Lochte and Turley, 1988; Deming and Baross,

1993; Gooday et al., 1990; Gooday, 2002) the importance of microbes in marine ecosystems and in carbon cycling is now firmly established. Microbes are major contributors to NPP in the marine environment and significant decomposers of marine OM (Gooday, 2002; Harvey, 2006, and references therein). However, knowledge of microbial life in the seabed is still in its infancy. Major early discoveries include: the discovery of millions of viable bacteria per gram of sediment at water depths of over 10,000 m (Zobell and Morita, 1959); the discovery of core material of high microbial diversity from subsurface sediments and the oceans crust during the Deep Sea Drilling Project in 1968; and the discovery by the ROV *ALVIN* of hydrothermal vents or 'black smokers' of rich biodiversity at the Pacific mid-oceanic ridge. Bacteria appear to comprise a large fraction of the total microbial community in the photic zone of the oceans, as illustrated in Fig. 1.8A for the North Pacific Ocean (Karner et al., 2001). However, bacterial dominance has been shown to decrease with depth in the water column, in tandem with the decreasing abundance of light and availability of labile OM (Madigan et al., 2012) (Fig. 1.8A). In contrast archaeal abundance, specifically pelagic Thaumarchaeota, have been observed to increase in relative abundance with depth (Karner et al., 2001).

Table 1.1. Number and biomass of prokaryotes in various habitats (after Whitman et al., 1998).

Environment	No. cells, X 10^{26}	Biomass, GtC[b]
Continental shelves	1.0	0.02
Ocean waters, upper 200 m	360	0.72
Ocean waters, below 200 m	650	1.3
Surface sediments, 0 to 10 cm	170	0.3
Oceanic subsurface[a]	35500	303
Soil	2600	26
Terrestrial subsurface[a]	2500 - 25000	22 - 215
Total, X 10^{28}	417 - 640	353 - 546

a. The subsurface compartments are defined as below 8 m in terrestrial systems and below 10 cm in oceans sediment.

b. Calculated with the assumption of 20 fg C $cell^{-1}$ for aquatic habitats and 10 fg C $cell^{-1}$ for sediment and soil.

The marine seafloor and subsurface is one of the most extensive microbial habitats on earth, whereby marine sediments cover more than two-thirds of the Earths's surface and microbial cells and activity are widespread in these sediments (Teske and Sørensen, 2008). In sites of particular nutrient and energy abundance microbial life can thrive, for example at huge bacterial mats in cold seep ecosystems (Fig. 1.8B)

(See section 1.4.2.2). Compared with the water column, the ocean seafloor provides a vast area of solid surfaces and heterogenous pore spaces, a high concentration of detrital OM per unit volume to support microbes. In addition transport processes, such as mixing and advection, which may limit microbial growth in the water column, are also normally limited to a few centimetres per year. Accordingly, seafloor sediments contain 10 – 10,000 fold more cells per unit volume than productive ocean-surface waters (Jørgensen, 2006). In the seabed, archaea seem to comprise a small proportion of the total microbial community of the oxic seafloor in terms of cell biomass, while bacteria dominate (Fig. 1.8C). However in the subseafloor, archaea have been shown to increase in abundance with depth and even dominate (Biddle et al., 2006; Lipp et al., 2008).

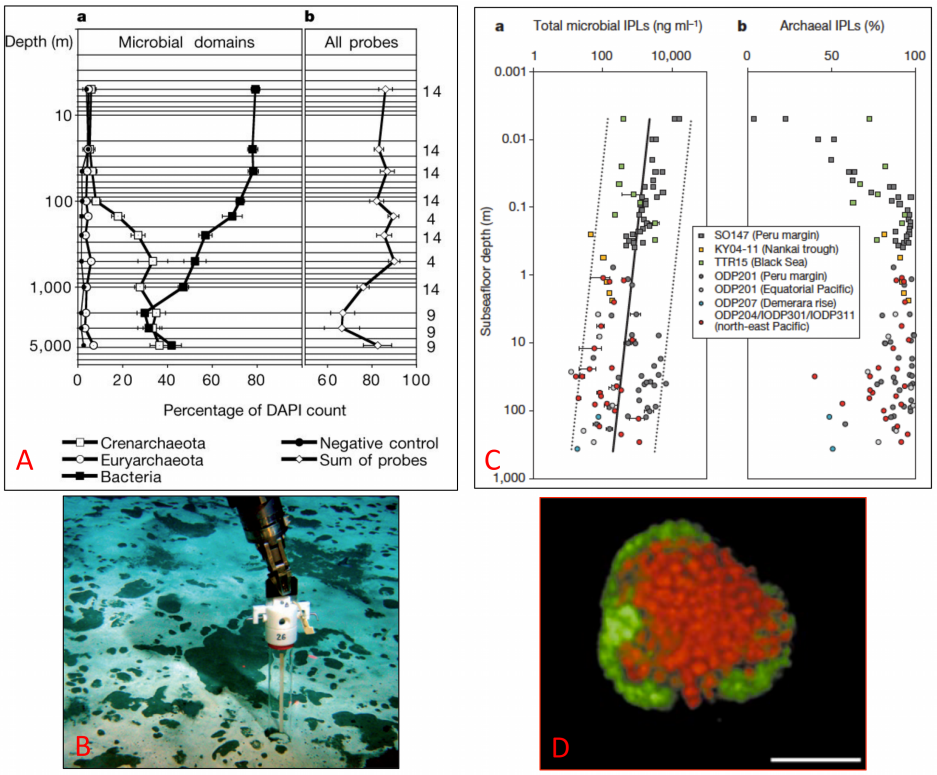

Figure 1.8. Marine microbial ecology. (A) [a] Mean annual water depth profiles of crenarchaeota, euryarchaeota and bacteria in the North Pacific. Numbers on x-axis represent percentage of total abundance (using the DAPI nucleic acid stain). [b] Corresponding depth profile of total bacteria, crenarchaeota and euryarchaeota. (Karner et al., 2001); (B) Remotely operated vehicle (ROV) sampling a deep sea bacterial mat, Haakon Mosby Mud Volcano (IFREMER, France); (C) [a] Subseafloor depth profiles of total intact polar lipids (IPLs) from a number of locations and [b] relative contribution of archaeal IPLs to total IPLs (Lipp et al., 2008); (D) Fluorescent in-situ hybridisation identification of an archaea (red)/sulfate-reducing bacteria (green) aggregate apparently mediating anaerobic oxidation of methane (AOM). (Boetius et al., 2000).

Prokaryotes are typically classified based on their metabolic diversity. Chemoorganotrophs obtain energy from the aerobic or anaerobic oxidation of organic compounds and storage of this energy in the energy-rich bonds of adenosine triphosphate. Some of these are strict (obligate) aerobes/anaerobes while others are facultative. Chemolithotrophs on the other hand oxidise inorganic compounds such as H_2, H_2S, NH_3 and Fe^{2+}. In contrast to chemotrophs, phototrophs convert light to energy by photosynthesis, with (oxygenic photosynthesis) or without (anoxygenic photosynthesis) the production of O_2. Furthermore microbes can be divided based on their requirement for carbon – heterotrophs, which obtain C from organic compounds, and autotrophs use CO_2 as their C source (Madigan et al., 2012).

The bacteria domain hosts an enormous variety of genera and species, with a considerable morphological and metabolic diversity. Proteobacteria is currently the largest phylum is and is sub-divided into Alpha-, Beta-, Delta-, Gamma-, Epsilon- and Zeta- classes. The Gram-positive phylum of bacteria includes *Bacillus, Clostridium, Streptomyces, Lactobacillus and Streptococcus*. The Cyanobacteria are phylogenetic relatives of the gram-positive bacteria and are oxygenic phototrophs. Two other major phyla are the green sulfur bacteria and the green nonsulfur bacteria. Species in these phyla are autotrophic. Other major bacterial phyla include the *Chlamydiae*, the *Deinococcus-Thermus*, the *Flavobacteria,* the *Thermatoga,* the *Thermodesulfobacterium* and the *Aquifex* groups. The proteobacteria appear to dominate the marine sedimentary environment in many cases. In deep gas hydrate-bearing sediments in the Cascadia margin, proteobacteria comprised 96% of all bacterial clones (Marchesi et al., 2001). Most marine bacterial groups described by culture-independent methods have not been cultured in the laboratory. Among those cultured the most common are alphaproteobacteria within the Roseobacter lineage. They occur in samples ranging from plankton, sediments, sea ice to animal surfaces and typically comprise 20% of communities in coastal waters, 15% in mixed layer ocean communities and less than 1% in waters deeper than a few hundred metres (Fuhrman and Hagström, 2008). In many cases the Gammaproteobacteria have been cultured and include members of the *Vibro, Alteromonas, Pseudoalteromonas, Marinomonas, Shewanella, Glacieola, Oceanospirillum* and *Colwellia* sp. These cultured bacteria have shown a tendency for rapid potential growth rates, display a large versatility for inorganic electron acceptors and are seemingly well suited to

feast-and-famine lifestyles (Fuhrman and Hagström, 2008). The Betaproteobacteria are a large group (perhaps 75 genera) of heterogenous and primarily uncultured bacteria, which appear to have diverse metabolic capabilities (Madigan et al., 2012).

Archaea are traditionally thought to exist in extreme environments such as hypersaline brines, geothermal environments and highly anoxic settings. However they are now known to be ubiquitous, including in aerobic marine and terrestrial habitats (DeLong and Pace, 2001). While marine subsurface archaea are now thought to be the most dominant microbial domain of the deep marine subsurface, they consist almost exclusively of uncultured, distinct phylogenetic lineages that have only been discovered in recent years (Vetriani et al., 1999). Based on molecular approaches marine sedimentary archaea have been divided into a number of lineages. Archaea can be divided into three major phyla – the Crenarchaeota, the Euryarchaeota and the recently classified Thaumarchaeota. The Nanoarchaeota and Korarchaeota are two other tentative phyla in the marine environment the Marine Benthic Group B (MBG-B), proposed by Vetriani et al. (1999), represents one of the most dominant archaeal lineages in 16s rRNA archaeal clone libraries. This group is synonymous with another group, called the Deep-Sea Archaeal Group (DAG), which was proposed by Inagaki et al. (2003). DSAG/MBG-B archaea have been detected and shown to be metabolically active in a wide variety of anoxic marine environments including methane-consuming Black Sea microbial mats and carbonate reefs (Knittel et al., 2005), surficial methane seeps in the Gulf of Mexico (Llyod et al., 2006), deep-sea sediments from the Okhotsk Sea (Inagaki et al., 2003), hydrate-bearing sediments of the Pacific Margin and in the Nankai Trough (Inagaki et al., 2006), organic-poor subsurface sediments from the Equatorial Pacific (Sørensen et al., 2004) and in diverse hydrothermal vent sites (Takai and Horikoshi, 1999). The Ancient Archaeal Group (AAG) and the Marine Hydrothermal Vent Group (MHVG) are two recently described groups, which currently have only been detected in a few studies. They appear to share the vent and subsurface habitat with the DSAG/MBG-B group. These groups were originally detected in hydrothermal vent sites near Japan (Takai and Horikoshi, 1999) but have since been described in cold, organic-rich Peru Margin subsurface sediments at ODP site 1227 (Sørensen and Teske, 2006).

The Miscellaneous Crenarchaeotic Group (MCG) is one of the most predominant groups in archaeal 16S rRNA clone libraries from marine deep subsurface sediments, and is known to be metabolically active. In contrast to the DSAG/MBG-B group, the MCG archaea have a more diverse habitat range that includes terrestrial and marine, hot and cold, surface and subsurface environments (Teske and Sørensen, 2008). Due to the rapidly increasing number of MCG clones from different environments this group has been sub-divided into numerous subgroups, which will not be discussed here (see Teske and Sørensen 2008, and references therein). The Marine Group I (MG-I) archaea account for a major fraction of all prokaryotic picoplankton in seawater (Karner et al., 2001), but are also known to exist in the subsurface at organic-poor open ocean sites in the Equatorial Pacific (Teske 2006) and in the Peru Margin (Sørensen et al., 2004). Some members of this group have been cultured and indicate that at least some of this group are aerobic, chemolithoautotrophic, nitrifying archaea that oxidise ammonia to nitrite (Teske and Sørensen, 2008).

The South African Goldmine Euryarchaeotal Group (SAGMEG) was originally described in the deep terrestrial subsurface in South African Gold mines (Takai et al., 2001), but were subsequently found in deep marine hydrate-bearing sediments (Reed et al., 2002), in marine subsurface sediments in the Sea of Okhotsk (Inagaki et al., 2003), and in marine sediments on the Peru Margin (Inagaki et al., 2006). Other groups including the Marine Benthic Groups A and D (MBG-A and MBG-D) are crenarchaeotal groups, the Terrestrial Miscellaneous Euryarchaeotal Group (TMEG) and the Miscellaneous Eurarcharotic Group (MEG) (previously known as Deep-Sea Hydrothermal Vent Euryarchaeotal Group 6) (Teske and Sørensen, 2008). Only three groups of microbes of limited diversity regulate global methane fluxes – aerobic methanotrophic bacteria, the methanogenic archaea and their close relatives, the anaerobic methanotrophic archaea (ANME). ANME represent a specialist Euryarchaeal lineage capable of AOM. ANME are discussed in further detail in section 1.4.2.2.

1.4 Seabed fluid flow

Seabed fluid flow is of fundamental importance to the geological, chemical and biological composition of the marine environment and also the composition of the atmosphere (Judd and Hovland, 2007). It is the upward transport of fluid that facilitates the formation of dramatic seabed and sub-seabed structures and also provides the ultimate carbon and/or energy source for microbes and upper trophic levels. Seabed fluid flow can be divided into hydrothermal vent systems and cold seeps. At hydrothermal vents highly reduced inorganic and organic compounds are produced by magmatic degassing and subsurface – rock reactions at temperatures of ~ 1000^{o}C. When this hot electron-donor-rich fluid is vented and meets electron-acceptor-rich seawater the energy becomes available for chemolithotrophic microbial primary producers. Dissolved material also precipitates, primarily as metal sulfides, to form the characteristic 'black smokers' (Jørgensen and Boetius, 2007). In contrast seepage fluids at cold seep settings include gas, hydrocarbons, pore water or groundwater. Cold seep fluid flow features are diverse and include trenches, mud volcanoes, mud diapirs, pockmarks, seabed domes, and methane-derived authigenic carbonate (MDAC) mounds and pavements (Judd and Hovland 2007). The focus of this review shall be on pockmarks.

Gas is by far the most common reported seepage fluid, which is broadly divided into microbial gas (MG) (also called biogenic gas) and thermogenic gas (TG) (Judd and Hovland, 2007). MG is primarily composed of CH_4 and is produced by the recycling of OM by microbial degradation (see section 1.3 above). MG is generally produced in shallow sedimentary layers (less than 1000 mbsf). On the other hand TG is composed of CH_4 and C_2 - C_4 hydrocarbons, and is formed much deeper in the sedimentary column (generally greater than 1000 mbsf) under conditions of high temperature and pressure. TG is generally isotopically heavier than MG, whereby CH_4 in MG generally has $\delta^{13}C$ (see section 1.5). values in the range of -60 to -80 ‰ and in TG ranges from -20 to -60 ‰ (Floodgate and Judd, 1992). $\delta^{13}C$ values ranges can vary considerably and during migration in the sedimentary column TG may be subjected to microbial activity, which would give a mixed $\delta^{13}C$ signal and hinder identification of the source of gas. Gas hydrates are also a significant potential source of subseabed fluid (Judd and Hovland, 2007). Under conditions of sufficient low temperatures and high pressures extensive deposits of gas hydrates exist, which are

composed of CH_4 molecules entrapped in a solid ice-like cage of water molecules. Changes in temperature and/or pressure or other disturbances may release significant quantities of CH_4 to shallow sediments and overlying waters (Kvenvolden, 1995; Buffett, 2000; Buffett and Archer, 2004; Hester and Brewer, 2009).

Gas seepage sources can also be differentiated based on the methane-to-higher-hydrocarbon ratio as shown in Equation 1.10.

$$C_{2+} = \left[1 - \left(\frac{C_1}{\sum C_{1-5}}\right)\right] x100$$

Eqn. 1.10

where C_1 is methane and ΣC_{2-5} is the sum of ethane, propane, butane and pentane. Ratios of 0.05% or less are characteristic of biogenic gas, while for dry and wet thermogenic gas ratios are less than 5% (mostly less than 1%) and greater than 5% respectively. Combination of Eqn. 1.10 with $\delta^{13}C$ and $\delta^{2}D$ provide the most comprehensive approach for characterising gas origins (Floodgate and Judd, 1992).

1.4.1 Evidence of shallow gas in the marine sediments and the water column

Evidence of shallow gas in marine sediments can be acquired remotely using a variety of geophysical (seismic) methods and also by direct sampling and geochemical analysis of sediment. Indirect evidence of the presence, present and/or past, of gas in sediments is provided by seepage-related structures, which include seafloor topographic depressions known as pockmarks and also topographic highs such mud diapirs and mud volcanos (see section 1.4.4). Other associated phenomena such as methane-derived authigenic carbonates (see section 1.4.3) and specific biological communities also provide an insight into seepage activity (Judd and Hovland, 2007) (see section 1.4.2.1). Seismic profiles of the sub-seabed are obtained by reflecting an acoustic pulse off of the seabed and sub-seabed layers (e.g. bedrock, sediment strata). This signal is received by a hydrophone array and processed to give a plot of georeferenced time on the *X*-axis and pulse two-way travel time on the *Y*-axis. In practice there is trade-off between depth of penetration and resolution, whereby high-frequency seismic systems (e.g. boomers and pingers) achieve resolutions of 1 metre or less but have limited penetration (generally much less than 50 m). Low-frequency

systems (e.g. airguns) have limited resolution but may achieve penetration depths of several kilometers. Echosounders operate on very high frequencies (~ 30 to 200 kHz) and are utilised for medium- to high-resolution seafloor mapping, while side scan sonars (60 to 400 kHz) are of particular use for identifying specific changes in seabed sediment type and fine scale topography. On seismic reflection profiles shallow gas may take the following forms:

Acoustic turbidity (AT): AT appears as chaotic reflections caused by scattering of acoustic energy. It generally removes all other structural information and appears as a smear on the record. As little as 1% gas presence may cause AT.

Enhanced reflections (ER): ER are coherent reflections that have increased amplitudes for part of their extent. ER often extend laterally from zones of AT.

Columnar disturbances (CD): CD (also referred to as gas chimneys) are distinct vertical features in which the normal seismic reflection sequence has been disturbed or destroyed by upward migrations of fluid.

Acoustic Blanking (AB): AB is zones of faint or absent seismic record, inferred as being caused by the presence of gas. This is thought to be due to disruption of sediment layering by fluid migration or by the absorption of acoustic energy in overlying gas-charged sediments.

Bright spots: High amplitude negative phase reflections in digital seismic data

For example, Fig. 1.9A shows a boomer profile at the Witch's Hole Pockmark in the North Sea (Judd and Hovland, 2007). The crater-like depression can be distinguished as well as numerous acoustic signatures such as areas of ER and AT, indicating shallow gas accumulations. Fig. 1.9B shows a multibeam echosounder bathymetry map from the Witch's Ground Basin, North Sea and highlights the extensive distribution and variety of sizes and morphologies that pockmarks (see section 1.4.2 below) can exhibit.

Water column seepage is generally classified as either macro- or micro-seepage, and can be assessed indirectly using acoustic techniques. Direct investigation by video ground-truthing using ROVs, underwater towed video (UWTV) systems, manned submersible or SCUBA diving, as well as direct sampling and geochemical analysis of the water column is also frequently employed. Macro-seepages are those that are large enough to be visible during video ground-truthing while micro-seepages are those that present as micro-bubbles or as dissolved gas. Micro-seepage may also be visualised as shimmering in the water column. Gas plumes may be detected on echosounder, side scan sonar and other high resolution seismic records, whereby plumes typically appear as darker targets similar to fish shoals (Judd and Hovland 2007).

1.4.2. Pockmarks

Pockmarks are seabed craters or depressions, which were first described in 1970 on the Scotian Shelf (King and MacLean, 1970). Since this initial discovery they have been described in a variety of settings and are now known to be globally ubiquitous. Pockmarks exhibit a variety of sizes and morphologies, as illustrated in Fig. 1.9 (A to C) and Fig. 10. Although pockmark size and depth can cover several orders of magnitude, they typically range in size and depth from 5 to 200 m and 0.5 to 20 m respectively. So-called ‘mega’ pockmarks exceeding these typical values have also been described (Kelley et al., 1994; Ondréas et al., 2005; Pilcher and Argent, 2007. A number of characteristic morphologies or pockmark types have been described to date:

Unit pockmarks are small uniform depressions, which range in size from about 1 to 10 m diameter and about 0.5 m in depth;

Normal pockmarks are larger circular craters ranging from 10 to 700 m diameter and 1 to 45 m deep. They exhibit varying angles of slope;

Elongated pockmarks have one axis much longer than the other and occur more commonly in areas influenced by strong bottom currents;

Eyed pockmarks have acoustically reflective material in its centre (coarse winnowed material, shell material or authigenic carbonates);

Strings or *trains* of pockmarks consist of numerous unit pockmarks showing curvilinear patterns or chains that may be kilometers in length and are often associated with fault patterns;

Complex pockmarks are clusters or amalgamations of pockmarks.

(Hovland and Judd, 1988; Judd and Hovland, 2007)

Furthermore the surface expression within the pockmark depression can be quite varied, and include cone-shaped and flat-bottomed surfaces. An underwater video still image from a ROV of a small (~ 2 m diameter) unit pockmark from the Central Nile deep sea fan is shown in Fig. 1.9C (Bayon et al., 2009). Reduced grey/black sediments occur within the crater as well as significant deposits of methane-derived authigenic carbonate (MDAC), thus indicating significant current or recent seepage.

The importance of pockmarks has been highlighted from a number of perspectives. As will be discussed in section 1.4.2.2 pockmarks and cold seeps in general have been shown to support distinct biological assemblages. The lack of knowledge regarding marine CH_4 cycling and its importance for climate changes and ocean and atmospheric chemistry has already been discussed (section 1.2). It is cold seeps settings, which have the greatest potential to impact local, regional and even global ocean chemistry and climate (Judd, 2003). Furthermore a link between pockmark occurrence and activity and the incidence of earthquakes and occurrence of petroleum deposits has been proposed (Hovland, et al., 2002). Thus the potential economic and commercial importance of pockmarks in relation to petroleum and gas prospecting and marine industrial cannot be underestimated (Judd and Hovland, 2007).

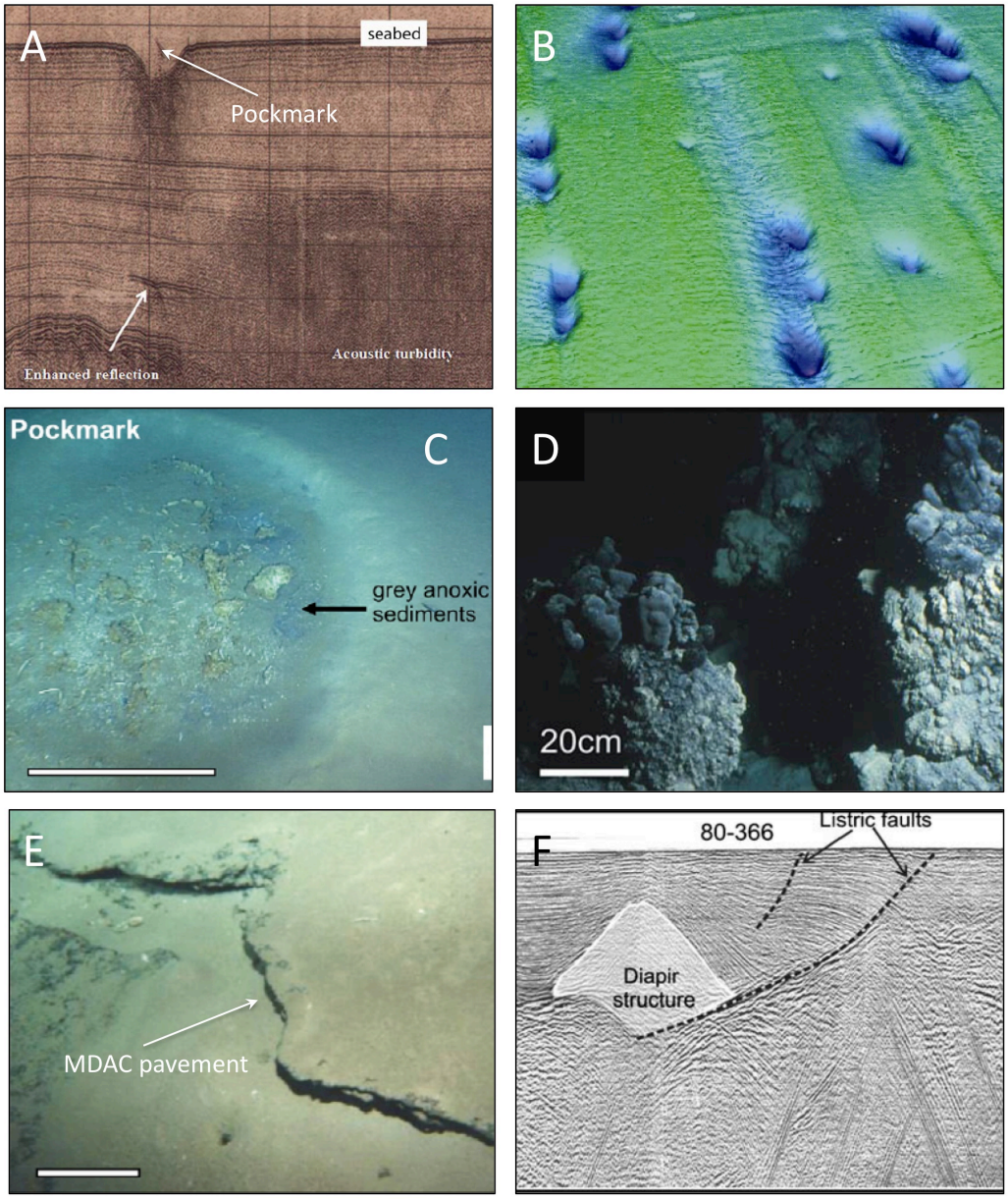

Figure 1.9. Marine seabed seepage features. (A) Boomer seismic profile across the Witch's Hole pockmark, North Sea, showing various seismic signals of gas accumulations (Judd and Hovland, 2007). (B) Multibeam echosounder (MBES) bathymetric map showing numerous pockmarks, Witch Ground Basin, North Sea (Judd and Hovland, 2007). (C) Underwater still image of a 3 m diameter unit pockmark in the Central Nile deep sea fan, containing anoxic sediment, authigenic carbonates and vestimentiferan tubeworms. The scale bar represents 1m. (Bayon et al., 2009) (D) Underwater image of methane-derived authigenic carbonate (MDAC) mounds, Black Sea (Reitner et al., 2005) (E) Underwater image of massive MDAC pavement, Central Nile deep sea fan (Bayon et al., 2009). The scale bar represents 1m. (F) Seismic profile showing a mud diapir (highlighted) in the Gulf of Cadiz, associated with Listric faults (Fernandez-Puga et al., 2007).

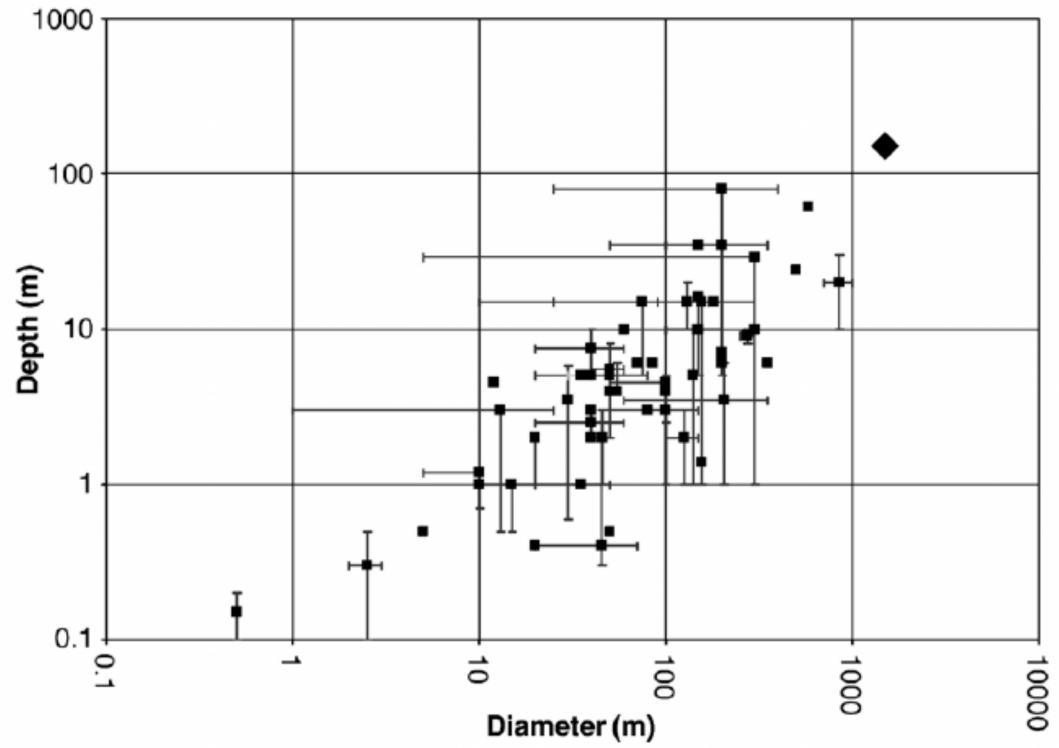

Figure 1.10. Plot illustrating the range of sizes and depth of pockmarks from 57 published locations globally (after Pilcher et al., 2007). Note the X and Y scales are logarithmic. The large diamond represents so-called 'mega' pockmarks as described by Pilcher et al. (2007). Single points represent the measured value for a single described pockmark or an average value for pockmarks within a field. Error bars represent the range in sizes within a particular pockmark field. The mean diameter and depth is 128 m and 9.5 m, respectively. Source data was obtained from Carvalho 2003; Dimitrov and Woodside 2003; Fader 1991; Games 2001; Hasiotis et al., 2002; Haskell et al., 1997, 1999; Hovland 1982, 1991, 1992, 2003; Hovland et al., 1987; Hovland and Judd 1988; Kelley et al., 1994; Maestro et al., 2002; Mosher et al., 2004; Pickrill 2006; Rise et al., 1999; Schroot and Schuttenhelm, 2003; Söderberg et al., 1992; and Soter 1999.

A summary of the geographical distribution of selected published pockmarks/pockmark fields is given in Table 1.2. Areas of extensive pockmark occurrence include the North Sea, the coasts and bays in proximity to Maine, offshore Greece and off the Norwegian coast. Undoubtedly these published occurrences reflect only a small proportion of total pockmarks.

Table 1.2. Geographic location and settings for selected known published pockmarks.

Location		Reference
NW Atlantic	Canadian Continental Shelf	Fader (1991)
	Scotian Shelf	King (1970), Mosher (2004)
	Belfast Bay & Gulf of Maine	Kelley (1994), Ussler (2003), Rogers (2006), Brothers (2011, 2012)
	Bering Shelf	Nelson (1979)
	St. Lawrence Estuary	Pinet (2008, 2010), Lavoie (2010)
	US Mid-Atlantic Shelf Break	Driscoll (2000), Hill (2004), Newman (2008)
NE Atlantic	Nyegga, Storegga Slide	Hovland (2005), Chen (2010)
	Gulf of Cadiz	Baraza and Ercilla (1996)
	San Simon Bay, NW Spain	Iglesias and Garcia-Gil (2007)
	Ebro Delta, Spain	Maestro (2002)
	Malin Shelf, NW Ireland	Szpak (2012)
	Porcupine Basin, NE Atlantic	Games (2001)
Mediterranean Sea	Patras & Corinth Gulf, Greece	Hasiotis (1996, 200), Soter (1999), Christodoulou (2003)
	Ibiza Channel	Acosta (2001)
	Central Nile Deep Sea fan	Bayon (2009)
	Eivissa Channel	Lastras (2004, 2006)
SE Atlantic	Lower Congo Basin, Gulf of Guinea	Gay (2003, 2006a,b, 2007), Olu-Le Roy (2007), Ondreas (200), Pilcher (2007), Sahling (2008)
SW Atlantic	Santos Basin, Brazilian Slope	Sumida (2004)
North Sea/Norway	Skaggerak	Hovland (1991), Rise (1999)
	Offshore Norway	Hovland (1987)
	Offshore Netherlands	Schroot and Schuttenhelm (2003)
	Moray Firth Basin	Cole (2000)
	Witch Ground Basin	Judd (1994)
	Oslofjord, Norway	Webb (2009), Hammer and Webb (2010)
	Norwegian Sea	Plassen and Vorren (2003), Mazzini (2006)
Pacific	Sur Basin, California	Paull (2002)
	South China Sea	Platt (1977), Sun (2011)
	Lake Rotoiti, New Zealand	Pickrill (1993)
Black Sea	Turkish Shelf	Cifci (2003)
	Fram Strait, Greenland Sea	Vogt (1994)
Barents Sea	Goliat hydrocarbon field	Chand (2009)
Arabian Sea	Western Indian Continental Margin	Karisiddaiah and Veerayya (2002)

1.4.2.1 Pockmark formation mechanisms

The leading theory for pockmark formation was first proposed by (Hovland and Judd, 1988) and is illustrated in Fig. 1.11. The major steps in pockmark formation, according to this theory are:

1) Gas generated at depth migrates through sediment in pores or along fissures and accumulates in porous layers below silty top layers of relative impermeability;

2) Pressure increases over time in these gas reservoirs leading to seabed doming;

3) This dome structure fails causing fractures and faults and a release of pressure;

4) This rapid pressure induces gas flow into the water column and expulsion of surrounding sediment matrix, forming a crater;

5) Finally settling and dispersal of sediment particles according to grain size by currents occurs.

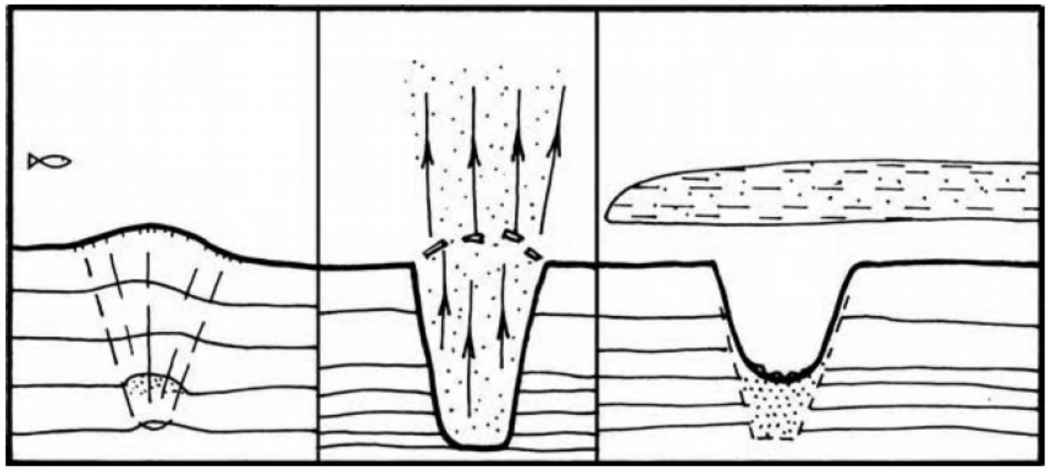

Figure 1.11. Conceptual model for pockmark formation. Pressure builds up in a shallow porous layer below an impermeable fine-grained sealing layer. This pressure is relieved by seabed doming (first panel). Eventually pore fluid pressure causes the sediment to yield, causing a rapid expulsion and fluidisation of the sediment matrix. Gas, water and sediment are expelled into the water column (second panel). Fine-grained sediments are suspended in the water column and transported by currents, while coarse material may deposit in or near the formed crater (after Hovland and Judd, 1988).

However other mechanisms for their formation have also been proposed such as gas hydrate escape (Hovland and Svensen, 2005;Vaular et al., 2010) pore water escape (Harrington, 1985), fresh/groundwater seepage (Whiticar, 2002; Christodoulou et al., 2003), ice-rafting (Paull et al., 1999), biological activity and meteorite impacts (Judd and Hovland 2007). The clearly diverse distribution (Table 1.2), sizes, morphologies (Fig. 1.10) and apparent ranges of seepage activity of known pockmarks likely reflect a variety of possible formation mechanisms and temporal activity. Frequently, surveyed pockmarks are not associated with evidence (be that geophysical and/or geochemical) of fluid migration and suggests that they either are inactive or that another formation mechanism may be possible (Paull et al., 2002; Ussler et al., 2003; Rogers et al., 2006). Thus there remains many questions as to how pockmarks are formed, become active and what factors control their temporal activity.

1.4.2.2 Pockmarks and biological productivity

Despite their ubiquitous occurrence, relatively little is known about the relationship between pockmarks and benthic biological diversity. Various reports have suggested that distinct biological assemblages and/or productivity may be associated with pockmarks. As outlined by Dando (2001) biodiversity and biomass may be expected to vary at pockmarks in relation to the surrounding seafloor by two factors:

1) Reduced bottom current flow and enhanced sedimentation within a pockmark due to the depression

2) Changes in sediment type, cementation, substrate and electron acceptor availability (e.g. H_2S and CH_4) as a result of current or past seepage (as discussed above)

Active cold seeps, with a significant supply of CH_4 may lead to dense microbial communities with high metabolic rates. With sufficient CH_4 supply, AOM facilitates the formation of MDAC and high concentrations of H_2S in pore waters (See section 1.12). The availability of high concentrations of CH_4, H_2S, and a hard substrate provides the basis for complex distinct ecosystems at these sites (Levin, 2005). Megafuanl diversity at cold seeps has recieved considerable attention (Sibuet and Olu, 1998; Tunnicliffe et al., 2003; Levin, 2005; Judd and Hovland, 2007; Cordes et al.,

2009). Megafaunal biomass at cold seeps in deep settings (> 500 m) generally far exceeds that of surrounding sediments and is dominated by bivalves such as mytilids, vesicomyids, lucinids and thyasirids, and vestimentiferan tube worms. Pogonophorans, cladorhizid sponges, gastropods and shrimp are also sometimes abundant. In many cases overall diversity may be reduced within a seep compared to surrounding environments (Levin 2005). In contrast to deep sea sites, macrofaunal biomass in coastal, shelf and upper slope cold seeps tend to differ little compared to surrounding sediments. This phenomenon is likely related to increased contribution photosynthesis and detrital OM and hence chemoautotrophy may be insignificant (Judd and Hovland, 2007, and references therein).

Active methane seeps have received significant attention from biogeochemists and geomicrobiologists over the past few years (Valentine and Reeburgh, 2000; Hinrichs and Boetius, 2002; Valentine, 2002, 2011; Caldwell et al., 2008; Knittel and Boetius, 2009). Microbial populations at active seeps are often dominated by groups involved in the AOM. AOM controls the atmospheric CH_4 efflux from oceans. In diffusive seabed settings this CH_4 is consumed within the SMTZ while at cold seeps and other gassy settings a significant fraction may escape into the water column (Valentine, 2000; Knittel and Boetius, 2009). AOM is carried out by at least three groups of archaea, belonging to the anaerobic methanotroph (ANME) lineage – the ANME-1, the ANME-2 and the ANME-3. ANME have been shown to exist in synthrophic consortia with sulfate-reducing bacteria in the *Desulfosarcina/Desulfococcus* and *Desulfobulba* genera. The overall reaction for AOM via reduction of SO_4^{2-} is illustrated in Fig. 1.12. However the exact nature of this association is poorly understood (Valentine, 2000; Knittel and Boetius, 2009). In addition, recent evidence has shown that a variety of other electron acceptors and synthrophic bacteria may be involved in AOM (Pernthalet et al., 2008; Beal et al., 2009) and that ANME may even be capable of mediating AOM without a partner (Milucka et al., 2012). It is also evident that there is considerable horizontal and vertical spatial variation in prokaryotic abundance and diversity at active cold seeps.

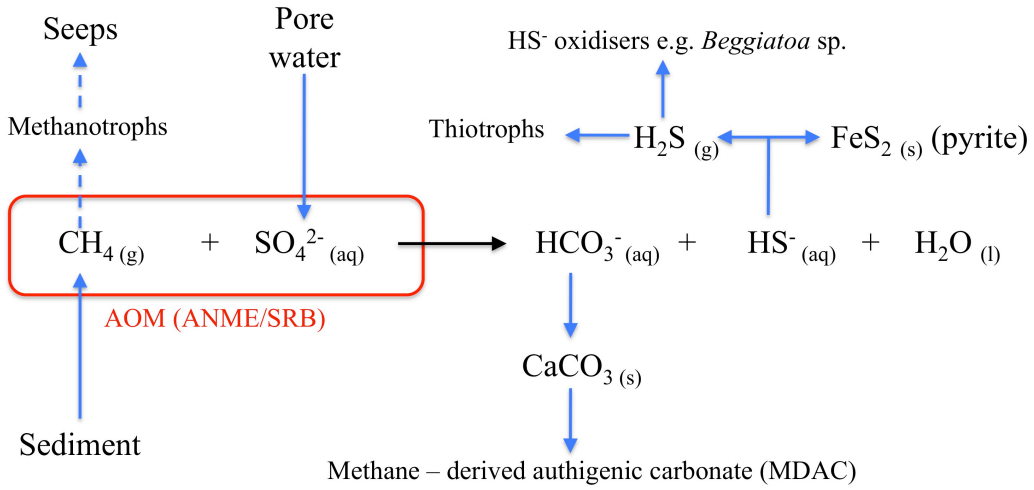

Figure 1.12. Anaerobic oxidation of methane (AOM) via reduction of SO_4^{2-}. This process forms the basis for complex cold seep ecosystems that utilise seeping CH_4 and produced H_2S and hard methane-derived carbonate.

Regarding pockmarks, however, evidence of increased biological productivity and distinct macrofaunal diversity is inconclusive (Judd and Hovland, 2007). Studies of microbial diversity within pockmarks are relatively rare. Previous research indicates that archaea and bacteria involved in AOM are significant in pockmarks with moderate-to-high CH_4 flux. Wegener et al. (2008) investigated biogeochemical processes and microbial diversity at pockmarks in the North Sea. ANME-2 were the most abundant archaea at the active Gullfaks and Tommeliten pockmarks while sulphur-oxidising and SRB were the most abundant bacteria. Shubenkova et al. (2010) analysed the microbial community structure of reduced pockmark sediments from 0 to 0.36 mbsf in the Gdansk Deep, Baltic Sea. They found three archaeal phylotypes, one belonging to the ANME-1 taxon while the other two were closely related to uncultured methanogens. Bacterial phylotypes were complex and included members of the *Proteobacteria*, *Chloroflexi*, *Firmicutes*, *Plantomycetales* and high G+C gram positive phyla. Archaea were more abundant than bacteria below 0.1 mbsf. Merkel et al. (2010) investigated the archaea performing AOM by methyl Coenymze M reductase and arrived at similar conclusions to Shubenkova et al. (2010), whereby ANME-1 were dominant ANME group.

Roalkvam et al. (2011) recently investigated the microbial diversity at the active G11 pockmark at Nyegga and found that in shallow sediments (< 0.04 mbsf) and surface microbial mats aerobic methanotrophs within the *Gammaproteobacteria*

dominate as well as sulphur-oxidising *Sulfurovum* (Epsilonproteobacteria). Stratification in ANME groups was observed with depth in the order of ANME-2a/b, ANME-1 and ANME-2c. Previously described sulfate-reducing partners of ANME were low in all samples. In a follow-up study Roalkvam et al. (2012) compared the findings from within the active G11 pockmark site to surrounding sediment exhibiting lower CH_4 flux. They found ANME were again dominant and also exhibited similar trends downcore. However the transition between ANME populations occurred over a wider spatial region and at greater depth in the site of lower CH_4 flux. Total 16S rRNA copies numbers for ANME groups were also two orders of magnitude lower in the site of micro-seepage. They also observed that ANME-1 from both sites clustered into a single OTU while ANME-2a/b were distinct. They concluded that ANME-1 is the most abundant and important consumer of CH_4 across the Nyegga cold seep setting.

The giant (~ 800 m diameter) active REGAB pockmark was the subject of a recent combined geomicrobiological and organic geochemical study (Boulabassi et al., 2009; Cambon-Bonavita et al., 2009). They found aggregates of ANME-2 and *Desulfosarcina/Desulfococcus* sulfate-reducing bacterial partners in sediments from four different chemosynthetic communities. Archaeal diversity was limited to the ANME cluster while bacterial diversity was more complex with members of the Proteobacteria, Bacilliales, Cytophaga/Flavobacteria, Verrucomicrobia, JS1 and Actinobacteria clusters found. Based on the occurrence of ^{13}C-depleted bacterial diplotene and 4α-methylsterols Boulasbassi et al. (2009) also proposed that aerobic methanotrophy was also occurring. As discussed here most studies of pockmarks (and for cold seeps generally) have focused on sites of significant current seepage activity. However, most mapped pockmarks are in fact seemingly inactive (Judd and Hovland 2007). Thus, as outlined by Levin (2005), there are a number of important questions relating to biological productivity at pockmarks and other cold seeps environments that remain to be answered:

1) Do species life histories reflect temporal variation in seepage activity and associated reduced compounds?

2) How do species adapt with temporary cessation of flow, expulsion events or rapid elevation of H_2S concentrations?

3) Are there successional stages that mirror development, input and breakdown of fluid flow?

1.4.3 Methane derived authigenic carbonate, mud volcanos and mud diapirs

MDAC has been found in a variety of seabed environments and ranges from small nodules and concretions, to slabs and pavements, to dramatic mounds or chimney features, with relief of several tens of metres. Fig. 1.10D shows MDAC deposits on the Crimean Shelf in the Black Sea (Reitner et al., 2005), while Fig. 1.10E shows massive MDAC pavements in the Central Nile deep sea fan (Bayon et al., 2009). MDAC formation is direct result of AOM, as illustrated in Fig. 1.12. Thus microbes are the primary driver for the formation of these vast geological features. CH_4 is oxidised to HCO_3^-, which increases the pore water alkalinity and eventual saturation causes precipitation of solid $CaCO_3$, or MDAC. MDAC has received considerable attention from physical, chemical and biological perspectives (Jensen et al., 1992; Aloisi et al., 2002; Reitner et al. 2005; Bayon et al. 2009; Feng et al. 2010).

Mud volcanoes are seafloor edifices from which seabed fluid (mud, seawater, gas, hydrocarbons) flows or erupts (Judd and Hovland, 2007) and are globally ubiquitous (Milkov, 2000). Gas is the most commonly reported escaping fluid and these features are usually associated with high fluid flux. For example the Hakon Mosby mud volcano is characterised by very high flux rates of CH_4 whereby greater than 60% of annual flux escapes into the water column (Niemann et al., 2006). On the other hand mud diapirs (also called shale diapirs) are seabed features where fluid-charged clay or mud rises through sedimentary layers due to buoyancy effects. These structures can be tens to hundreds of metres in diameter and their size and morphology depends on the depth and size of the gas accumulation that triggers their formation (Judd and Hovland, 2007). In contrast to mud volcanoes, there may not be evidence of fluid flow and the term is generally applied to intrusive features i.e. ones that are only expressed in the subsurface. However, there is considerable crossover between these terms. Both mud volcanos and mud diapirs have been reported worldwide, often in areas of known hydrocarbon potential (Milkov, 2000). A sub-bottom acoustic profile showing a mud diapir associated with faults in the Gulf of Cadiz, is shown in Figure 1.10F. (Fernández-Puga et al., 2007).

1.5. Lipid biomarkers for marine organic matter

In identifying petroporyphryins, a geochemical class of compounds possessing a tetrapyrrole structure, in shales, bitumens and crude oils, Treibs (1934) can be considered the first to utilise the concept of molecular organic biomarkers. There are two principal criteria by which to measure the utility of an organic biomarker, namely source specificity and conservative behaviour. Source specificity refers to the link between the molecular marker under investigation and its putative source. Ideally this would be direct and specific, but in practice these criteria are met to varying degrees. In addition it is often the case that a proposed biomarker for a certain source becomes less and less source specific over time. Conservative behaviour refers to the requirement that a biomarker should retain a degree of the original information from the source molecule over the appropriate time scale of study. In other words a proposed biomarker should possess a degree of chemically recalcitrance in the environment in order to be of use. Again this criterion is rarely achieved completely since once introduced to the environment all molecules are subject to a complex array of physical, chemical and biological processes that may alter its spatial distribution, fate and chemical composition (Eganhouse, 1997).

Lipids meet many of the characteristics of the aforementioned criteria for a good biomarker, and in addition can be directly extracted and analysed from environmental samples, in particular as result of the development of gas chromatography-mass spectrometry. Thus, lipid biomarkers have been extensively utilised in studying organic matter cycling (Volkman, 2006, and references therein). The most commonly used definition for lipids is that they are a range of compounds that are soluble in organic solvents (Christie, 1982). This includes a diverse range of compounds such as fatty acids, steroids, acylglycerols, phospholipids, terpenes, carotenoids and fat-soluble vitamins. Lipids can be divided into two broad classes - simple or complex, or more commonly as neutral or polar. The structures for a range of common lipids of relevance as biomarkers are given in Fig. 1.13.

There are a number of means by which lipid biomarkers can impart useful information about a process under investigation. These include individual molecular structure, occurrence of molecular assemblages and also isotope compositions. Biosynthesis produces a diverse array of organic compounds with unique specific biological functions. However, due to the directed nature of biosynthesis, the number

of synthesised compounds that occur naturally are a fraction of the theoretical possibilities. Thus structural similarities between the source, contemporary biogenic biomarkers and fossil (relict) biomarkers provide information on precursor-product relationships. In addition structural differences and alteration may also be useful by reflecting post-depositional diagenetic processes (Eganhouse, 1997). In addition to specific molecular structures that occur due to biological synthesis and diagenesis, characteristic distributions of homologous series of compounds are often produced and may provide more powerful source and process-related information.

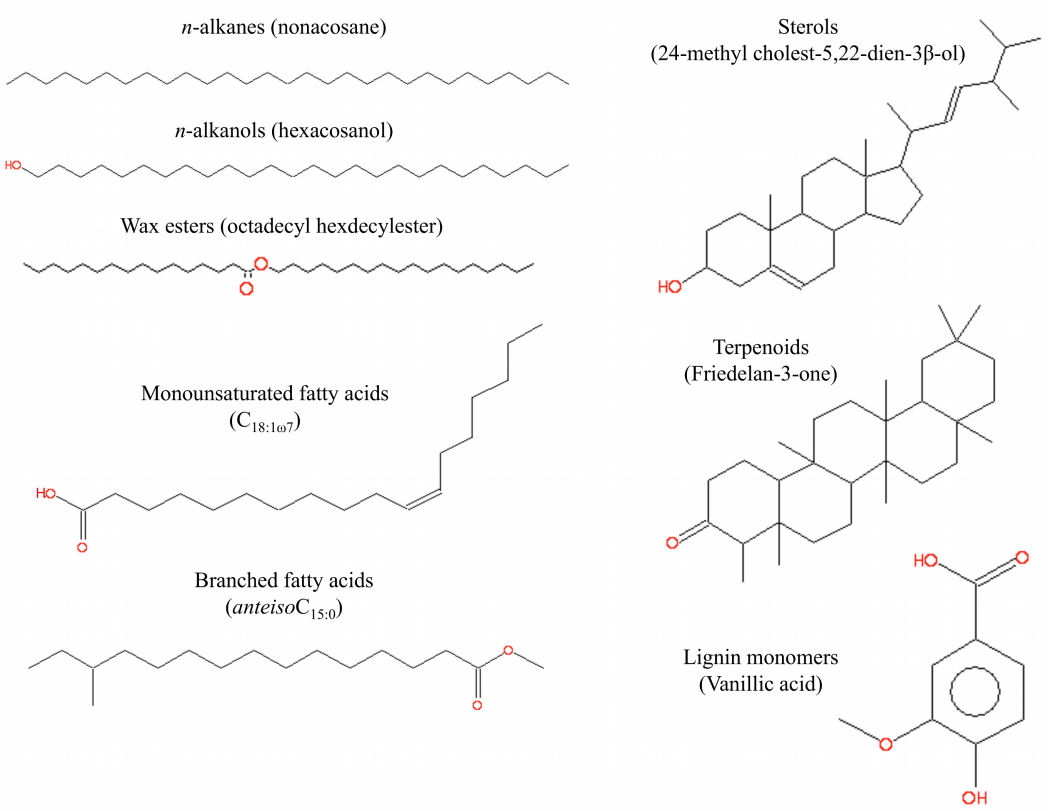

Figure 1.13. Structures of selected major lipid classes utilised as biomarkers to characterise marine organic matter (OM).

Over the past twenty years or so, the utility of lipid biomarkers has been augmented further by the advent of compound-specific stable isotope analysis, in particular for ^{13}C. Variations in the relative isotopic abundance are a consequence of the preferential reaction of once isotopic species over another, whereby in general the lighter isotope in favoured, and are calculated according to the following equation:

$$\delta^{13}C = \left[\frac{R_{sample} - R_{standard}}{R_{standard}} \right] \times 10^3$$

Eqn. 1.11

where values are reported in per mil (‰) *R* is the ratio of measured ^{13}C to ^{12}C and is measured relative to the Vienna PeeDee Belemnite (VPDB) standard (VPDB, $\delta^{13}C$ = 0‰, with $^{13}C/^{12}C$ = 0.0112372 absolute ratio) .

For example most primary producers (80 to 90% of land plants) incorporate carbon into their biomass via the Calvin (C_3) pathway. This pathway discriminates against incorporation of ^{13}C, resulting in a shift in $\delta^{13}C$ values of about -18 to -20‰ from the isotopic ratio of the inorganic carbon source. Thus OM produced by terrestrial plants utilising the C_3 pathway have typical $\delta^{13}C$ values of -27‰ ($CO_{2(g)}$ $\delta^{13}C$ ~ 7‰), while OM derived from water column phytoplankton have $\delta^{13}C$ values of around -20 ‰ (HCO_3^- $\delta^{13}C$ ~ 0‰). The isotopic fractionation during biosynthesis produces further fractionation of $\delta^{13}C$ for certain biomolecules from the $\delta^{13}C$ value of the bulk biomass. Lipids typically have the lightest $\delta^{13}C$ values, with $\delta^{13}C$ value depleted by 5 to 8 ‰ relative to bulk biomass (Hoefs, 2009). In addition within these biomolecules particular compounds classes may differ in their $\delta^{13}C$ values due to their specific biosynthetic pathways (Rullkütter, 2006).

Nevertheless $\delta^{13}C$ analysis of bulk and compound-specific OM has proved very useful in studying OM cycling in the environment. The commonly observed difference in $\delta^{13}C$ of ~7 ‰ between terrestrial OM and marine OM has been used to trace the origin of recent OM in coastal and shelf sediments (Westerhausen et al., 1993; Prahl et al., 1994). Compound-specific $\delta^{13}C$ analysis has also been particularly important in studying AOM in sedimentary environments. Microbial CH_4 is typically isotopically light, with $\delta^{13}C$ values in the range of -60 to -100 ‰. Methanotrophs using CH_4 as a carbon source have membrane lipids, which may be as light as -120‰. Studies combining molecular ecological analysis and compound-specific $\delta^{13}C$ analysis have successfully elucidated many of the process and key microbial players involved in AOM (Hinrichs and Boetius, 1999; Pancost et al., 2000; Orphan et al., 2001).

In modern marine biomarker research a multi-biomarker approach, together with extensive supporting information (e.g. oceanographic transport processes, water column nutrient chemistry, sediment accumulation rates, pore water geochemistry,

nucleic-acid based investigation of microbial diversity) and appropriate multivariate statistical treatment is required to obtain significant conclusions on marine processes (Yunker et al., 2005; Parkes et al., 2007; Schmidt et al., 2010). A summary of selected biomarkers commonly utilised for marine environments is given in Table 1.3. A discussion of these biomarkers is beyond the scope of this review and the reader is referred to comprehensive reviews by (Peters and Moldowan, 1993; White et al., 1997; Pancost and Boot, 2004; Peters et al., 2004; Volkman, 2006; Niemann and Elvert, 2008).

Table 1.3. Summary of major biomarker/biomarker classes used to characterise marine organic matter (OM).

Biomarker/Biomarker class	Primary Source	Original/Key reference
Hydrocarbons		
C_{25} to C_{35} odd *n*-alkanes	Epicuticular plant waxes	Eglinton and Hamilton (1967)
C_{17} to C_{21} alkanes	Phytoplankton, algae	Blumer et al. (1970, 1971), Volkman et al. (1998), Sinninghe-Damste et al. (1999)
$C_{17:1}$, $C_{19:1}$, $C_{21:5}$, $C_{21;6}$ alkenes	Phytoplankton	Blumer et al. (1970, 1971), Sinninghe-Damste et al. (1999)
Diplotene	Bacteria, terrestrial ferns	Rohmer et al. (1984), Venkatesan (1988), Elvert (2001)
$C_{37:2}$ Alkene	Cocclithophoridae e.g. *E. huxleyi*	Conte et al. (1994)
C_{25} & C_{30} highly branched isoprenoids	Diatoms, specifically *Rhizosolenia, Haslea, Navicula, Pleurosigma* genera	Belt et al. (1996, 2000, 2001), Massé et al. (2004)
Crocetane (& isomers)	Archaea	Tornabene et al. (1979), De Rosa & Gambacorta (1988)
Pentamethylicosane (& isomers)		
Phytadiene	Zooplankton (Phytol metabolism)	Avigan and Blumer (1968), Blumer et al. (1969)
Squalene		
Pristane		
Unresolved complex matrix	Petroleum	Peters and Moldowan (1993)
C_{29}/C_{30} steranes/hopanes		
Phytane		
Alkyl polyaromatic hydrocarbons		
Non-alkyl polyaromatic hydrocarbons	Combustion products	Jiang et al. (1998)
Fatty acids		
n-C_{14}-C_{16} SATFA	Nonspecific marine	Cranwell (1982)
n-C_{22}-C_{32} SATFA	Epicuticular plant waxes	Eglinton and Hamilton (1967)
$C_{16:1\omega5}$	Sulfate-reducing bacteria	Elvert (2003)
$C_{18:1\omega9}$	Zooplankton	Sargent (1976)
$C_{18:1\omega7}$	Bacteria	Cranwell (1982)
$C_{20:4}$, $C_{20:5}$	Fresh phytoplankton (diatoms)	Canuel and Martens (1993)
iso & *anteiso* $<C_{20}$ odd	Bacteria	Edlund et al. (1985)
10Me $C_{16:0}$	Sulfate-reducing bacteria	
cy$C_{17:0\omega5,6}$		Elvert (2003)
TriMe $C_{13:0}$	Zooplankton (Phytol metabolism)	Prahl et al. (1984), Rontani and Volkman (2003)
Trime C_{16}:0		
Terpenoids		
Friedelin	Higher plants	
β-amyrin	Higher plants	Brassell et al. (1983), Versteegh et al. (2004)
Taraxerol, lupeol	Higher plants, mangroves	
Alcohols		
C_{12} to C_{22} *n*-alkanols	Zooplankton, microalgae	Kattner and Krause (1989), Volkman et al. (1998)

C_{22} to C_{32} even *n*-alkanols	Epicuticular plant waxes	Eglington and Hamilton (1967)
Phytol	Chlorophyll-*a* side chain	Johns et al. (1980)
Dihydrophytol	Zooplankton (Phytol metabolism)	Prahl et al. (1984)
C_{28} to C_{30} Alkyl-diols	Eustigmatophytes	Volkman (1992), Volkman et al. (1999)
Mono-alkyl glyceryl ethers	Bacteria	Rütters et al. (2001)
Archaeol	Archaea	Koga et al. (1998)
sn-2-hydroxyarchaeol	Anaerobic methanotrophic archaea	Sprott et al. (1990), Hinrichs et al. (2000)
Glycerol dialkyl glycerol ethers (GDGTs)	Archaea	Hopmans et al. (2000), Schouten et al. (2012)
Non-isoprenoidal GDGTs		
Diploterol		
β,β-bishomohopanol	Bacteriohopanetetrol/aminobacteriohopanetriol degradation)	Rohmer et al. (1984); Innes et al. (1997)
β,β-homohopanol	Bacteriohopanepentol/aminobacteriohopanetetrol degradation	
	Aminobacteriohopanepentol	
Sterols		
$C_{26}\Delta^{5,22}$, $C_{26}\Delta^{22}$	Marine invertebrates, diatoms	Idler et al. (1970); Boutry et al. (1971)
$C_{27}\Delta^{5}$	Nonspecific marine (In high abundance – zooplankton)	
5β-$C_{27}\Delta^{0}$	Sewage	Hatcher and McGillivary (1979); Venkatesan and Mirsadeghi (1988)
$C_{27}\Delta^{5,22}$, $C_{28}\Delta^{5,22}$, $C_{28}\Delta^{5,22}$	Phytoplankton	Volkman et al. (1998)
$C_{28}\Delta^{5,24(28)}$	Diatoms	
$C_{28}\Delta^{5}$, $C_{29}\Delta^{5,22}$, $C_{29}\Delta^{5}$	Higher plants (also microalgae)	
$C_{30}\Delta^{22}$	Dinoflagellates	Boon et al. (1979)
Other		
C_{32} to C_{36} Wax esters	Zooplankton	Sargent et al. (1977), Boon and De Leeuw (1979), Burns et al. (2003)
$>C_{40}$ Wax esters	Higher plants	Cranwell and Volkman (1981)
$C_{37:2}$ & $C_{37:3}$ Alkenones	Cocclithophoridae e.g. *E. huxleyi*	Conte et al. (1994)
Vanillyl phenols	Woody gymnosperms	Hedges and Mann (1979)
Syringyl phenols	Woody angiosperms	
Cinnamyl phenols	Non-woody material	

1.6 Project Overview

Ireland's marine territory currently stands at approximately 10 times its land surface area, and as such the potential for exciting discoveries of scientific, economic and commercial importance are evident. The Irish National Seabed Survey (INSS), which ran from 1999 to 2005, and its successor, the Integrated Mapping for the Sustainable Development of Ireland's Marine Resource (INFOMAR) program has successfully mapped much of Ireland's offshore seabed. It is becoming increasingly evident that Ireland's seafloor environment is diverse, yet untapped from scientific and economic viewpoints. Seabed mapping has highlighted the existence of a number of seabed fluid (primarily gas) flow features in diverse settings. However, in contrast to British and North Sea waters, for example, knowledge regarding these phenomena in Irish waters is distinctly lacking. Recently mapped pockmarks in the Malin Sea and in Dunmanus Bay and carbonate mound features in the Irish Sea, are almost certainly a fraction of what has yet to be discovered. These recently mapped features remain to be ground-truthed in earnest and investigated from biological or geochemical perspectives. Thus, one of the objectives of this project was to investigate these features from a broad geochemical, geomicrobiological and geophysical perspective. Another goal of this project was to conduct broader studies of the major sources, transport and fate of organic matter in the Irish marine environment. The importance and potential of studying the sedimentary environment from a purely scientific or knowledge-building perspective is evident, but there is also of considerable potential commercial and economic value, in particular in terms of energy resources and novel biotechnological applications. This project involved geophysical and underwater video ground-truthing, geochemical techniques such gas and pore water analysis, lipid biomarker analysis and nuclear magnetic resonance, as well as culture-independent molecular ecological approaches such as denaturing gradient gel electrophoresis and phylogenetic analysis of clone libraries. As such it was a collaborative project involving Dublin City University (organic geochemistry), Queen's University Belfast (molecular microbial ecology), University of Toronto, Scarborough (nuclear magnetic resonance) and the Geological Survey of Ireland (geophysics). The research expeditions were funded by the Irish Marine Institute via the INFOMAR program and the PhD project was funded by the Irish Research Council for Science, Engineering and Technology (IRCSET).

1.7 References

Acosta, J., Muñoz, A., Herranz, P., Palomo, C., Ballesteros, M., Vaquero, M., et al., 2001. Pockmarks in the Ibiza Channel and western end of the Balearic Promontory (western Mediterranean) revealed by multibeam mapping. Geo-Marine Letters 21, 123-130.

Aloisi, G., Bouloubassi, I., Heijs, S.K., Pancost, R.D., Pierre, C., Sinninghe-Damsté, J.S., et al., 2002. CH_4-consuming microorganisms and the formation of carbonate crusts at cold seeps. Earth and Planetary Science Letters 203, 195-203.

Avigan, J., Blumer, M., 1968. On the origin of pristane in marine organisms. Journal of Lipid Research 9, 350-352.

Baldock, J.A., Masiello, C.A., Gélinas, Y., Hedges, J.I., 2004. Cycling and composition of organic matter in terrestrial and marine ecosystems. Marine Chemistry 92, 39-64.

Balkwill, D.L., Leach, F.R., Wilson, J.T., McNabb, J.F., White, D.C., 1988. Equivalence of microbial biomass measures based on membrane lipid and cell wall components, adenosine triphosphate, and direct counts in subsurface aquifer sediments. Microbial Ecology 16, 73-84.

Baraza, J., Ercilla, G., 1996. Gas-charged sediments and large pockmark-like features on the Gulf of Cadiz slope (SW Spain). Marine and Petroleum Geology 13, 253-261.

Barrett, S.M., Volkman, J.K., Dunstan, G.A., LeRoi, J.M., 1995. Sterols of 14 species of marine diatoms (Bacillariophyta). Journal of Phycology 31:360-369.

Bayon, G., Loncke, L., Dupré, S., Caprais, J.C., Ducassou, E., Duperron, S., et al., 2009. Multi-disciplinary investigation of fluid seepage on an unstable margin: The case of the Central Nile deep sea fan. Marine Geology 261, 92-104.

Beal, E.J., House, C.H., Orphan, V.J., 2009. Manganese-and iron-dependent marine methane oxidation. Science 325, 184-187.

Behrenfeld, M.J., Falkowski, P.G., 1997. A consumer's guide to phytoplankton primary productivity models. Limnology and Oceanography 42, 1479-1491.

Belt, S.T., Allard, W.G., Massé, G., Robert, J., Rowland, S.J., 2001. Structural characterisation of C30 highly branched isoprenoid alkenes (rhizenes) in the marine diatom Rhizosolenia setigera. Tetrahedron Letters 42, 5583-5585.

Belt, S.T., Allard, W.G., Massé, G., Robert, J., Rowland, S.J., 2000. Highly branched isoprenoids (HBIs): identification of the most common and abundant sedimentary isomers. Geochimica et Cosmochimica Acta 64, 3839-3851.

Belt, S.T., Cooke, D.A., Robert, J., Rowland, S., 1996. Structural characterisation of widespread polyunsaturated isoprenoid biomarkers: A C25 triene, tetraene and pentaene from the diatom *Haslea ostrearia simonsen*. Tetrahedron Letters 37, 4755-4758.

Benner, R., 2004. What happens to terrestrial organic matter in the ocean? Marine Chemistry 92, 307 – 310

Benner, R., Pakulski, J.D., McCarthy, M., Hedges, J.I., Hatcher, P.G., 1992. Bulk chemical characteristics of dissolved organic matter in the ocean. Science 255, 1561-1564.

Berner, R.A., 1981. A new geochemical classification of sedimentary environments. Journal of Sedimentary Research 51, 359-365.

Berner, R.A., 1980. Early diagenesis: A theoretical approach. Princeton University Press.

Biddle, J.F., Lipp, J.S., Lever, M.A., Lloyd, K.G., Sørensen, K.B., Anderson, R., et al. 2006. Heterotrophic Archaea dominate sedimentary subsurface ecosystems off Peru. Proceedings of the National Academy of Sciences U S A 103, 3846-3851.

Blumer, M., Guillard, R.R.L., Chase, T., 1971. Hydrocarbons of marine phytoplankton. Marine Biology 8, 183-189.

Blumer, M., Mullin, M.M., Guillard, R.R.L., 1970. A polyunsaturated hydrocarbon (3, 6, 9, 12, 15, 18-heneicosahexaene) in the marine food web. Marine Biology 6, 226-235.

Blumer, M., Robertson, J.C., Gordon, J.E., Sass, J., 1969. Phytol-derived C19 di- and triolefinic hydrocarbons in marine zooplankton and fishes. Biochemistry 8, 4067-4074.

Boon, J.J., de Leeuw, J.W., 1979. The analysis of wax esters, very long mid-chain ketones and sterol ethers isolated from Walvis Bay diatomaceous ooze. Marine Chemistry 7, 117-132.

Boon, J.J., Rijpstra, W.I.C., De Lange, F., De Leeuw, J.W., Yoshioka, M., Shimizu, Y., 1979. Black Sea sterol—a molecular fossil for dinoflagellate blooms. Nature 277, 125-127.

Borowski, W.S., Paull, C.K., Ussler, W., 1996. Marine pore-water sulfate profiles indicate in situ methane flux from underlying gas hydrate. Geology 24, 655-658.

Bouloubassi, I., Nabais, E., Pancost, R.D., Lorre, A., Taphanel, M.H., 2009. First biomarker evidence for methane oxidation at cold seeps in the Southeast Atlantic (REGAB pockmark). Deep Sea Research Part II 56, 2239-2247.

Boutry, J.L., Alcaide, A., Barbier, M., 1971. Sur la présence d'un sterol en C_{26} dans un plancton marin végétal. Comptes Rendus l'Academie des Sciences 272, 1022–1023.

Brassell, S.C., Eglinton, G., Marlowe, I.T., Pflaumann, U., Sarnthein, M., 1986. Molecular stratigraphy: a new tool for climatic assessment. Nature 320, 129-133.

Brassell, S.C., Eglinton, G., Maxwell, J.R., 1983. The geochemistry of terpenoids and steroids. Biochemical Society Transactions 11, 575-586.

Brothers, L.L., Kelley, J.T., Belknap, D.F., Barnhardt, W.A., Andrews, B.D., Legere, C., et al. 2012. Shallow stratigraphic control on pockmark distribution in north temperate estuaries. Marine Geology 329-331, 34-45

Brothers, L.L., Kelley, J.T., Belknap, D.F., Barnhardt, W.A., Andrews, B.D., Maynard, M.L., 2011. More than a century of bathymetric observations and present-day shallow sediment characterization in Belfast Bay, Maine, USA: implications for pockmark field longevity. Geo-Mar Letters 31, 237-248.

Buffett, B., Archer, D., 2004. Global inventory of methane clathrate: sensitivity to changes in the deep ocean. Earth Planetary Science Letters 227, 185-199.

Buffett, B.A., 2000. Clathrate hydrates. Annual Review of Earth and Planetary Science 28, 477-507.

Burns, K.A., Volkman, J.K., Cavanagh, J.-A., Brinkman, D., 2003. Lipids as biomarkers for carbon cycling on the Northwest Shelf of Australia: results from a sediment trap study. Marine Chemistry 80, 103-128.

Caldwell, S.L., Laidler, J.R., Brewer, E.A., Eberly, J.O., Sandborgh, S.C., Colwell, F.S., 2008. Anaerobic oxidation of methane: mechanisms, bioenergetics, and the ecology of associated microorganisms. Environmental Science and Technology 42, 6791-6799.

Cambon-Bonavita, M.A., Nadalig, T., Roussel, E., Delage, E., Duperron, S., Caprais, J.C., et al., 2009. Diversity and distribution of methane-oxidizing microbial

communities associated with different faunal assemblages in a giant pockmark of the Gabon continental margin. Deep Sea Research Part II 56, 2248-2258.

Canuel, E.A., Martens, C.S., 1993. Seasonal variations in the sources and alteration of organic matter associated with recently-deposited sediments. Organic Geochemistry 20, 563-577.

Carlson, C., Bates, N., Hansell, D., Steinberg, D., 2001. Carbon cycle. In: Steele JH, Thorpe SA, Turekian KK (Eds.). Encyclopedia of Ocean Sciences, Elsevier Academic Press p390-400.

Carvalho, J., Kuilman, L.W., Sonangol, P.P., Luanda, A., 2003. Deepwater Angola; Seafloor Pock-Marks as Hydrocarbon Indicators? AAPG International Conference & Exhibition Technical Program, Barcelona.

Chand, S., Rise, L., Ottesen, D., Dolan, M., Bellec, V., Bøe R., 2009. Pockmark-like depressions near the Goliat hydrocarbon field, Barents Sea: Morphology and genesis. Marine and Petroleum Geology 26, 1035-1042.

Chen, Y., Ussler, W., Haflidason, H., Lepland, A., Rise, L., Hovland, M., et al., 2010. Sources of methane inferred from pore-water $\delta^{13}C$ of dissolved inorganic carbon in Pockmark G11, offshore Mid-Norway. Chemical Geology 275, 127-138.

Chester, R., Jickells, T., 2012. Marine geochemistry. Wiley-Blackwell: Susses, UK.

Christie, W.W., 1982. Lipid analysis. Pergamon Press: Oxford, UK.

Christodoulou, D., Papatheodorou, G., Ferentinos, G., Masson, M., 2003. Active seepage in two contrasting pockmark fields in the Patras and Corinth gulfs, Greece. Geo-Marine Letters 23, 194-199.

Çifçi, G., Dondurur, D., Ergün, M., 2003. Deep and shallow structures of large pockmarks in the Turkish shelf, Eastern Black Sea. Geo-Mar Letters 23, 311-322.

Clark, Jr R., Blumer, M., 1967. Distribution of n-paraffins in marine organisms and sediment. Limnology and Oceanography 12, 79-87.

Cole, D., Stewart, S., Cartwright, J., 2000. Giant irregular pockmark craters in the Palaeogene of the outer Moray Firth basin, UK North Sea. Marine and Petroleum Geol 17:563-577.

Collister, J.W., Rieley, G., Stern, B., Eglinton, G., Fry, B., 1994. Compound-specific $\delta\ ^{13}C$ analyses of leaf lipids from plants with differing carbon dioxide metabolisms. Organic Geochemistry 21, 619-627.

Conte, M.H., Thompson, A., Eglinton, G., 1994. Primary production of lipid biomarker compounds by *Emiliania huxleyi*. Results from an experimental mesocosm study in fjords of southwestern Norway. Sarsia 79, 319-331.

Coppola, L., Gustafsson, Ö., Andersson, P., Eglinton, T.I., Uchida, M., Dickens, A.F., 2007. The importance of ultrafine particles as a control on the distribution of organic carbon in Washington Margin and Cascadia Basin sediments. Chemical Geology 243, 142-156.

Cordes, E.E., Bergquist, D.C., Fisher, C.R., 2009. Macro-ecology of Gulf of Mexico cold seeps. Annual Review of Marine Science 1, 143-168.

Cowie, G.L., Hedges, J.I., 1992. The role of anoxia in organic matter preservation in coastal sediments: relative stabilities of the major biochemicals under oxic and anoxic depositional conditions. Organic Geochemistry 19, 229-234.

Cranwell, P.A., 2006. Chain-length distribution of n-alkanes from lake sediments in relation to post-glacial environmental change. Freshwater Biology 3, 259-265.

Cranwell, P.A., 1982. Lipids of aquatic sediments and sedimenting particulates. Progress in Lipid Research 21, 271-308.

Cranwell, P.A., Volkman, J.K., 1981. Alkyl and steryl esters in a recent sediment. Chemical Geology 32, 29-43.

Damsté, J.S.S., Rijpstra, W.I.C., Hopmans, E.C., Prahl, F.G., Wakeham, S.G., Schouten, S., 2002. Distribution of membrane lipids of planktonic Crenarchaeota in the Arabian Sea. Applied and Environmental Microbiology 68, 2997-3002.

Dando, P., 2001. A review of pockmarks in the UK part of the North Sea, with particular respect to their biology. Department of Trade and Industry Strategic Environmental Assessment Technical Report: UK.

Dando, P., Austen, M., Burke, R., Kendall, M., Kennicutt, M., Judd, A., et al., 1991. Ecology of a North Sea pockmark with an active methane seep. Marine Ecology Progress Series 70, 49-63.

Danovaro, R., Corinaldesi, C., Luna, G., Dell'Anno, A., 2006. Molecular tools for the analysis of DNA in marine environments. In: Volkman, J.K. (Ed.). Marine Organic Matter: Biomarkers, Isotopes and DNA. Springer-Verlag: Berlin p105-126.

De Rosa, M., Gambacorta, A., 1988. The lipids of archaebacteria. Progress in Lipid Research 27, 153-175.

DeFlaun, M.F., Mayer, L.M., 1983. Relationships between bacteria and grain surfaces in intertidal sediments. Limnology and Oceanography 28, 873-881.

DeLong, E.F., Pace, N.R., 2001. Environmental diversity of bacteria and archaea. Systematic Biology 50, 470-478.

Demaison, G.J., Moore, G.T., 1980. Anoxic environments and oil source bed genesis. America Association of Petroleum Geologists Bulletin 64, 1179-1209.

Deming, J., Baross, J., 1993. The early diagenesis of organic matter: bacterial activity. Organic Geochemistry. Plenum Press: New York.

Denman, K.L., Brasseur, G., Chidthaisong, A., Ciais, P., Cox, P.M., Dickinson, R.E., et al. 2007. Couplings between changes in the climate system and biogeochemistry. In: Solomon, S., Qin, D., Manning, M., Chen, Z., Marquis, M., Averyt, K.B., et al., (Eds.). Climate Change 2007: The physical science basis. Contribution of Working Group I to the Fourth Assessment Report of the Intergovernmental Panel on Climate Change Cambridge, Cambridge University Press: United Kingdom and USA, p. 499-589.

Derenne, S., Largeau, C., 2001. A review of some important families of refractory macromolecules: composition, origin, and fate in soils and sediments. Soil Science 166, 833-847.

Dickens, A.F., Gélinas, Y., Hedges, J.I., 2004. Physical separation of combustion and rock sources of graphitic black carbon in sediments. Marine Chem 92, 215-223.

Dimitrov, L., Woodside, J., 2003. Deep sea pockmark environments in the eastern Mediterranean. Marine Geology 195, 263-276.

Driscoll, N.W., Weissel, J.K., Goff, J.A., 2000. Potential for large-scale submarine slope failure and tsunami generation along the US mid-Atlantic coast. Geology 28, 407-410.

Edlund, A., Nichols, P.D., Roffey, R., White, D.C., 1985. Extractable and lipopolysaccharide fatty acid and hydroxy acid profiles from Desulfovibrio species. Journal of Lipid Research 26, 982-988.

Eganhouse, R.P., 1997. Molecular Markers in Environmental Organic Geochemistry. American Chemical Society: Washington.

Eglinton, G., Hamilton, R.J., 1967. Leaf epicuticular waxes. Science 156, 1322-1335.

Eglinton, T.I., Repeta, D.J., 2004. Organic matter in the contemporary ocean. In:

Holland, H.D., Turekian, K.K. (Eds.). Treatise on Geochemistry Volume 6, The Oceans and Marine Geochemistry, Elsevier Pergamon, Amsterdam, pp. 145–180.

Eglinton, T.I., 2012. Geochemistry: A rusty carbon sink. Nature 483, 165-166.

Elvert, M., Whiticar, M.J., Suess, E., 2001. Diploptene in varved sediments of Saanich Inlet: indicator of increasing bacterial activity under anaerobic conditions during the Holocene. Marine Geology 174, 371-383.

Elvert, M., Boetius, A., Knittel, K., Jørgensen, B.B., 2003 Characterization of Specific Membrane Fatty Acids as Chemotaxonomic Markers for Sulfate-Reducing Bacteria Involved in Anaerobic Oxidation of Methane. Geomicrobiol Journal 20, 403-419.

Fabbri, D., Sangiorgi, F., Vassura, I., 2005. Pyrolysis–GC–MS to trace terrigenous organic matter in marine sediments: a comparison between pyrolytic and lipid markers in the Adriatic Sea. Analytica Chimica Acta 530, 253-261.

Fader, G.B.J., 1991. Gas-related sedimentary features from the eastern Canadian continental shelf. Continental Shelf Research 11, 1123-1153.

Falkowski, P., Scholes, R.J., Boyle, E., Canadell, J., Canfield, D., Elser, J., Gruber, N., Hibbard, K., Högberg, P., Linder, S., et al., 2000. The global carbon cycle: A test of our knowledge of Earth as a system. Science 290, 291–296.

Feng, D., Chen, D., Peckmann, J., Bohrmann, G., 2010. Authigenic carbonate crusts from methane seeps of the northern Congo fan: microbial formation mechanism. Marine and Petroleum Geology 27, 748-756.

Fernández-Puga, M., Vázquez, J., Somoza, L., Díaz del Rio, V., Medialdea, T., Mata, M., et al., 2007. Gas-related morphologies and diapirism in the Gulf of Cádiz. Geo-Mar Letters 27, 213-221.

Floodgate, G., Judd, A., 1992. The origins of shallow gas. Continental Shelf Research 12, 1145-1156.

Forster, P., Ramaswamy, V., Artaxo, P., Berntsen, T., Betts, R., Fahey, D.W., et al., 2007. Changes in atmospheric constituents and in radiative forcing. In: Solomon, S., Qin, D., Manning, M., Chen, Z., Marquis, M., Averyt, K.B., et al., (eds.). Climate Change 2007: The physical science basis. Contribution of Working Group I to the Fourth Assessment Report of the Intergovernmental Panel on Climate Change Cambridge, Cambridge University Press: United Kingdom and USA, p. 129-234

Froelich, P.N., Klinkhammer, G.P., Bender, M.L., Luedtke, N.A., Heath, G.R., Cullen, D., et al., 1979. Early oxidation of organic matter in pelagic sediments of the eastern equatorial Atlantic: suboxic diagenesis. Geochimica et Cosmochimica Acta 43, 1075-1090.

Frostegård, Å., Tunlid, A., Bååth, E., 2011. Use and misuse of PLFA measurements in soils. Soil Biology and Biochemistry 43, 1621-1625.

Fuhrman, J.A., Hagström, Å., 2008. Bacterial and archaeal community structure and its patterns. Microbial Ecology of the Oceans, 2nd Ed. p45-90.

Games, K., 2001. Evidence of shallow gas above the Connemara oil accumulation, Block 26/28, Porcupine Basin. Geological Society, London, Special Publications 188, 361-373.

Gay A, Lopez M, Berndt C, Seranne M. 2007. Geological controls on focused fluid flow associated with seafloor seeps in the Lower Congo Basin. Mar Geol 244:68-92.

Gay A, Lopez M, Cochonat P, Levaché D, Sermondadaz G, Seranne M. 2006. Evidences of early to late fluid migration from an upper Miocene turbiditic channel revealed by 3D seismic coupled to geochemical sampling within seafloor pockmarks, Lower Congo Basin. Mar Pet Geol 23:387-399.

Gay A, Lopez M, Cochonat P, Sultan N, Cauquil E, Brigaud F. 2003. Sinuous pockmark belt as indicator of a shallow buried turbiditic channel on the lower slope of the Congo Basin, West African Margin. Geological Society, London, Special Publications 216:173-189.

Gay A, Lopez M, Ondreas H, Charlou JL, Sermondadaz G, Cochonat P. 2006. Seafloor facies related to upward methane flux within a Giant Pockmark of the Lower Congo Basin. Mar Geol 226:81-95.

Gooday AJ. 2002. Biological responses to seasonally varying fluxes of organic matter to the ocean floor: a review. J Oceanogr 58:305-332.

Gooday AJ, Turley CM, Allen JA. 1990. Responses by Benthic Organisms to Inputs of Organic Material to the Ocean Floor: A Review [and Discussion}. Phil Trans R Soc A 331:119-138.

Hammer Ø, Webb KE. 2010. Piston coring of Inner Oslofjord pockmarks, Norway: constraints on age and mechanism. Norw J Geol 90:79-91.

Hansell, D.A., Carlson, C.A., 1998. Deep-ocean gradients in the concentration of dissolved organic carbon. Nature 395, 263–266.

Harrington, P., 1985. Formation of pockmarks by pore-water escape. Geo-Marine Letters 5, 193-197.

Harvey, H., 2006. Sources and cycling of organic matter in the marine water column. In: Volkman JK (Ed.). Marine Organic Matter: Biomarkers, Isotopes and DNA Springer-Verlag: Berlin p1-25.

Hasiotis, T., Papatheodorou, G., Ferentinos, G., 2002. A string of large and deep gas-induced depressions (pockmarks) offshore Killini peninsula, western Greece. Geo-Marine Letters 22, 142-149.

Hasiotis, T., Papatheodorou, G., Kastanos, N., Ferentinos, G., 1996. A pockmark field in the Patras Gulf (Greece) and its activation during the 14/7/93 seismic event. Marine Geology 130, 333-344.

Haskell, N., Nissen, S., Hughes, M., Grindhaug, J., Dhanani, S., Heath, R., et al., 1999. Delineation of geologic drilling hazards using 3-D seismic attributes. The Leading Edge 18, 373-382.

Haskell, N., Nissen, S., Whitman, D., Antrim, L., 1997. Structural features on the West African continental slope delineated by 3-D seismic coherency: abstract. America Association of Petroleum Geologists Bulleting 81, 1382.

Hatcher, P.G., McGillivary, P.A., 1979. Sewage contamination in the New York Bight. Coprostanol as an indicator. Environmental Science and Technology 10, 1225-1229.

Head, I., Saunders, J., Pickup, R., 1998. Microbial evolution, diversity, and ecology: a decade of ribosomal RNA analysis of uncultivated microorganisms. Microbial Ecology 35, 1-21.

Hedges, J.I., Baldock, J.A., Gélinas, Y., Lee, C., Peterson, M., Wakeham, S.G., 2001. Evidence for non-selective preservation of organic matter in sinking marine particles. Nature 409, 801-804.

Hedges, J.I., Baldock, J.A., Gélinas, Y., Lee, C., Peterson, M.L., Wakeham, S.G., 2002. The biochemical and elemental compositions of marine plankton: A NMR perspective. Marine Chemistry 78, 47-63.

Hedges, J.I., Eglinton, G., Hatcher, P.G., Kirchman, D.L., Arnosti, C., Derenne, S., et al., 2000. The molecularly-uncharacterized component of nonliving organic matter in natural environments. Organic Geochemistry 31, 945-958.

Hedges, J.I., Keil, R.G., Benner, R., 1997. What happens to terrestrial organic matter in the ocean? Organic Geochemistry 27, 195-212.

Hedges, J.I., Oades, J.M., 1997. Comparative organic geochemistries of soils and marine sediments. Organic Geochemistry 27, 319-361.

Hedges, J.I., Keil, R.G., 1999. Organic geochemical perspectives on estuarine processes: sorption reactions and consequences. Marine Chemistry 65, 55-65.

Hedges, J.I., Keil, R.G., 1995. Sedimentary organic matter preservation: an assessment and speculative synthesis. Marine Chemistry 49, 81-115.

Hedges, J.I., Mann, D.C., 1979. The characterization of plant tissues by their lignin oxidation products. Geochimica et Cosmochimica Acta 43, 1803-1807.

Herndl, G.J., Reinthaler, T., Teira, E., Van Aken, H., Veth, C., Pernthaler, A., et al., 2005. Contribution of Archaea to total prokaryotic production in the deep Atlantic Ocean. Applied and Environmental Microbiology 71, 2303-2309.

Hester, K.C., Brewer, P.G., 2009. Clathrate hydrates in nature. Annual Review of Marine Science 1, 303-327.

Hill, J.C., Driscoll, N.W., Weissel, J.K., Goff, J.A., 2004. Large-scale elongated gas blowouts along the US Atlantic margin. Journal of Geophysical Research 109, B09101.

Hinrichs, K., Boetius, A., 2002. The anaerobic oxidation of methane: new insights in microbial ecology and biogeochemistry. In: Wefer, G., Billett, D., Hebbeln, D., Jørgensen, B.B., Schlüter, M., Van Weering, T. (Eds.) Ocean Margin Systems. Springer-Verlag Berlin Heidelberg, pp 457-477.

Hinrichs, K.U., Hayes, J.M., Sylva, S.P., Brewer, P.G., DeLong, E.F., 1999. Methane-consuming archaebacteria in marine sediments. Nature 398, 802-805.

Hinrichs, K.U., Summons, R.E., Orphan, V., Sylva, S.P., Hayes, J.M., 2000. Molecular and isotopic analysis of anaerobic methane-oxidizing communities in marine sediments. Organic Geochemistry 31, 1685-1701.

Hoefs, J., 2009. Stable isotope geochemistry. 6th ed. Springer: Germany.

Hoefs, M., Schouten, S., De Leeuw, J., King, L.L., Wakeham, S.G., Damste, J., 1997. Ether lipids of planktonic archaea in the marine water column. Applied and Environmental Microbiology 63, 3090-3095.

Hopmans, E.C., Schouten, S., Pancost, R.D., van der Meer, M.T.J., Sinnighe Damsté, J.S., 2000. Analysis of intact tetraether lipids in archaeal cell material and sediments by high performance liquid chromatography/atmospheric pressure chemical ionization mass spectrometry. Rapid Communications in Mass Spectrometry 14, 585-589.

Hovland, M., 2003. Geomorphological, geophysical, and geochemical evidence of fluid flow through the seabed. Journal of Geochemical Exploration 78, 287-291.

Hovland, M., 1992. Hydrocarbon Seeps in Northern Marine Waters: Their Occurrence and Effects. Palaios 7, 376-382.

Hovland, M., 1991. Large pockmarks, gas-charged sediments and possible clay diapirs in the Skagerrak. Marine and Petroleum Geology 8, 311-316.

Hovland, M., 1982. Pockmarks and the recent geology of the central section of the Norwegian Trench. Marine Geology 47, 283-301.

Hovland, M., Gardner, J., Judd, A., 2002. The significance of pockmarks to understanding fluid flow processes and geohazards. Geofluids 2, 127-136.

Hovland, M., Judd, A., 1988. Seabed pockmarks and seepages: impact on geology, biology, and the marine environment. Springer: London

Hovland, M., Svensen, H., 2006. Submarine pingoes: Indicators of shallow gas hydrates in a pockmark at Nyegga, Norwegian Sea. Marine Geology 228, 15-23

Hovland, M., Svensen, H., Forsberg, C.F., Johansen, H., Fichler, C., Fosså, J.H., et al. 2005. Complex pockmarks with carbonate-ridges off mid-Norway: Products of sediment degassing. Marine Geology 218, 191-206.

Hovland, M., Talbot, M.R., Qvale, H., Olaussen, S., Aasberg, L., 1987. Methane-related carbonate cements in pockmarks of the North Sea. Journal of Sedimentary Research 57, 881-892.

Hugenholtz, P., Goebel, B.M., Pace, N.R., 1998. Impact of culture-independent studies on the emerging phylogenetic view of bacterial diversity. Journal of Bacteriology 180, 4765-4774.

Idler, D.R., Wiseman, P.M., Safe, L.M., 1970. A new marine sterol, 22-trans-24-norcholesta-5,22-dien-3β-ol. Steroids 16, 451-461.

Iglesias, J., García-Gil, S., 2007. High-resolution mapping of shallow gas accumulations and gas seeps in San Simón Bay (Ría de Vigo, NW Spain). Some quantitative data. Geo-Marine Letters 27, 103-114.

Inagaki, F., Nunoura, T., Nakagawa, S., Teske, A., Lever, M., Lauer, A., et al., 2006. Biogeographical distribution and diversity of microbes in methane hydrate-bearing deep marine sediments on the Pacific Ocean Margin. Proceedings of the National Academy of Sciences U S A 103, 2815-2820.

Inagaki, F., Suzuki, M., Takai, K., Oida, H., Sakamoto, T., Aoki, K., et al., 2003. Microbial communities associated with geological horizons in coastal subseafloor sediments from the Sea of Okhotsk. Applied and Environmental Microbiology 69, 7224-7235.

Innes, H.E., Bishop, A.N., Head, I.M., Farrimond, P., 1997. Preservation and diagenesis of hopanoids in Recent lacustrine sediments of Priest Pot, England. Organic Geochemistry 26, 565-576.

Jensen, P., Aagaard, I., Burke, Jr R., Dando, P., Joergensen, N.O., Kuijpers, A., et al. 1992. “Bubbling reefs" in the Kattegat: Submarine landscapes of carbonate-cemented rocks support a diverse ecosystem at methane seeps. Marine Ecology Progress Series 83, 103-112.

Jiang, C., Alexander, R., Kagi, R.I., Murray, A.P., 1998. Polycyclic aromatic hydrocarbons in ancient sediments and their relationships to palaeoclimate. Organic Geochemistry 29, 1721-1735.

Johns, R.B., Gillan, F.T., Volkman, J.K., 1980. Early diagenesis of phytyl esters in a contemporary temperate intertidal sediment. Geochimica et Cosmochimica Acta 44, 183-188.

Jørgensen, B.B., 2006. Bacteria and marine biogeochemistry. In: Schulz, H.D., Zabel, M., (Eds.). Marine Geochemistry. 2nd ed. Springer: Germany p169-206.

Jørgensen, B.B., 1982. Mineralization of organic matter in the sea bed—the role of sulphate reduction. Nature 296, 643-645

Jørgensen, B.B., Boetius, A., 2007. Feast and famine—microbial life in the deep-sea bed. Nature Reviews Microbiology 5, 770-781.

Jørgensen, B.B., Kasten, S., 2006. Sulfur cycling and methane oxidation. In: Schulz, H.D., Zabel, M., (Eds.). Marine Geochemistry. 2nd ed. Springer:Germany p. 271-310.

Judd, A.G., Hovland, M., 2007. Seabed fluid flow: the impact on geology, biology and the marine environment. Cambridge University Press: Cambridge, UK.

Judd, A.G., 2003. The global importance and context of methane escape from the seabed. Geo-Mar Letters 23, 147-154.

Judd, A.G., Hovland, M., 1992. The evidence of shallow gas in marine sediments. Continental Shelf Research 12, 1081-1095.

Judd, A., Long, D., Sankey, M., 1994. Pockmark formation and activity, UK block 15/25, North Sea. Bulletin of the Geological Society of Denmark 41, 34-49.

Kaiser, K., Benner, R., 2009. Biochemical composition and size distribution of organic matter at the Pacific and Atlantic time-series stations. Marine Chemistry 113, 63-77.

Karisiddaiah, S., Veerayya, M., 2002. Occurrence of pockmarks and gas seepages along the central western continental margin of India. Current Science 82, 52-57.

Karner, M.B., DeLong, E.F., Karl, D.M., 2001. Archaeal dominance in the mesopelagic zoneof the Pacific Ocean. Nature 409, 507-510.

Kattner, G., Krause, M., 1989. Seasonal variations of lipids (wax esters, fatty acids and alcohols) in calanoid copepods from the North Sea. Marine Chemistry 26, 261-275.

Kelley, J.T., Dickson, S.M., Belknap, D.F., Barnhardt, W.A., Henderson, M. 1994. Giant sea-bed pockmarks: evidence for gas escape from Belfast Bay, Maine. Geology 22, 59-62.

King, L.H., MacLean, B., 1970. Pockmarks on the Scotian shelf. Geological Society of America Bulletin 81, 3141-3148.

King, L.L., Pease, T.K., Wakeham, S.G., 1998. Archaea in Black Sea water column particulate matter and sediments—evidence from ether lipid derivatives. Organic Geochemistry 28, 677-688.

Knebel, H.J., Scanlon, K.M., 1985. Sedimentary framework of Penobscot Bay, Maine. Marine Geology 65, 305-324.

Knittel, K., Boetius, A., 2009. Anaerobic oxidation of methane: progress with an unknown process. Annual Review of Microbiology 63, 311-334.

Knittel, K., Lösekann, T., Boetius, A., Kort, R., Amann, R., 2005. Diversity and distribution of methanotrophic archaea at cold seeps. Applied and Environmental Microbiology 71, 467-479.

Koga, Y., Morii, H., Akagawa-Matsushita, M., Ohga, M., 1998. Correlation of Polar Lipid Composition with 16S rRNA Phylogeny in Methanogens. Further Analysis of Lipid Component Parts. Bioscience Biotechnology and Biochemistry 62, 230-236.

Kögel-Knabner, I., 2002. The macromolecular organic composition of plant and microbial residues as inputs to soil organic matter. Soil Biology and Biochemistry 34, 139-162.

Kvenvolden, K.A., 1995., A review of the geochemistry of methane in natural gas hydrate. Organic Geochemistry 23, 997-1008.

Lalonde, K., Mucci, A., Ouellet, A., Gelinas, Y., 2012 . Preservation of organic matter in sediments promoted by iron. Nature 483, 198-200.

Lastras, G., Canals, M., Amblas, D., Ivanov, M., Dennielou, B., Droz, L., et al., 2006. Eivissa slides, western Mediterranean Sea: morphology and processes. Geo-Marine Letters 26, 225-233.

Lastras, G., Canals, M., Urgeles, R., Hughes-Clarke, J., Acosta, J., 2004. Shallow slides and pockmark swarms in the Eivissa Channel, western Mediterranean Sea. Sedimentology 51, 837-850.

Lavoie, D., Pinet, N., Duchesne, M., Bolduc, A., Larocque, R., 2010. Methane-derived authigenic carbonates from active hydrocarbon seeps of the St. Lawrence Estuary, Canada. Marine and Petroleum Geology 27, 1262-1272.

Levin, L.A., 2005. Ecology of cold seep sediments: interactions of fauna with flow, chemistry and microbes. Oceanography and Marine Biology Annual Review 43, 1-46.

Lipp, J.S., Morono, Y., Inagaki, F., Hinrichs, K.U., 2008. Significant contribution of Archaea to extant biomass in marine subsurface sediments. Nature 454, 991-994.

Llyod, K.G., Lapham, L., Teske, A., 2006. An anaerobic methane-oxidising community of ANME-1b archaea in hypersaline Gulf of Mexico sediments. Applied and Environmental Microbiology 72, 7218-7230.

Lochte, K., Turley, C., 1988. Bacteria and cyanobacteria associated with phytodetritus in the deep sea. Nature 333, 67-69.

Loh, A.N., Bauer, J.E., Druffel E.R.M., 2004. Variable ageing and storage of dissolved organic components in the open ocean. Nature 430, 877-881.

Longhurst, A., Sathyendranath, S., Platt, T., Caverhill, C., 1995. An estimate of global primary production in the ocean from satellite radiometer data. Journal of Plankton Research 17, 1245-1271.

Lösekann, T., Knittel, K., Nadalig, T., Fuchs, B., Niemann, H., Boetius, A., et al., 2007. Diversity and abundance of aerobic and anaerobic methane oxidizers at the Haakon Mosby Mud Volcano, Barents Sea. Appl Environ Microbiol 73, 3348-3362.

Madigan, M.T., Martinko, J.M., Stahl, D.A., Clark, D.P., 2012. Brock Biology of Microorganisms. 13th ed. Pearson University Press: San Francisco.

Maestro, A., Barnolas, A., Somoza, L., Lowrie, A., Lawton, T., 2002. Geometry and structure associated to gas-charged sediments and recent growth faults in the Ebro Delta (Spain). Marine Geology 186, 351-368.

Manahan, S.E., 2004. Environmental chemistry. CRC Press: Florida, USA.

Mannino, A., Harvey, H.R., 2004. Black carbon in estuarine and coastal ocean dissolved organic matter. Limnology and Oceanography 49, 735-740.

Marchesi, J.R., Weightman, A.J., Cragg, B.A., John, Parkes, R., Fry, J.C., 2001. Methanogen and bacterial diversity and distribution in deep gas hydrate sediments from the Cascadia Margin as revealed by 16S rRNA molecular analysis. FEMS Microbiology Ecology 34, 221-228.

Massé, G., Belt, S.T., Allard, G.W., Lewis, A.C, Wakeham, S.G., Rowland, S.J., 2004. Occurrence of novel monocyclic alkenes from diatoms in marine particulate matter and sediments. Organic Geochemistry 35, 813-822.

Mazzini, A., Svensen, H., Hovland, M., Planke, S., 2006. Comparison and implications from strikingly different authigenic carbonates in a Nyegga complex pockmark, G11, Norwegian Sea. Marine Geology 231, 89-102.

McCarthy, M.D., Hedges, J.I., Benner, R., 1998. Major bacterial contribution to marine dissolved organic nitrogen. Science 281, 231-234.

McCarthy, M., Hedges, J., Benner, R., 1996. Major biochemical composition of dissolved high molecular weight organic matter in seawater. Marine Chemistry 55, 281-297.

Merkel, A.Y., Chernykh, N.A., Kanatpatskii, T.A., Pimenov, N.V., 2010. Detection of methanotrophic archaea in pockmark sediments (Gdansk Deep, Baltic Sea) by sequence analysis of the gene encoding the α subunit of Methyl Coenzyme M reductase. Microbiology 79, 849-852

Michaelis, W., Seifert, R., Nauhaus, K., Treude, T., Thiel, V., Blumenberg, M., et al. 2002. Microbial reefs in the Black Sea fueled by anaerobic oxidation of methane. Science 297, 1013-1015.

Middelburg, J.J., Nieuwenhuize, J., van Breugel, P., 1999. Black carbon in marine sediments. Marine Chemistry 65, 245-252.

Milkov, A., 2000. Worldwide distribution of submarine mud volcanoes and associated gas hydrates. Marine Geology 167, 29-42.

Milucka, J., Ferdelman, T.G., Polerecky, L., Franzke, D., Wegener, G., Schmid, M., et al. 2012. Zero-valent sulphur is a key intermediate in marine methane oxidation. Nature 491, 541-546.

Mosher, D.C., Piper, D.J.W., Campbell, D.C., Jenner, K.A., 2004. Near-surface geology and sediment-failure geohazards of the central Scotian Slope. America Association of Petroleum Geologists Bulletin 88, 703-723.

Myers, R.M., Fischer, S.G., Lerman, L.S., Maniatis, T., 1985. Nearly all single base substitutions in DNA fragments joined to a GC-clamp can be detected by denaturing gradient gel electrophoresis. Nucleic Acids Research 13, 3131-3145.

Nealson, K.H., 1997. Sediment bacteria: who's there, what are they doing, and what's new? Annual Review of Earth and Planet Sciences 25, 403-434.

Nelson, H., Thor, D., Sandstrom, M., Kvenvolden, K., 1979. Modern biogenic gas-generated craters (sea-floor "pockmarks") on the Bering Shelf, Alaska. Geological Society of America Bulletin 90, 1144-1152.

Newman, K.R., Cormier, M.H., Weissel, J.K., Driscoll, N.W., Kastner, M., Solomon, E.A., et al., 2008. Active methane venting observed at giant pockmarks along the US mid-Atlantic shelf break. Earth and Planetary Science Letters 267, 341-352.

Nickel, J.C., di Primio, R., Mangelsdorf, K., Stoddart, D., Kallmeyer, J., 2012. Characterization of microbial activity in pockmark fields of the SW-Barents Sea. Marine Geology 332-334, 152-162

Niemann, H., Elvert, M., 2008. Diagnostic lipid biomarker and stable carbon isotope signatures of microbial communities mediating the anaerobic oxidation of methane with sulphate. Organic Geochemistry 39, 1668-1677.

Niemann, H., Lösekann, T., de Beer, D., Elvert, M., Nadalig, T., Knittel, K., et al. 2006. Novel microbial communities of the Haakon Mosby mud volcano and their role as a methane sink. Nature 443, 854-858.

Ogawa, H., Tanoue, E., 2003. Dissolved Organic Matter in Oceanic Waters. Journal of Oceanography 59, 129-147.

Olsen, G.J., Lane, D.J., Giovannoni, S.J., Pace, N.R., Stahl, D.A., 1986. Microbial ecology and evolution: a ribosomal RNA approach. Annual Reviews of Microbiology 40, 337-365.

Ondréas, H., Olu, K., Fouquet, Y., Charlou, J.L., Gay, A., Dennielou, B., et al., 2005. ROV study of a giant pockmark on the Gabon continental margin. Geo-Marine Letters 25, 281-292.

Orphan, V.J., Hinrichs, K.U., Ussler III, W., Paull, C.K., Taylor, L.T., Sylva, S.P., et al., 2001. Comparative analysis of methane-oxidizing archaea and sulfate-reducing bacteria in anoxic marine sediments. Applied and Environmental Microbiology 67, 1922-1934.

Orphan, V.J., House, C.H., Hinrichs, K.U., McKeegan, K.D., DeLong, E.F., 2001. Methane-consuming archaea revealed by directly coupled isotopic and phylogenetic analysis. Science 293, 484-487.

Pace, N.R., 1997. A molecular view of microbial diversity and the biosphere. Science 276, 734-740.

Pancost, R.D., Boot, C.S., 2004. The palaeoclimatic utility of terrestrial biomarkers in marine sediments. Marine Chemistry 92, 239-261.

Pancost, R.D., Sinninghe Damste, J.S., de Lint, S., van der Maarel, M.J., Gottschal, J.C., 2000. Biomarker evidence for widespread anaerobic methane oxidation in Mediterranean sediments by a consortium of methanogenic archaea and bacteria. The Medinaut Shipboard Scientific Party. Applied and Environmental Microbiology 66, 1126-1132.

Parkes, R.J., Cragg, B.A., Banning, N., Brock, F., Webster, G., Fry, J.C., et al., 2007. Biogeochemistry and biodiversity of methane cycling in subsurface marine sediments (Skagerrak, Denmark). Environmental Microbiology 9, 1146-1161.

Parsons, T., Stephens, K., Strickland, J., 1961. On the chemical composition of eleven species of marine phytoplankters. Journal of the Fisheries Board of Canada 18, 1001-1016.

Paull, C., Ussler III. W., Maher, N., Greene, H., Rehder, G., Lorenson, T., et al., 2002. Pockmarks off Big Sur, California. Marine Geology 181, 323-335.

Paull, C., Ussler III, W., Borowski, W., 1999. Freshwater ice rafting: an additional mechanism for the formation of some high-latitude submarine pockmarks. Geo-Marine Letters 19, 164-168.

Pauly, G.G., Van Vleet, E.S., 1986. Acyclic archaebacterial ether lipids in swamp sediments. Geochimica et Cosmochimica Acta 50, 1117-1125.

Pedersen, T.F., Calvert, S.E., 1990. Anoxia vs productivity; what controls the formation of organic-carbon-rich sediments and sedimentary rocks? America Association of Petroleum Geologists Bulletin 74, 454-466.

Pernthaler, A., Dekas, A.E., Brown, C.T., Goffredi, S.K., Embaye, T., Orphan, V.J., 2008. Diverse syntrophic partnerships from deep-sea methane vents revealed by direct cell capture and metagenomics. Proceedings of the National Academy of Sciences USA 105, 7052-7057.

Peters, K.E., Moldowan, J.M., 1993. The biomarker guide: Interpreting molecular fossils in petroleum and ancient sediments. Prentice-Hall, NJ USA.

Peters, K.E., Walters, C.C., Moldowan, J.M., 2004. The biomarker guide Volume 1. Biomarkers and Isotopes in the Environment and Human History. Cambridge University Press: Cambridge, UK and USA.

Petit, J.R., Jouzel, J., Raynaud, D., Barkov, N., Barnola, J., Basile, I., et al., 1999. Climate and atmospheric history of the past 420,000 years from the Vostok ice core, Antarctica. Nature 399, 429-436.

Pickrill, R., 2006. Shallow seismic stratigraphy and pockmarks of a hydrothermally influenced lake, Lake Rotoiti, New Zealand. Sedimentology 40, 813-828.

Pilcher, R., Argent, J., 2007. Mega-pockmarks and linear pockmark trains on the West African continental margin. Marine Geology 244, 15-32.

Pinet, N., Duchesne, M., Lavoie, D., 2010. Linking a linear pockmark train with a buried Palaeozoic structure: a case study from the St. Lawrence Estuary. Geo-Marine Letters 30, 517-522.

Pinet, N., Duchesne, M., Lavoie, D., Bolduc, A., Long, B., 2008. Surface and subsurface signatures of gas seepage in the St. Lawrence Estuary (Canada): Significance to hydrocarbon exploration. Marine and Petroleum Geology 25, 271-288.

Plassen, L., Vorren, T.O., 2003. Fluid flow features in fjord-fill deposits, Ullsfjorden, North Norway. Norsk Geologisk Tidsskrift 83, 37-42.

Platt, J., 1977. Significance of pockmarks for engineers. Offshore Engineer 45.

Pomeroy, L.R., 1974. The ocean's food web, a changing paradigm. Bioscience 24, 499-504.

Prahl, F.G., Eglinton, G., Corner, E.D., O'Hara, S.C., 1984. Copepod fecal pellets as a source of dihydrophytol in marine sediments. Science 224, 1235-1237.

Prahl, F.G., Ertel, J.R., Goni, M.A., Sparrow, M.A., Eversmeyer, B., 1994. Terrestrial organic carbon contributions to sediments on the Washington margin. Geochimica et Cosmochimica Acta 58, 3035-3048.

Rappé, M.S., Giovannoni, S.J., 2003. The uncultured microbial majority. Annual Reviews of Microbiology 57, 369-394.

Rau, G.H., Takahashi, T., Des Marais, D.J., 1989. Latitudinal variations in plankton delta ^{13}C: implications for CO_2 and productivity in past oceans. Nature 341, 516-518.

Redfield, A.C., Ketchum, B.H., Richards, F.A.. 1963. The influence of organisms on the composition of seawater. In: Hill, M.N. (Ed.). The Sea. 2nd ed. Wiley Interscience: New York p26-77.

Reed, D.W., Fujita, Y., Delwiche, M.E., Blackwelder, D.B., Sheridan, P.P., Uchida, T., et al., 2002. Microbial communities from methane hydrate-bearing deep marine sediments in a forearc basin. Applied and Environmental Microbiology 68, 3759-3770.

Reitner, J., Peckmann, J., Reimer, A., Schumann, G., Thiel, V., 2005. Methane-derived carbonate build-ups and associated microbial communities at cold seeps on the lower Crimean shelf (Black Sea). Facies 51, 66-79.

Rise, L., Sættem, J., Fanavoll, S., Thorsnes, T., Ottesen, D., Bøe, R., 1999. Sea-bed pockmarks related to fluid migration from Mesozoic bedrock strata in the Skagerrak offshore Norway. Marine and Petroleum Geology 16, 619-631.

Roalkvam, I., Dahle, H., Chen, Y., Jørgensen, S.L., Haflidason, H., Steen, I.H., 2012. Fine-scale community structure analysis of ANME in Nyegga sediments with high and low methane flux. Frontiers in Microbiology 3, 1-13.

Roalkvam, I., Jørgensen, S.L., Chen, Y., Stokke, R., Dahle, H., Hocking, W.P., et al., 2011. New insight into stratification of anaerobic methanotrophs in cold seep sediments. FEMS Microbiology Ecology 78, 233-243.

Rogers, J.N., Kelley, J.T., Belknap, D.F., Gontz, A., Barnhardt, W.A., 2006. Shallow-water pockmark formation in temperate estuaries: A consideration of origins in the western gulf of Maine with special focus on Belfast Bay. Marine Geology 225, 45-62.

Rohmer, M., Bouvier-Nave, P., Ourisson, G., 1984. Distribution of Hopanoid Triterpenes in Prokaryotes. Journal of General Microbiology 130, 1137-1150.

Rontani, J., Volkman, J.K., 2003. Phytol degradation products as biogeochemical tracers in aquatic environments. Organic Geochemistry 34, 1-35.

Rullkötter, J., 2006. Organic matter: The driving force for early diagenesis. In: Schulz, H.D., Zabel, M., (Eds.). Marine Geochemistry. 2nd ed. Springer: Germany p125-168.

Rutters, H., Sass, H., Cypionka, H., Rullkötter, J., 2001. Monoalkylether phospholipids in the sulfate-reducing bacteria *Desulfosarcina variabilis* and *Desulforhabdus amnigenus*. Archives of Microbiology 176, 435-442.

Sahling, H., Bohrmann, G., Spiess, V., Bialas, J., Breitzke, M., Ivanov, M., et al., 2008. Pockmarks in the Northern Congo Fan area, SW Africa: Complex seafloor features shaped by fluid flow. Marine Geology 249, 206-225.

Sargent, J.R., 1976. The structure, metabolism and function of lipids in marine organisms. In: Malins, D.C., Sargent, J.R., (Eds.). Biochemical and biophysical perspectives in marine biology Vol. 3. London: Academic Press p.149-212.

Sargent, J.R., Gatten, R.R., McIntosh, R., 1977. Wax esters in the marine environment — their occurrence, formation, transformation and ultimate fates. Marine Chemistry 5, 573-584.

Sarmiento, J.L., Gruber, N., 2006. Ocean Biogeochemical Dynamics. Princeton University Press, Princeton, NJ, p.503.

Schmidt, F., Hinrichs, K., Elvert, M., 2010. Sources, transport, and partitioning of organic matter at a highly dynamic continental margin. Marine Chemistry 118, 37-55.

Schouten, S., Rijpstra, W., Kok, M., Hopmans, E., Summons, R., Volkman, J., et al., 2001. Molecular organic tracers of biogeochemical processes in a saline meromictic lake (Ace Lake). Geochimica et Cosmochimica Acta 65, 1629-1640.

Schouten, S., Hopmans, E.C., Sinninghe Damsté, J.S., 2012. The organic geochemistry of glycerol dialkyl glycerol tetraether lipids: a review. Organic Geochemistry 54, 19-61.

Schouten, S., Sinninghe Damsté, J.S., de Leeuw, J.W., 1995. A novel triterpenoid carbon skeleton in immature sulphur-rich sediments. Geochimica et Cosmochimica Acta 59, 953-958.

Schrenk, M.O., Huber, J.A., Edwards, K.J., 2010. Microbial provinces in the subseafloor. Annual Review of Marine Science 2, 279-304.

Schroot, B., Schuttenhelm, R., 2003. Expressions of shallow gas in the Netherlands North Sea. Netherlands Journal of Geosciences 82, 91-106.

Schubert, C.J., Calvert, S.E., 2001. Nitrogen and carbon isotopic composition of marine and terrestrial organic matter in Arctic Ocean sediments: implications for nutrient utilization and organic matter composition. Deep Sea Research Part I 48, 789-810.

Schulz, H.D., 2006. Quantification of early diagenesis: Dissolved constituents in marine pore water. In: Schulz, H.D., Zabel, M. (Eds.) Marine Geochemistry, 2nd ed. Springer: Germany p124.

Shubenkova, O., Likhoshvai, A., Kanapatskii, T., Pimenov, N., 2010. Microbial community of reduced pockmark sediments (Gdansk Deep, Baltic Sea). Microbiology 79, 799-808.

Sibuet, M., Olu, K., 1998. Biogeography, biodiversity and fluid dependence of deep-sea cold-seep communities at active and passive margins. Deep Sea Research Part II 45, 517-567.

Simoneit, B.R.T., 1977. Organic matter in eolian dusts over the Atlantic Ocean. Marine Chemistry 5, 443-464.

Simoneit, B.R.T., Cardoso, J., Robinson, N., 1991. An assessment of terrestrial higher molecular weight lipid compounds in aerosol particulate matter over the South Atlantic from about 30–70^{o}S. Chemosphere 23, 447-465.

Simpson, A.J., Simpson, M.J., Smith, E., Kelleher, B.P., 2007. Microbially derived inputs to soil organic matter: are current estimates too low? Environmental Science and Technology 41, 8070-8076.

Simpson, M.J., Hatcher, P.G., 2004. Overestimates of black carbon in soils and sediments. Naturwissenschaften 91, 436-440.

Sinninghe Damsté, J.S., Rijpstra, W.I.C., Schouten, S., Peletier, H., van der Maarel, M.J.E.C., Gieskes, W.W.C., 1999. A C_{25} highly branched isoprenoid alkene and C_{25} and C_{27} *n*-polyenes in the marine diatom *Rhizosolenia setigera*. Organic Geochemistry 30, 95-100.

Söderberg, P., Flodén, T., 1992. Gas seepages, gas eruptions and degassing structures in the seafloor along the Strömma tectonic lineament in the crystalline

Stockholm Archipelago, east Sweden. Continental Shelf Research 12, 1157-1171.

Sørensen, K.B., Lauer, A., Teske, A., 2004. Archaeal phylotypes in cold metal-rich, low activity deep subsurface sediment off the Peru Basin, ODP Leg 201, Site 1231. Geobiology 2, 151-161.

Sørensen, K.B., Teske, A., 2006. Stratified communities of active archaea in deep marine subsurface sediments. Applied and Environmental Microbiology 72, 4596-4603.

Soter, S., 1999. Macroscopic seismic anomalies and submarine pockmarks in the Corinth–Patras rift, Greece. Tectonophysics 308, 275-290.

Sprott, G.D., Brisson, J.R., Dicaire, C.J., Pelletier, A.K., Deschatelets, L.A., Krishnan, L., et al. 1999. A structural comparison of the total polar lipids from the human archaea *Methanobrevibacter smithii* and *Methanosphaera stadtmanae* and its relevance to the adjuvant activities of their liposomes. Biochimica et Biophysica Acta 1440, 275-288.

Sprott, G.D., Dicaire, C.J., Choquet, C.G., Patel, G.B., Ekiel, I., 1993. Hydroxydiether lipid structures in *Methanosarcina* spp. and *Methanococcus voltae*. Applied and Environmental Microbiology 59, 912-914.

Sprott, G.D., Ekiel, I., Dicaire, C., 1990. Novel, acid-labile, hydroxydiether lipid cores in methanogenic bacteria. Journal of Biological Chemistry 265, 13735-13740.

Suess, E., 1980. Particulate organic carbon flux in the oceans - surface productivity and oxygen utilization. Nature 288, 260-263.

Sugimura, Y., Suzuki, Y., 1988. A high-temperature catalytic oxidation method for the determination of non-volatile dissolved organic carbon in seawater by direct injection of a liquid sample. Marine Chemistry 24, 105-131.

Sumida, P.Y.G., Yoshinaga, M.Y., Madureira, L.A.S.P., Hovland, M., 2004. Seabed pockmarks associated with deepwater corals off SE Brazilian continental slope, Santos Basin. Marine Geology 207, 159-167.

Sun, Q., Wu, S., Hovland, M., Luo, P., Lu, Y., Qu, T., 2011. The morphologies and genesis of mega-pockmarks near the Xisha Uplift, South China Sea. Marine and Petroleum Geology 28, 1146-1156.

Suzuki, Y., Sugimura, Y., Itoh, T., 1985. A catalytic oxidation method for the determination of total nitrogen dissolved in seawater. Marine Chemistry 16, 83-97.

Szpak, M., Monteys, X., O'Reilly, S., Simpson, A., Garcia, X., Evans, R.L., et al., 2012. Geophysical and geochemical survey of a large marine pockmark on the Malin Shelf, Ireland. Geochemistry Geophysics Geosystems 13, Q01011.

Takai, K., Horikoshi, K., 1999. Genetic diversity of archaea in deep-sea hydrothermal vent environments. Genetics 152, 1285-1297.

Takai, K., Moser, D.P., DeFlaun, M., Onstott, T.C., Fredrickson, J.K., 2001. Archaeal diversity in waters from deep South African gold mines. Applied and Environmental Microbiology 67, 5750-5760.

Teixidor, P., Grimait, J.O., Pueyo, J.J., Rodriguez-Valera, F., 1993. Isopranylglycerol diethers in non-alkaline evaporitic environments. Geochimica et Cosmochimica Acta 57, 4479-4489.

Teske, A.P., Sorensen, K.B., 2008. Uncultured archaea in deep marine subsurface sediments: have we caught them all? ISME Journal 2, 3-18.

Teske, A.P., 2006. Microbial communities of deep marine subsurface sediments: molecular and cultivation surveys. Geomicrobiology Journal 23, 357-368.

Tissot, B.P., Welte, D.H., 1984. Petroleum Formation and Occurrence. Springer-Verlag:Berlin.

Tornabene, T.G., Langworthy, T.A., Holzer, G., Oró, J., 1979. Squalenes, phytanes and other isoprenoids as major neutral lipids of methanogenic and thermoacidophilic “archaebacteria”. Journal of Molecular Evolution 13, 73-83.

Tunnicliffe, V., Juniper, S.K., Sibuet, M., 2003. Reducing environments of the deep-sea floor. In: Tyler, P.A. (Ed.). Ecosystems of the Deep Ocean: Ecosystems of the World Elsevier: London p81-110**.**

Upasani, V.N., Desai, S.G., Moldoveanu, N., Kates, M., 1994. Lipids of extremely halophilic archaeobacteria from saline environments in India: a novel glycolipid in Natronobacterium strains. Microbiology 140, 1959-1966.

Ussler, W., Paull, C.K., Boucher, J., Friederich, G., Thomas, D., 2003. Submarine pockmarks: a case study from Belfast Bay, Maine. Marine Geology 202, 175-192.

Valentine, D.L., 2011. Emerging topics in marine methane biogeochemistry. Annual Review of Marine Science 3, 147-171.

Valentine, D.L., 2002. Biogeochemistry and microbial ecology of methane oxidation in anoxic environments: a review. Antonie Van Leeuwenhoek 81, 271-282.

Valentine, D.L., Reeburgh, W.S., 2000. New perspectives on anaerobic methane oxidation. Environ Microbiology 2, 477-484.

Vaular, E.N., Barth, T., Haflidason, H., 2010. The geochemical characteristics of the hydrate-bound gases from the Nyegga pockmark field, Norwegian Sea. Organic Geochemistry 41, 437-444.

Venkatesan, M.I., 1988. Organic geochemistry of marine sediments in Antarctic region: Marine lipids in McMurdo Sound. Organic Geochemistry 12, 13-27.

Venkatesan, M.I., Mirsadeghi, F.H., 1992. Coprostanol as sewage tracer in McMurdo Sound, Antarctica. Marine Pollution Bulletin 25, 328-333.

Versteegh, G.J.M., Schefuß, E., Dupont, L., Marret, F., Sinninghe Damsté, J.S., Jansen, J.H.F., 2004. Taraxerol and Rhizophora pollen as proxies for tracking past mangrove ecosystems. Geochimica et Cosmochimica Acta 68, 411-422.

Vetriani, C., Jannasch, H.W., MacGregor, B.J., Stahl, D.A., Reysenbach, A.L., 1999. Population structure and phylogenetic characterization of marine benthic archaea in deep-sea sediments. Applied and Environmental Microbiology 65, 4375-4384.

Vogt, P.R., Crane, K., Sundvor, E., Max, M.D., Pfirman, S.L., 1994. Methane-generated (?) pockmarks on young, thickly sedimented oceanic crust in the Arctic: Vestnesa ridge, Fram strait. Geology 22, 255-258.

Volk, T., Hoffert, M.I., 1985. Ocean carbon pumps: Analysis of relative strengths and efficiencies in ocean-driven atmospheric CO2 changes. Geophysical Monograph Series 32, 99-110.

Volkman, J.K., 2006. Lipid markers for marine organic matter. In: Volkman, J.K. (Ed.) Marine Organic Matter: Biomarkers, Isotopes and DNA. Springer:Berlin p27-70.

Volkman, J.K., 2003. Sterols in microorganisms. Applied Microbiology and Biotechnology 60, 495-506.

Volkman, J.K., 1986. A review of sterol markers for marine and terrigenous organic matter. Organic Geochemistry 9, 83-99.

Volkman, J.K., Barrett, S.A., Blackburn, S.I., 1999. Eustigmatophyte microalgae are potential sources of C_{29} sterols, C_{22}-C_{28} n-alcohols and C_{28}-C_{32} n-alkyl diols in freshwater environments. Organic Geochemistry 30, 307-318.

Volkman, J.K., Barrett, S.M., Blackburn, S.I., Mansour, M.P., Sikes, E.L., Gelin, F., 1998. Microalgal biomarkers: A review of recent research developments. Organic Geochemistry 29, 1163-1179.

Volkman, J.K., Barrett, S.M., Dunstan, G.A., Jeffrey, S.W., 1992. C_{30} and C_{32} alkyl diols and unsaturated alcohols in microalgae of the class Eustigmatophyceae. Organic Geochemistry 18, 131-138.

Wakeham, S.G., Canuel, E.A., Lerberg, E.J., Mason, P., Sampere, T.P., Bianchi, T.S., 2009. Partitioning of organic matter in continental margin sediments among density fractions. Marine Chemistry 115, 211-225.

Wakeham, S., Canuel, E., 2006. Degradation and Preservation of Organic Matter in Marine Sediments. In: Volkman, J.K. (Ed.) Marine Organic Matter: Biomarkers, Isotopes and DNA. Springer:Berlin p295-321.

Walinsky, S.E., Prahl, F.G., Mix, A.C., Finney, B.P., Jaeger, J.M., Rosen, G.P., 2009. Distribution and composition of organic matter in surface sediments of coastal Southeast Alaska. Continental Shelf Research 29, 1565-1579.

Webb, K.E., Hammer, Ø., Lepland, A., Gray, J.S., 2009. Pockmarks in the inner Oslofjord, Norway. Geo-Marine Letters 29, 111-124.

Wegener, G., Shovitri, M., Knittel, K., Niemann, H., Hovland, M., Boetius, A., 2008. Biogeochemical processes and microbial diversity of the Gullfaks and Tommeliten methane seeps (Northern North Sea). Biogeoscience Discussions 5, 971- 1015.

Westerhausen, L., Poynter, J., Eglinton, G., Erlenkeuser, H., Sarnthein, M., 1993. Marine and terrigenous origin of organic matter in modern sediments of the equatorial East Atlantic: the $\delta^{13}C$ and molecular record. Deep Sea Research Part I 40, 1087-1121.

White, D.C., Davis, W.M., Nickels, J.S., King, J.D., Bobbie, R.J., 1979. Determination of the sedimentary microbial biomass by extractible lipid phosphate. Oecologia 40, 51-62.

White, D.C., Ringelberg, D.B., Macnaughton, S.J., Srinivas, A., David, S., 1997. Signature Lipid Biomarker Analysis for Quantitative Assessment In Situ of Environmental Microbial Ecology. In: Eganhouse, R.P. (Ed.) Molecular markers in environmental chemistry. American Chemical Society, ACS Symposium Series 671 p22-34.

Whiticar, M.J., 2002. Diagenetic relationships of methanogenesis, nutrients, acoustic turbidity, pockmarks and freshwater seepages in Eckenförde Bay. Marine Geology 182, 29-53

Whitman, W.B., Coleman, D.C., Wiebe, W.J., 1998. Prokaryotes: the unseen majority. Proceedings of the National Academy Sciences 95, 6578-6583.

Woese, C.R., Fox, G.E., 1977 Phylogenetic structure of the prokaryotic domain: the primary kingdoms. Proceedings of the National Academy Sciences 74, 5088-5090.

Wuebbles, D.J., Hayhoe, K., 2002. Atmospheric methane and global change. Earth Science Reviews 57, 177-210.

Xu, Y., Jaffé, R., 2007. Lipid biomarkers in suspended particles from a subtropical estuary: Assessment of seasonal changes in sources and transport of organic matter. Marine Environmental Research 64, 666-678.

Yunker, M.B., Belicka, L.L., Harvey, H.R., Macdonald, R.W., 2005. Tracing the inputs and fate of marine and terrigenous organic matter in Arctic Ocean sediments: A multivariate analysis of lipid biomarkers. Deep Sea Research Part II 52, 3478-3508.

Chapter 2

Biomarkers reveal the effects of hydrography on the sources and fate of marine and terrestrial organic matter in the western Irish Sea

This chapter has been accepted to Estuarine, Coastal and Shelf Science:

O'Reilly, S.S., Szpak, M.T., Flanagan, P.V., Monteys, X., Murphy, B.T., Jordan, S.F., Allen, C.C.R, Simpson, A.J., Mulligan, S.M., Sandron, S., Kelleher, B.P., 2013. Biomarkers reveal the effects of hydrography on the sources and fate of marine and terrestrial organic matter in the western Irish Sea. Estuarine, Coastal and Shelf Science, accepted manuscript.

2.1 Introduction

Cycling of organic matter (OM) is the key biological process in the marine environment (Chester and Jickells, 2012). Knowledge of sources and the reactivity of OM, in addition to factors controlling its distribution in estuarine, coastal and shelf sediments are of key importance for understanding global biogeochemical cycles (Baldock et al., 2004). Marine systems contribute an estimated 44 to 50 GtC a^{-1} of new OM to the biosphere and are approximately equal to the terrestrial system (Harvey, 2006). Continental margins account for approximately 90% of global sedimentary organic matter (SOM) and thus are an important component of the marine organic matter (MOM) pool (Hedges and Keil, 1995). Coastal and shelf SOM is typically derived from a complex distribution of autochthonous water column sources, in addition to allochthonous terrestrial sources. The sources and fate of MOM in these settings are diverse and dependent on the intensity of both autochthonous and allochthonous input (Harvey, 2006). In addition differences in OM molecular composition, regional sedimentological and oceanographic regimes, and processes mediating the preservation and mineralisation of OM are important parameters in MOM cycling (Hedges and Keil, 1995).

Autochthonous SOM is primarily derived from particulate sinking detritus from the photic zone, whereby the OM flux is typically proportional to the amount of primary production and inversely so with water depth (Rullkötter, 2006). This is reflected in the fact that in coastal settings 25 to 50% of primary production reaches the seafloor, compared to typically less than 1% in deep sea settings (Suess 1980). Rivers transport about 1% of terrestrial productivity (60 Gt C a^{-1}) to the marine environment, while aeolian input can be an order of magnitude lower (~0.1 Gt C a^{-1}) (Hedges et al., 1997). Thus riverine input is the major source of terrestrial OM (TOM) in marine settings, in particular in coastal and shelf settings. Despite significant attention for a number of decades, the fate of TOM in the marine environment remains poorly understood (Hedges et al., 1997; Baldock et al., 2004).

The Irish Sea, lying between the landmasses of Great Britain and Ireland, has received little attention from the perspective of OM cycling. Although relatively small in size, it is characterised by large regional differences in oceanographic and sedimentological conditions, nutrient chemistry and ecology (Kennington and Rowlands, 2006). In particular a seasonal gyre occurs in the western Irish Sea each year, and is formed when thermal stratification isolates a dome of cold dense bottom

water in the deep (> 100 m) western Irish Sea basin. The resulting density fields drive a cyclonic gyre, which dominates the circulation of the region during late spring and summer and separates the surrounding well-mixed areas by tidal mixing fronts (Hill et al., 1994; Horsburgh et al., 2000). Frontal zones are generally considered high productivity settings (Tolosa et al., 2005) and mean chlorophyll concentrations between well-mixed (~ 23 mg m^{-3}) and stratified offshore waters (~ 16 mg m^{-3}) in the western Irish Sea attest to this (Gowen and Stewart, 2005). It has been proposed that this summer gyre may act as a retention system for planktonic larvae of commercially valuable *Nephrops norvegicus* (Hill et al., 1996), for larval and juvenile fish, and for zooplankton (Dickey-Collas et al., 1996, 1997), and possibly for anthropogenic contaminants (Hill et al., 1997). Furthermore, documented changes in the Irish Sea as a result of anthropogenic activity include: increases in nutrient concentrations and primary productivity (Allen et al., 1998); an increase in mean sea surface temperature of about 1°C over the last four decades; and also distinct regional differences in salinity and nutrient relationships and in the timing and duration of phytoplankton blooms (Evans et al., 2003). It is evident that without baseline knowledge of natural processes it will be difficult to ascertain the environmental and ecological effects of climate change.

However, despite the fundamental role of OM in the marine environment and for marine ecosystems, few studies have focused on OM cycling in the Irish Sea (Gowen et al., 1995, 2000; Trimmer et al., 1999, 2003), and to our knowledge none have studied the composition, sources and fate of OM in the Irish Sea. In this study we applied a suite of molecular level lipid biomarkers in conjunction with bulk physical and chemical parameters to study TOM and MOM cycling in surface sediments and net tow particulate matter collected from well-mixed coastal and offshore summer-stratified waters in the western Irish Sea. Although lipids represent a small fraction of OM, their diversity, specificity and relative recalcitrance makes them useful for studying the sources, transport and fate of OM, especially when combined with other bulk measurements and compound specific stable carbon isotope ($\delta^{13}C$) analysis (e.g. Westerhausen et al., 1993; Zimmerman and Canuel, 2001; Belicka et al., 2002, 2004; Jeng et al., 2003; Schmidt et al., 2010; Burns and Brinkman, 2011). This study combined analysis of biomarkers with typically high preservation potential (e.g. *n*-alkanes, sterols) with biomarkers with low preservation potential (e.g. ester-linked phospholipids; White et al., 1979, 1997) across the mixed and stratified zones. Thus

the aims of this study were to: (i) investigate the relative contribution of marine and terrestrial input to SOM in coastal and offshore surface sediments; (ii) elucidate likely transport mechanisms by investigating the spatial distribution of SOM; and (iii) investigate whether the distinct seasonal gyre plays a role in transport and fate of OM in this setting.

2.2 Oceanographic and Environmental Setting

The Irish Sea (Fig. 2.1) is connected with the Atlantic Ocean by the North Channel on the north and St. George's Channel on the south. Water depths range from less than 20 m in the coastal areas and bays to over 100 m in the central region. Localised depressions of 130 to over 200 m also occur. Water transport through the sea is generally considered to be northwards, with flow rates in the region of 2 to 8 km^3 d^{-1} (Gowen and Stewart, 2005, and references therein), but there is also exchange to the North and seawater movement tends to be highly variable (Kennington and Rowlands, 2006). Local meteorological conditions are known to have a major influence on transport through the two channels (Knight and Howarth, 1999). Waters are generally well mixed throughout the Irish Sea and ensure vertically homogeneous water column conditions over the year (Hill et al., 1994). However, waters in the western region are generally deeper (> 100 m), exhibit lower tidal energies and have higher salinity values (Gowen et al., 1995), factors attributing to the strong seasonal gyre that develops in the summer months upon onset of the summer thermocline (Hill et al., 1994). This results in an offshore summer stratified region (SSR), which is distinct from coastal and southern mixed regions (CMR and SMR respectively) (Fig. 2.1). The northwest region (north of 53.2°N) is characterised by weaker hydrodynamic conditions, allowing the deposition of fine-grained particles and is dominated by a smooth muddy seabed. This is in contrast to the southern region (south of 53.2°N), which is subject to comparatively high-energy currents and is characterised by gravelly sands and cobbles and high energy bedforms such as sand streaks, sand ribbons, gravel furrows and sand waves (Croker et al., 2005). Thus sediment type closely reflects the distinct hydrographic zones in the western Irish Sea (Trimmer et al., 2003). The Irish Sea has an estimated total catchment area of about 43,000 km^2, whereby the greatest freshwater input is understood to be in the eastern Irish Sea, from the Solway Firth to Liverpool Bay (Bowden, 1980).

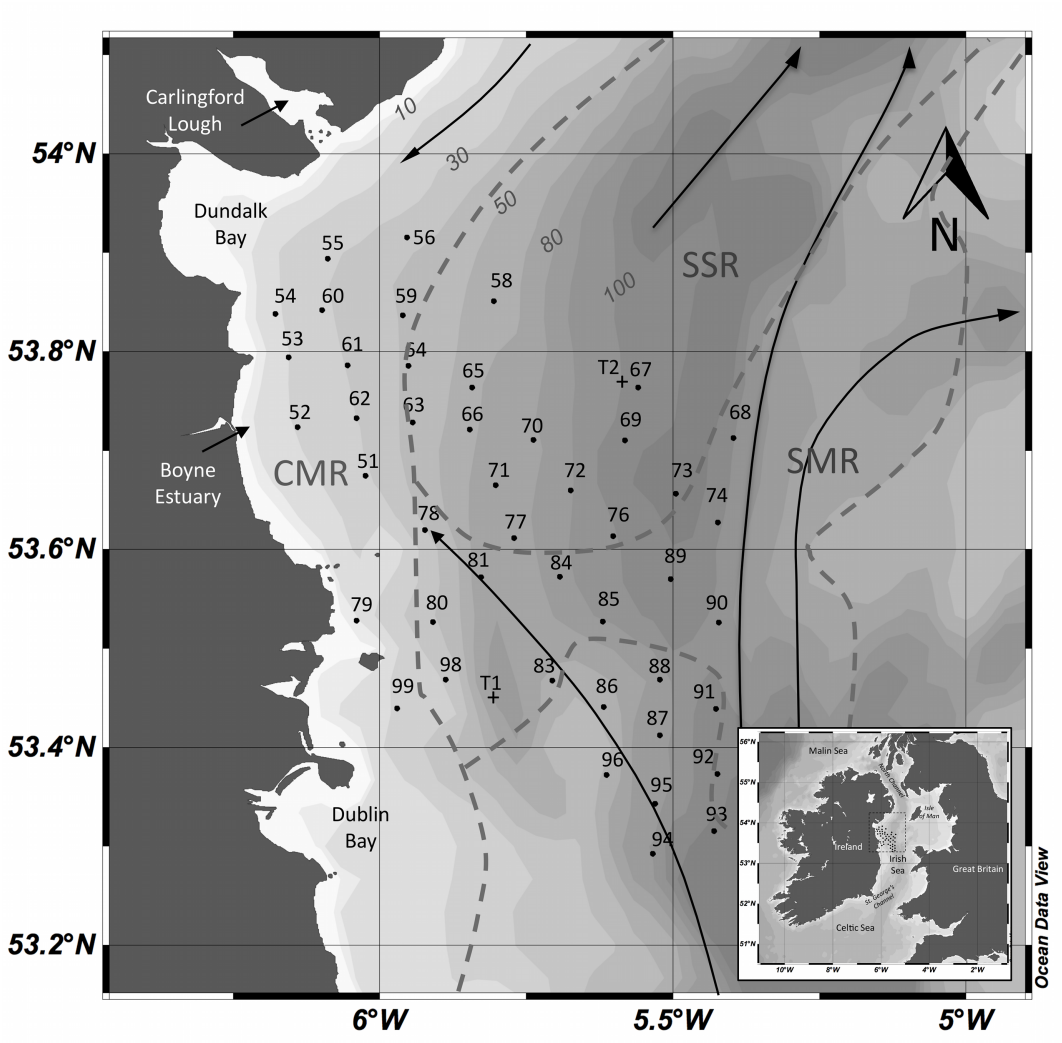

Figure 2.1. Map of the Irish Sea and study area location. Sediment boxcore stations are numbered and marked with a black circle. Plankton net tow stations are shown as crosses (T1 and T2). Broken grey lines represent approximate summer hydrographic regions (from Gowen et al., 1995) and black arrows represent the near-bottom residual circulation (from Ramster et al. 1969). SSR – Summer Stratified Region, CMR – Coastal Mixed Region, SMR – Southern Mixed Region.

2.3 Materials and Methods

2.3.1 Sampling and bulk analysis

Surface sediments were sampled in June 2010 during INFOMAR (Integrated Mapping for the Sustainable Development of Ireland's Marine Resource) survey CV10_28 aboard the RV Celtic Voyager. Sediment pushcores (n = 55) were taken using a Reineck boxcorer. Samples for lipid analysis were stored at -20°C onboard and at -20°C in the laboratory. Vertical tow nets (30 cm diameter, 20 μm mesh size) were deployed in vertical haul (0 to 30 m water depth) at two stations, T1 in waters in the SMR and T2 in waters in the SSR (Fig. 2.1). Two casts were deployed at each

station and pooled together to yield a representative sample. Large debris and larger organisms were removed and the particulates were vacuum-filtered through pre-combusted GF/A filters. Particle size analysis (n = 50) was performed with laser granulometry (Malvern MS2000). For total organic carbon (TOC) and total nitrogen (TN) analysis, sediment (n = 20) was sub-sampled from 0 to 2 cm from pushcores and inorganic carbon was removed by addition of 1 M HCl and analysed using an Exeter Analytical CE440 elemental analyser.

2.3.2 Lipid biomarker analysis

Sediment samples (0 to 2 cm) were freeze-dried, ground and sieved, while plankton net tow samples were filtered through pre-furnaced GF/A filters and subsequently freeze-dried. Freeze-dried samples were extracted by a modified Bligh-Dyer method (White et al., 1997). After addition of 2:1:0.8 (v/v) methanol, chloroform and phosphate buffer (pH 7.2), samples were sonicated for 2 min and subsequently extracted on a horizontal shaker for 18 hr. After centrifugation, organic and aqueous phases from the supernatant were split by addition of solvent to achieve a solvent ratio 1:1:0.9 (v/v). The total extract was collected and concentrated by rotary evaporation. After desulfurisation with activated copper overnight, extracts were fractionated by solid phase extraction according to Pinkart et al. (1998). Briefly, a portion of total extract was added to aminopropyl cartridges (Alltech 500 mg Ultra-Clean) and eluted with 5 mL chloroform (neutrals), 5 mL acetone (glycolipids), and finally with 5 mL 6:1 (v/v) methanol/chloroform, followed by 5 mL 0.05 M sodium acetate in 6:1 (v/v) methanol/chloroform. These were combined to comprise the polar lipid fraction.

The neutral lipid fractions were derivatised with N,O-bis(trimethylsilyl)trifluoroacetamide/pyridine (9:1, v/v) (70°C, 2.5 hr). Phospholipids in the polar fraction were derivatised using 0.5 M sodium methoxide (50°C, 30 min). PLFA monounsaturation position was confirmed by formation of dimethyl disulfide adducts as outlined by Nichols et al. (1986). One microlitre aliquots of derivatised extracts were injected in splitless mode onto an Agilent 6890N gas chromatograph interfaced with an Agilent 5975C mass spectrometer (MS). Separation was achieved on a HP-5MS fused silica capillary column (Agilent: 30 m x 0.25 mm I.D. and film thickness of 0.25 μm). The injector and MS source were held at 280°C and 230°C, respectively. The column temperature program was as follows: 65°C injection and hold for 2 min, ramp at 6°C min^{-1} to 300°C; followed by isothermal hold at 300°C for

20 min. The MS was operated in electron impact mode with an ionisation energy of 70 eV and a mass scan range set from m/z 50 to 650. Data was acquired and processed using Chemstation software (revision 2.0 E). All reported compounds were confirmed using a combination of mass spectral libraries, interpretation of mass fragmentation patterns, compound retention times and by comparison with literature. 5-α-cholestane was used as an internal standard and procedural blanks were run to monitor background interferences. See Appendix A for details of GC-MS analyte quantification.

Selected samples (BC52, BC72, BC78, BC85) were analysed by a gas chromatograph under conditions as described above, but coupled to a continuous flow isotope ratio mass spectrometer (IsoPrime) via a combustion furnace (GC5, CuO/Pt 650). $\delta^{13}C$ values were measured against a reference gas CO_2 of known $\delta^{13}C$ value. $\delta^{13}C$ values were reported against a stable isotope reference standard (*n*-alkanes mixture B2, Indiana University, US; See Appendix B). All samples were measured in duplicate and average $\delta^{13}C$ values are reported after correction for addition of derivative groups where necessary. The standard deviation for the instrument, based on replicate standard injection was calculated to be ± 1.00‰ or better. Only well-resolved major analytes are reported here, and are limited to major compounds within biomarker classes.

2.3.3 Data and statistical analysis

Biomarker data is primarily expressed relative to TOC or percentage abundance rather than simply against dry mass weight of sediment. This helps remove gross variation based solely on grain size and helps identify changes in relative input (e.g. Canuel and Martens, 1993; Westerhausen et al., 1993; Hu et al., 2006; Belicka et al., 2004). Statistically significant correlations between measured bulk parameters and biomarker classes were calculated using PAST by calculating Pearson correlation coefficients (*r*) with PAST software (v1.75) (Hammer et al., 2001). *P* values less than 0.05 were considered statistically significant. Distribution maps of lipid biomarker data were constructed in Ocean Data View (Schlitzer, 2002) using the diva gridding algorithm. Hierarchical cluster analysis was performed in PAST in an attempt to simplify multivariate data. Ward's minimum variance method (Ward Jr, 1963) was used to cluster bulk and lipid biomarker data shown in Table 2.1.

Table 2.1. Boxcore sample station locations and summary of bulk parameters and biomarker data

Station	BC51	BC52	BC53	BC54	BC55	BC56	BC58	BC63	BC64	BC65	BC66	BC67	BC70	BC72	BC73	BC76	BC78	BC79	BC81	BC85
Latitude	53.675	53.724	53.794	53.838	53.894	53.916	53.851	53.728	53.786	53.764	53.721	53.764	53.711	53.660	53.656	53.613	53.620	53.528	53.572	53.527
Longitude	-6.024	-6.140	-6.155	-6.178	-6.089	-5.954	-5.806	-5.944	-5.951	-5.843	-5.847	-5.559	-5.738	-5.675	-5.495	-5.602	-5.923	-6.040	-5.828	-5.620
Depth (m)	29.6	19.1	24.4	21.5	31.9	41.9	41.9	42.8	42.8	54.1	54.9	102.7	77.7	90.7	110.8	102.7	45.5	12.4	66.6	95.8
Grain Size	3.06	3.11	3.83	3.54	3.04	4.4	5.18	4.01	4.13	4.59	4.36	5.46	4.91	4.93	4.36	4.91	3.05	2.31	3.28	3.19
Sorting	2.1	2.1	2.2	1.9	2.2	2.2	2.0	2.2	2.2	2.2	2.2	1.9	2.0	2.1	2.3	2.1	1.9	1.0	2.0	2.4
Clay (%)	6.8	9.0	13.3	8.2	9.0	20.6	24.0	15.0	15.8	19.5	17.3	27.2	20.4	23.5	20.6	26.3	6.1	0.7	8.6	12.0
Silt (%)	20.1	17.9	39	28	24.3	57.7	66.2	44.5	47.9	58.1	54.2	66.2	64.9	60.9	49	58.2	16.8	4.4	23.6	25.4
Mud (%)	26.9	26.9	52.3	36.2	33.3	78.3	90.2	59.5	63.7	77.6	71.5	93.4	85.4	84.4	69.6	84.5	22.9	5.1	32.3	37.4
Sand (%)	73.1	73.1	47.7	63.8	66.7	21.7	9.8	40.5	36.3	22.4	28.5	6.6	14.6	15.6	30.4	15.5	77.1	94.9	67.7	62.6
TOC (%)	0.4	0.55	1.09	0.67	0.83	1.05	1.21	0.65	1.15	1.19	1.01	1.57	1.18	1.27	1.52	1.33	0.66	0.09	0.75	1.07
TN (%)	0.04	0.05	0.11	0.02	0.05	0.12	0.12	0.06	0.07	0.11	0.08	0.18	0.13	0.13	0.12	0.11	0.03	nd	0.06	0.08
C/N	10.5	11.0	9.9	33.5	16.6	8.8	10.1	10.8	16.4	10.8	12.6	8.7	9.1	9.8	12.7	12.1	22.0	nd	12.5	13.4
LC_{HC}	147	167	319	116	90	138	78	96	65	109	100	87	102	89	77	129	54	135	67	125
CPI_{HC}	3.8	3.1	3.4	5.3	2.1	4	3.4	3.2	3.7	2.6	3.5	2.8	3.3	2.9	3.2	2.6	3	2.4	2.6	3.5
LC_{OH}	116	166	299	84	110	183	77	89	59	108	115	72	86	78	63	121	54	159	86	156
CPI_{OH}	5.1	5.7	11.6	7	8.4	7.4	6.8	5.7	6.7	6	6.5	6.5	6.1	6	6.3	5.9	10.8	4.5	6.2	8.1
Σsterols	299	392	731	276	346	817	165	47	115	207	479	143	201	129	142	247	262	907	454	361
ΣC_{26}	17	21	32	16	14	31	9	nd	8	13	18	10	14	10	9	15	11	60	30	16
ΣC_{27}	107	141	223	100	123	203	38	16	29	56	109	37	66	31	43	75	99	363	129	137
ΣC_{28}	101	132	255	91	114	378	61	11	40	68	221	54	58	44	46	78	90	258	204	110
ΣC_{29}	59	83	181	58	73	168	45	7	30	54	108	33	50	33	36	64	50	203	76	79
ΣC_{30}	15	15	40	11	22	38	12	12	9	15	23	10	13	11	9	15	12	23	14	18
ΣPLFA	1188	564	317	749	575	355	481	211	280	223	502	502	557	252	208	199	378	1351	999	577
ΣSATFA	344	174	94	206	183	114	146	82	83	60	151	127	156	91	63	53	139	420	315	164
ΣMUFA	483	233	117	290	227	140	183	66	109	90	180	186	215	96	86	79	147	521	359	215
ΣPUFA	124	54	18	72	50	22	24	3	17	19	38	39	50	9	17	18	30	97	144	67
ΣbrFA	237	103	89	183	115	79	128	61	72	55	133	151	136	57	43	48	62	312	181	130
Phytol	7	8	17	5	15	34	3	2	2	6	19	7	6	4	3	6	5	13	18	10
Pristane	1	1	23	3	2	23	4	1	<1	14	2	2	1	<1	2	1	2	2	2	2
Phytane	nd	nd	52	1	1	50	2	<1	<1	29	<1	<1	<1	<1	1	<1	nd	2	<1	<1
Phytadienes	17	7	nd	11	9	6	9	3	5	nd	14	8	9	5	6	nd	nd	12	26	nd
C_{25} HBI	15	10	8	6	8	16	5	nd	2	5	11	3	4	1	6	5	nd	4	5	nd
Terpenoids	6	6	11	4	4	11	3	6	3	5	7	3	4	4	5	7	5	8	8	12

All biomarker data reported in μg g OC^{-1}; nd – not detected; LC_{HC} – Long chain odd carbon number *n*-alkanes; CPI_{HC} – $0.5[(C_{25}+C_{27}+C_{29}+C_{31}+C_{33})/(C_{24}+C_{26}+C_{28}+C_{30}+C_{32})+(C_{25}+C_{27}+C_{29}+C_{31}+C_{33})/(C_{26}+C_{28}+C_{30}+C_{32}+C_{34})$ (Zhang et al., 2006); LC_{OH} – Long chain even carbon number *n*-alkanols; CPI_{OH} – $0.5[(C_{24}+C_{26}+C_{28}+C_{30}+C_{32})/(C_{23}+C_{25}+C_{27}+C_{29}+C_{31})+(C_{24}+C_{26}+C_{28}+C_{30}+C_{32})/(C_{25}+C_{27}+C_{29}+C_{31}+C_{33})$ (Zhang et al., 2006); PLFA – Phospholipid fatty acids; SATFA – Saturated fatty acids; MUFA – Monounsaturated fatty acids; PUFA – Polyunsaturated fatty acids; brFA – branched (and cyclic) fatty acids; C_{25} HBI – C_{25} Highly branched isoprenoids

2.4 Results

2.4.1 Bulk physical and chemical parameters

Results for bulk physical and chemical analysis for the twenty boxcore stations studied in detail are shown in Table 2.1. Sediment grain size ranged from 26 µm to 1467 µm across the region, with a clear distribution of fine-grained poorly to very poorly sorted silty sand/sandy silt north of 53.5°N and moderately sorted to well sorted sand to the south (Fig. 2.2A to C). A strong positive correlation between clay and silt fractions and water depth was observed (clay; $r = 0.68$, $P = 0.001$). Offshore, silt and clay accounts for 50 to over 70% and 15 to over 25% of sediment type in this region, respectively (clay; Fig. 2.2D). There was a stronger correlation between clay and water depth compared to silt ($r = 0.68$ compared to 0.53). TOC ranged from 1.57% in deeper waters in the centre of the mudbelt i.e. the SSR, to 0.03% south of the mudbelt closer to the coast i.e. the SMR (Fig. 2.2E), and are in agreement with previous reports (Charlesworth and Gibson, 2002).

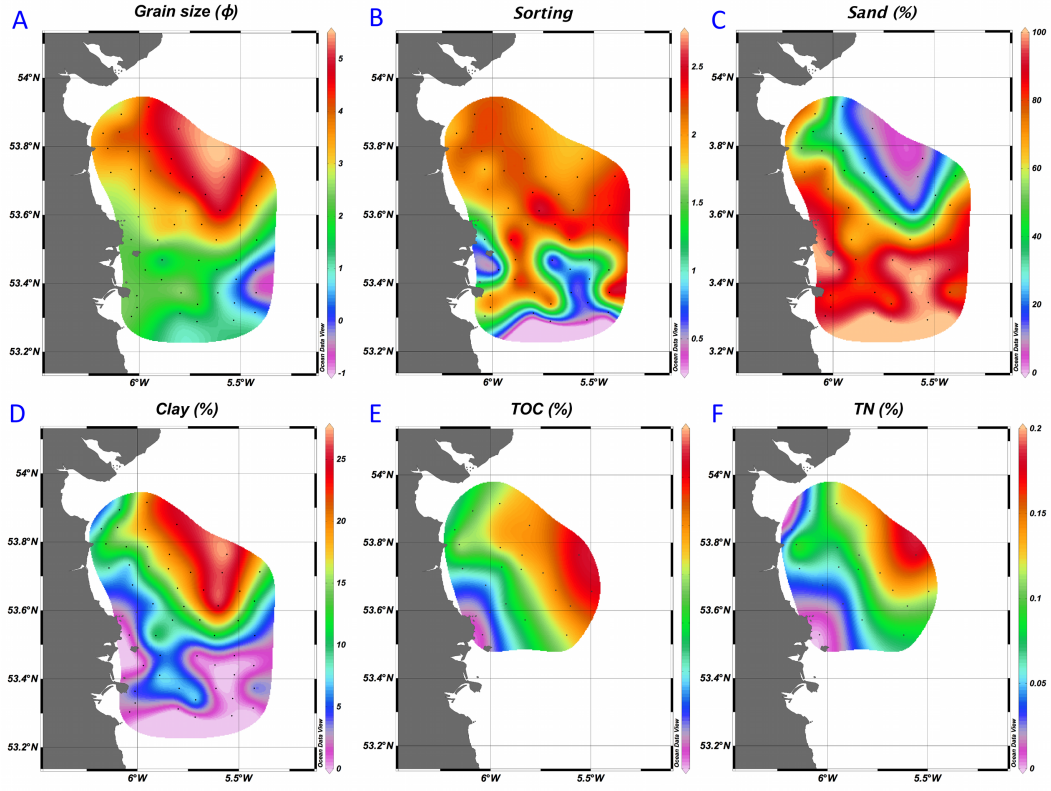

Figure 2.2. Spatial distribution of bulk physical and chemical parameters in western Irish Sea surface sediments: A. grain size (ϕ); B. sorting; C. sand (%); D. clay (%); E. total organic carbon (TOC; %); and F. total nitrogen (TN; %).

TOC is very strongly positively correlated with mud (r = 0.86, P <0.001), and exhibits a stronger correlation with the clay fraction (r = 0.89, P <0.001) compared to silt (r = 0.84, P <0.001). TN distribution largely reflects TOC (Fig. 2.2F) and also displays similar correlations to slay and silt. C/N values ranged from 8.7 in the deepest offshore station (BC67) to over 33.5 in fine-grained coastal sediment at BC54.

Table 2.2: Plankton vertical tow net sampling stations and summary of biomarker data.

Station	T1	T2
Region	Mixed	Stratified
Latitude	53.4422	53.7638
Longitude	-5.8114	-5.5590
Σsterols	1428.2	413.4
ΣC_{26}	111.3	31.2
ΣC_{27}	962.5	210.8
ΣC_{28}	251.5	129.5
ΣC_{29}	73.1	30.4
ΣC_{30}	29.8	11.5
ΣPLFA	1080.0	439.8
ΣSATFA	515.5	252.2
ΣMUFA	211.1	120.8
ΣPUFA	333.1	59.2
ΣbrFA	20.4	7.6
Alkanols	207.6	12.9
Alkenols	247.0	31.1
Phytol	27.8	21.0
WE	954.8	11.7
ΣHydrocarbons	28.2	45.9
Alkanes	3.2	4.7
Alkenes	1.5	4.8
C_{25} HBI	12.5	16.5
Phytadienes	7.6	19.3
Pristane	3.3	0.6
Phytane	nd	nd

All biomarker data reported in μg g dw^{-1}, nd – not detected

2.4.2 Aliphatic hydrocarbons and alcohols

Aliphatic hydrocarbons and alcohols observed in surface sediments and particulate matter are summarised in Table 2.1 and 2.2, respectively. Compound and compound class abbreviations used throughout the text are detailed in Table 2.3. *n*-alkanes and *n*-alkanols were among the major lipids found in the neutral lipid fractions from these surface sediments (Table 2.1). *n*-alkanes ranged from C_{16} to C_{33}, with LC_{HC} being most abundant (24.7 to 63.3% of total). $C_{29:0}$ was the most abundant LC_{HC} at most stations. *n*-alkanols ranged from C_{14} to C_{32} and were dominated by LC_{OH} (61.4 to 77.7% of total). LC_{HC} and LC_{OH} were very strongly positively correlated (r = 0.96, P < 0.001) and their spatial distribution was similar overall, with the highest abundance found in fine-grained coastal sediments (highest at BC53; Table 2.1). No significant correlation was observed for LC_{HC} or LC_{OH} and water depth, grain size or sediment

type. However TOC and TN were strongly correlated with these lipids classes, whereby TN exhibited stronger correlations. When normalised to TOC, LC_{OH} and LC_{HC} revealed clear distributions, whereby a transition from highest concentrations in the CMR and SMR to lowest concentrations in the SSR was evident (Fig. 2.3B and C). The CPI_{HC}, defined following the equation of Zhang et al. (2006) (see Table 2.1 for the complete equation) was 3.2 on average and ranged from 2.1 to 5.3. Calculated CPI_{OH} averaged 6.9 and ranged from 4.5 to 11.6. CPI_{HC} and CPI_{OH} were highest in fine-grained coastal sediments in the CMR (Fig. 2.3D; CPI_{OH}). $\delta^{13}C$ values for measured LC_{OH} ranged from -34.86 ± 0.10 to -35.93 ± 0.21‰, while for LC_{HC} ranged from -32.48 ± 0.11 to -33.35 ± 0.71‰ (Fig. 2.4).

n-alkanes were also identified in particulate matter but in contrast to sediments were limited to C_{15} (most abundant), C_{18}, C_{19} and C_{22}. $C_{19:1}$ also occurred and was more abundant than the *n*-alkanes, in particular at T2. Pristane was observed in highest abundance at stations BC53, BC56 and BC65 up to 23 ug g OC^{-1}. Generally however, concentrations were less than 2 µg g OC^{-1}. Pristane was found in much higher concentrations (3.3 µg g dw^{-1}) at T1 in the CMR compared to T2 in the SSR (0.6 µg g dw^{-1}). Phytane was present at most boxcore stations and was found at highest concentrations in BC53, BC56 and BC65 (up to 52 µg g OC^{-1}), while it was not detected at either net tow stations. At these stations phytane was over double the abundance of pristane while at all other boxcore stations abundance of pristane was more abundant. Phytadienes were observed (reported cumulatively) at much higher abundance at T2. In total hydrocarbons were about twice the concentration at T2 compared to T1 (29.4 compared to 15.7 ug g dw^{-1} respectively).

n-alkanols were also found in high abundance in net tows and ranged from C_{14} to C_{26}. However, in contrast to the aliphatic hydrocarbons, alcohols were found in much higher abundance at T1 (501.1 ug g dw^{-1}) compared to T2 (65.1 ug g dw^{-1}). In addition *n*-alkenols occurred in high abundance, and represented 51% of total aliphatic alcohols at T1 and 48% at T2. These included C_{16}, C_{18}, C_{20}, C_{22}, C_{24} and C_{26} alkenols. *n*-alkenols less than C_{20} were not observed at T2 and at both stations $C_{22:1}$ was the major homolog. Methyl-branched alkanols were also observed at T1 but not at T2, and ranged from C_{14} to C_{18} chain lengths. Phytol was present at all sediment stations and ranged from 2 ug g OC^{-1} up to 34 ug g OC^{-1}. In the net tows abundances were 27.8 ug g dw^{-1} and 21.0 ug g dw^{-1} for T1 and T2 respectively. Phytol was strongly positively correlated with the sterol classes and C_{25} HBIs. In particular a very

strong positive correlation was observed between phytol and C_{28} sterols ($r = 0.93$, $P < 0.0001$).

Table 2.3. Summary of major biomarkers, biomarkers classes and proxies used, with abbreviations used in the text and references.

Biomarker	Abbreviation/ Name used	Likely Source
Sterols		
24-norcholesta-5, 22-dien-3β-ol	$C_{26}\Delta^{5,22}$	Zooplankton, degradation of phytoplankton sterols[1]
24-norcholesta-22-en-3β-ol	$C_{26}\Delta^{22}$	
22-trans-cholesta-5,22-dien-3β-ol	$C_{27}\Delta^{5,22}$	Zooplankton detritus[2]
trans-27-nor-24-methyl-cholest-22-en-3β-ol	$C_{27}\Delta^{22}$	Dinoflagellates[3], benthic invertebrates[4]
cholest-5-en-3β-ol	$C_{27}\Delta^{5}$	Macrofauna, zooplankton biomass/detritus[5]
5-α(H)-cholestan-3β-ol	$C_{27}\Delta^{0}$	Bacterial reduction of C_{27} stenols[6]
cholesta-5,24-dien-3β-ol	$C_{27}\Delta^{5,24}$	Marine phytoplankton, diatoms[5]
24-methylcholesta-5,22-dien-3β-ol	$C_{28}\Delta^{5,22}$	Marine phytoplankton, diatoms[1,7]
24-methylcholesta-22-en-3β-ol	$C_{28}\Delta^{22}$	Marine invertebrates (sponges)[8], phytoplankton[9]
24-methylcholesta-5-en-3β-ol	$C_{28}\Delta^{5}$	Higher plants[10], green algae[1]
24-methyl-5-α(H)-cholestan-3β-ol	$C_{28}\Delta^{0}$	Bacterial reduction of C_{28} stenols[6]
24-methylcholesta-5-24(28)-dien-3β-ol	$C_{28}\Delta^{5,24(28)}$	Diatoms, marine phytoplankton[1,7]
24-ethylcholesta-5,22-dien-3β-ol	$C_{29}\Delta^{5,22}$	Terrestrial higher plants[10], some marine algae[11]
24-ethylcholesta-5-en-3β-ol	$C_{29}\Delta^{5}$	Terrestrial higher plants[10], some marine algae[11]
24-ethylcholesta-5,24(28)-dien-3β-ol	$C_{29}\Delta^{5,24(28)}$	Green microalgae[1]
4α,23,24-trimethyl-5α-cholesta-22-en-3β-ol	$C_{30}\Delta^{22}$	Dinoflagellates[1,5]
Phospholipid fatty acids		
Saturated straight chain fatty acids	SATFA	Marine plankton, non-specific[12,13,14]
Monounsaturated straight chain fatty acids	MUFA	Marine plankton, non-specific[12,13,14]
Polyunsaturated fatty acids	PUFA	Marine plankton[13,14,15]
branched (and cyclic fatty acids)	brFA	Bacterial biomass[16]
Eicosapentaenoic acid	$C_{20:5\omega3}$	Marine microalgae, diatoms[2,11]
Docosahexaenoic acid	$C_{22:6\omega3}$	Dinoflagellates, zooplankton[2,13,17]
9-cis-hexadecenoic acid	$C_{16:1\omega7}$	Marine microalgae[11,12], bacterial biomass[16]
11-cis-octadecenoic acid	$C_{18:1\omega7}$	
Long chain odd carbon *n*-alkanes (C_{25} to C_{33})	LC_{HC}	Terrestrial higher plants[18,19]
Long chain even carbon *n*-alcohols (C_{26} to C_{32})	LC_{OH}	
n-alkane carbon preference index	CPI_{HC}	Terrestrial vs. marine proxy[20,21,22]
n-alkanol carbon preference index	CPI_{OH}	
Friedelan-3-one	Friedelin	Terrestrial higher plants[6]
Urs-12-en-3β-ol	β-amyrin	
Wax esters (C_{28} to C_{34})	WE	Zooplankton, particularly copepods[18]
C_{25} Highly branched isoprenoids	C_{25} HBIs	Diatoms, marine and benthic[23,24]
3,7,11,15-tetramethyl-2-hexadecen-1-ol	Phytol	Chlorophyll degradation (zooplankton grazing)[25,26]
2, 6, 10, 14-trimethylpentadecane	Pristane	Phytol degradation (zooplankton grazing)[25,26], archaeal ether lipids[27], petroleum[28]
2,6,10,14-tetramethylhexadecane	Phytane	

Sterol nomenclature is according to $C_x\Delta^y$, where *x* refers to the number of carbons and *y* refers to the position of the unsaturation(s) on the carbon skeleton. PLFA are named according to $aC_{b:c\omega d}$ where *a* indicates the presence of a methyl branching (*i* – iso, *ai* – anteiso, 10Me - methyl on 10th carbon from methyl end, cyc – cycloproyl), *b* indicates the total number of carbons, *c* indicates the number of double bonds and *d* indicates the position of the first double bond from the methyl end. References: 1. Volkman (2003), 2. Colombo et al. (1996), 3. Thomson et al. (2004), 4. Goad and Withers (1982), 5. Volkman (1986), 6. Volkman (2006), 7. Rampen et al. (2010), 8. Smallwood and Wolf (1999), 9. Hudson et al. (2001), 10. Huang and Meinschein (1976), 11. Volkman et al. (1998), 12. Volkman et al. (1989), 13. Carrie et al. (1998), 14. Hu et al. (2006), 15. Canuel and Martens (1993), 16. White et al. (1997), 17. Kattner and Hagen (2009), 18. Eglinton and Hamilton (1967), 19. Kolatukuddy (1970), 20. Clark Jr and Blumer (1967), 21. Cranwell (2006), 22. Zhang et al. (2006), 23. Grosse et al (2004), 24. Massé et al. (2004), 25. Brooks et al. (1969), 26. Didyk et al. (1978), 27. Rowland (1990), 28. Peters and Moldowan (1993).

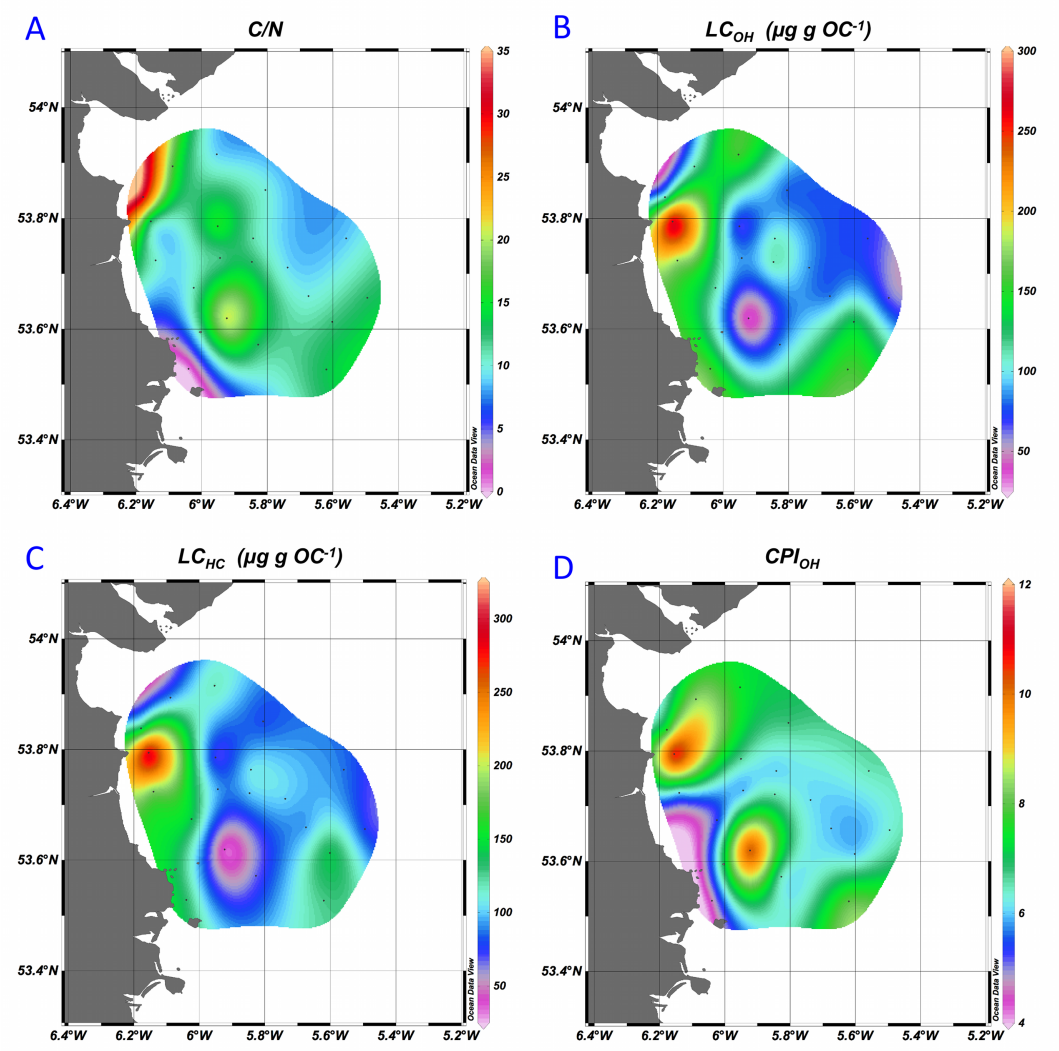

Figure 2.3. Spatial distribution of terrestrial organic matter (TOM) in the study area based on A. Bulk C/N ratio; B. long chain *n*-alkanols (LC_{OH}); C. long chain *n*-alkanes (LC_{HC}); and D. *n*-alkanol carbon preference index (CPI_{OH}).

2.4.3 Sterols and triterpenoids

Summary data for the occurrence and distribution of sterols for sediment samples and plankton net tows are given in Table 2.1 and 2.2, respectively. A suite of up to twenty-two sterols and stanols were identified in surface sediments and seventeen from the particulate matter. Total sterols were strongly positively correlated with LC_{HC} ($r = 0.71$, $P < 0.001$) and LC_{OH} ($r = 0.84$, $P < 0.001$) but a stronger relationship was observed between total sterols and LC_{OH}. Of the main sterol classes, C_{28} sterols exhibited the lowest correlation coefficient for LC_{HC} ($r = 0.57$, $P < 0.02$). Higher molecular weight sterols ($\geq C_{29}$) were more strongly correlated with LC_{HC} than the lower molecular weight sterols (C_{26} to C_{28}). This relationship was also observed for

LC_{OH}. Most sediment samples were dominated (average of 58.9% of total sterols) by $C_{27}\Delta^5$, $C_{28}\Delta^{5,22}$, $C_{28}\Delta^{5,24(28)}$, $C_{28}\Delta^5$, $C_{29}\Delta^5$, $C_{27}\Delta^{5,22}$ and $C_{30}\Delta^{22}$. Other sterols identified included $C_{26}\Delta^{5,22}$, $C_{26}\Delta^{22}$, $C_{27}\Delta^{22}$, $C_{27}\Delta^{5,24}$, $C_{28}\Delta^{22}$, $C_{29}\Delta^{5,22}$ and $C_{29}\Delta^{5,24(28)}$. C_{27} to C_{29} stanols accounted for an average of 10.8% of the sterol fractions.

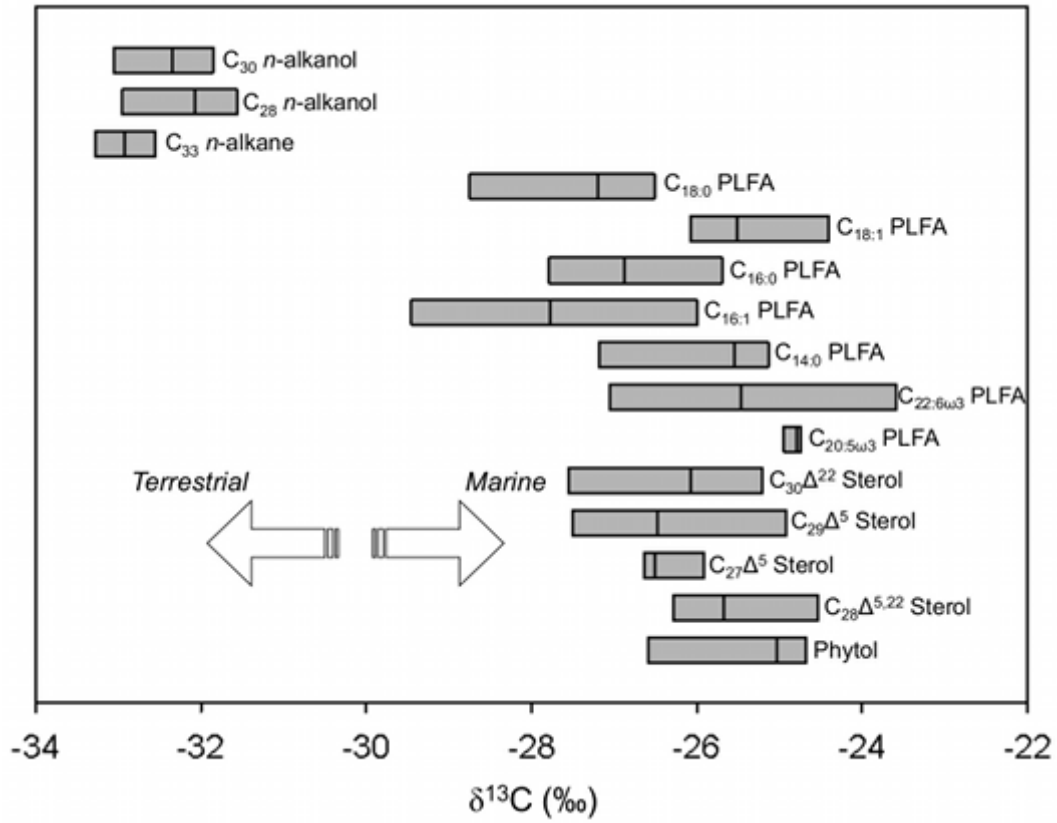

Figure 2.4. Horizontal boxplot of selected biomarker $\delta^{13}C$ values distinguishing marine and terrestrial organic matter. Each boxplot depicts the range of $\delta^{13}C$ values observed for the analyte at selected stations (n = 4; BC52, BC72, BC78, BC85 for PLFAs and BC55, BC66, BC72 and BC73 for neutral lipids). The black line represents the average $\delta^{13}C$ values.

The spatial distribution of sterols showed distinct trends within this setting. Total sterols, normalised for TOC content, revealed a clear 2- to 3-fold increase in the CMR and SMR compared to the SSR (Fig. 2.5A) and there is an increased relative proportion of a number of sterols in stations from mixed hydrographic regions (Fig. 5B to D). $\delta^{13}C$ values for measured major sterols, including C_{29} sterols, ranged from -24.38 ± 0.51‰ to -27.63 ± 0.26‰ (Fig. 2.4). Sterol occurrence in net tows generally reflected those found in sediments. However station T1 in the SMR revealed an approximately 3-fold greater abundance of total sterols (1428.2 μg g^{-1} dw compared to 413.4 μg g^{-1}) than at station T2 from the SSR (Table 2.2). Major sterols from T1 included $C_{27}\Delta^5$, $C_{27}\Delta^{5,24}$, $C_{27}\Delta^{5,22}$, $C_{28}\Delta^{5,24(28)}$ and $C_{26}\Delta^{5,22}$, and together represented

79.5% of total sterols (Fig. 2.6). In contrast to station T1, $C_{28}\Delta^{5,24(28)}$ was the major sterol at station T2, accounting for 23.2% of total sterols, while $C_{27}\Delta^{5}$ accounted for 22.3%. Two triterpenoids were positively identified in most surface sediment samples - friedelin and β-amyrin. They occurred in overall low abundance and were not observed in net tows. In addition they were strongly positively correlated with LC_{OH} (r = 0.77, P<0.0001) and LC_{HC} (r = 0.58, P<0.007).

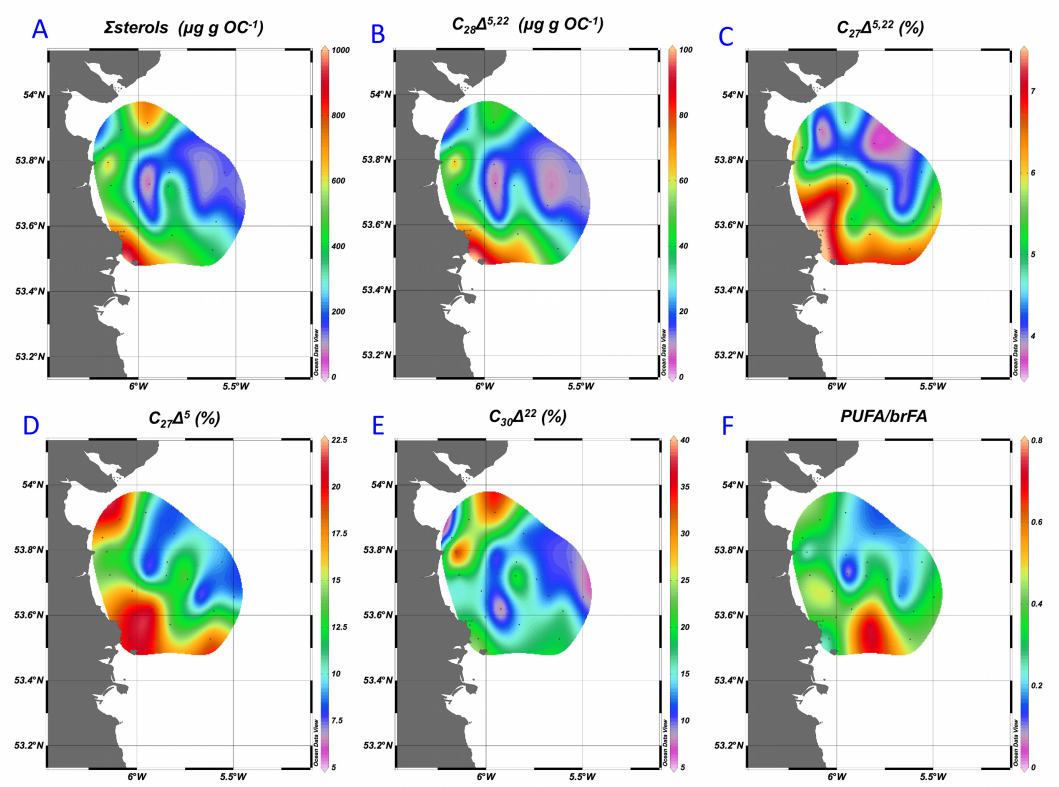

Figure 2.5. A. total sterol concentration (µg g OC^{-1}); B. $C_{28}\Delta^{5,22}$ (µg g OC^{-1}); C. $C_{27}\Delta^{5,22}$ (% of total sterols); D. $C_{27}\Delta^{5}$ (% of total sterols); E. $C_{30}\Delta^{22}$ (% of total sterols); and F. the ratio of polyunsaturated to branched phospholipid fatty acids (PUFA/brFA). Sterol nomenclature is according to $C_x\Delta^y$, where x refers to the number of carbons and y refers to the position of the unsaturation(s) on the carbon skeleton.

2.4.4 Other neutral lipids

WE abundance was negligible in surface sediments but were found in high concentrations (954.8 µg g dw^{-1}) at station T1 in the SMR, and were much lower (11.7 µg g dw^{-1}) at T2 in the SSR (Table 2.2). WE ranged from C_{28} WE with C_{14} *n*-alkanols and C_{14} saturated straight chain fatty acids (SATFA) ($C_{14:0/14:0}$), to C_{34} WE with C_{16} *n*-alkanols and C_{18} monounsaturated straight chain fatty acids (MUFA) ($C_{16:0/18:1}$). WE with MUFA dominated, whereby $C_{16:0/18:1}$ and $C_{16:0/16:1}$ represented

69.2% of total WE at T1. Four C_{25} HBIs were also observed in plankton net stations and in surface sediment stations. These were identified based on retention indices and published spectra by Belt et al. (2000). The structures observed here were $C_{25:4}$, $C_{25:3}$ and two $C_{25:5,}$ which correspond to structures XV, XIV, XII and XI of Belt et al. (2000). On average, the abundance (per g OC) of C_{25} HBIs in the CMR (8 µg g OC^{-1}) was higher than at the SSR (5 µg g OC^{-1}). C_{25} HBIs were also observed at station T1 and T2. However T1 HBI were limited to $C_{25:4}$ (XV) and $C_{25:3}$ (XIV), while at T2, these aforementioned HBI were accompanied by $C_{25:4}$ (XVII) and $C_{25:5}$ (XII). In both cases $C_{25:4}$ (XV) was the major compound. The total concentrations of C_{25} HBI were 12.5 µg g dw^{-1} at T1 and 16.5 µg g dw^{-1} at T2.

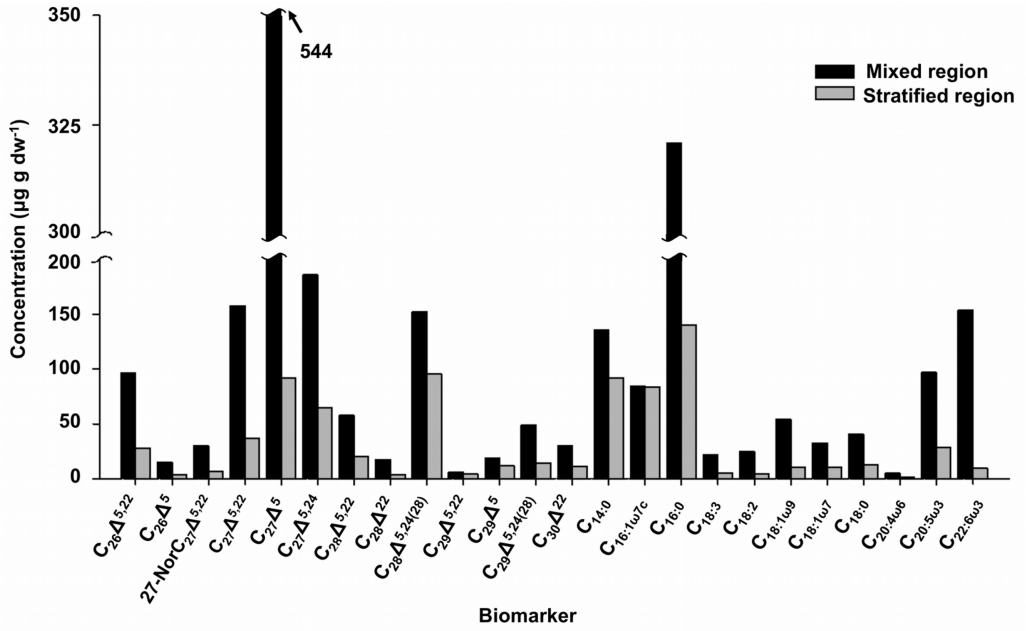

Figure 2.6. Concentrations of major sterol and phospholipid fatty acids in plankton net tow samples from mixed and stratified regions.

2.4.5 Phospholipid fatty acids

Summary data for the occurrence and distribution of phospholipids fatty acids (PLFAs) for sediment samples and net tows are given in Tables 2.1 and 2.2, respectively. Sixty-three PLFA were identified in the sediments and thirty-eight in net tows. Specific PLFA classes comprised a mixture of SATFA, MUFA, PUFA, brFA, and ranged from C_{12} to C_{24} (C_{14} to C_{24} for nets tows). MUFA were the most abundant PLFA class, followed by SATFA, brFA and finally PUFA. In the surface sediments SATFA comprised between 25.1% and 38.8% of total PLFAs found. The lowest

proportion of SATFA relative to total PLFA was found at BC67 located in the deeper offshore region while the highest proportion of SATFA relative to total PLFA was found at BC63 in shallower water. PUFA represented an average of 7.8% of total PLFA while brFA accounted for on average 23.4% of total PLFA.

SATFA ranged from C_{12} to C_{24} in surface sediments and there was a strong even carbon number predominance. $C_{16:0}$ was the major SATFA found at all sediment stations, representing an average of 11.3 and 20.5% of total PLFA. MUFA ranged from C_{14} to C_{24} in chain length and exhibited a clear bimodal distributions whereby $C_{16:1\omega7c}$ and $C_{18:1\omega7c}$ were the dominant members. These accounted for an average of 11.5% and 13.9% of total PLFA, respectively. ω9 MUFA dominated for the MUFA ≥ C_{20}. Taken together $C_{16:0}$, $C_{16:1\omega7c}$ and $C_{18:1\omega7c}$ accounted for an average of 41.0% of total PLFA. brFA accounted for an average of 23.4% of total PLFA in surface sediments. *i*$C_{15:0}$, *ai*$C_{15:0}$ and 10Me$C_{16:0}$ were the dominant brFA and accounted for on average 53.8% of brFA, or 12.6% of total PLFA. Other brFA encountered were iso and anteiso C_{13} to C_{19}. A number of cyclic fatty acids were also observed in these samples and included one cyclopropyl C_{17} and two cyclopropyl C_{19} FA. These comprised on average of 1.9% of total PLFA in surface sediments. PUFA ranged from C_{16} to C_{24} and were dominated by $C_{20:4\omega6}$, $C_{20:5\omega3}$, $C_{22:6\omega3}$. These PUFA accounted for an average of 1.8, 2.9 and 0.7% of total PLFA respectively.

Total PLFA abundance was not significantly correlated with water depth, sediment type, TOC, TN or with neutral compound classes. This was also the case for SATFA, MUFA and PUFA classes. $\delta^{13}C$ values for major PLFA from station BC52 (CMR), BC72 (SSR), BC78 (SMR) and BC85 (SSR) ranged from -23.23‰ to -29.76‰ (Fig. 2.4). $C_{14:0}$ ranged from -25.04 ± 0.17‰ at station BC85 to -27.68 ± 0.10‰ at BC72. $C_{16:1}$ ranged from 25.65 ± 0.22‰ at BC85 to -29.76 ± 0.26‰. $C_{16:0}$ $\delta^{13}C$ values ranged from 25.42 ± 0.18‰ at BC85 to 27.97 ± 0.21‰ at BC72. $C_{18:1}$ was more enriched compared to C_{16} PLFA, ranging from 24.11 ± 0.18‰ at BC85 to 26.18 ± 0.11‰ at BC72. There was a shift in the overall trend for $C_{18:0}$ whereby the more depleted $\delta^{13}C$ values were observed at BC85 (29.07 ± 0.06‰) and BC72 exhibited the most enriched $\delta^{13}C$ values (26.47 ± 0.14‰). $\delta^{13}C$ for $C_{20:5\omega3}$ revealed very little variability in $\delta^{13}C$ values, whereby values ranging from -24.75 ± 0.25‰ (BC72) to -24.99 ± 0.09‰ (BC52). $C_{22:6\omega3}$ $\delta^{13}C$ values varied over a wider range, from -23.23 ± 0.27‰ (BC52) to -27.30 ± 0.15‰ (BC78).

The major PUFA, $C_{20:5\omega3}$ and $C_{22:6\omega3}$, represented 4.9% of total PLFA in the CMR/SMR while in the SSR accounted for 3% of total. *i*$C_{15:0}$, *ai*$C_{15:0}$ and 10Me$C_{16:0}$ represented an average of 12.1% of total PLFA in the CMR/SMR while in the SSR they represented 14.1% of total PLFA. For the particulate matter PLFA abundance at station T1 was over double that of T2 (1080.0 μg g dw^{-1} compared to 439.8 μg g dw^{-1}, respectively) (Fig. 2.6). In particular the major PUFA, $C_{20:5\omega3}$ and $C_{22:6\omega3}$, were present in much greater abundance at station T1. This is consistent with the increased relative abundance of PUFA in surface sediments in the CMR/SMR. $C_{22:6\omega3}$ was the dominant PUFA at station T1 while $C_{20:5\omega3}$ was the dominant at T2. $C_{18:3\omega3}$ and $C_{18:2\omega3}$ were other significant PUFA in the nets tows.

2.5 Discussion

Lipid biogeochemistry is a complex mixture of different sources and relative fluxes, and includes input from the terrestrial environment via plant matter and anthropogenic contaminants, phytoplankton, zooplankton, macroalgae and bacteria. Due to their recalcitrance the source of certain lipids in sediments and other samples may be attributed to specific classes of organisms. The focus of the present study was on the sources and cycling of natural TOM and MOM. Thus anthropogenic sources of OM will not be discussed here. In addition biomarkers derived from prokaryotes such as brFA and MAGE will not be discussed in detail here. A table summarising the primary biomarkers used in this study, along with common names, abbreviations used in the text, likely sources and key references is given in Table 2.3.

2.5.1 Sources, distribution and fate of marine organic matter

Fatty acids of marine plankton typically range from C_{14} to C_{22} (Carrie et al., 1998), whereby C_{14}, C_{16} and C_{18} SATFA are typically the major homologs (e.g. Volkman et al., 1989; Carrie at al., 1998; Hu et al., 2006). These fatty acids are generally ubiquitous and not source-specific. However, overall these fatty acids have broadly similar $\delta^{13}C$ values as the measured marine sterols (Fig. 2.4), and the average $\delta^{13}C$ value for these lipids (-26.7‰) is consistent with a dominant marine origin (Pancost et al., 1997). $C_{16:1\omega7}$ was a major fatty acid and is synthesised by a variety of marine organisms, such as diatoms, dinoflagellates, prymnesiophytes and haptophytes (Volkman et al., 1989, 1998), as well as bacteria (White et al., 1997). A dominant

marine microalgal source is likely, especially considering the average $\delta^{13}C$ values of -27.7‰ (as total C_{16} MUFA). A similar assessment can be made for $C_{18:1\omega7}$. The broad range of $\delta^{13}C$ values of measured PLFA likely reflects the variable marine and benthic sources for these lipids. C_{16} and C_{18} SATFA and C_{16} MUFA were more depleted in ^{13}C than other PLFA and reflects their ubiquity and input from other, possibly terrestrial, sources. Nevertheless a marine planktonic input for these lipids in considered the primary source in this setting. This conclusion is supported by their occurrence as major lipids in sampled particulate matter (Fig. 2.6).

PUFA are generally more specific marine fatty acids and are primarily produced by planktonic microalgae in marine settings (Volkman et al., 1989, 1998). PUFA are considered labile and subject to rapid losses and alteration by bacteria and zooplankton grazing (Hu et al., 2006). Thus their occurrence, especially as ester-linked constituents, in marine sediments, is indicative of input of microalgal biomass or fresh detritus from the water column (Canuel and Martens, 1993; Carrie et al., 1998). PUFA were present at all sediment stations (Table 2.1) and exhibited average $\delta^{13}C$ values that indicate a major marine water column input (Fig. 2.4). Furthermore, PUFA abundance, expressed against TOC, is on average greater in the hydrographically well mixed CMR and SMR (70.6 μg g OC^{-1}) compared to stations associated with the SSR (23.3 μg g OC^{-1}). This is also reflected in the net tows whereby PUFA abundance at T1 was 333.1 μg g dw^{-1} and at T2 was 59.2 μg g dw^{-1}. This suggests that there is a greater average productivity and input of fresh algal biomass in the well-mixed region compared to stratified offshore waters. The spatial distribution of algal PUFA is discussed in more detail in section 5.3.

Sterols were dominated by C_{27} and C_{28} sterols, which are typically the major sterols in marine plankton and invertebrates, while C_{29} sterols and C_{27} sterols are the predominant sterols in higher plants and in animals respectively (Huang and Meinschein, 1976). Sterols are not completely metabolised or degraded quickly under reducing conditions, and hence are typically selectively preserved in sediments compared to more labile molecules such as sugars or phospholipids (Huang and Meinschein, 1979). In this sense they are not strictly associated with fresh input. However sterols provide a record of past MOM input to sediments and, with PLFAs, may help elucidate recent and longer-term MOM production and input. C_{28} and C_{27} were the major sterol classes at all sediment stations (Table 2.1) and also in net tows

(Table 2.2), indicating a major contribution of planktonic OM to MOM. This is supported by the average $\delta^{13}C$ values for well resolved sterols (Fig. 2.4).

Phytol (the ester-linked side chain of chlorophyll) is probably the most abundant acyclic isoprenoid in nature and is considered to be the major source of other isoprenoids with twenty or less carbons in geological samples - for example pristane, phytane and phytadienes (Brooks et al., 1969; Didyk et al., 1978; Rontani and Volkman, 2003). Phytol $\delta^{13}C$ values are consistent with a marine planktonic origin (Fig. 2.4). Chlorophyll hydrolysis to yield free phytol, and subsequent production of pristane and phytadienes, is mainly associated with herbivorous grazing activity (Blumer et al., 1969; Rontani and Volkman, 2003). Alternative sources for pristane and phytane include archaeal ether lipids (Rowland, 1990) and oil spills (Peters and Moldowan, 1993). It has been reported that phytadienes may also be produced as artifacts during the analytical process (Grossi et al., 1996). However the occurrence of phytadienes in most sediment stations and in high abundance in net tows strongly indicate that at least the major proportion of these are present as a result of *in situ* processes. Phytol abundance at sediment stations in the mixed regions averaged 13.2 μg g OC^{-1} while at stations in stratified waters was 5.8 μg g OC^{-1}. Thus the abundance of phytol and its proposed degradation products highlight the considerable processing and turnover of MOM in the water column and upon deposition. However, it must be noted that although there a positive correlations between phytol and is degradation products, the variable distribution indicates that there a number of sources for these compounds in this setting. The occurrence of polyaromatic hydrocarbons in appreciable amounts in surface sediments (data not shown) highlights the significant input of OM from anthropogenic sources. Thus, more diagnostic lipids are discussed below and provide a greater insight to for specific groups of marine organisms contributing to MOM in this setting.

2.5.1.1 Phytoplankton

Although the phytoplankton composition of the Irish Sea is generally not well-characterised, recent investigations have shown that over seventy species/species groups of diatoms are known to occur (Kennington and Rowlands, 2006), and diatoms appear to dominate the seasonal bloom (Gowen and Stewart, 2005). Diatoms are a vital link in marine food webs, accounting for one-fifth of global marine primary productivity and represent an important source of MOM (Nelson et al., 1995).

Important diatom species and groups in the seasonal bloom appear to be *Skeletonema costatum*, species belonging to *Chaetoceros*, *Pseudonitzschia* and *Thalassiosira* (McKinney et al., 1997), and *Guinardia delicatula* (Gowen et al., 2000). Diatoms are characterised by high abundances of $C_{16:1\omega7c}$, $C_{18:1\omega7c}$, $C_{20:5\omega3}$ (Colombo et al., 1996; Volkman et al., 1998). In addition $C_{28}\Delta^{5,22}$ and $C_{28}\Delta^{5,24(28)}$ are major sterols in many diatom species, while $C_{27}\Delta^{5}$, $C_{29}\Delta^{5}$ and $C_{27}\Delta^{5,22}$ are also commonly present (Volkman 2003; Rampen et al., 2010). Of these sterols $C_{28}\Delta^{5,24(28)}$ is considered the most specific for diatoms. C_{25} HBIs have also been attributed to marine and benthic diatoms (Grosse et al., 2004; Masse et al., 2004). $C_{16:1\omega7c}$, $C_{18:1\omega7c}$, $C_{20:5\omega3}$ accounted for a major proportion of total PLFA in sediment samples. Both $C_{28}\Delta^{5,22}$ and $C_{28}\Delta^{5,24(28)}$ were sterols at all sediment stations and in particulate matter. Surface sediments in the CMR and SMR yielded, on average, a greater relative abundance of these sterols. For particulate matter, the abundance of these sterols was also much greater in the mixed region compared to the stratified region (Fig. 2.6). C_{25} HBIs were observed in most surface sediment samples. This indicates that fresh diatom biomass is a significant source of OM to surface sediments throughout the region, and that there was a greater relative abundance of diatom biomass and detritus in particulate matter and surface sediments in well mixed waters. However, relative to total sterols, $C_{28}\Delta^{5,24(28)}$ was a more significant sterol in the stratified region (Fig. 2.6), which suggest that during sampling diatoms comprised a greater proportion of total plankton in the stratified waters compared to the mixed region.

About sixty species/species groups of dinoflagellates have also been identified in the Irish Sea (Kennington and Rowlands, 2006) and they are considered to represent an important component of the bloom also (Gowen and Stewart, 2005). Species belonging to *Gymnodinium spp.*, *Peredinium spp.*, *Ceratium spp.* and *Scrippsiella spp*. appear to be the major dinoflagellate groups in the Irish Sea during the spring/summer season. $C_{30}\Delta^{22}$ is a major sterol in many dinoflagellates and considered a source-specific biomarker (Volkman, 2003). $C_{30}\Delta^{22}$ was a major sterol in both sediments and net tows. This confirms that dinoflagellates are a major member of the plankton in the Irish Sea and a major contributor to MOM and SOM. The PUFA $C_{22:6\omega3}$ has also previously been utilised as a biomarker for dinoflagellate input (e.g. Colombo et al., 1996; Budge and Parrish, 1998; Carrie et al., 1998). However no strong correlation was observed between $C_{22:6\omega3}$ and $C_{30}\Delta^{22}$ in this study, reflecting the variety of other sources of $C_{22:6\omega3}$.

Green algae (division Chlorophyta) are characterised by C_{16} and C_{18} PUFA with ω3 and ω6 isomerism and low amounts of C_{20} and C_{22} PUFA (Volkman et al., 1989; Dunstan et al., 1992; Zhukova and Aizdaicher, 1995; Meziane and Tsuchiya, 2000). Major sterols associated with green algae are $C_{28}\Delta^{5}$, $C_{28}\Delta^{5,7,22}$, $C_{28}\Delta^{7,22}$, $C_{29}\Delta^{5,22}$, $C_{29}\Delta^{5}$ and $C_{29}\Delta^{5,24(28)}$ (Volkman, 2003). The Δ^{7} sterols are major sterols in many Chlorophyceae while the Prasinophyceae lack these sterols and instead have $C_{28}\Delta^{5,24(28)}$, $C_{28}\Delta^{5}$ and $C_{29}\Delta^{5,24(28)}$ as major sterols. C_{16} and C_{18} PUFA were observed in all sediment stations and in net tows, which highlights the importance of green algae as primary producers in the Irish Sea. However Δ^{7} sterols were not observed in either sediments or net tows, based on the absence of sterols with the characteristic mass spectral peaks at m/z 213, 229 and 255. $C_{29}\Delta^{5,24(28)}$ was identified from both sediments and net tows, which suggests that Prasinophyceae rather than Chlorophyceae may be the dominant class of green microalgae in the western Irish Sea. In summary it has been demonstrated based on the occurrence of multiple biomarkers that diatoms, dinoflagellates and green microalgae are major primary producers in the western Irish and components of the seasonal plankton bloom. These organisms are a major source of MOM and, based on the surface sediments, also provide a major fraction of SOM to the benthos.

2.5.1.2 Zooplankton

Zooplankton, in particular copepods, play a key role in energy transfer from primary to higher trophic levels (Kattner and Hagen, 2009). The importance of zooplankton grazing on the pelagic mineralisation of fresh phytoplankton detritus in the Irish Sea has been emphasised (Dickey-Collas et al., 1996, Gowen et al., 1999; Trimmer et al., 1999), and it has been suggested that zooplankton grazing alone may account for up to 56% of daily spring production (Gowen et al., 2000). In particular copepods are the dominant zooplankton group in the Irish Sea, comprising almost 70% of the total according to Kennington and Rowlands (2006). *Pseudocalanus elongatus* is the dominant species reported in the Irish Sea, comprising almost 40% of total copepods (approximately 26% of total zooplankton) (Kennington and Rowlands, 2006). Other major copepods are *Temora longicornis* and *Acartia clausi*. $C_{16:1\omega7}$, $C_{20:5\omega3}$ and $C_{22:6\omega3}$ are typically major fatty acids in zooplankton (Williams 1965; Kattner and Hagen, 2009). As discussed $C_{16:1\omega7}$ is also widespread among marine organisms and is not considered source specific for zooplankton here. $C_{27}\Delta^{5}$ is also ubiquitous in the

marine environment. However in high concentrations it is typically associated with zooplankton biomass and detrital matter (Volkman, 1986). $C_{27}\Delta^{5,22}$ is also typical of zooplankton carcasses, molts and faeces (Colombo et al., 1996) and the co-occurrence of both of these sterols in high relative abundance compared to other sterols in this study indicates considerable zooplankton input.

More specific biomarkers for zooplankton are WE, which are synthesised in high amounts by numerous zooplankton, in particular copepods (Kattner and Hagen, 2009). WE biosynthesis by zooplankton plays a key role in this process by facilitating lipid accumulation and storage (Kattner and Hagen, 2009). Herbivorous calanoid copepods are known to intensely synthesise wax esters in marine settings with marked seasonality (Lee et al., 1971), such as those present in the western Irish Sea. In particulate samples WE reflected $C_{27}\Delta^{5,22}$ and $C_{27}\Delta^{5}$ whereby total WE abundance was over eighty times higher at T1 compared to T2. The low abundance of WE in sediments indicates that these are rapidly hydrolysed to the constituent *n*-alkanol and *n*-fatty acid in the water column. WE are typically the major lipid class of *P. elongatus*, accounting for almost 50% of total lipids in specimens from the North Sea (Kattner and Krause, 1989). Neither *T. longicornis* or *A. clausi* synthesise WE in appreciable amounts (Kattner et al., 1981; Fraser et al., 1989). Thus the high concentrations of WE found in this setting are most likely attributable to *P. elongatus*. Taken together results suggest that WE-synthesising calanoid copepods, such as *P. elongatus*, play an important role in the annual mineralisation and cycling of spring bloom biomass. These observations are consistent with previous reports emphasising the importance of copepods for OM mineralisation in the Irish Sea (Dickey-Collas et al., 1996, Gowen et al., 1999; Trimmer et al., 1999).

2.5.2 Terrestrial organic matter and terrestrial versus marine input

Homologous series of long-chain *n*-alkanes and *n*-alkanols are typical terrigenous lipids found in marine sediments (Gearing et al., 1976; Farrington and Tripp, 1977; Huang et al., 2000). These are predominantly derived from higher plant waxes, which make up protective coating on leaves and stems (Eglinton and Hamilton, 1967; Kolattukudy, 1970). Plant LC_{HC} normally range from C_{25} to C_{33} with an odd-over-even carbon number predominance while plant LC_{OH} typically range from C_{26} to C_{32} and exhibit an even-over-odd carbon number predominance (Eglinton and Hamilton, 1967). In contrast, algae and bacteria typically synthesise odd or even C_{14} to C_{24} *n*-

alkyl lipids (Volkman et al., 1998). Thus the relative abundance of these *n*-alkanes and proxies such as the CPI are useful for assigning relative OM contributions from terrestrial and marine signals (Clark Jr and Blumer, 1967; Cranwell, 2006; Zhang et al., 2006) (See Table 2.1 for details of the equations used). The CPI_{HC} values greater than four indicate a dominant higher plant source while lower values indicate either a dominant bacterial/algal input and/or degradative processes (Pancost and Boot, 2004, and references therein). CPI_{OH} can provide similar utility due to the dominance of long chain C_{26} to C_{32} even carbon members in plants (Zhang et al., 2006). Average CPI_{HC} values were 3.2, which indicates that although there is a considerable OM contribution from terrestrial sources, this does not appear to dominate over MOM. Thus a mixed marine/terrestrial OM contribution is evident. CPI_{HC} ranged from 2.1 to 5.3, with the higher values generally observed in the shallow CMR in proximity to Dundalk bay and the Boyne Estuary. Similar observations and conclusions can be drawn from the CPI_{OH}. $\delta^{13}C$ values for major LC_{OH} (C_{28} and C_{30}) ranged from -31.48 ± 0.22 to -33.22 ± 0.23‰, while for LC_{HC} (C_{31}) ranged from -32.48 ± 0.11 to -33.35 ± 0.71‰. In addition these values are about 7‰ more depleted than other typical marine lipids (Fig. 2.4), confirming their terrestrial source.

C_{29} sterols, such as $C_{29}\Delta^{5,22}$ and $C_{29}\Delta^{5}$ are typical major sterols in higher plants (e.g. Huang and Meinschein, 1976; Pancost and Boot, 2004) and often utilised as markers of terrestrial input in marine settings. However these sterols are also synthesised by a variety of marine plankton (Volkman et al., 1998, and reference therein). In this study C_{29} sterols were more strongly correlated with LC_{HC} than the lower molecular weight sterols (C_{26} to C_{28}), suggesting a terrestrial origin. However these sterols were also observed in net tows (Fig. 2.6) and $\delta^{13}C$ analysis of $C_{29}\Delta^{5}$ indicates a clear marine origin (Fig. 2.4). Thus these sterols are of limited use as terrestrial biomarkers in this setting. A mixed marine/terrestrial origin for LC_{OH} is also apparent based on their strong correlation with marine sterols (r = 0.84, P < 0.001). This is likely related to $C_{26:0}$, which was a major *n*-alkanol in net tows. However $\delta^{13}C$ analysis confirms than LC_{OH} greater then C_{26} are predominantly terrestrial. The plant triterpenoids friedilin and β-amyrin are considered highly specific biomarkers for vascular plants (Volkman, 2006) and their presence throughout the study area confirms the widespread distribution of TOM. The strong correlations between these triterpenoids and LC_{HC} and LC_{OH} support the conclusion that plant waxes are also the major source LC_{HC} and LC_{OH}.

$\delta^{13}C$ values for major LC_{OH} (C_{28} and C_{30}) ranged from -31.48 ± 0.22 to -33.22 ± 0.23‰, while for LC_{HC} (C_{31}) ranged from -32.48 ± 0.11 to -33.35 ± 0.71‰. Higher plants and phytoplankton discriminate against the energetically less favourable $^{13}CO_2$ during photosynthesis and the magnitude of this isotope fractionation is reflected in the type of metabolism and the growth environment (Collister, et al., 1994). Plants utilising the C_3 (Calvin-Benson) pathway (most plants) typically exhibit $\delta^{13}C$ values of around -25 to -30‰, while plants utilising the C_4 (Hatch-Slack) pathway typically exhibit $\delta^{13}C$ values ranging from -10‰ to -16‰ (Bird et al., 1995; Huang et al., 2000). Furthermore since the average bulk $\delta^{13}C$ values between land plants and marine primary producers are known to differ by about 7‰, whereby marine biomass is comparatively enriched in ^{13}C compared to terrestrial biomass, this difference can be used to between marine and terrestrial input in the marine environment (e.g. Westerhausen et al., 1993; Chikaraishi and Naraoka, 2003). Isotopic fractionation not only causes depletion of $\delta^{13}C$ values in bulk biomass relative to atmospheric CO_2, but specific compounds classes exhibit different $\delta^{13}C$ values due to further isotope fractionation associated with specific biosynthetic pathways (Pancost and Pagani 2006). Lipids are known to be depleted in ^{13}C by 5 to 8‰ relative to bulk biomass. Plant *n*-alkanes have recieved significant attention and are found to be typically depleted relative to biomass by about 6‰ (Collister et al., 1994; Chikaraishi and Naraoka, 2003). This fractionation is thought to be similar for similar *n*-alkyl lipids such as *n*-alkanols (Pancost and Pagani, 2006). As shown in Fig. 2.4, $\delta^{13}C$ values for proposed terrestrial and marine biomarkers revealed a clear distinction between isotopically lighter terrestrial, and heavier marine OM. $\delta^{13}C$ values of -32 to -33‰ are within the commonly observed ranges for plant-derived OM, and assuming a depletion of between -5 and -8‰, the major plant input in the western Irish Sea is likely derived from C_3 plant biomass.

TOM can be transported to marine environments by a variety of mechanisms, of which freshwater riverine runoff is considered to be the primary source in coastal and shelf settings (Bird et al., 1995, Harvey, 2006). The western Irish Sea is in close proximity to a number of bays and estuaries, which include Carlingford Lough, Dundalk Bay and the Boyne Estuary. The observation that bulk C/N ratios, plant-derived biomarkers and CPI values all peaked in well-sorted fine-grained coastal sediments in proximity to Dundalk Bay and the Boyne Estuary (Fig. 2.3), indicate local riverine input are the most important transport routes for TOM input. These

results are consistent with previous reports showing that fluvial input of dissolved inorganic nitrogen and ortho-phosphate to the western Irish Sea are generally highest in Dundalk Bay, Carlingford Lough, the Boyne estuary and in Dublin Bay (McGovern et al., 2002). Riverine input is considered much lower than in the eastern Irish Sea (Gowen et al., 2000), and this is reflected in the decreased sedimentary input of TOM from the shallow coastal regions to offshore sediments (Fig. 2.3). Near-surface and near-bottom residual circulation from the eastern Irish Sea (Liverpool Bay) to the western Irish Sea is not apparent (Ramster et al., 1969), and suggests that transport of TOM from east to west may be of minor importance. However, the influence of TOM from the eastern Irish Sea to the western Irish Sea is unknown at present. Furthermore, the transport of terrestrial material from the south, via St. George's Channel and from the North, via the North Channel needs to be considered further in future studies regarding the source and fate of TOM in the Irish Sea.

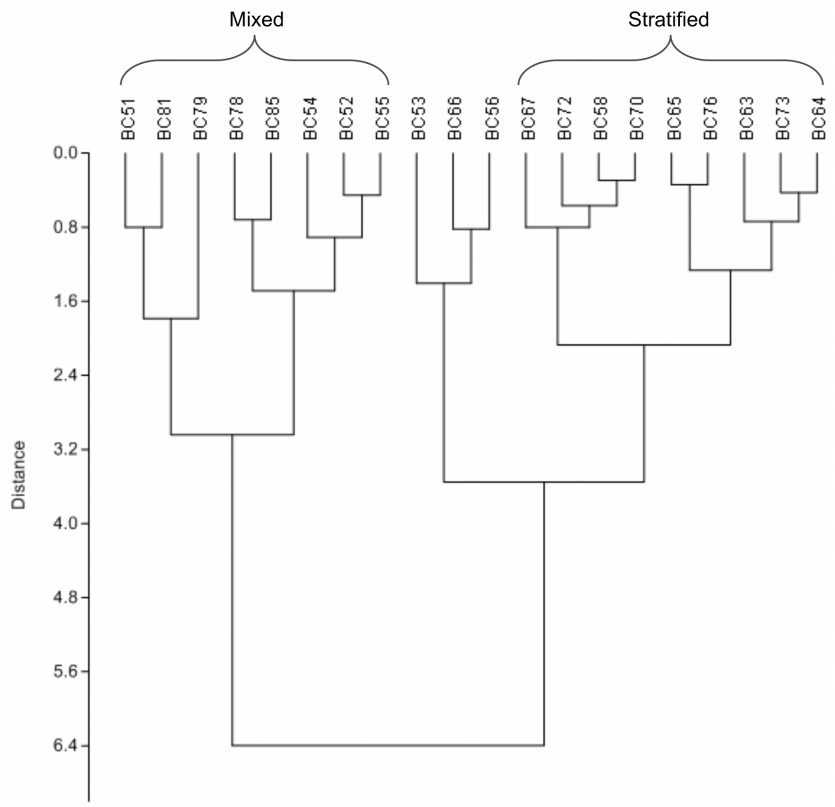

Figure 2.7. Hierarchical cluster analysis of multivariate bulk parameter and biomarker data, as shown in Table 2.1, revealing a clear distinction between the dataset that corresponds with the distinct seasonal hydrographic zonation.

2.5.3 Hydrographic control on organic matter cycling.

The spatial distribution of grain size and sediment type are primarily controlled by the hydrographic conditions and resulting depositional regime. In this way the transition from coarse-grained sandy sediments to more fine-grained sediments found in deeper waters (> 50 m depth) delineates the average location of mixed and stratified hydrographic regions that develop each year in the western Irish Sea (Fig. 2.2). It has been proposed that the establishment of the summer gyre may play a role in controlling the spatial distribution of *Nephrops norvegicus* larvae (Hill et al., 1996), larval and juvenile fish, and zooplankton (Dickey-Collas et al., 1996, 1997), and anthropogenic contaminants (Hill et al., 1997). Assessing the distribution of marine- and terrestrial- derived fresh and recalcitrant OM provides one means of assessing the effect these frontal zones on natural processes. Results presented in this study from a multi-biomarker approach provide evidence that the seasonal stratification in the western Irish Sea is a key factor controlling the production, distribution and fate of MOM.

PUFA were major PLFA at both plankton nets stations (up to 30.8% of total PLFA). PUFA abundance at T1 was almost 6 times greater than at T2 (Fig. 2.6), indicating a greater abundance of fresh microalgal biomass in the SMR compared to the SSR during the sampling period. There was a clear decrease in the overall relative abundance of PUFA from the water column to surface sediments, whereby the relative abundance of PUFA decreased to an average of 7.8%. This reflects the rapid degradation of fresh planktonic biomass in the water column and is in agreement with previous observations that much of the seasonal primary productivity in the western Irish Sea is remineralised in the water column (Gowen et al., 2000; Trimmer et al., 1999). These observations made during sampling are reflected in surface sediments also, and is illustrated by the ratio of algal/bacterial PLFA (Fig. 2.5F). PUFA are diagnostic of microalgal biomass while brFA indicate an increased relative contribution of bacterial biomass (White et al., 1997). The ratio of PUFA/brFA was approximately half in the SSR compared to the mixed regions. Thus an increased relative abundance of PUFA is apparent in the CMR/SMR while the brFA is more abundant in the SSR. Thus these trends in biomass production and distribution may be periodical. However, temporal sampling would be required to confirm this. The increased residence time of marine biomass in the water column, together with lower primary production, and lower dissolved inorganic nutrient availability (Gowen et al.,

1995, 1996) are likely the most important reasons for the indicated decreased input of fresh MOM to surface sediments within the gyre.

The spatial distribution of $C_{27}\Delta^{5}$ and $C_{27}\Delta^{5,22}$ is similar and has an increased relative abundance in the mixed region, in particular to the south (Fig. 2.5C and D). This indicates that there is increased abundance of zooplankton and hence likely grazing activity in the mixed region in comparison to seasonally stratified waters. This conclusion is strongly supported by the occurrence of these sterols at T1 in concentrations greater than five times that found at T2. Furthermore WE were over eighty times more abundant at T1 compared to T2. In contrast to the sterol profiles at T1, $C_{28}\Delta^{5,24(28)}$ was the major sterol at T2 (Fig. 2.6). This reflects the greater relative abundance of diatoms in the SSR during the sampling period in the 2010 seasonal bloom. The occurrence of C_{25} HBIs in greater abundance in the SSR particulate samples compared to the SMR, again supports the conclusion that diatoms represented a greater relative proportion of total phytoplankton within the gyre during the sampling period. The distribution of C_{25} HBIs in surface sediments suggests an increased relative input to the CMR however, compared to the SSR and SMR. This may be due to a number of possible factors such as the higher average primary productivity in the coastal mixed region, the increased zooplankton activity in the mixed region and also the lower residence time of these lipids in the water column at these shallower water depths.

It has been demonstrated that the ratio of $C_{22:6\omega3}$ to $C_{20:5\omega3}$ may provide an indication of relative dinoflagellate to diatom input (Volkman et al., 1989; Budge and Parrish, 1998). This ratio was highest in a number of stations in the CMR (average = 0.27) and SMR (average = 0.30), while typically being lower in the SSR (average = 0.20). Thus, this suggests an average increased abundance of dinoflagellates and dinoflagallate detritus in the mixed regions and is supported by the spatial distribution of $C_{30}\Delta^{22}$ (Fig. 2.5E). The three-fold greater abundance of $C_{29}\Delta^{5,24(28)}$ and of C_{16}/C_{18} PUFA at T1 compared to T2 indicates that there was an increased abundance of green microalgae in well-mixed zones compared to the stratified waters during the summer. This is also reflected in the increased abundance (μg g OC^{-1}) of these PUFA in surface sediments at stations BC79, BC81 and BC85 in the southern region. Based on the abundance of $C_{28}\Delta^{5,24(28)}$, $C_{30}\Delta^{22}$ and $C_{29}\Delta^{5,24(28)}$ in net tows, diatoms represented about fives times more biomass than dinoflagellates and three times more than the

green microalgae at T1. At T2 these figures were about three times and two times, respectively.

The distribution of C/N, LC_{OH} and LC_{HC}, normalised to TOC content reflects the hydrographic conditions also whereby these are highest in coastal fine-grained sediments in proximity to Dundalk Bay and the Boyne Estuary (particularly station BC53). The spatial distribution of these plant lipids also suggests that the regional near-bottom residual flows that exist in the western Irish Sea (Ramster and Hill, 1969) as shown in Fig. 2.1 may facilitate transport of riverine TOM from the south coast and from the northern coast and deposition in the low energy hydrographic areas near Dundalk Bay. The clear decrease in abundance of LC_{OH} and LC_{HC}, expressed against TOC content (Fig. 2.3B and C) offshore suggests that the seasonal gyre may influence TOM transport and deposition in the region.

Hierarchical cluster analysis of bulk and biomarker data (Fig. 2.7) from all stations support the aforementioned conclusion that the hydrographic regime plays a major role on the production, distribution and deposition of OM in the western Irish Sea. Two major groupings were formed whereby all stations in the SSR cluster together and eight out of ten stations (BC53 and BC56) in the mixed CMR and SMR cluster together. In summary the distribution of biomarkers from phytoplankton and zooplankton are clearly distinct between the mixed waters and the stratified waters in the Irish Sea. Evidence presented here suggests that there is an overall higher primary productivity and zooplankton grazing and that this effects the composition and distribution of SOM across this region. This is likely a result of a number of factors such as OM water column residence time and the earlier and longer production season in coastal and mixed waters compared to offshore waters. It must be noted however, that changes in phyto- and zooplankton abundance and distribution over the course of the spring/summer bloom, as well as annual variation, have not been addressed here. Nevertheless, we propose that the hydrographic regime in the western Irish Sea and the establishment of the western gyre plays a role in the production, distribution and fate of OM in the western Irish Sea.

2.6 Conclusions

The occurrence of $C_{28}\Delta^{5,22}$, $C_{28}\Delta^{5,24(28)}$ sterols, as well as ester-linked PUFA and C_{25} HBIs in surface sediments and the water column in this setting highlighted the importance of diatoms for primary production and as a component of SOM in the Irish Sea. $C_{30}\Delta^{22}$, C_{16}/C_{18} PUFA and $C_{29}\Delta^{5,24(28)}$ also confirm the importance of dinoflagellates and chlorophyta primary producers. The key role of copepod zooplankton in mineralising the seasonal pytoplanton bloom was also revealed based on the widespread occurrence of PUFA, $C_{27}\Delta^{5}$, $C_{27}\Delta^{5,22}$ and WE. The spatial distribution of these diagnostic compounds reflects the importance the distinct hydrographic regime and the summer gyre for controlling the production, distribution and fate of MOM. The widespread distribution of higher plant alkyl lipids and triterpenoids, revealed the importance of allochtonous TOM as a component of OM in the Irish Sea. The TOM fraction is composed predominantly of recalcitrant plant wax constituents and highlighted the preservation of TOM from source to deposition in surface sediments. The spatial distribution of terrestrial biomarkers indicates that the major transport route is via riverine input from the Boyne Estuary and Dundalk Bay. Near-bottom residual currents and seasonal hydrographic zonation also likely play a role in the transport and fate of TOM.

2.7 References

Allen, J., Slinn, D., Shammon, T., Hartnoll, R, Hawkins, S., 1998. Evidence for eutrophication of the Irish Sea over four decades. Limnology and Oceanography 43, 1970-1974.

Baldock, J.A., Masiello, C.A., Gelinas, Y., Hedges, J.I., 2004. Cycling and composition of organic matter in terrestrial and marine ecosystems. Marine Chemistry 92, 39-64.

Belicka, L.L., Macdonald, R.W., Harvey, R.H., 2002. Sources and transport of organic carbon to shelf, slope, and basin surface sediments of the Arctic Ocean. Deep Sea Research I 49, 1463-1483.

Belicka, L.L., Macdonald, R.W., Yunker, M.B., Harvey, R.H., 2004. The role of depositional regime on carbon transport and preservation in Arctic Ocean sediments. Marine Chemistry 86, 65-88.

Belt, S.T., Allard, W.G., Massé, G., Robert, J.-M., Rowland, S.J., 2000. Highly branched isoprenoids (HBIs): Identification of the most common and abundant sedimentary isomers. Geochimica et Cosmochimica Acta 64, 3839-3851.

Bird, M.I., Summons, R.E., Gagan, M.K., Roksandic, Z., Dowling, L., Head, J., Fifield, K.L., Cresswell, R.G., Johnson, D.P., 1995. Terrestrial vegetation change inferred from *n*-alkane $\delta^{13}C$ analysis in the marine environment. Geochimica et Cosmochimica Acta 59, 2853-2857.

Blumer, M., Robertston, J.C., Gordon, J.E., Sass, J., 1969. Phytol-derived C19 di- and triolefinic hydrocarbons in marine zooplankton and fishes. Biochemistry 8, 4067-4074.

Bowden, K., 1980. Physical and dynamical oceanography of the Irish Sea. In: Banner, F.T., Collins, M.B., Massie, K.S., (Eds). The North-West European Shelf Seas: The Sea Bed and the Sea in Motion II. Physical and Chemical Oceanography and Physical Resources. Elsevier, Amsterdam pp. 391-413.

Brooks, P.W., Gould, K., Smith, J., 1969. Isoprenoid hydrocarbons in coal and petroleum. Nature 222, 257-259.

Budge, S.M., Parrish, C.C., 1998. Lipid biogeochemistry of plankton, settling matter and sediments in Trinity Bay, Newfoundland. II. Fatty acids. Organic Geochemistry 29, 1547-1559.

Burns, K., Brinkman, D., 2011. Organic biomarkers to describe the major carbon inputs and cycling of organic matter in the central Great Barrier Reef region. Estuarine Coastal and Shelf Science 93, 132-141.

Canuel, E.A., Martens, C.S., 1993. Seasonal variations in the sources and alteration of organic matter associated with recently deposited sediments. Organic Geochemistry 20, 563-577.

Carrie, R.H., Mitchell, L., Black, K.D., 1998. Fatty acids in surface sediment at the Hebridean shelf edge, west of Scotland. Organic Geochemistry 29, 1583-1593

Charlesworth, M., Gibson, C., 2002. PAH contamination of western Irish Sea sediments. Marine Pollution Bulletin 44, 1421-1426.

Chester, R., and Jickells, T., 2012. Marine geochemistry. Wiley-Blackwell, London.

Chikaraishi, Y., Naraoka, H., 2003. Compound-specific δD–δ^{13}C analyses of *n*-alkanes extracted from terrestrial and aquatic plants. Phytochemistry 63, 361-371.

Clark, Jr. R., Blumer, M., 1967. Distribution of *n*-paraffins in marine organisms and sediment. Limnology and Oceanography 12, 79-87.

Collister, J.W., Rieley, G., Stern, B., Eglinton, G., Fry, B., 1994. Compound-specific δ^{13}C analyses of leaf lipids from plant with differing carbon dioxide metabolisms. Organic Geochemistry 21, 619-627.

Colombo, J.C., Silverberg, N., Gearing, J.N., 1996. Lipid biogeochemistry in the Laurentian Trough I. Fatty acids, sterols and aliphatic hydrocarbons in rapidly settling particles. Organic Geochemistry 25, 211-225.

Cranwell, P., 2006. Chain-length distribution of *n*-alkanes from lake sediments in relation to post-glacial environmental change. Freshwater Biology 3, 259-265.

Croker, P.F., Kozachenko, M. Wheeler, A.J., 2005. Gas-related seepage features in the western Irish Sea (IRL-SEA6). Tech Rep Strategic Environmental Assessment of the Irish Sea (SEA6). Department of Trade and Industry, United Kingdom.

Dickey-Collas, M., Brown, J., Fernand, L., Hill, A., Horsburgh, K., Garvine, R.. 1997. Does the western Irish Sea gyre influence the distribution of pelagic juvenile fish? Journal of Fisheries Biology 51, 206-229.

Dickey-Collas, M., Gowen, R., Fox, C., 1996. Distribution of Larval and Juvenile Fish in the Western Irish Sea: Relationship to Phytoplankton, Zooplankton

Biomass and Reccurrent Physical Features. Marine and Freshwater Research 47, 169-181.

Didyk, B.M., Simoneit, B.R.T., Brassel, S.C., Eglinton, G., 1978. Organic geochemical indicators of paleoenvironmental conditions of sedimentation. Nature 272, 216-222.

Dunstan, G.A., Volkman, J.K., Jeffrey, S.W., Barrett, S.M., 1992. Biochemical composition of microalgae from the green algal classes *Chlorophyceae* and *Prasinophyceae* 2. Lipid classes and fatty acids. Journal of Experimental Marine Biology and Ecology 161, 115-134.

Eglinton, G., Hamilton, R.J., 1967. Leaf epicuticular waxes. Science 156, 1322-1335.

Evans, G.L., Williams, P.J.B., Mitchelson-Jacob, E.G., 2003. Physical and anthropogenic effects on observed long-term nutrient changes in the Irish Sea. Estuarine Coastal and Shelf Science 57, 1159-1168.

Farrington, J.W., Tripp, B.W., 1977. Hydrocarbons in western North Atlantic surface sediments. Geochimica et Cosmochimica Acta 41, 1627-1641.

Fraser, A.J., Sargent, J.R., Gamble, J.C., 1989. Lipid class and fatty acid composition of *Calanus finmarchicus* (Gunnerus), *Pseudocalanus* sp. and *Temora longicornis* (Muller) from a nutrient-enriched seawater enclosure. Journal of Experimental Marine Biology and Ecology 130, 81-92.

Gearing, P., Gearing, J.N., Lytle, T.F., Lytle, J.S., 1976. Hydrocarbons in 60 northeast Gulf of Mexico shelf sediments: a preliminary survey. Geochimica et Cosmochimica Acta 40, 1005-1017.

Goad, L. J., Withers, N., 1982. Identification of 27-nor-(24R)–24-methyl cholesta-5, 22-dien–3β-ol. Lipids 17, 853–858.

Gowen, R.J., Stewart, B., 2005. The Irish Sea: nutrient status and phytoplankton. Journal of Sea Research 54, 36-50.

Gowen, R., McCullough, G., Kleppel, G., Houchin, L., Elliott, P., 1999. Are copepods important grazers of the spring phytoplankton bloom in the western Irish Sea? Journal of Plankton Research 21, 465-483.

Gowen, R., Mills, D., Trimmer, M., Nedwell, D., 2000. Production and its fate in two coastal regions of the Irish Sea: the influence of anthropogenic nutrients. Marine Ecology Progress Series 208, 51-64.

Gowen, R., Stewart, B., Mills, D., Elliott, P., 1995. Regional differences in stratification and its effect on phytoplankton production and biomass in the northwestern Irish Sea. Journal of Plankton Research 17, 753-769.

Grossi, V., Baas, M., Schogt, N., Kelin Breteler, W.C., de Leeuw, J.W., Rontani, J.-F., 1996. Formation of phytadienes in the water column: myth or reality? Organic Geochemistry 24, 833-839.

Grossi, V., Beker, B., Geenavasen, J.A.J., Schouten, S., Raphel, D., Fontaine, M.-F., Sinninghe Damsté, J.S., 2004. C_{25} highly branched isoprenoid alkenes from the marine benthic diatom *Pleurosigma strigosum*. Phytochemistry 65, 3049-3055.

Hammer, O., Harper, D.A.T., Ryan, P.D., 2001. Paleotonlogical statistics software package for education and data analysis. Paleontologia Electronica 4, 2-9.

Harvey, H., 2006. Sources and cycling of organic matter in the marine water column. In: Volkman, J.K. (Ed.) Marine Organic Matter: Biomarkers, Isotopes and DNA. Springer, Berlin pp. 1-25.

Hedges, J.I., Keil, R.G., Benner, R., 1997. What happens to terrestrial organic matter in the ocean? Organic Geochemistry 27, 195-212.

Hedges, J.I., Keil, R.G., 1995. Sedimentary organic matter preservation: an assessment and speculative synthesis. Marine Chemistry 49, 81-115.

Hill, A., Brown, J., Fernand, L., 1997. The summer gyre in the western Irish Sea: shelf sea paradigms and management implications. Estuarine Coastal and Shelf Science 44, 83-95.

Hill, A., Brown, J., Fernand, L., 1996. The western Irish Sea gyre: a retention system for Norway lobster (*Nephrops norvegicus*)? Oceanologica Acta 19, 3-4.

Hill, A., Durazo, R., Smeed, D., 1994. Observations of a cyclonic gyre in the western Irish Sea. Continental Shelf Research 14, 479-490.

Horsburgh, K., Hill, A., Brown, J., Fernand, L., Garvine, R., Angelico, M., 2000. Seasonal evolution of the cold pool gyre in the western Irish Sea. Progress in Oceanography 46, 1-58.

Hu, J., Zhang, H., Peng, P., 2006. Fatty acid composition of surface sediments in the subtropical Pearl River estuary and adjacent shelf, Southern China. Estuarine Coastal and Shelf Science 66, 346-356.

Huang, W.Y., Meinschein, W.G., 1976. Sterols as source indicators of organic materials in sediments. Geochimica et Cosmochimica Acta 40, 323-330.

Huang, W.Y., Meinschein, W.G., 1979. Sterols as ecological indicators. Geochimica et Cosmochimica Acta 43, 739-745.

Huang, Y., Dupont, L., Sarnthein, M., Hayes, J.M., Eglinton, G., 2000. Mapping of C_4 plant input from North West Africa into North East Atlantic sediments. Geochimica et Cosmochimica Acta 64, 3505-3513.

Hudson, E.D., Parrish, C.C., Helleur, R.J., 2001. Biogeochemistry of sterols in plankton, settling particles and recents sediments in a cold ocean ecosystem (Trinity Bay, Newfoundland). Marine Chemistry 76, 256-270.

Jeng, W.L., Lin, S., Kao, S.J., 2003. Distribution of terrigenous lipids in marine sediments off northeastern Taiwan. Deep-Sea Research Part II 50, 1179-1201.

Kattner, G., Hagen, W., 2009. Lipids in marine copepods: Latitudinal characteristics and perspective to global warming. In: Arts, M.T., Brett, M.T., Kainz, M. (Eds.). Lipids in Aquatic Ecosystems. Springer, New York pp. 257-280.

Kattner, G., Krause, M., 1989. Seasonal variations of lipids (wax esters, fatty acids and alcohols) in calanoid copepods from the North Sea. Marine Chemistry 26, 261-275.

Kattner, G., Krause, M., Trahms, J., 1981. Lipid composition of some typical North Sea copepods. Marine Ecology Progress Series 4, 69-74.

Kennington, K., Rowlands, Ll., 2006. SEA6 Technical Report–Plankton Ecology of the Irish Sea. Department of Trade and Industry, United Kingdom.

Knight, P., Howarth, M., 1999. The flow through the North Channel of the Irish Sea. Continental Shelf Research 19, 693-716.

Kolattukudy, P., 1970. Plant waxes. Lipids 5, 259-275.

Lee, R., Nevenzel, J., Paffenhöfer, G.A., 1971. Importance of wax esters and other lipids in the marine food chain: phytoplankton and copepods. Marine Biology 9, 99-108.

Massé, G., Belt, S.T., Allard, W.G., Lewis, C.A., Wakeham, S.G., Rowland, S.J., 2004. Occurrence of novel monocyclic alkenes from diatoms in marine particulate matter and sediments. Organic Geochemistry 35, 813-822.

Meziane, T., Tsuchiya, M., 2000. Fatty acids as tracers of organic matter in the sediment and food web of a mangrove/intertidal flat ecosystem, Okinawa, Japan. Marine Ecology Progress Series 200, 49-57.

McGovern, E., Monaghan, E., Bloxham, M., Rowe, A., Duffy, C., Quinn, A., et al., 2002. Winter nutrient monitoring of the Western Irish Sea – 1990 to 2000. Marine Environmental Health Series 4, Dublin.

McKinney E, Gibson C, Stewart B. 1997. Planktonic diatoms in the North-West Irish Sea: a study by automatic sampler. Biology and Environment: Proceedings of the Royal Irish Academy 97, 197–202.

Nelson, D.M., Tréguer, P., Brzezinski, M.A., Leynaert, A., Quéguiner, B., 1995. Production and dissolution of biogenic silica in the ocean: revised global estimates, comparison with regional data and relationship to biogenic sedimentation. Global Biogeochemical Cycles 9, 359-359.

Nichols, P.D., Guckert, J.B., White, D.C., 1986. Determination of monosaturated fatty acid double-bond position and geometry for microbial monocultures and complex consortia by capillary GC-MS of their dimethyl disulphide adducts. Journal of Microbiological Methods 5, 49-55.

Pancost, R.D., Freeman, K.H., Wakeham, S.G., Robertson, C.Y., 1997. Controls on carbon isotope fractionation by diatoms in the Peru upwelling region. Geochimica et Cosmochimica Acta 61, 4983-4991.

Pancost, R.D., Boot, C.S., 2004. The palaeoclimatic utility of terrestrial biomarkers in marine sediments. Marine Chemistry 92, 239-261.

Pancost, R.D., Pagani, M., 2006. Controls on the carbon isotope compositions of lipids in marine environments. In: Volkman, J.K. (Ed.). Marine Organic Matter: Biomarkers, Isotopes and DNA. Springer, Berlin p209-249.

Peters, K.E., Moldowan, J.M., 1993. The biomarker guide: interpreting molecular fossils in petroleum and ancient sediments. Prentice Hall, New Jersey.

Pinkart, H.C., Devereux, R., Chapman, P.J., 1998. Rapid separation of microbial lipids using solid phase extraction columns. Journal of Microbiological Methods 34, 9-15.

Rampen, S., Abbas, B., Schouten, S., Sinninghe-Damste, J., 2010. A comprehensive study of sterols in marine diatoms (Bacillariophyta): implications for their use as tracers for diatom productivity. Limnology and Oceanography 55, 91-105.

Ramster, J., Hill, H., 1969. Current system in the northern Irish Sea. Nature 224, 59 – 61.

Rontani, J.F., Volkman, J.K., 2003. Phytol degradation products as biogeochemical tracers in aquatic environments. Organic Geochemistry 34, 1-35.

Rowland, S.J., 1990. Production of isoprenoid hydrocarbons by laboratory maturation of methanogenic bacteria. Organic Geochemistry 15, 9-16.

Rullkötter, J., 2006. Organic matter: The driving force for early diagenesis. In: Schulz, H.D., Zabel, M., (Eds.). Marine Geochemistry. 2nd ed. Springer: Berlin p125-168.

Schlitzer R. 2002. Interactive analysis and visualization of geoscience data with Ocean Data View. Computers and Geoscience 28, 1211-1218.

Schmidt, F., Hinrichs, K., Elvert, M., 2010. Sources, transport, and partitioning of organic matter at a highly dynamic continental margin. Marine Chemistry 118, 37-55.

Smallwood, B.J., Wolf, G.A., 1999. Megafauna can control the quality of organic matter in marine sediments. Naturwissenschaften 86, 320-324.

Suess, E., 1980. Particulate organic carbon flux in the oceans - surface productivity and oxygen utilization. Nature 288, 260-263.

Thomson, P.G., Wright, S.M., Bolch, C.J.S., Nichols, P.D., Skerratt, J.H., McMinn, A. 2004. Antarctic distribution, pigment and lipid composition, and molecular identification of the brine dinoflagellate *Polarella glacialis* (Dinophyceae). Journal of Phycology 40, 867-873.

Tolosa, I., Le Blond, N., Marty, J.C., de Mora, S., Prieur, L., 2005. Export fluxes of organic carbon and lipid biomarkers from the frontal structure of the Alboran Sea (SW Mediterranean Sea) in winter. Journal of Sea Research 54, 125-142.

Trimmer, M., Gowen, R., Stewart, B., 2003. Changes in sediment processes across the western Irish Sea front. Estuarine Coastal and Shelf Science 56, 1011-1019.

Trimmer, M., Gowen, R., Stewart, B., Nedwell, D., 1999. The spring bloom and its impact on benthic mineralisation rates in western Irish Sea sediments. Marine Ecology Progress Series 185, 37-46.

Volkman, J.K., 2006. Lipid markers for marine organic matter. In: Volkman, J.K. (Ed.). Marine Organic Matter: Biomarkers, Isotopes and DNA. Springer, Berlin pp. 27-70.

Volkman, J.K., 2003. Sterols in microorganisms. Applied Microbial and Biotechnology 60, 495-506.

Volkman, J.K., 1986. A review of sterol markers for marine and terrigenous organic matter. Organic Geochemistry 9, 83-99.

Volkman, J.K., Jeffrey, S.W., Nichols, P.D., Rogers, G.I., Garland, C.D., 1989.Fatty acid and lipid composition of 10 species of microalgae used in mariculture. Journal of Experimental Marine Biology and Ecology 128, 219-240.

Volkman, J.K., Barrett, S.M., Blackburn, S.I., Mansour, M.P., Sikes, E.L., Gelin, F., 1998. Microalgal biomarkers: A review of recent research developments. Organic Geochemistry 29, 1163-1179.

Ward, Jr. J.H., 1963. Hierarchical grouping to optimize an objective function. Journal of the American Statistical Association 58, 236-244.

Westerhausen, L., Poynter, J., Eglinton, G., Erlenkeuser, H., Sarnthein, M., 1993. Marine and terrigenous origin of organic matter in modern sediments of the equatorial East Atlantic: the $\delta^{13}C$ and molecular record. Deep-Sea Research Part I 40, 1087-1121.

White, D.C., Davis, W.M., Nickels, J.S., King, J.D., Bobbie, R.J., 1979. Determination of the sedimentary microbial biomass by extractible lipid phosphate. Oecologia 40, 51-62.

White, D.C., Ringelberg, D.B., Macnaughton, S.J., Srinivas, A., Schram, D., 1997. Signature Lipid Biomarker Analysis for Quantitative Assessment In Situ of Environmental Microbial Ecology In: Eganhouse, R.P. (Ed.). Molecular Markers in Environmental Chemistry. American Chemical Society, Washington DC p22-34.

Williams, P.M., 1965. Fatty Acids Derived from Lipids of Marine Origin. Journal of Fisheries Research Board of Canada 22, 1107-1122.

Zhang, Z., Zhao, M., Eglinton, G., Lu, H., Huang, C.Y., 2006. Leaf wax lipids as paleovegetational and paleoenvironmental proxies for the Chinese Loess Plateau over the last 170kyr. Quaternary Science Reviews 25, 575-594.

Zhukova, N., Aizdaicher ,N.A., 1995. Fatty acid composition of 15 species of marine microalgae. Phytochemistry 39, 351-356.

Zimmerman, A., Canuel, E., 2001. Bulk organic matter and lipid biomarker composition of Chesapeake Bay surficial sediments as indicators of environmental processes. Estuarine Coastal and Shelf Science 53, 319-341.

Chapter 3

Shallow water methane-derived authigenic carbonate mounds at the Codling Fault Zone, western Irish Sea

O'Reilly, S.S., Hryniewicz, K., Little, C.T.S., Monteys, X., Szpak, M.T., Croker, P., Allen, C.C.R., Kelleher, B.P. Shallow water methane-derived authigenic carbonate mounds at the Codling Fault Zone, western Irish Sea.

This chapter is planned for submission to Marine Geology.

3.1 Introduction

Methane is an important trace gas in the atmosphere and a potent greenhouse gas (Svensen et al., 2004; Forster et al., 2007). Seepage of methane from the ocean's seafloor is of global occurrence, yet one that is poorly quantified and understood (Fleischer et al., 2001; Knittel and Boetius, 2009). One result of seabed seepage is the formation of distinctive seafloor structures, such as pockmarks, mud diapirs, mud volcanoes and methane-derived authigenic carbonates (MDAC). MDAC, which may form pavements or mound structures, are produced as a direct result of methane supply from the subsurface to shallow sediment and the sediment-water interface (e.g. Bohrmann et al., 1998; Aloisi et al., 2000; Greinert et al. 2002; Bayon et al., 2009). There, methane is utilized by a consortium of anaerobic methane-oxidizing archaea (ANME) and sulfate-reducing bacteria (SRB) in the anaerobic oxidation of methane (AOM) reaction (Hinrichs et al. 1999; Boetius et al. 2000; Reitner et al. 2005) according to Equation 3.1:

$$CH_{4(g)} + SO_4^{2-}{}_{(aq)} \rightarrow HCO_3^-{}_{(aq)} + HS^-{}_{(aq)} + H_2O_{(l)}$$

Eqn. 3.1

The reaction is maintained in expense of marine sulfate dissolved in pore waters (Boetius et al., 2000; Tsunogai et al. 2002; Niemann et al., 2005). If the supply of methane is sufficient, AOM leads to supersaturation of pore fluids with respect to HCO_3^- and in result facilitates the formation of MDAC (Hovland et al., 1987; Stakes et al. 1999; Greinert et al., 2001; Mazzini et al., 2005; Naehr et al., 2007; Paull et al., 2007; Feng et al., 2008). HS^- typically precipitated as pyrite (FeS_2) on reaction with Fe in pore fluids (e.g. Peckmann et al., 2001; Pechmann and Thiel, 2004). Recent evidence indicates that the bacterial partners involved in AOM may be more diverse than previously thought (Beal et al., 2009) and that ANME may be able to perform AOM without bacterial partners (Milucka et al., 2012). AOM is responsible for the oxidation of possibly 90% of marine methane (Knittel and Boetius, 2009) and hence AOM and MDAC formation are important for regulation of ocean to atmosphere carbon fluxes (e.g. Aloisi et al., 2002). Methane consumption via AOM is estimated to be in the range of 5 to 20% of net modern atmospheric methane flux (20 to 100 $x10^{12}$ g a^{-1}) (Valentine and Reeburgh, 2000). Many sites of active methane seepage have been shown to support unique macro- and micro-faunal biodiversity (e.g. Dando

et al., 1991; Jensen et al., 1992; Sibuet and Olu 1998; Van Dover et al., 2003; Olu-Le Roy et al., 2004). In addition gas seepage features are important in relation to marine industrial and petroleum safety (Hovland et al., 2002) and also in petroleum and gas prospecting (Judd and Hovland, 2007).

Most cold seeps with extensive MDAC have been reported from the deep sea (e.g. Ritger et al., 1987; von Rad et al., 1996; Chen et al., 2005; Feng et al., 2010; Haas et al., 2010; Crémière et al., 2012; Magalhães et al., 2012), while regions of extensive MDAC occurrence within the photic zone (0 to ~200 m water depth) are less common. Shallow cold seep settings with extensive MDAC occurrence include the Coal Oil Point Seep field, off Santa Barbara (Kinnaman et al., 2010), St. Lawrence Estuary, Canada (Lavoie et al., 2010), Monterey Bay (Stakes et al., 1999), the Kattegat (Jørgensen et al., 1989; Jensen et al., 1992), the Adriatic (Capozzi et al., 2012), the northwestern Black Sea (Peckmann et al., 2001), the North Sea (Hovland and Judd, 1988), and recently the Texel 11 and Holden's Reef sites in the Irish Sea (Judd et al., 2007). Seep-specialist macrofaunal communities typically flourish in deep sea active cold seeps compared to shallower settings, likely due to the increased influence and input of photosynthetic carbon in shallow depths (Levin, 2005). However, this distribution is more complex than simple bathymetric zonation and shallow cold seeps with extensive seep-associated biological communities have also been documented (e.g. Dando et al., 1991; Little et al., 2002; Levin, 2005, and references therein).

Twenty three mounds features have recently been identified along the Codling Fault Zone (CFZ) in the east perimeter of the Kish Bank Basin in the western Irish Sea (Croker et al., 2005). The CFZ is a major northwest-southeast trending strike-slip fault and consists of a complex fault zone several kilometers wide (Jackson et al., 1995; Croker et al., 2005). Croker et al. (2005) divided the fault into three zones: the northern muddy zone containing the Lambay Deep and its associated mud diapir; the central sandy zone characterised by large sand waves; and the southern zone characterised by current-swept seabed and patches of coarse sediments. The CFZ mounds have been identified in the central zone and appear to have a relief of 5 to 10 m. They are typically greater than 250 m in length and over 80 m in width. Croker et al. (2005) proposed that the CFZ is the most active site of gas seepage in the Irish designated zone of the Irish Sea. A number of the CFZ mounds were investigated in 2010 during INFOMAR survey CV10_28. The purpose of this study was to further

ground-truth the CFZ carbonate mound features to confirm whether these features are formed by methane seepage, to provide evidence of current active seepage, and finally to compare this site to other extensive MDAC occurrences in shallow and deep sea settings.

3.2 Environmental and Geological Setting

The western Irish Sea encompasses two Mesozoic sedimentary basins, namely the Kish Bank Basin and the southwest section of the Central Irish Basin, and is primarily underlain with Permian and Carboniferous rocks. Quaternary deposits up to 150 m thick occur, but are laterally discontinous, locally revealing exposed bedrock (Croker et al., 2005). The northwest Irish Sea (north of $53^{o}10^{'}$) is characterised by relatively weak hydrodynamic conditions, resulting in the seabed being dominated by fine silty mud. This is in contrast to the southern region where the CFZ is located. This region is subject to comparatively high-energy currents and is characterised by gravelly sands and cobbles, and high-energy bedforms such as sand streaks, sand ribbons, gravel furrows and sand waves (Croker et al., 2005). The water depth here is 50 to 60 m at the west of the fault and 80 to 120 m to its east. For a detailed discussion of the setting and geology of the study area see Dobson and Whittington (1979) and Jackson et al. (1995).

3.3 Materials and Methods

Bathymetry data was collected as part of the INFOMAR (Integrated Mapping for the Sustainable Development of Ireland's Marine Resources) program, using a Kongsberg Simrad EM1002 multibeam echosounder. Data was acquired using a heave-corrected SES Probe 5000 3.5 kHz transceiver in conjunction with a hull-mounted $4^{o}x4^{o}$ transducer array. Acquisition parameters, data logging and interpretation were carried out using the CODA Geokit suite. Water column echofacies were monitored using a Kongsberg Simrad EA400 single beam echosounder operated at 38 kHz. A Kongsberg Simrad OE14-208 underwater towed video system, housed in a Seatronics frame was used to obtain video and image stills of the mound features and surrounding seabed. Sediment sampling was conducted using Shipek and Van Veen grabs. Hardground material was retrieved from three stations, G103, G107 and G109, as shown in Fig. 3.1. Details for the sampling stations are given in Table 3.1. Samples

for geochemical analysis were stored at -20°C onboard and at -80°C in the laboratory. The redox potential (E_h) of sampled sediments was assessed using an ORP ProcessProbe Ag/AgCl redox probe (Bradley James Corp., Bedford, UK).

Unoriented rock slabs from G109 were cut using a diamond rock cutter and polished with sandpaper. Some polished slabs were used to prepare uncovered petrographic thin sections of standard size (48 mm x 28mm). Optical petrographic microscopy was performed using Leica DC 300 digital camera mounted on Leica DMLP microscope under the magnifications of 2.5, 5, 10, 20 and 40x. Relative abundances of grains in relation to pore space were estimated using comparison charts (Bacelle and Bosellini, 1965). Finely ground, hand-drilled carbonate samples from G109 were analysed for stable $\delta^{13}C$ and $\delta^{18}O$ isotope ratios using a Finnigan MAT 251 and MAT 253 mass spectrometers coupled to automated Kiel devices. The results are measured in relation to standard VPDB, with long-term analytical precision around 0.05% for $\delta^{13}C$ and 0.1% for $\delta^{18}O$. $\delta^{13}C$ measurement of methane from sediment samples to headspace vials from a core catcher was performed on a Finnegan MAT DeltaPlus irMS after conversion to CO_2 (Organic Mass Spectromety Facility, Woods Hole Oceanographic Institute).

Standard X-ray diffraction in order to identify main minerals was performed on mortar-ground samples using Siemens D5005 powder X-ray diffractometer. Scanning electron microscopy was performed using a Hitachi S3400-N scanning electron microscopy operated at an accelerating voltage of 15.0 kV and a working distance of 10 mm. Elemental composition was assessed using an INCA Energy energy dispersive spectrometer (Oxford Instruments, UK) fitted to a Hitachi SU-70 SEM. SEM-energy dispersive spectroscopy (EDS) was performed at an accelerating voltage of 15.0 kV and a working distance of 16 mm. Elemental data was processed with the INCA suite software.

Sampled hardgrounds were acid solubilised (2 M HCl) and extracted according to Niemann et al. (2005) by ultrasonication-assisted extraction with the following solvent regime: 2:1 (v/v) methanol/DCM (x2), 1:2 (v/v) methanol/DCM (x2) and DCM (x2). Total lipid extracts were saponified with 6% KOH in methanol (80°C for 3 hr) and neutral lipids and fatty acids (at ~ pH 1) were recovered by liquid-liquid extraction (x3) with 9:1 (v/v) hexane/diethyl ether. Neutral lipids were derivatised with N,O- bis(trimethylsilyl) trifluoroacetamide/pyridine (9:1, v/v), while fatty acids were methylated with 14% BF_3 in methanol at 70°C for 1 hr. Fatty acid

methyl ester (FAME) monounsaturation position was confirmed by formation of dimethyl disulfide (DMDS) adducts as outlined by Nichols et al. (1986). Analysis was performed on an Agilent 6890N gas chromatograph interfaced with an Agilent 5975C mass selective detector. The column temperature program was as follows: 65^{o}C injection and hold for 2 min, ramp at 6^{o}C min^{-1} to 300^{o}C, followed by isothermal hold at 300^{o}C for 20 min. Quantification was performed using 5-α-cholestane internal standard (Appendix A). Samples were analysed in duplicate by continuous flow isotope ratio mass spectrometry (IsoPrime) using identical GC conditions as above. $\delta^{13}C$ values were calibrated against a stable isotope reference standard comprising a mixture of 15 *n*-alkanes (Mixture B2, Indiana University; See Appendix B)). Average $\delta^{13}C$ values are reported after correction for addition of derivative groups where necessary. Fatty acid nomenclature is according to $xC_{y\omega z}$, where *x* refers to the number of carbon atoms present, *y* refers to the number of double bonds on the carbon chain and *z* refers to the position of the first double bond from the methyl end.

A sample of retrieved carbonate and a control sand sample were extracted in duplicate using the POWERSOIL DNA isolation kit (MO BIO, Carlsbad, US). PCR reactions (50 μL) were carried out using DNA Engine DYAD Peltier Thermal Cycler. DGGE primer 2 (5'-ATTACCGCGGCTGCTGG-3') and DGGE primer 3 (5'-CGCCCGCCGCGCGCGGCGGGCGGGGCGGGGGCACGGGGGGCCTACGGGA GGCAGCAG-3') (Muyzer et al., 1993). A touch-down PCR was performed as follows: denaturation step of 95^{o}C for 5min; followed by 20 cycles of 95^{o}C for 1 min, 60^{o}C for 1 min and 72^{o}C for 3 min, with a 0.5^{0}C decrease per cycle for the annealing step. This was followed by 8 cycles of 95^{0}C for 1 min, 55^{o}C for 1 min and 72^{o}C for 1 min. Archaeal 16S rRNA sequences were first amplified using S-D-Arch-0025-a-S-17 (5'-CTGGTTGATCCTGCCAG-3') forward primer and S-*-Univ-0907-a-A-20 (5'-CCGTCAATTCMTTTRAGTTT-3') reverse primer (Vetriani et al., 1999). PCR was performed as follows: denaturation step of 94^{o}C for 3 min; followed by 40 cycles of 94^{o}C for 30 s, 48^{o}C for 30 s, and 72^{o}C for 30 s; and finally an elongation step of 72^{o}C for 5 min. A nested PCR was then performed as above but replacing DGGE primer 3 with the archaeal specific GC-clamped primer A344f (GC) (5'CGCCCGCCGCGCCCCGCGCCCGTCCCGCCGCCCCCGCCACGGGGCGCA GCAGGCGCGA-3') (Vetriani et al., 1999). DGGE was performed using the CBS Scientific DGGE 2401 system with denaturing gradients from 20 to 80% (80% denaturant consisted of 5.6 M urea and 32% v/v formamide), at constant voltage and

temperature of 90V and 60°C respectively, for 16 hrs. The gels were then stained using 1X SYBRGold nucleic acid stain (Invitrogen, Paisley, UK) for 45 min and imaged by transillumination.

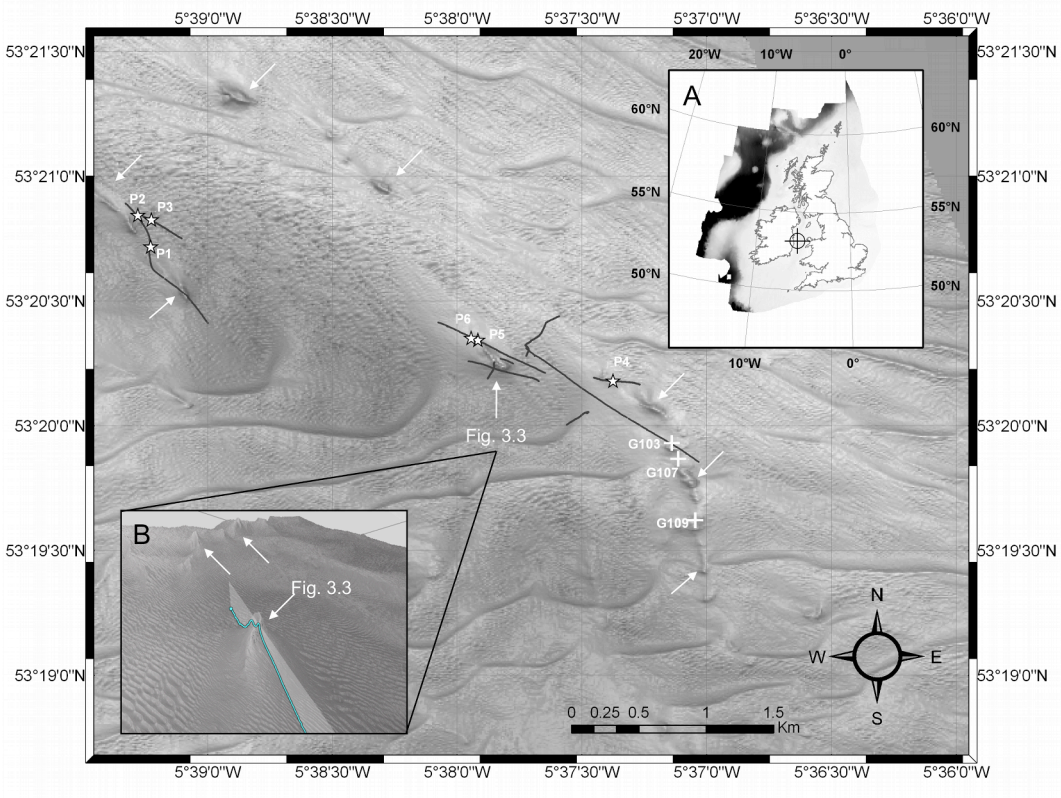

Figure 3.1. The Codling Fault Zone mound features (white arrows), sampling stations that recovered hardground material (white crosses), underwater video tracklines (dark grey lines), and representative underwater image stills of exposed carbonates or black reduced sediment (white stars). A. Location of the area of study; B. A 3D Fledermaus image showing the topography of some of the mounds (Data source – Monteys, X.).

3.4 Results

3.4.1 Underwater towed video, sampling and single beam echosounder

Video and image stills of the seabed at and in the vicinity of the mound targets were collected (Fig. 3.2). Representative underwater image stills are shown in Fig. 3.2A to F. Sediment type was primarily fine- to coarse-grained sand, with frequently a high proportion of intact and fragmented bivalve shells. There was widespread occurrence of exposed and semi-exposed hardgrounds on the seabed in the vicinity of target sites (Fig. 3.2A and B). These features appeared to be largely buried by sand. Fig. 3.2C shows an underwater still image of an area of exposed stacked pavement. This shows large 10 to 20 cm thick slabs and likely represents the characteristic morphology of

the CFZ mounds. Patches of black, apparently reduced seabed several centimetres across were also recorded (Fig. 3.2D and F) during video surveying as well as frequent cemented tube worms (Fig. 3.2D). A high density of asterozoans (likely ophiuroids) was observed in the vicinity of the mounds (not shown). In addition, possible hydroids colonising hardgrounds were also recorded (Fig. 3.2D to F).

Table 3.1. Summary data of collected cemented carbonates from the Codling Fault Zone.

Station		G103	G107	G109
Latitude		53.3319	53.3308	53.3265
Longitude		-5.6192	-5.6187	-5.61780
Water Depth (m)		58	61	67
Sediment		Black reducing coarse sand, hydroids,	Dark greyish brown sand, hydroids	Dark greyish brown sand and black reducing
Hardgrounds (approx. %)		Cemented worm tubes (70%)	20%	50%
E_h (mV)		-177	-	-
Bulk $\delta^{13}C$ (‰)		-	-37.0	-48.1 to -53.0
Bulk $\delta^{18}O$ (‰)		-	3.5	1.7 - 2.4
Major Elements (%)		Ca (68), Si (15), Al (5), Na (4)	Si (59), Ca (37), Cl (4)	Ca (96), Si (4)
Fatty acids (µg g^{-1})		1.11	1.58	3.4
(%)	SATFA[1]	32.7	35.7	39.1
	MUFA[2]	37.6	25	33.2
	PUFA[3]	13.5	27.7	16.7
	brFA[4]	16.2	11.7	11
	$iC_{15:0}$	2.7	1.1	1.8
	$aiC_{15:0}$	2	0.6	1.8
	$C_{16:1\omega5}$	1.7	0.6	1.3
	$10MeC_{16:0}$	3.2	1.9	1.1
	$iC_{17:0}$	1.8	1.2	2.5
	$aiC_{17:0}$	0.6	0.6	0.7
	$C_{17:1\omega6}$	0.6	n.d.	0.3
	$cycC_{17:0}$	0.8	0.4	0.4
	$cycC_{18:0}$	0.6	n.d.	0.4
Sterols (µg g^{-1})		1.32	4.46	1.72
(%)	C_{26}	9.8	9.9	6.8
	C_{27}	69.1	70.9	59.8
	C_{28}	15	14.3	22.4
	C_{29}	6.2	4.8	11
n-alkanols (ng g^{-1})[5]		19	24	47
MAGE (ng g^{-1})[6]		49	36	161
Phytol (ng g^{-1})		n.d.	n.d.	22
Crocetane (ng g^{-1})[7]		<1	n.d.	1
PMI (ng g^{-1})[8]		9	n.d.	10
Archaeol (ng g^{-1})		1	n.d.	7

1. Saturated fatty acids
2. Monounsaturated fatty acids
3. Polyunsaturated fatty acids
4. Branched (including cyclic) fatty acids
5. C_{14} to C_{26} *n*-alkanols
6. Monoalkyl glyceryl ethers ranging from C_{14} to C_{20}
7. Co-eluting – concentrations estimated based on abundance of key m/z fragments
8. Pentamethyleicosane

Grab sampling of sites G103, G107 and G109 retrieved hardground fragments and some black sediment. The locations of these grabs are shown in Fig. 3.1 and all summary data is given in Table 3.1. Sampled black surface sediments (Fig. 3.2G and I) were confirmed to be reducing, exhibiting E_h readings as low as -177 mV.

Colonising hydroids were also retrieved, still physically attached to sampled hardgrounds (Fig. 3.2G and H). These possibly belong to the genus *Nemertesia*, which have been found in carbonate mound sites in the mid-Irish Sea (Judd, 2005). Grab sampling stations G103, G107 and G109 contained cemented tube worms (Fig. 3.2G). These are likely to have been formed by sedentary sabellarid polychaetes, possibly *Sabellaria spinulosa*, which are abundant at other hard grounds in the Irish Sea (Whomersley et al., 2010). Single beam echosounder transects across one of the mounds (Fig. 3.1B) yielded characteristic acoustic echofacies in the water column. These appear as a rising vertical plume from close to the apex of the mound (Fig. 3.3). This acoustic signal is either caused by fish shoals or gas bubbles. However, fish shoals would normally display a broader more horizontal profile (Judd and Hovland, 2007), and by virtue of the source and vertical profiles this is very likely a gas plume emanating from the mound itself. The plume was detected rising a number of metres into the water column and the profile indicates at least moderate seepage is taking place at the CFZ.

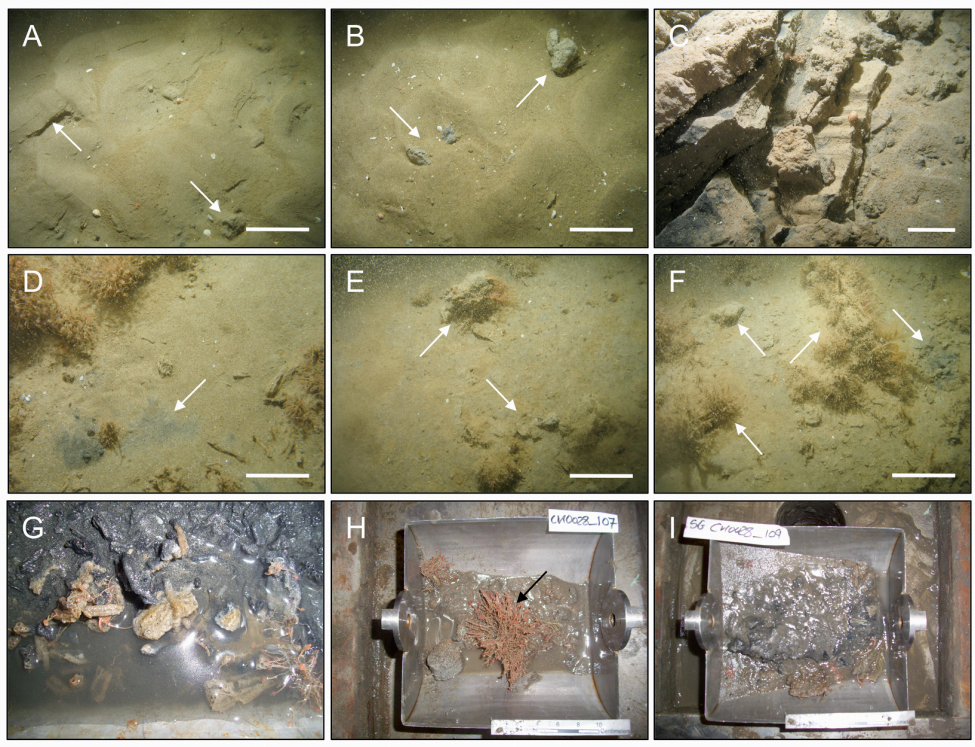

Figure 3.2. Underwater towed video (A to F) and grab sampling (G to I) of Codling Fault mound targets. A. Semi-exposed nodules and pavement (P1); B. Semi-exposed hardgrounds (P2); C. Pavement stacking (P3); D. Reduced surface sediment (P4) E. Large exposed hardgounds (P5) F. Exposed colonised and non-colonised hardgrounds (P6); G. G103, H. G107, I. G109 – a hardground colonised by a *Nemertesia* hydroid (black arrow); Unlabelled scale bars = 25cm; The locations for underwater still images and sampling stations are given in Fig. 3.1 and Table 3.1.

3.4.2 Mineralogy and petrographic analysis

A number of sampled hardgrounds were also analysed using SEM-EDS analysis (Fig. 3.4). EDS spectra were dominated by calcium, silica, carbon and oxygen, confirming that the hard grounds are composed of carbonate and carbonate-cemented quartz grains (Fig. 3.4A and B). Individual quartz grains cemented by this carbonate are shown in Fig. 3.4C. Sulphur was also identified from EDS spectra, in particular for G109 (Fig. 3.4B). SEM micrographs highlighted the occurrence of amorphous to well-developed framboidal pyrite as the source of this sulphur (Fig. 3.4D and E). Based on the crystal shapes observed in SEM, the carbonate appears to a primarily acicular aragonite. Further petrographic analysis (Fig. 3.5) and X-ray diffraction (Fig. 3.6) of G109 confirmed that quartz and aragonite are the major mineral constituents of the rock. The rock can be subdivided into two main components. A detrital component is composed mostly of quartz with small admixtures of other grains. It comprises mudstone lithoclasts, glaucony grains (Fig. 3.5B) and bioclasts. Among bioclasts possible red algae (Fig. 3.5B), echinoderms (Fig. 3.5B), bivalve fragments (Fig. 3.5C), balanid barnacles (Fig. 3.5D), foraminifera and gastropods (Fig. 3.5E and F) have been identified. This component can be linked with quartz and magnesian calcite, as identified by XRD (Fig. 3.6). The total grain fabric constitutes around 60% of the rock volume. Pore space partially occluded by the authigenic component occupies the remaining 40% of rock volume. The authigenic component is composed almost solely of aragonite (Fig. 3.6). It is represented by the microcrystaline variety, lining the surface of some of the grains and occasionally forming clothed microfabrics, followed by more abundant acicular crystals cementing the pore space (Fig. 3.5).

3.4.3 Carbonate and gas $\delta^{13}C$ analysis

Measured $\delta^{13}C$ isotope values for G109 were significantly low, reaching down to -53.7‰ (Fig. 3.7). $\delta^{13}C$ values for methane sampled from surface sand at the CFZ measured -70.0‰.

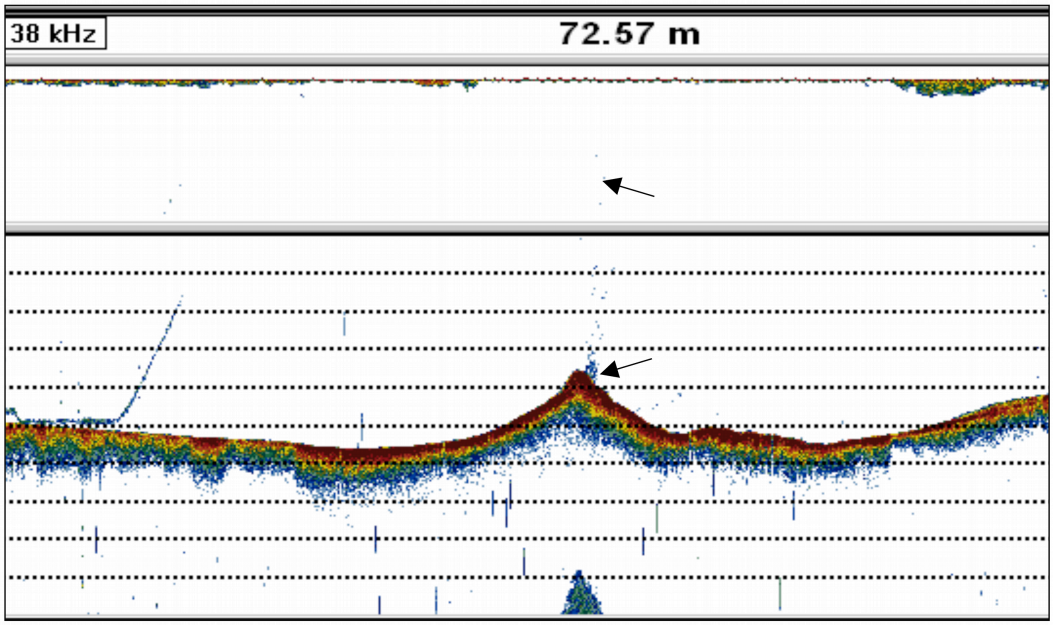

Figure 3.3. Single beam echosounder profile showing topography of one of the Codling Fault mounds and active gas seepage to the water column from close to its apex (black arrows). The broken horizontal lines represent about 10 m water depth. The location of the mound is shown in Fig. 3.1 (inset B). (Data Source – Monteys, X.).

3.4.4 Lipid biomarkers and compound specific $\delta^{13}C$ analysis

Fatty acids distribution was similar between three carbonate samples whereby a range of saturated, monounsaturated, polyunsaturated, methyl- and cyclopropyl fatty acids were observed (Fig. 3.8A). Fatty acids ranged from C_{12} to C_{26} homologs. $C_{16:0}$ was the major fatty acid in all samples. $C_{14:0}$ and $C_{18:0}$ were other major saturated fatty acids. Monounsaturated $C_{16:1\omega7}$ and $C_{18:1\omega7}$ were also major fatty acids, followed by the polyunsaturated fatty acids $C_{20:5\omega3}$, $C_{20:4\omega6}$, $C_{22:6\omega3}$ and $C_{22:5\omega6}$. Iso and anteiso methyl branched fatty acids were also abundant and were dominated by odd carbon C_{15} and C_{17} homologs. These included *i*$C_{15:0}$, *ai*$C_{15:0}$, *i*$C_{16:0}$, 10Me$C_{16:0}$ and *i*$C_{17:0}$. The average (n = 2) measured $\delta^{13}C$ values for selected lipids from G103, G107 and G109 are given in Fig. 3.9. The $\delta^{13}C$ measurements for fatty acids ranged from -24‰ to as low as -39‰. A general trend of between -25‰ to -29‰ was observed with overall little variation between samples for each compound. However the branched fatty acids *ai*$C_{15:0}$, *i*$C_{16:0}$, 10Me$C_{16:0}$ and $C_{17:1}$ were more depleted (below -30‰) for G109, as well as with *i*$C_{16:0}$ for G107. Sterols were the major lipid class in the neutral lipid fractions. $C_{27}\Delta^5$ was the major sterol in all samples. $C_{26}\Delta^{5,22}$, $C_{27}\Delta^{5,22}$, $C_{28}\Delta^{5,22}$, $C_{29}\Delta^{5,22}$, $C_{29}\Delta^5$ and $C_{29}\Delta^{5,24(28)}$ were also identified. $\delta^{13}C$ values were about -28‰ for

well-resolved major sterols (Fig. 9). Other major lipids included phytol, *n*-alkanols (C_{14} to C_{26}), a range of mono-alkyl glycerol ethers (MAGE) with *n*-alkyl chain lengths from C_{14} to C_{20}. Pentamethylicosane was identified in G109 in low abundance, as well as crocetane co-eluting with phytane. Archaeol was tentatively identified in low abundance in G103 also based on the peaks at m/z 130, 278 and 426. The abundance of these lipids was too low to permit $\delta^{13}C$ measurement.

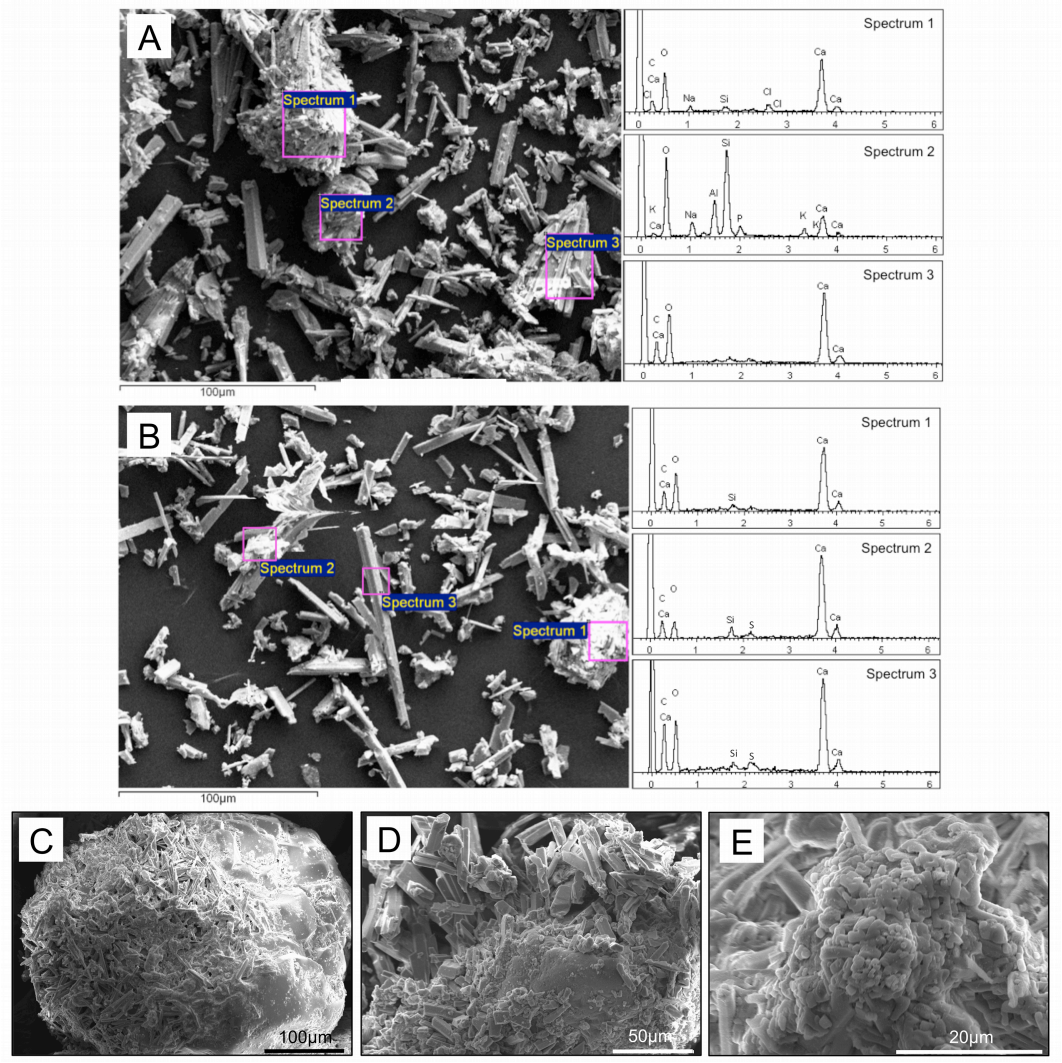

Figure 3.4. A, B. Representative SEM-EDS analyses of the composition of sampled hard grounds (locations given in Fig. 3.1 and Table 3.1). C. SEM micrograph showing carbonate-cemented quartz grain. D. Aragonite crystals and framboidal pyrite. E. Detail of framboidal pyrite close-up.

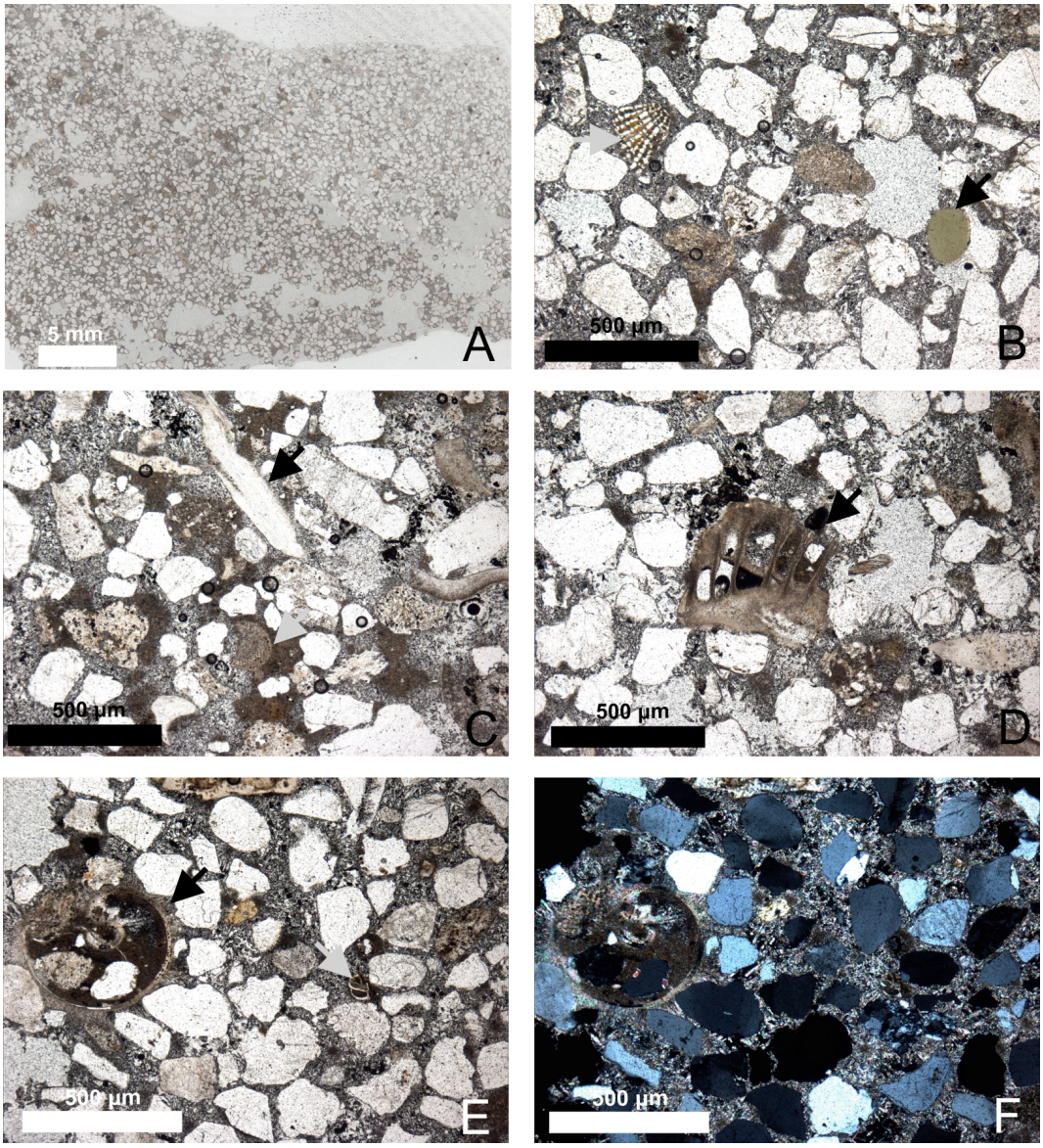

Figure 3.5. Aragonite cemented allochemic sandstone with bioclasts (G109). All microphotographs from PMO 217.327; A. Low magnification view of petrographic thin section. Note the large contribution of quartz grains in the rock volume. Empty cavities visible in the lover part of the picture are a product of sample preparation. B. Detail showing a possible glaucony granule (black arrow) and a an echinoderm skeletal fragment (grey arrow). C. Detail showing a bivalve fragment, possible an oyster (black arrow) and a red algal fragment (grey arrow). D. Detail showing a balanid barnacle fragment (black arrow) E. Detail showing a gastropod (black arrow) and a possible foraminiferan (grey arrow). F. Same are as in E, but with polarized light. (Data source – Hryniewicz, K.; Little, C.T.S.)

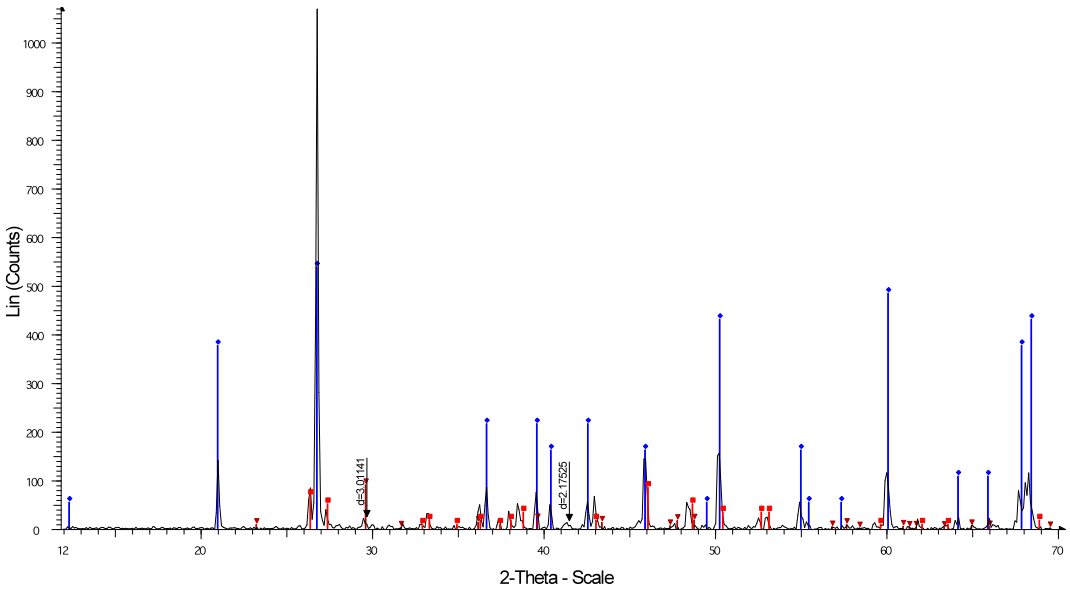

Figure 3.6. X-ray powder diffractogram of sample G109. The blue rhombi represent quartz, red squares represent aragonite and red triangles represent Mg-calcite (Data source – Hryniewicz, K.; Little, C.T.S.).

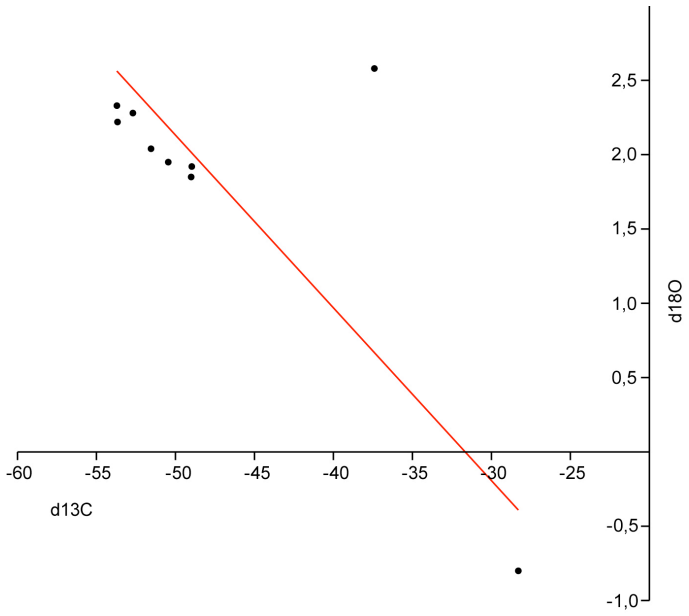

Figure 3.7. Carbon and oxygen stable isotope data from sample G109. Regression line in red (Data source – Hryniewicz, K.; Little, C.T.S.).

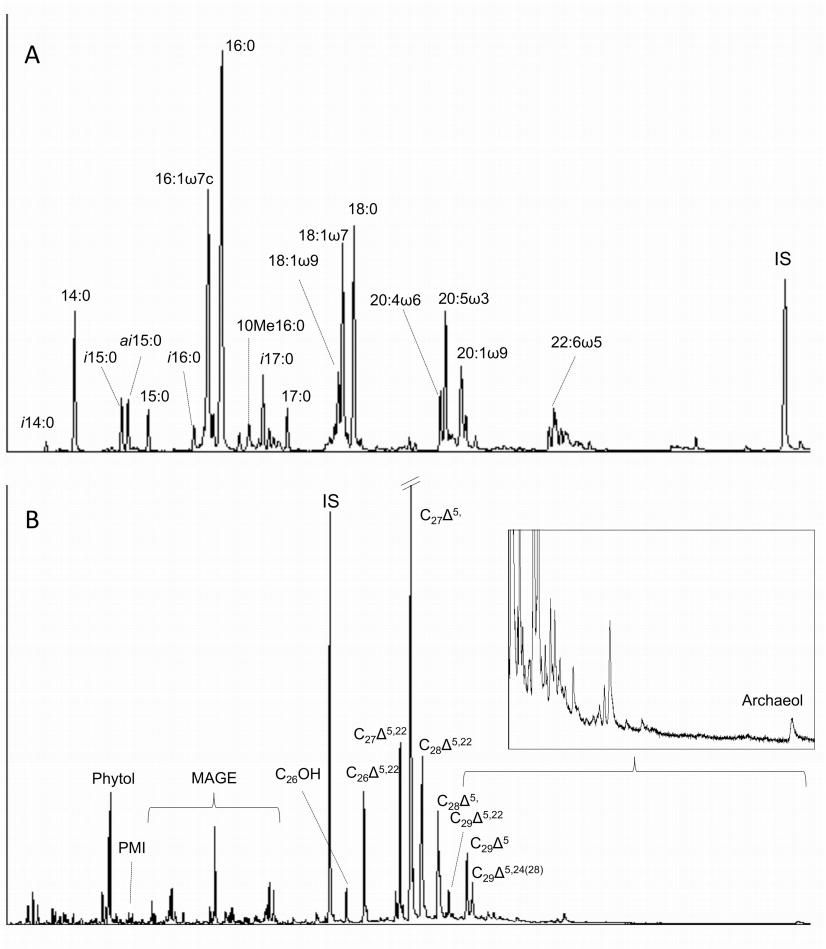

Figure 3.8. Total ion chromatograms of a representative phospholipid fatty acid sample (A) and an alcohol fraction (B) from extracted aragonite-cemented quartz. Major compounds are labeled. Fatty acid nomenclature is according to *X:Y*ω*Z,* where *X* refers to the number of carbon atoms present, *Y* refers to the number of double bonds on the carbon chain and *Z* refers to the position of the first double bond from the methyl end. Sterol nomenclature is according to $C_X\Delta^Y$ where *Y* refers to the position of double bond(s) on the sterol skeleton.

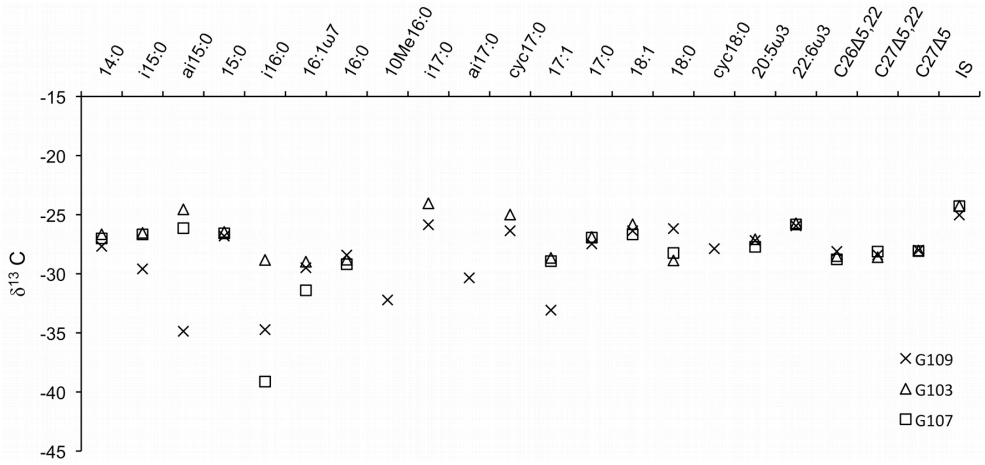

Figure 3.9. Measured $\delta^{13}C$ values for selected biomarkers extracted from samples G103, G107 and G109. See Fig. 3.1 for station location. IS = internal standard (5-α-cholestane).

3.5 Discussion

Methanogenesis in marine sediments can be subdivided into three main stages. The first stage takes place during shallow burial, when in temperatures lower than 50°C organic matter is being converted into methane by series of biochemical processes (Mah et al., 1977). In later burial at 80°C to 120°C, thermal cracking of organic matter forms gaseous and liquid hydrocarbons, which are further cracked to methane in when temperatures reach ca. 150°C (Claypool and Kvenvolden, 1983). Each of the formation stages leaves a characteristic trace in isotopic and chemical composition of the resulting gas (Schoell, 1988; Whiticar, 1999), which can be used to trace back the origin of the methane (e.g. Martens et al., 1991; Ivanov et al., 2010). Usually, the biogenic methane is significantly depleted in the heavy carbon isotope, with $\delta^{13}C$ values below -50‰, with thermogenic methane ranging between -50‰ to -30‰ (Sackett, 1978; Peckmann and Thiel, 2004; Judd and Hovland, 2007).

Heavily depleted carbon isotope (as low as -53.71‰) data from hardgrounds sampled at stations G107 and G109 confirm that the CFZ mounds are MDAC. Thus the CFZ mounds are, along with the Texel 11 and the Holden's Reef sites, the third confirmed occurrence of MDAC in the Irish Sea (Judd, 2005; Judd et al., 2007). Usually MDAC is less depleted than parent gas due to mixing with carbon from other sources, so the exact correlation between carbonate and parent gas is not straightforward (e.g. Bohrmann et al., 1998, Peckmann et al., 2001, Schmidt et al., 2002; Peckmann and Thiel, 2004). The amount of mixing is unknown, but seeping methane was likely isotopically lighter than cements and therefore of biogenic origin. The $\delta^{13}C$ for methane recovered from surface sediment in this region measured -70‰, and again supports the conclusion that the source of gas is biogenic rather than thermogenic. Accumulations of unidentified shallow gas north of the study area has been suggested previously to be of biogenic origin (Yuan et al., 1992). Gas generation within these sediments is possible, however the volume of gas generated from thin and fairly recent sediment (Belderson, 1964) is probably much lower than that observed (Clayton, 1992; Judd and Hovland, 2007). Because the area of study is dominated by sands (Belderson, 1964; Croker et al., 2005), the gas is most likely sourced from the deeper subsurface. Subcropping Palaeozoic and Mesozoic rocks of the Kish Bank Basin (Naylor et al., 1993) are obvious candidates, with Carboniferous coals subjected to biogenesis of methane being of particular interest here (e.g. Flores

et al., 2008; Li et al., 2008; Ulrich and Bower, 2008; cf. Moore, 2012). Alternatively, significant mixing and microbial reworking of seeping thermogenic gas in the shallow subsurface would result in a further depleted isotope signal from the original thermogenic signature and may be occurring here. Thus the exact source of the gas remains difficult to determine at present.

Active water column seepage from the CFZ mounds has been documented on one other occasion at a separate feature in the CFZ to the southeast (Croker et al., 2005). Based on surveys to date, the CFZ appears to be a site of an active macro-seepage. $\delta^{13}C$ analysis has confirmed that the precipitated carbonate is MDAC and SEM-EDS and has also highlighted the presence of co-precipitated pyrite. Sulfate reduction is also evidenced by the presence of patches of black reducing sediments at the sediment-water interface (Fig. 3.2D and F). AOM is therefore a significant process regulating the flux of methane from the CFZ mounds and the formation of carbonate mounds exposed at this site. The size and thickness of the slabs shown in Fig. 3.2C indicate considerable seepage over geological time (Fig. 3.2C), and together with echosounder data, indicates active methane seepage from the CFZ mounds is ongoing. Marine settings experiencing long-term erosion will eventually expose MDAC formed by AOM and, since carbonate-cemented sediments are more resistant to erosion than uncemented sediments, exhumed MDAC will accumulate as lag deposits in erosional environments (Paull and Ussler, 2008). The CFZ is a dynamic erosional setting with strong hydrographic conditions, and it is likely that the mounds formed in the shallow subsurface and have become exposed over time. The topography of these features are also likely extensively eroded post-exposure.

Both the character of the detrital and authigenic component suggests carbonate authigenesis within the sediment. This seems to be a common phenomenon in most of the seeps in the marine environment (e.g. Naehr et al., 2007; Pierre and Fouquet 2007; Himmler et al., 2011), since AOM is localized to the anoxic zone at some depth within the sediment (Hinrichs et al. 1999, Boetius et al. 2000). Aragonite forms in favour over calcite in settings with relatively high alkalinity and increased sulfate concentrations (Walter, 1986; Burton, 1993). In this way in seep settings aragonite is preferentially formed closer to the sediment-water interface (Beauchamp and Savard, 1996; Aloisi et al., 2002). Formation of authigenic carbonate proceeds downward from the initial sulfate-methane transition to form carbonate crust (Greinert et al., 2002; Bayon et al., 2009). As AOM proceeds, marine sulfate enclosed in the pore

water is successively consumed, giving way for more extensive precipitation of calcite in the succeeding stages (e.g. Aloisi et al., 2002; Bayon et al., 2009). Dominance of aragonite over calcite in carbonates sampled (Fig. 3.6) implies their formation in sulfate-rich environment, most likely shaped by seawater reflux trough permeable sandy sediment (Fig. 3.5).

Nemertesia and *Sabellaria* are epifaunal animals, which require a solid substrate for colonisation (Whomersley et al., 2010). *Sabellaria spinulosa* favours a sandy erosional environment but requires a hard ground in order to get established. This species was found in very high densities covering MDAC in the mid-Irish Sea (Whomersley et al., 2010) and may be an important coloniser of carbonate grounds throughout the Irish Sea. No known seep-associated macrofauna, such as siboglinid tubeworms or thyasirid bivalves (Dando et al., 1991) were observed during video surveying. Nor were bacterial mats, which are commonly reported in active methane seep environments (e.g. Niemann et al. 2005, Bouloubassi et al. 2009). Chemosymbiotic macrofauna such as Siboglinidae are rarely reported in shallow shelf and coastal cold seeps and are largely restricted to deep-sea active cold seep settings (Judd and Hovland 2007). Thus they would not be expected to occur in a setting such as the CFZ seeps. However it is evident that these hard grounds are of significant importance as a solid substrate for normal marine epifauna, allowing for diverse ecosystems to develop (Whomersley et al., 2010), as has been observed in the North Sea (Dando et al., 1991; Jensen et al., 1992).

The CFZ seep carbonates contain major fatty acids previously reported among SRB implicated in AOM (Aloisi et al., 2002; Elvert et al., 2003; Niemann and Elvert 2008). These included $i\mathrm{C}_{15:0}$, $ai\mathrm{C}_{15:0}$, $\mathrm{C}_{16:1\omega5c}$, $\mathrm{C}_{17:1\omega6c}$ and $\mathrm{cyc}\mathrm{C}_{17:0}$ (Fig. 3.8A). $ai\mathrm{C}_{15:0}$, $i\mathrm{C}_{16:0}$ and $\mathrm{C}_{17:1}$ fatty acids, in particular for G109 (and $i\mathrm{C}_{16:0}$ for G107) were more depleted than other fatty acids, which suggests that SRB involved in AOM are present. However, in general measured $\delta^{13}\mathrm{C}$ values for most fatty acids were not significantly depleted in $^{13}\mathrm{C}$ (Fig. 3.9) and suggests that methane is not a primary substrate for the dominant bacterial populations in this setting, as has been found in some other active seep settings (e.g. Pancost et al., 2000; Elvert et al., 2003, Niemann et al., 2005). Monoalkyl glyceryl ethers (MAGE) have previously been reported as diagnostic lipids for SRB implicated in AOM (Pancost et al., 2001; Rütters et al., 2001). However, $\delta^{13}\mathrm{C}$ measurements indicate that water column input is the major source of MAGE in this study (Fig. 3.9). This conclusion is supported by the

widespread occurrence of MAGE in sediments and in the water column in the western Irish Sea (unpublished data).

Commonly reported archaeal lipids such as crocetane (co-eluting with phytane), pentamethyleicosane and archaeol were observed, but in low abundance (Fig. 3.8B). This indicates archaea are a minor contributor to overall organic matter within these hardgrounds. These lipids are frequently among the most abundant and ^{13}C-depleted at active methane seeps (Pancost et al., 2000; Aloisi et al., 2002; Niemann et al., 2005; Bouloubassi et al., 2009). In this case biomarkers diagnostic for microalgal water column input, such as sterols, phytol and C_{14} to C_{22} *n*-alkanols (Volkman, 2006) were dominant in all samples. This suggests that water column input derived from marine plankton, as well as benthic microalgae, is the dominant organic matter signal in the cemented sands. This is not surprising considering that the CFZ zone is located in shallow shelf waters in a setting of known high primary productivity (Gowen and Stewart, 2005) and a dominant input of organic matter from the water column should be expected. $\delta^{13}C$ values therefore likely reflect this major input from photosynthetic and related heterotrophic processes and may be diluting signals from microbial biomass that could be incorporating methane (Aquilina et al., 2010).

It is noteworthy however, that certain bacterial fatty acids were more depleted relative to other lipids and measured values were as low as -40‰ (Fig. 3.9), which suggests that an unknown proportion of these fatty acids may be associated with SRB involved in AOM. Similar moderately depleted fatty acids diagnostic for SRB were obtained by Kinnaman et al. (2010) from MDAC concretions at 10 m water depth in the Brian Seep off Santa Barbara. AOM consortium biomass and their associated lipids are spatially highly variable and typically is highest in defined locales below the sediment surface where AOM rates are highest (e.g. Elvert et al., 2005; Aquilina et al., 2010). Therefore further targeted surveys in proximity to a venting site and from subsurface MDAC may reveal further the nature of the microorganisms involved in AOM at this setting. DGGE screening of archaeal and bacterial 16S rDNA indicates that the bacterial community structure is very similar to that obtained from surrounding sand (Fig. 3.10). This would suggest that the dominant bacterial populations are either derived from extant benthic sedimentary bacteria of else from water column bacteria. Thus, DGGE seems to support the results from biomarker analysis. In contrast the archaeal population structure appears to be distinct and

exhibits greater diversity than sandy sediment in the region. This suggest that the archaea may be playing a more significant role in CH_4 oxidation and MDAC formation

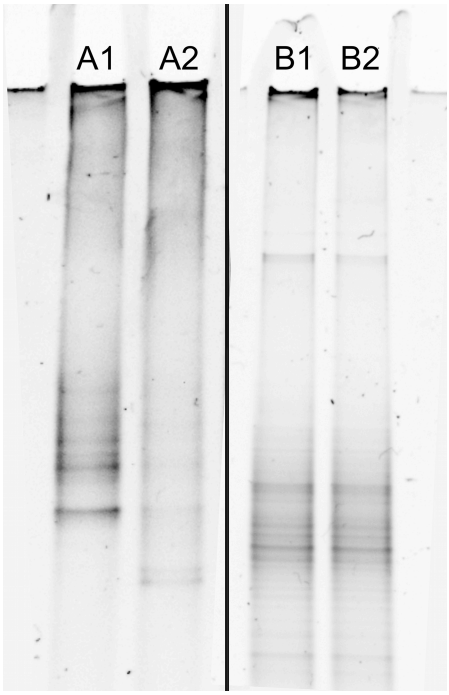

Figure 3.10. 16S rRNA DGGE profiles of archaeal (A) and bacterial (B) populations from MDAC (A1 and B1) and sand (A2 and B2).

3.6 Conclusions

Bulk isotope analysis and mineralogical analysis has confirmed that the carbonate mound features at the CFZ in the Irish Sea, similar to the Holden's Reef and the Texel 11 sites, are MDAC. The principal authigenic form appears to be aragonite. Active seepage was recorded from one of the mounds, with gas plumes detected in the water column. Underwater video footage highlighted the presence of largely sand-covered stacked carbonate pavements. The occurrences of high densities of cemented sabellarid tubes and extensive macrofaunal colonisation of carbonates indicate the CFZ mounds, like at other MDAC sites in the Irish Sea, represent an important solid substrate and habitat for local macrofauna. The common occurrence of patches of reduced sediment and the association of authigenic aragonite with framboidal pyrite indicate that AOM is taking place in shallow subsurface. In contrast to other deep sea methane seeps with widespread MDAC, lipid biomarker analysis suggests that microbial organic matter derived from methane is of minor significance in

comparison to algal detrital organic matter from the water column. The co-existence of $\delta^{13}C$–depleted authigenic aragonite and isotopically light methane indicates a biogenic origin of the seeping gas, possibly related to Carboniferous coal deposits. However microbial reworking of deep thermogenic methane cannot be ruled out at present.

3.7 References

Aloisi, G., Pierre, C., Rouchy, J.-P., Foucher, J.-P., Woodside, J. and the MEDINAUT Scientific Party. 2000. Methane-related authigenic carbonates of eastern Mediterranea Sea mud volcanoes and their possible relation to gas hydrate destabilization. Earth and Planetary Science Letters 184, 321-338.

Aloisi, G., Bouloubassi I., Heijs S.K., Pancost R.D., Pierre C., Sinninghe Damsté J.S., Gottschal J.C., Forney, L.J., 2002. CH_4-consuming microorganisms and the formation of carbonate crusts at cold seeps. Earth and Planetary Science Letters 203, 195-203.

Bacelle, L., Bosellini, A., 1965. Diagrammi per la stima visiva della composizione percentuale nelle rocce sedimentarie. Annali della Universitá di Ferrara, Sezione IX, Science Geologiche e Paleontologiche 1:59-62.

Bayon, G., Henderson, G.M., Bohn, M., 2009. U-Th stratigraphy of a cold seep carbonate crust. Chemical Geology 260, 47-56.

Belderson, R.H., 1964. Holocene sedimentation in the western half of the Irish Sea. Marine Geology 2,147-163.

Beal, E.J., House, C.H., Orphan, V.J., 2009. Manganese-and iron-dependent marine methane oxidation. Science 325, 184-187.

Boetius, A., Ravenschlag, K., Schubert, C.J., Rickert, D., Widdel, F., Gieseke, A., et al., 2000. A marine microbial consortium apparently mediating anaerobic oxidation of methane. Nature 407, 623-626.

Boetius, A., Suess, E., 2004. Hydrate Ridge: a natural laboratory for the study of microbial life fueled by methane from near-surface gas hydrates. Chemical Geology 2005, 291-310.

Bohrmann, G., Greinert, J., Suess, E., Torres, M., 1998. Authigenic carbonates from the Cascadia subduction zone and their relation to gas hydrate stability. Geology 26, 647-650.

Bouloubassi, I., Nabais, E., Pancost, R.D., Lorre, A., Taphanel, M.H., 2009. First biomarker evidence for methane oxidation at cold seeps in the Southeast Atlantic (REGAB pockmark). Deep Sea Research Part II 56, 2239-2247.

Burton, E.A., 1993. Controls on marine carbonate cement mineralogy: review and

reassessment. Chemical Geology 105, 163–179.

Capozzi, R., Guido, F.L., Oppo, D., Gabbianelli, G., 2012. Methane-Derived Authigenic Carbonates (MDAC) in northern-central Adriatic Sea: Relationships between reservoir and methane seepages. Marine Geology 332-334, 174-188.

Chen, D.F., Huang, Y.Y., Yuan, X.L., Cathles III, L. M., 2005 Seep carbonates and preserved methane oxidizing archaea and sulfate reducing bacteria fossils suggest recent gas venting on the seafloor in the Northeastern South China Sea. Marine and Petroleum Geology 22, 613-621

Claypool, G.E., Kvenvolden, K.A., 1983. Methane and other hydrocarbon gases in marine sediment. Annual Review of Earth Sciences 11, 299-327.

Clayton, C., 1992. Source volumetrics of biogenic gas generation. In: Vially, R. (Ed.) Bacterial Gas. Paris, Editions Technip, 191-204.

Crémière, A., Pierre, C., Blanc-Valleron, M.-M., Zitter, S., Çağatay, M.N., Henry, P., 2012. Methane-derived authigenic carbonates along the North Anatolian fault system in the Sea of Marmara (Turkey). Deep-Sea Research I 66, 114-130.

Croker, P.F., 1995. Shallow gas accumulation and migration in the western Irish Sea. Geological Society of London, Special Publications 93, 41-58.

Croker, P.F., Kozachenko, M., Wheeler, A.J., 2005. Gas-related seepage features in the western Irish Sea IRL-SEA6. Tech Rep Strategic Environmental Assessment of the Irish Sea (SEA6). Petroleum Affairs Division: Dublin, Ireland

Dando, P., Austen, M., Burke, R., Kendall, M., Kennicutt, M., Judd, A., Moore, D.C., O'Hara, S.C.M., Schmaljohann, R., Southward, A.J., 1991. Ecology of a North Sea pockmark with an active methane seep. Marine Ecology Progress Series 70, 49-63

Dobson, M., Whittington, R., 1979. The geology of the Kish Bank Basin. Journal Geological Society London 136, 243-249.

Elvert, M., Boetius, A., Knittel, K., Jørgensen, B.B., 2003. Characterization of specific membrane fatty acids as chemotaxonomic markers for sulfate-reducing bacteria involved in anaerobic oxidation of methane. Geomicrobiology Journal 20, 403-419.

Feng, D., Chen, D., Roberts, H.H., 2008. Sedimentary fabrics in the authigenic carbonates from Bush Hill: implication for seabed fluid flow and its dynamic signature. Geofluids 8, 301-310.

Feng, D., Chen, D., Peckmann, J., Bohrmann, G., 2010. Authigenic carbonates from methane seeps of the northern Congo fan: Microbial formation mechanism. Marine and Petroleum Geology 27, 748-756.

Fleischer, P., Orsi, T., Richardson, M., Anderson, A., 2001. Distribution of free gas in marine sediments: a global overview. Geo-Marine Letters 21, 103-122.

Flores, R.M., Rice, C.A., Stricker, G.D., Warden, A., Ellis, M.S., 2008. Methanogenic pathways of coal-bed gas in the Powder River Basin, United States: The geologic factor. International Journal of Coal Geology 27, 52-75.

Flügel, E., 2004. Microfacies of carbonate rocks. Analysis, Interpretation and Application. Springer Verlag, Berlin Heidelberg, p976.

Forster, P., Ramaswamy, V., Artaxo P., Berntsen, T., Betts, R., Fahey, D.W., et al., 2007. Changes in atmospheric constituents and in radiative forcing. In: Solomon, S., Qin, D., Manning, M., Chen, Z., Marquis, M., Averyt, K.B., et al., (Eds.). Climate Change 2007: The physical science basis. Contribution of Working Group I to the Fourth Assessment Report of the Intergovernmental Panel on Climate Change, Cambridge, Cambridge University Press: United Kingdom and USA, p129-234.

Friedman, G.M., 1959. Identification of carbonate minerals by staining methods. Journal of Sedimentary Petrology 29, 87-97.

Gowen R.J., Stewart B., 2005. The Irish Sea: nutrient status and phytoplankton. Journal of Sea Research 54, 36-50.

Greinert, J., Bohrmann, G., Suess, E., 2001. Gas hydrate-associated carbonates and methane-venting at Hydrate Ridge: Classification, distribution and origin of authigenic lithologies. In: Paull, C.K., Dillon, P.W. (Eds.). Natural Gas Hydrates: Occurrence, Distribution and Detection. Geophysical Monograph 124, 99-113.

Greinert, J., Bohrmann, G., Elvert, M., 2002. Stromatolitic fabric of authigenic carbonate crusts: result of anaerobic methane oxidation at cold seeps in 4,850 m water depth. Interational Journal Of Earth Sciences 91, 698-711.

Haas A., Peckmann, J., Elvert, M., Sahling, H., Bohrmann, G., 2010. Patterns of carbonate authigenesis at the Kouilou pockmarks on the Congo deep-sea fan. Marine Geology 268, 129-136.

Himmler, T., Brinkmann, F., Bohrmann, G., Peckmann, J., 2011. Corrosion patterns of seep-carbonates from the eastern Mediterranean Sea. Terra Nova 23, 206-212

Hinrichs, K.-U., Hayes, J.M., Sylva, S.P., Brewer, P.G. DeLong, E.F., 1999. Methane-consuming archaebacteria in marine sediments. Nature 398, 802-805.

Hovland, M., Talbot, M.R., Qvale, H., Olaussen, S., Aasberg, L., 1987. Methane-related carbonate cements in pockmarks of the North Sea. Journal of Sedimentary Petrology 57, 881-892.

Hovland, M., Gardner, J., Judd, A., 2002. The significance of pockmarks to understanding fluid flow processes and geohazards. Geofluids 2, 127-136.

Hovland, M., Svensen, H., Forsberg, C.F., Johansen, H., Fichler, C., Fosså, J.H., Jonsson, R., Rueslåtten, H., 2005. Complex pockmarks with carbonate-ridges off mid-Norway: Products of sediment degassing. Marine Geology 218, 191-206.

Ivanov, M., Mazzini, A., Blinova, V., Kozlova, E., Laberg. J.-S., Matveeva, T., Taviani, M., Kaskov, N., 2010. Seep mounds on the Southern Vøring Plateau. Marine and Petroleum Geology 27, 1235-1261.

Jackson, D.I., Jackson, A.A., Evans, D., Wingfield, R.T.R., Barnes, R.P., Arthur, M.J., 1995. The geology of the Irish Sea. BGS UK Offshore regional Rep, HMSO, London.

Jensen, P., Aagaard, I., Burke, Jr R.A., Dando, P.R., Jørgensen, N.O., Kuijpers, A., Laier, T., O'Hara, S.C.M., Schmaljohann, R., 1992. 'Bubbling reefs in the Kattegat: Submarine landscapes of carbonate-cemented rocks support a diverse ecosystem at methane seeps. Marine Ecology Progress Series 83, 103-112.

Jones, G.B., Floodgate, G., Bennell, J., 1986. Chemical and microbiological aspects of acoustically turbid sediments: preliminary investigations. Marine Georesources and Geotechnology 6, 315-332.

Jørgensen, N.O., 1989. Holocene methane-derived dolomite-cemented sandstone

pillars from the Kattegat, Denmark. Marine Geology 88, 71-81.

Judd, A., Croker, P., Tizzard, L., Voisey, C., 2007. Extensive methane-derived authigenic carbonates in the Irish Sea. Geo-Marine Letters 27, 259-267.

Judd, A., Hovland, M., 2007. Seabed fluid flow: the impact on geology, biology and the marine environment. Cambridge University Press: Cambridge, UK.

Judd, A.G., 2005. Strategic Environmental Assessment of the Irish Sea (SEA6): The distribution and extent of methane-derived authigenic carbonate. Department of Trade and Industry, United Kingdom.

Kinnaman, F.S., Kimball, J.B., Busso, L., Birgel, D., Ding, H., Hinrichs, K.-U., Valentine, D.L., 2010. Gas flux and carbonate occurrence at a shallow seep of thermogenic natural gas. Geo-Marine Letters 30, 355-365.

Knittel, K., Boetius, A., 2009. Anaerobic oxidation of methane: progress with an unknown process. Annual Review of Microbiology 63, 311-334.

Lavoie, D., Pinet, N., Duchesne, M., Bolduc, A., Larocque, R., 2010. Methane-derived authigenic carbonates from active hydrocarbon seeps of the St. Lawrence Estuary, Canada. Marine and Petroleum Geology 27, 1267-1272.

Levin, L.A., 2005. Ecology of cold seep sediments: interactions of fauna with flow, chemistry and microbes. Oceanography and Marine Biology: An annual Review 43, 1-46.

Li, D., Hendry, P., Faiz, M., 2008. A survey of the microbial populations in some Australian coalbed methane reservoirs. International Journal of Coal Geology 27, 14-24.

Little, C.T.S., Campbell, K.A., Herrington, R.J., 2002. Why did ancient chemosynthetic seep and vent assemblages occur in shallower water than they do today? Comment. International Journal of Geosciences 91, 149-153.

Mah, R.A., Ward, D.M., Baresi, L., Glass, T.L., 1977. Biogenesis of methane. Annual Review of Microbiology 31, 309-341.

Magalhães, V.H., Pinheiro, L.M., Ivanov, M.K., Kozlova, E., Blinova, V., Kolganova, J., Vasconcelos, C., McKenzie, J.A., Bernasconi, et al., 2012. Formation processes of methane-derived authigenic carbonates from the Gulf of Cadiz. Sedimentary Geology 243-244, 155-168.

Martens, C.S., Chanton, J.P., Paull, C.K., 1991. Biogenic methane from abyssal brine seeps at the base of the Florida escarpment. Geology 19, 851-854.

Mazzini, A., Aloisi, G., Akhmanov, G.G., Parnell, J., Cronin, B.T., Murphy, P., 2005. Integrated petrographic and geochemical record of hydrocarbon seepage on the Vøring Plateau. Journal of the Geological Society 162, 815-827.

Milucka, J., Ferdelman, T.G., Polerecky, L., Franzke, D., Wegener, G., Schmid, M., Lieberwirth, I., Wagner, M., Widdel, F., Kuypers, M.M., 2012. Zero-valent sulphur is a key intermediate in marine methane oxidation. Nature 491,541-546.

Moore, T.A., 2012. Coalbed methane: A review. International Journal of Coal Geology 101, 36-81.

Mount, J., 1985. Mixed siliciclastic and carbonate sediments: a proposed first-order textural and compositional classification. Sedimentology 32, 435-442.

Muyzer, G., De Waal, E.C., Uitterlinden, A.G., 1993. Profiling of complex microbial populations by denaturing gradient gel electrophoresis analysis of polymerase chain reaction-amplified genes coding for 16S rRNA. Appled and Environmental Microbiology 59, 695-700.

Naehr, T.H., Eichhubl, P., Orphan, V.J., Hovland, M., Paull, C.K., Ussler III, W., Lorenson, T.D., Greene, H.G., 2007. Authigenic carbonate formation at hydrocarbon seeps in continental margin sediments: a comparative study. Deep-Sea Research II, 54, 1268-1291.

Naylor, D., Haughey, N., Clayton, G. & Graham, J.R., 1993. The Kish Bank Basin, offshore Ireland. In: Parker, J.R. (Ed.). Petroleum Geology of Northwest Europe: Proceedings of the 4th Conference. Petroleum Geology Conference series 4, 845-855.

Nichols, P.D., Guckert, J.B., White, D.C., 1986. Determination of monosaturated fatty acid double-bond position and geometry for microbial monocultures and complex consortia by capillary GC-MS of their dimethyl disulphide adducts. Journal of Microbiological Methods 5, 49-55.

Niemann, H., Elvert, M., 2008. Diagnostic lipid biomarker and stable carbon isotope signatures of microbial communities mediating the anaerobic oxidation of methane with sulphate. Organic Geochemistry 39, 1668-1677.

Niemann, H., Elvert, M., Hovland, M., Orcutt, B., Judd, A., Suck, I., Gutt, J., Joye, S., Damm, E., Finster, K., Boetius, A., 2005. Methane emission and consumption at a North Sea gas seep (Tommeliten area). Biogeosciences Discussions 2, 1197-1241.

Olu-Le Roy, K., Sibuet, M., Fiala-Medioni, A., Gofas, S., Salas, C., Mariotti, A., Foucher, J.P. Woodside, J., 2004: Cold seep communities in the deep eastern Mediterranean Sea: composition, symbiosis and spatial distribution on mud volcanoes. Deep-Sea Research I 51, 1915-1936.

Pancost, R.D., Bouloubassi, I., Aloisi, G., Sinninghe Damsté, J.S., 2001. Three series of non-isoprenoidal dialkyl glycerol diethers in cold-seep carbonate crusts. Organic Geochemistry 32, 695-707.

Pancost, R.D., Sinninghe Damste, J.S., de Lint, S., van der Maarel, M.J., Gottschal, J.C., 2000. Biomarker evidence for widespread anaerobic methane oxidation in Mediterranean sediments by a consortium of methanogenic archaea and bacteria. The Medinaut Shipboard Scientific Party. Applied and Environmental Microbiology 66, 1126-1132.

Paull, C.K., Ussler III, W., 2006. Re-evaluating the significance of seafloor accumulations of methane-derived carbonates: seepage or erosion indicators? Proceedings of the 6th International Conference on Gas Hydrates, Vancouver, Canada.

Paull. C.K., Ussler III, W., Peltzer, E.T., Brewer, P.G., Keaten, R., Mitts, P.J., et al., 2007. Authigenic carbon entombed in methane-soaked sediments from the northeastern transform margin of the Guayamas Basin, Gulf of California. Deep-Sea Research II, 54, 1240-1267.

Peckmann J., Reimer A., Luth U., Luth C., Hansen B.T., Heinicke C., Hoefs, J. Reitner, J., 2001. Methane-derived carbonates and authigenic pyrite from the northwestern Black Sea. Marine Geology 177, 129-150.

Peckmann, J., Thiel, V., 2004. Carbon cycling at ancient methane seeps. Chemical Geology 205, 443-467.

Pierre, C., Fouquet, Y., 2007. Authigenic carbonates from methane seeps of the Congo deep-sea fan. Geo-Marine Letters 27, 249-257.

Reitner, J., Peckmann, J., Reimer, A., Schumann, G., Theil, V., 2005. Methane-derived carbonate build-ups and associated microbial communities at cold seeps on the lower Crimean shelf (Black Sea). Facies 51, 66-79.

Ritger, S., Carson, B., Suess, E., 1987. Methane-derived authigenic carbonates formed by subduction-induced pore-water expulsion along the Oregon/Washington margin. Geological Society of America Bulletin 98, 147-156.

Rütters, H., Sass, H., Cypionka, H., Rullkötter, J. 2001., Monoalkylether phospholipids in the sulfate-reducing bacteria *Desulfosarcina variabilis* and *Desulforhabdus amnigenus*. Archives of Microbiology 176, 435-442.

Sackett, W.M., 1978. Carbon and hydrogen isotope effects during the thermocatalytic production of hydrocarbons in laboratory simulation experiments. Geochemica et Cosmochemica Acta 42, 571-580.

Schmidt, M., Botz, R., Winn, K., Stoffers, P., Thiessen, O., Herzig, P., 2002. Seeping hydrocarbons and related carbonate mineralization in sediments south of Lihir Island (New Ireland fore arc basin, Papua New Guinea). Chemical Geology 186, 249-264.

Sibuet, M., Olu, K., 1998. Biogeography, biodiversity and fluid dependence of deep-sea cold-seep communities at active and passive margins. Deep-Sea Research II 45, 517-567.

Stakes, D.S., Orange, D., paduan, J.B., Salamy, K.A., Maher, N., 1999. Cold seeps and authigenic carbonate formation in Monterey Bay, California. Marine Geology 159, 93-109.

Svensen, H., Planke, S., Sørenssen, A.-M., Jamtveit, B., Myklebust, R., Eidem, T.R., Rey, S.S., 2004. Release of methane from a volcanic basin as a mechanism for initial Eocene global warming. Nature 429, 542-545.

Tsunogai, U., Yoshida, N., Gamo, T., 2002. Carbon isotopic evidence of methane oxidation through sulfate reduction in sediment beneath cold seep vents on the seafloor at Nankai Trough. Marine Geology 187, 145-160.

Ulrich, G., Bower, S., 2008. Active methanogenesis and acetate utilization in Powder River Basin coals, United States. International Journal of Coal Geology 76, 25-33.

van Dover, C.L., Aharon, P., Bernhard, J.M., Caylor, E., Doerries, M., Flickinger, W., et al., 2003. Blake Ridge methane seeps: characterization of a soft-sediment, chemosyntetically based ecosystem. Deep-Sea Research I 50, 281-230.

Valentine, D.L., Reeburgh, W.S., 2000. New perspectives on anaerobic methane oxidation. Environmental Microbiology 2, 477-484.

Vetriani, C., Jannasch, H.W., MacGregor, B.J., Stahl, D.A., Reysenbach, A.L., 1999. Population structure and phylogenetic characterization of marine benthic archaea in deep-sea sediments. Applied and Environmental Microbiology 65, 4375-4384.

von Rad, U., Rösch, H., Berner, U., Geyh, M., Marchig, V., Schulz, H., 1996. Authigenic carbonates derived from oxidized methane vented from the Makran accretionary prism off Pakistan. Marine Geology 136, 55-77.

Walter, L.M., 1986. Relative efficiency of carbonate dissolution and precipitation during diagenesis: a progress report on the role of solution chemistry. In: Gauties, D.L., (Ed.), Roles of organic matter in mineral diagenesis, SEPM (Society for Sedimentary Geology) Special Publication 38, 1-12.

Whiticar, M.J., 1999. Carbon and hodrogen isotope systematics of bacterial formation and oxidation of methane. Chemical Geology 161, 291-314.

Whomersley, P., Wilson, C., Clements, A., Brown, C., Long, D., Leslie, A., Limpenny, D., 2010. Understanding the marine environment - seabed habitat investigation of submarine structures in the mid Irish Sea and Solan Bank Area of Search (AoS). JNCC Report No. 430.

Yuan, F., Bennell, J., Davis, A., 1992. Acoustic and physical characteristics of gassy sediments in the western Irish Sea. Continental Shelf Research 12, 1121-1134.

Chapter 4

An assessment of microbial diversity at a large pockmark on the Malin Shelf, NW Ireland

DGGE, clone library data and PLFA data presented in Chapter 4 has been published in the Open Journal of Marine Science:

Flanagan, P.V., Kelleher, B.P., O'Reilly, S.S., Szpak, M.T., Monteys, X., Kelly, P.P., Kulakova, A.N., Kulakov, L.A., Allen, C.C.R., 2013. A depth-resolved insight into benzoyl CoA reductase and benzoate dioxygenase gene copy numbers within a marine sediment associated with methane seepage. Open Journal of Marine Science 6, 1-9.

4.1 Introduction

Scientific and technological advances in mapping, observing and sampling of the seafloor over the past number of decades has highlighted a global seafloor populated by dramatic and diverse landscapes and geological features, which include cold seeps, deep-water coral reefs, mud volcanoes, mud diapirs, methane-derived authigenic carbonate (MDAC) mounds, hydrothermal vents, seamounts, ridges, trenches and pockmarks (Jørgensen and Boetius, 2007). Marine pockmarks are considered seafloor surface expressions of fluid expulsion, first described in 1970 (King and MacLean, 1970). The leading formation theory assumes rapid expulsion of overpressurised fluid through relatively impermeable fine-grained sedimentary seabed layers (Judd and Hovland, 2007). Fluids implicated in pockmark formation include microbial and thermogenic hydrocarbon gas (primarily CH_4), hydrothermal fluids and groundwater (Judd and Hovland, 2007). Sites of active gas seepage have received significant attention and are often characterized by gas flares to the water column (e.g. Dando et al., 1991), methane-derived authigenic carbonate (MDAC) crusts (e.g. Bayon et al., 2009), giant sulphur-oxidising bacterial mats (e.g. Dando, et al. 1991, Wegener et al., 2008), and seepage-associated macrofauna such as Vesicomyidae and Mytilidae bivalves families, and Siboglinidae tube worms (e.g. Ondreas et al., 2005; Olu-Le Roy et al., 2007).

There have been relatively few studies investigating the microbial diversity of pockmarks, and most have focused on actively seeping features (Wegener et al., 2008; Cambon-Bonavita et al., 2009; Omorogie et al., 2009; Shubenkova et al., 2010; Deutzmann et al., 2011; Lazar et al., 2011; Roalkvam et al., 2011). Microbial communities from pockmarks associated with active seepage are often dominated by consortia of methanotrophic archaea (ANME) and sulphate-reducing bacteria (SRB) of the Deltaproteobacteria class (e.g. Wegener et al. 2008; Cambon-Bonavita et al., 2009), which appear to be major microbes involved in anaerobic oxidation of methane (AOM) in a variety of seepage settings (Boetius et al., 2000; Jørgensen and Boetius, 2007; Judd and Hovland, 2007). In contrast, there has been relatively little focus on the biological diversity at dormant or very low seepage activity pockmarks. Of all the mapped pockmarks to date, the majority do not exhibit active seepage and many do not appear to be associated with evidence of gas accumulations at all (Judd and Hovland, 2007).

The Malin Deep pockmark field is situated on the Irish continental shelf, 70 km NW of Ireland. This region is structurally complex, bordered by the Stanton Banks fault to the north and the Malin Terrace to the south. The Skerryvore fault, a major normal fault, divides the region into the Donegal Basin and the West Malin Basin (Dobson and Whittington, 1992). The Malin Deep seafloor is characterized by complex seabed geology with a variety of sediment facies, which include recent sand bedforms, gravel lags and coarser clasts, but the seafloor in the vicinity of the pockmark ranges from fine-grained sand to silt (Monteys et al., 2008a; Monteys et al., 2008b; Szpak et al., 2012). Shallow seismic and towed electromagnetic investigation of the pockmark highlighted the presence of a shallow subsurface gas pocket below the pockmark and gas signatures in and around the feature, but without active venting from the pockmark itself and no evidence of gas migration to the top 20 m of sediment (Szpak et al., 2012). Underwater towed video (UWTV) investigations of the region did not record any MDAC crusts or mounds, bacterial mats or evidence of increased biological productivity. In addition nuclear magnetic resonance analysis of sedimentary organic matter (OM) and towed electromagnetic surveying suggested microbial biomass and activity was reduced inside the pockmark compared to surrounding sediments. Deep (> 20 mbsf) lateral migration of gas to surrounding sediment was also proposed (Szpak et al., 2012). Therefore the pockmark itself appears to be in a stage of inactivity or is possibly dormant.

Therefore, the aims of this study were to analyze the microbial community diversity at a inactive/dormant pockmark setting as a possible means for comparison to reported pockmark settings with active seepage, and also to characterise the community diversity and biomass abundance to address the suggestion of decreased microbial activity within the feature.

4.2 Materials and Methods

4.2.1 Sampling and DNA extraction

A 6 m vibrocore, VC045, was recovered using a Geo-Resources 6000 vibrocorer at a water depth of 180 m in 2008 from within the pockmark depression (55.85680^{o}N Lat., -8.13720^{o}E Long.) during INFOMAR CE_08 survey aboard the RV Celtic Explorer (Fig. 4.1). The core was sectioned, wax-sealed and refrigerated for the duration of the cruise prior to multi sensor core logging, and subsequent sub-sampling and freezing at -80^{o}C back in the laboratory. DNA was extracted at three sediment depths from freshly exposed sediment from the sediment core, at 0.2 metres below seafloor (mbsf), 2.1 mbsf and 5.9 mbsf according to the method of Zhou et al. (1996). Crude DNA concentration and purity was estimated spectrophotometrically. The crude total DNA was further purified on a 1% low-melting point agarose gel electrophoresis and DNA bands were purified from the agarose gel using the Illustra GFX PCR and gel band purification kit (GE Healthcare, Buckinghamshire, UK).

4.2.2 16S rRNA PCR and denaturing gradient gel electrophoresis

PCR reactions (50 µL) were carried out using DNA Engine DYAD Peltier Thermal Cycler. DGGE primer 2 (5'-ATTACCGCGGCTGCTGG-3') and DGGE primer 3 (5'-CGCCCGCCGCGCGCGGCGGGCGGGGCGGGGGCACGGGGGGCCTACGGGA GGCAGCAG-3') were used to amplify the variable V3 region of the bacterial 16S rRNA gene as outlined by Muyzer et al. (1993). A touch-down PCR was performed as follows: denaturation step of 95^{o}C for 5min; followed by 20 cycles of 95^{o}C for 1 min, 60^{o}C for 1 min and 72^{o}C for 3 min, with a 0.5^{o}C decrease per cycle for the annealing step. This was followed by 8 cycles of 95^{o}C for 1 min, 55^{o}C for 1 min and 72^{o}C for 1 min. 16S archaeal rRNA gene sequences were amplified from the purified genomic DNA using a nested approach as outline by Vetriani et al. (1999). Archaeal 16S rRNA sequences were first amplified using S-D-Arch-0025-a-S-17 (5'-CTGGTTGATCCTGCCAG-3') forward primer and S-*-Univ-0907-a-A-20 (5'-CCGTCAATTCMTTTRAGTTT-3') reverse primer (Vetriani et al., 1999). PCR was performed as follows: denaturation step of 94^{o}C for 3min; followed by 40 cycles of 94^{o}C for 30s, 48^{o}C for 30 s, and 72^{o}C for 30s; and finally an elongation step of 72^{o}C for 5min. A nested PCR was then performed as above but DGGE primer 3 with 344f(GC)(5'CGCCCGCCGCGCCCCGCGCCCGTCCCGCCGCCCCCGCCACGGG

GCGCAGCAGGCGCGA-3'). DGGE was performed as described previously (see Materials and Methods, Chapter 3) DGGE band sequencing was performed as described previously (Muyzer et al., 1993). Prominent DGGE bands were excised and eluted DNA used as PCR templates using non-GC clamp DGGE primer 1 (5'-CCTACGGGAGGCAGCAG-3') instead of DGGE primer 3 and P2 primers, and previously mentioned PCR conditions. Amplified products were sequencing in the forward direction by DNA Sequencing & Services (University of Dundee, Scotland). 16S rRNA sequences were subjected to NCBI BLAST search to identify sequences with highest similarity. DGGE profiles were subjected to statistical image analysis using Phoretix 1D v10.3 (TotalLab) software package. Cluster analysis was performed using UPGMA and Ochiai coefficient based similarities.

4.2.3 16S rRNA bacterial clone library construction and phylogenetic analysis

Clone libraries were prepared from bacterial 16S rRNA sequences from 2.1 metres below seafloor (mbsf) and 5.9 mbsf using the CloneJET PCR cloning kit (Fermentas, Pittsburgh, USA) according to manufacturer's guidelines. 16S rRNA clone inserts were reamplified from colony PCR reactions using 63f (5'-CAGGCCTAACACATGCAAGTC-3') forward primer and 1387r (5'-GGGCGGWGTGTACAAGGC-3') reverse primer (Marchesi et al., 1998). Operational taxonomic units (OTUs) were grouped by restriction analysis using Fastdigest RSaI and HaeIII (Fermentas, Pittsburgh, USA) restriction enzymes. Restriction profiles were analysed on 1.4% agarose gel and each gel was standardized to allow comparison between gels. Clones showing identical restriction profiles were assigned to the same OTU group and a total of 60 clones from 2.1 mbsf and 52 clones from 5.9 mbsf were assigned to OTU groups. Initially at least 30% of clones from each group were sequenced in full using pJET1.2 forward and reverse sequencing primers. Amplified products were sequencing in the forward direction and reverse direction by DNA Sequencing and Services (University of Dundee, Scotland). Nucleotide sequence similarities were analysed by NCBI GenBank BLAST search and those found to be 98% or greater in similarity were considered the same and grouped as a phylotype. Sequence anomalies were checked using Pintail (v1.0) (Ashelford et al., 1994). Sequence alignment was performed by ClustalW algorithm (Thompson et al., 1994) in the MEGA5 software package (Tamura et al., 2011).

Maximum-likelihood phylogenetic trees were constructed based on the Tamura-Nei model (Tamura and Nei 1993) in the MEGA5 software package, with 16S rRNA bacterial reference sequences obtained from GenBank. Trees were subjected to bootstrap analysis (n = 1000) (Felsenstein 1985) to assess confidence levels and bootstrap values of 50 or higher are reported here. The nucleotide sequence data reported in this study were deposited in the GenBank nucleotide sequence database under the accession numbers JQ349446 to JQ349503.

4.2.4 Phospholipid fatty acid analysis

Lyophilized sediment samples were extracted using the modified Bligh-Dyer method, according to White and Ringelberg (1998). Total lipid extracts (TLEs) were desulphurised by mixing with activated copper powder overnight. TLEs were fractionated into neutral, glycolipids and polar lipids using solid phase extraction on solvent-cleaned aminopropyl cartridges (Alltech 500mg Ultra-Clean, USA) according to Pinkart et al. (1998). Phospholipids were transesterified by mild alkaline methanolysis using 0.5M sodium methoxide (Sigma Aldrich) for 30min at 50^{o}C. Fatty acid methyl esters (FAMEs) were analysed using an Agilent 6890 gas chromatograph (GC) coupled to Agilent 5973 N quadruopole mass selective detector (MSD). 1 μL aliquots of derivatised extracts were injected in splitless mode. Separation was achieved on a HP-5MS fused silica capillary column (Agilent: 30 m x 0.25 mm I.D. and film thickness of 0.25 μm). The injector and MS source were held at 280 ^{0}C and 230 ^{0}C respectively. The column temperature program was as follows: 65 ^{0}C injection and hold for 2 min, ramp at 6^{o}C min^{-1} to 300^{o}C; followed by isothermal hold at 300^{o}C for 20 min. The MS was operated in electron impact mode with an ionisation energy of 70 eV and a mass scan range set from 50 to 650 Da. Data was acquired and processed using Chemstation software (revision 2.0 E). FAME Monounsaturation position were identified according to Nichols et al. (1986). Quantification was performed using to 5-α-cholestane internal standard (See Appendix A).

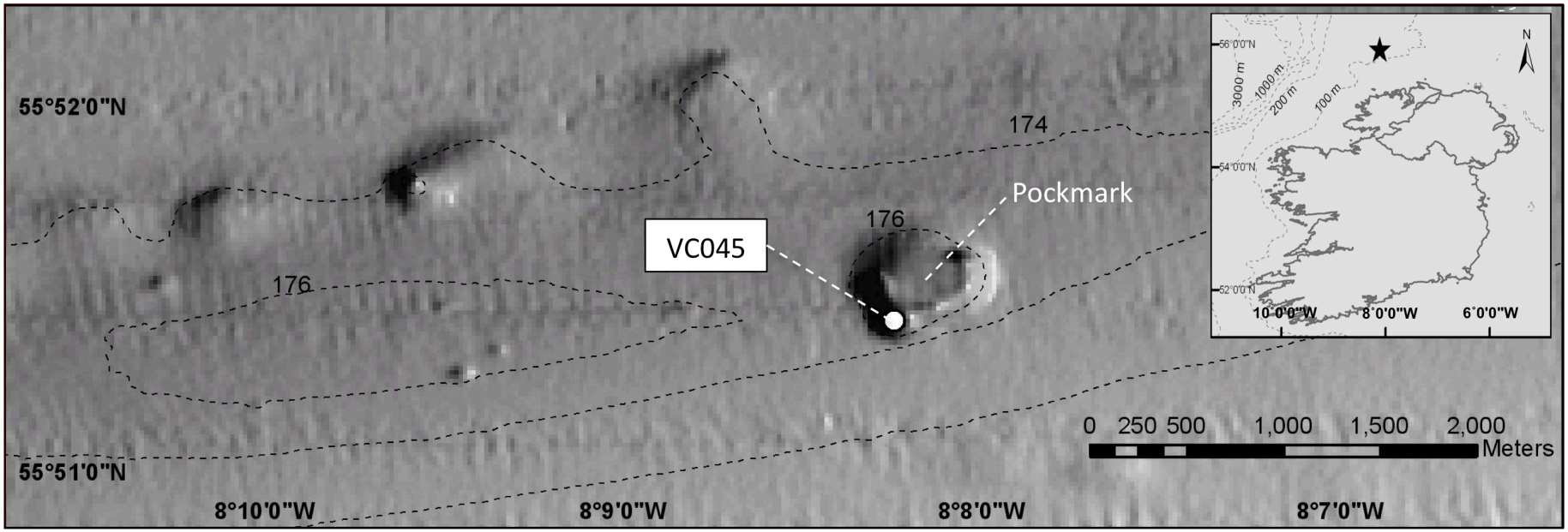

Figure 4.1. Multibeam shaded relief bathymetry of the Malin Deep and the studied pockmark. The sampling site for VC045, taken from within the pockmark is shown. Figure adapted from Szpak et al. (2012).

4.3 Results and Discussion

4.3.1 Microbial community is dominated by non-seep related assemblages

DGGE profiling of bacterial and archaeal diversity was performed at three depths in the VC045 core and hierarchical cluster analysis of DGGE lanes is given in Fig. 4.2. The results of sequencing major bands in DGGE gels is given in Table 4.1. Based on the cluster analysis, bacterial community composition at 2.1 mbsf and 5.9 mbsf showed 68% similarity, while the community as 0.2 mbsf displayed 62% similarity to these depths (Fig. 4.2a). Bacterial community composition was less than 55% similar to marine sediments taken from a shallow pockmark in Dunmanus Bay (see Chapter 5) and the three samples from VC045 grouped together. This indicates that there is a distinct bacterial community at this site compared to the Dunmanus Bay sediments. DGGE band sequencing of some excised bands (Table 4.1) indicates that there is a clear dominance of the γ-proteobacteria and α-proteobacteria, in particular *Psychrobacter* (Bands B2, B4, B5 and B6) and *Sulfitobacter* (Bands B3 and B8). The majority of sequenced bands from bacterial DGGE gels belonged to these genera, neither of which have been reported at cold seep settings previously.

DGGE screening of archaeal communities indicates that groups related to phylotypes from diverse settings such as turbidites in the Gulf of Mexico (Table 4.1, A1), deep sea sediments in the Sea of Okhotsk (A2 and A6), cold-water corals in the Porcupine Seabight (A5), sediments in Eel River Basin (A3) and deep sea sediments in the Pacific Ocean margin (A4) are present. Based on the number of bands present, the archaeal community diversity appears to be quite low in diversity. A number of these affiliated sequences have been reported at active CH_4 seepage environments. For example the Eel River Basin is a site of active CH_4 seepage (e.g. Orphan et al., 2001; Beal et al., 2009) and the Pacific Ocean margin (Nunoura et al., 2008) is a site of substantial gas hydrate deposits. However, Nunoura et al. (2009) concluded that archaeal populations investigated were not specifically associated with gas hydrates and Beal et al. (2009) found that only 5% of total archaeal diversity was associated with known ANME groups. Most sequences reported here are not associated with known methanogenic or methanotrophic archaea. DGGE band A1 however, was closely related to previously reported phylotypes in the ANME-1 lineage (e.g. Nunoura et al., 2009). This suggests ANME-1 populations may be present.

Nevertheless evidence here suggests that the archaeal diversity is low at this setting and that most screened phylotypes are not related to known lineages engaged in AOM, as are found in active cold seep settings. This supports previous reports by Szpak et al. (2012) that the pockmark itself is not currently actively seeping.

Table 4.1. Bacterial and archaeal DGGE band sequencing and BLAST similarities.

Band	Depth (mbsf)	Organism (Accession No.)	Match[1]	Reference
B1	0.2	*Alcanivorax* sp. ANT-2400 S4 (GQ153640.1)	96	Tapilatu (2009)
B2	0.2	*Psychrobacter* sp. KOPRI 25504 (GU062550.1)	98	Kim (2010)
B3	0.2	*Sulfitobacter* sp. COL-20 (HQ534315.1)	100	Lo Giudice (2012)
B4	2.1	*Psychrobacter* sp. KOPRI 25504 (GU062550.1)	98	Kim (2010)
B5	2.1	*Psychrobacter* sp. C11 (DQ831958.1)	96	Lo Giudice (2007)
B6	2.1	*Psychrobacter* sp. KOPRI 25504 (GU062550.1)	100	Kim (2010)
B7	5.9	*Halomonas* sp. DPB4_(MB)_50.2mbsf (DQ344858.1)	100	Biddle (2005)
B8	5.9	*Sulfitobacter* sp. COL-20 (HQ534315.1)	95	Lo Giudice (2012)
B9	5.9	*Pseudoalteromonas* sp. TB27 (JF273878.1)	99	Papaleo (2011)
B10	5.9	*Thiomicrospira* sp. Milos-T2 (AJ237758.1)	95	Brinkhoff (1999)
A1	0.2	Uncultured ANME-1 euryarchaeote clone slm_arc_110 (HQ700669.1)	99	Nunoura (2009)
A2	2.1	Uncultured archaeon clone OHKA2.13 (AB094530)	99	Inagaki (2003)
A3	2.1	Uncultured archaeon clone FeSO4_A_116 (GQ356853.1)	99	Beal (2009)
A4	5.9	Uncultured euryarchaeote clone: ODP1251AQ1.19 (AB364330.1)	93	Nunoura (2008)
A5	5.9	Uncultured archaeon clone 3H3M_ARC63 (JN229818.1)	98	Hoshino (2011)
A6	5.9	Uncultured archaeon clone: OHKA2.13 (AB094530.1)	99	Inagaki (2003)

Note 1: % match based on NCBI MegaBLAST search algorithm

16S rRNA bacterial clone libraries indicate that the Proteobacteria were the major phylum, representing 93.4 and 98.1% of the bacterial population at 2.1 and 5.9 mbsf respectively. These belonged to the Gamma- Alpha and Beta- classes, whereby respectively they represent the 73.8, 18.0 and 1.6% of the population at 2.1 mbsf and 54.7, 36.5 and 5.7% of the population at 5.9 mbsf (Fig. 3). A complete OTU table for the clone libraries is given in Table 4.2 and a 16S rRNA phylogenetic tree showing positions of clones from this study is shown in Fig. 4.4. In agreement with DGGE results, the major groups are closely related to the *Psychrobacter* and *Sulfitobacter* species. At 2.1mbsf clones closely related to *Psychrobacter* represent 59.0% of the clone library and those related to *Sulfitobacter* represent 18.0% of the library, while at 5.9 mbsf there is a shift in population structure of both groups to 40.3 and 36.5%, respectively. Other major phylotypes found at 2.1 mbsf were related to *Alcanivorax borkumensis* SK2 (Yakimov et al., 1998), related to uncultured actinobacteria, previously reported at low-activity cold seeps in the Weddell Sea, Antarctica (Niemann et al., 2009) and *Pseudoalteromonas arctica* (Bernbom et al., 2011).

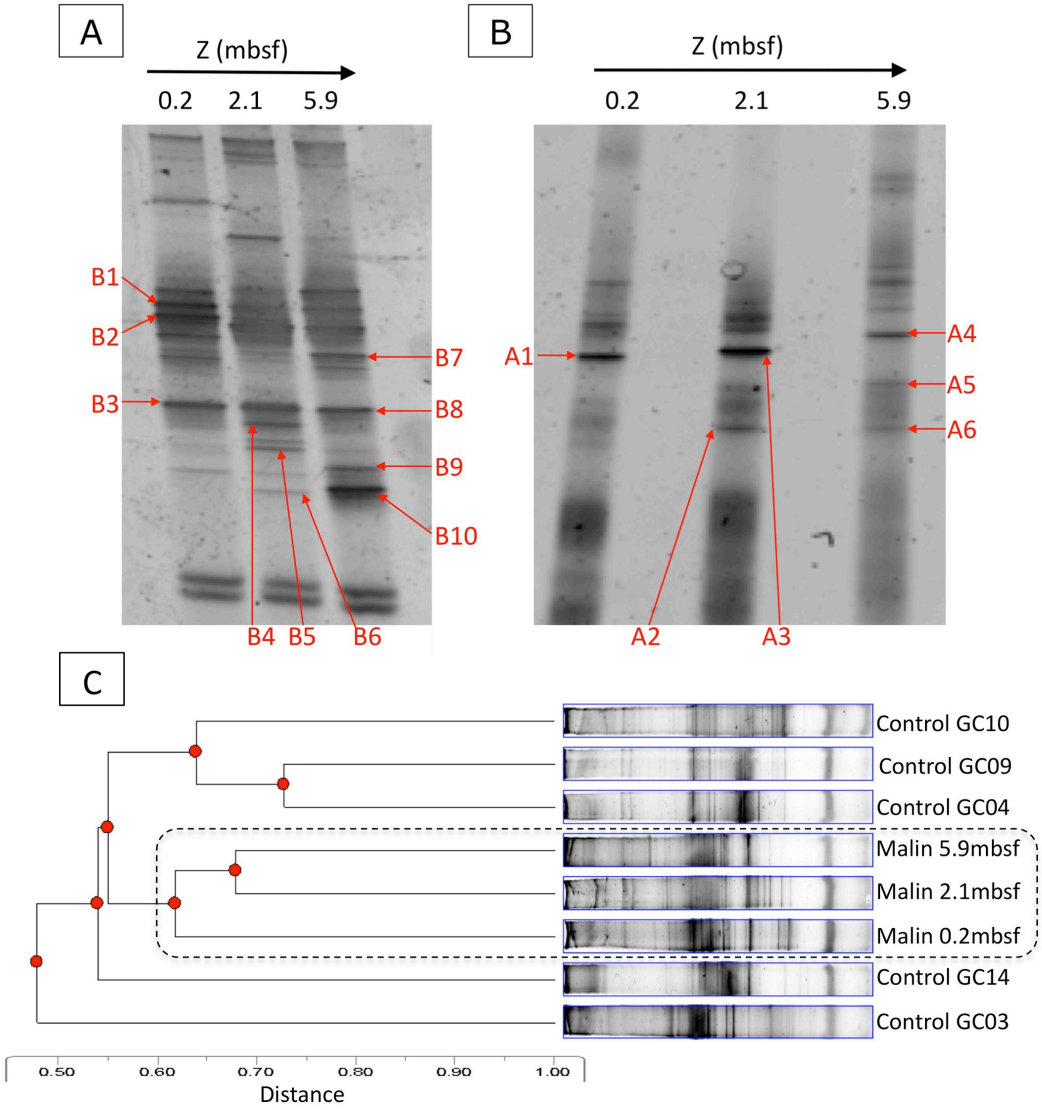

Figure 4.2. DGGE profiles of bacterial (A) and archaeal (B) community composition at 0.2, 2.1 and 5.9mbsf from VC045. Excised bands are labeled and referred to in Table 4.1 Digitised bacterial DGGE lanes were clustered by UPGMA clustering and Ochiai coefficient-based similarities (C). The distance scale indicates Euclidean distance. Bacterial DGGE lanes from the Malin site were compared to control marine sediment samples taken from 1 mbsf sediment from Dunmanus Bay, Ireland (See chapter 5).

Table 4.2. Operational taxonomic units from 16S rRNA bacterial 2.1 and 5.9mbsf clone libraries

OTU	Accession Number	Clones Sequenced /Total	Closest Phylotype (Accession No.)	Match	OTU % in library	Reference
			2.1mbsf library			
1	JQ349463	17/35	*Psychrobacter nivimaris* strain 88/2-7 (NR_028948.1)	≥97	59.0	Heuchert (2004)
2	JQ349486	4/11	*Sulfitobacter pontiacus* ChLG-10 (NR_026418.1)	≥97	18.0	Sorokin (1995)
3	JQ349489	1/4	*Alcanivorax borkumensis* SK2 (NR_029340.1)	98	6.7	Yakimov (1998)
4	JQ349490	1/3	Uncultured actinobacterium clone ANTXXIII_706-4_Bac69 (FN429805.1)[2]	98	4.9	Niemann (2009)
5	JQ349494	1/2	*Pseudoalteromonas arctica* strain C53q-3a (JN681829.1)	98	3.3	Bernbom (2011)
6	JQ349491	1/1	Uncultured bacterium clone 3H3M_69 (JN230300.1)[3]	98	1.6	Hoshino (2011)
7	JQ349492	1/1	Uncultured bacterium clone Propane SIP20-4-09 (GU584779.1)	98	1.6	Redmond (2010)
8	JQ349493	1/1	*Thauera* sp. R-28312 (AM084110.1)	96	1.6	Heylen (2006)
9	JQ349496	1/1	Pseudoalteromonas tetraodonis strain IAM 14160 (NR_041787.1)	99	1.6	Ivanova (2001)
10	JQ349495	1/1	Pseudomonas sp. PM1 16S (EU768833.1)	99	1.6	Ren (2011)
OTU	**Accession Number**	**Clones sequenced**	**5.9mbsf library**			
1	JQ349448	15/21	*Psychrobacter marincola* strain KMM 277 (NR_025458.1)[1]	≥97	40.3	Romanenko (2002)
2	JQ349479	7/19	*Sulfitobacter litoralis* strain Iso 3 (NR_043547.1)	≥92	36.5	Park (2007)
3	JQ349498	1/4	Uncultured Pseudomonas sp. C-51 (FJ900868.1)	99	7.7	Ren (2011)
4	JQ349503	1/2	Uncultured bacterium 16S rRNA gene clone D3DH031 (FQ660126.1)	95	3.8	Martin (2012)
5	JQ349497	1/2	*Pseudoalteromonas arctica* strain C53q-3a (JN681829.1)	98	3.8	Bernbom (2011)
6	JQ349500	1/1	Uncultured bacterium clone Propane SIP20-4-09 (GU584779.1)	99	1.9	Redmond (2010)
7	JQ349499	1/1	Uncultured actinobacterium clone ANTXXIII_706-4_Bac69 (FN429805.1)[2]	98	1.9	Niemann (2009)
8	JQ349501	1/1	*Variovorax paradoxus* EPS (CP002417.1)	99	1.9	Lucas (2010)
9	JQ349502	1/1	*Colwellia aestuarii* strain SMK-10 (NR_043509.1)	98	1.9	Jung (2006)

Note 1: OTU group dominated by clones closest to *Psychrobacter marincola* but clones most related to *Psychrobacter celer* strain SW-238 (NR_043225.1), *Psychrobacter pacifisensis* strain NIBH P2K6 (NR_027187.1) are also present.

Note 2: Closest cultured relatives are distantly related (~82% match) to sulphate reducing δ-proteobacteria *S. palmitis*, *S. svalbardensis*

Note 3: Closest cultured relatives are distantly related (82-84% match) to the sulphate reducing δ-proteobacteria *Dessulfobacca acetoxidans*, *Desulfobacterium anilini* and *Desulfacinum subterraneum*

Less abundant groups, representing less than 2% of the library each, are those closely related to an uncultured bacterium reported in cold-water corals at the Porcupine Seabight (Hoshino et al., 2011), an uncultured bacterium reported at hydrocarbon seeps off the Coast of Santa Barbara (Redmond et al., 2010), *Pseudoalteromonas tetradonis* (Ivanova et al., 2001), an uncultured *Pseudomonas* reported in water flooded petroleum reservoirs (Ren et al., 2011) and distantly related (96%) to a denitrifying bacterium in activated sludge (Heylen et al., 2006). The bacterial clone library at 5.9 mbsf is similar in composition to the bacterial

community composition at 2.1 mbsf but there are distinct differences in the relative proportions. The *Alcanivorax* OTU is not present while the *Pseudomonas* OTU is the largest OTU (7.7%) after *Psychrobacter* and *Sulfitobacter*. An OTU group distantly related to an uncultured bacterium implicated in polyaromatic hydrocarbon degradation in soils (Martin et al., 2012) represented 3.3% of this library but was not found at 2.1 mbsf. OTU groups closely related to *Colwellia aestuarii* (Jung et al., 2006) and *Variovorax paradoxus* (Lucas et al., 2010), which were not found at shallower depths, are present at 5.9 mbsf. The closest cultured relatives to OTU group 4 and 7 from 2.1 mbsf and 5.9 mbsf libraries were distantly related (~82% match) to sulphate reducing *Desulfobacter palmitis*, *Desulfuromonas svalbardensis.* In addition the closest cultured relatives to OTU group 6 at 2.1 mbsf were distantly related (82-84% match) to the sulphate reducing *Dessulfobacca acetoxidans*, *Desulfobacterium anilini* and *Desulfacinum subterraneum.* These groups may be responsible for the observed SO_4^{2-} depletion (Fig. 4.3).

The clone library results are in good overall agreement with DGGE band sequencing, whereby bacteria closely related to *Psychrobacter* and *Sulfitobacter* appear be dominant. *Psychrobacter* are a genus of psychrotolerant or psychrophillic non-motile heterotrophic gram-negative rods or coccobacilli (Juni and Heym, 1986; Bowman et al., 1996). A number of distinct species have been isolated from a wide variety of environments, such as marine sediments (Bozal et al., 2003; Romanenko et al., 2004), Antarctic ornithogenic soils (Bowman et al., 1996), sea ice (Bowman et al., 1997), coastal seawater (Yumoto et al., 2003) and deep-sea trenches and troughs (Maruyama et al., 2000; Dang et al., 2009). *Sulfitobacter* are a genus of bacteria belonging to the Alphaproteobacteria, were first isolated from the Black Sea (Sorokin 1995), but have since been shown to be ubiquitous in the marine environment (Park et al., 2007). They are part of the *Roseobacter* lineage, which is believed to compose up to 25% of marine microbial communities, in particular in coastal and polar settings (Wagner-Döbler and Biebl, 2006). *Sulfitobacter* are primarily gram-negative obligate heterotrophs, which are motile and generate metabolic energy through sulfite oxidation. Thus they are found to be particularly abundant in environments with abundant inorganic sulphur, such as marine sediments (Sorokin, 1995). However these genera have not been found in active cold seep settings or associated with CH_4 cycling, and this is likely the case in this setting also.

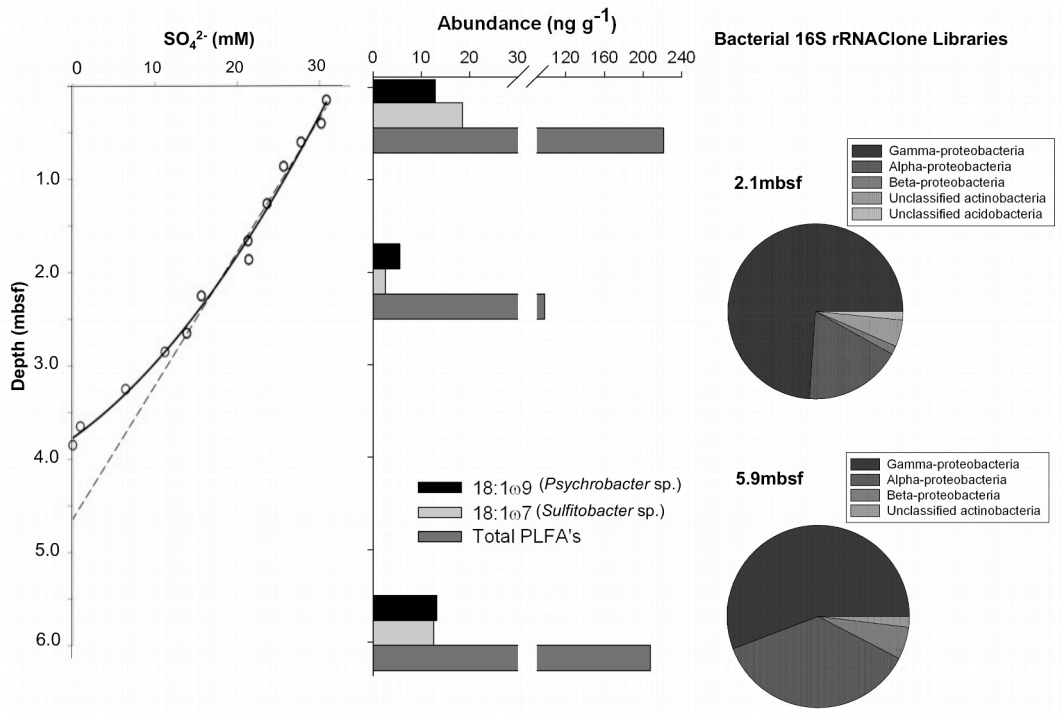

Figure 4.3. Phospholipid fatty acid abundance downcore and composition of bacterial clone libraries from 2.1mbsf and 5.9mbsf. Pore water sulphate profiles are also shown (Pore water data from Szpak et al., 2012).

4.3.2 Occurrence of *Psychrobacter* and *Sulfitobacter* genera

Although many *Psychrobacter* and *Sulfitobacter* species have been cultured to date, little is known about their importance or role in the environment. To our knowledge there are only three previous studies reporting both *Psychrobacter* and *Sulfitobacter* in environmental clone libraries in significant proportions as seen in this study (Inagaki et al., 2003; Prabagaran et al., 2007; McKew et al., 2012). Prabagaran et al. (2007) found that both *Psychrobacter* and *Sulfitobacter* were among the major genera present in contaminated Antarctic seawater and concluded that they might be engaged in oil biodegradation. Inagaki et al. (2003) have also reported a high proportion of these genera in periodic volcanic ash layers in a 58.1 m sediment core from the Sea of Okhotsk. They were not present in pelagic clay layers, which suggests there was lithological control on the success of these genera. McKew et al. (2012) recently reported that *Psychrobacter* and *Sulfitobacter* accounted for up to 63.4% and 61.8% of sequences, respectively, from clone libraries in Caribbean and Indonesian marine sponges. These genera have also been reported among major cultured isolates associated with marine sponges in Antarctic (Papaleo et al., 2012) and N.W. Atlantic coastal waters (Kennedy et al., 2009).

Ettoumi et al. (2010) reported *Psychrobacter* among the major groups present in Tyrrhenian Sea sediments. Rodrigues et al. (2009) reported a geographical distribution of *Psychrobacter* in polar soils and sediments and demonstrated that this genus was dominant in polar settings but only marginally successful in non-polar environments. Mean bottom water temperatures on the NW Irish Shelf range from as low as 5°C in winter to generally less than 10°C in summer, due to thermal stratification of overlying water masses (Hiscock, 1998). Based on optimal growth temperatures (10 to 16°C) and ranges of known cultured *Psychrobacter* (Bowman et al., 1997; Heuchert et al., 2004), seabed temperatures on the Malin Shelf may thus favour the success of this genus. *Sulfitobacter* are also frequently reported as significant members of 16 rDNA clone libraries in cold marine environments (Labrenz et al., 2000; Brakstad and Lodeng, 2004; Kurosawa et al. 2010; Guibert et al., 2012).

There are few studies of microbial diversity in coastal waters in this region (e.g. Gallagher et al., 2004; Hoshino et al., 2011; Egan et al., 2012). Hoshino et al. (2011) and Egan et al. (2012) did not report *Psychrobacter* or *Sulfitobacter*. However Gallagher et al. (2004) found both *Psychrobacter* and *Sulfitobacter* species in water samples from the Porcupine Abyssal Plain. *Psychrobacter* represented 10% or less of clones from water depths of 100 m, 1000 m and 10 m above the seafloor, while they represented 15% of clone libraries from sediment contact water. *Sulfitobacter* represented about 13% of clones from sediment contact water, and were not found at other depths. Thus these genera appear to be ubiquitous regionally. Geographical and oceanographic conditions are likely important controls on their occurrence regionally. These populations are unlikely involved in CH_4 production or oxidation and further support the conclusion that at present the investigated large pockmark is dormant.

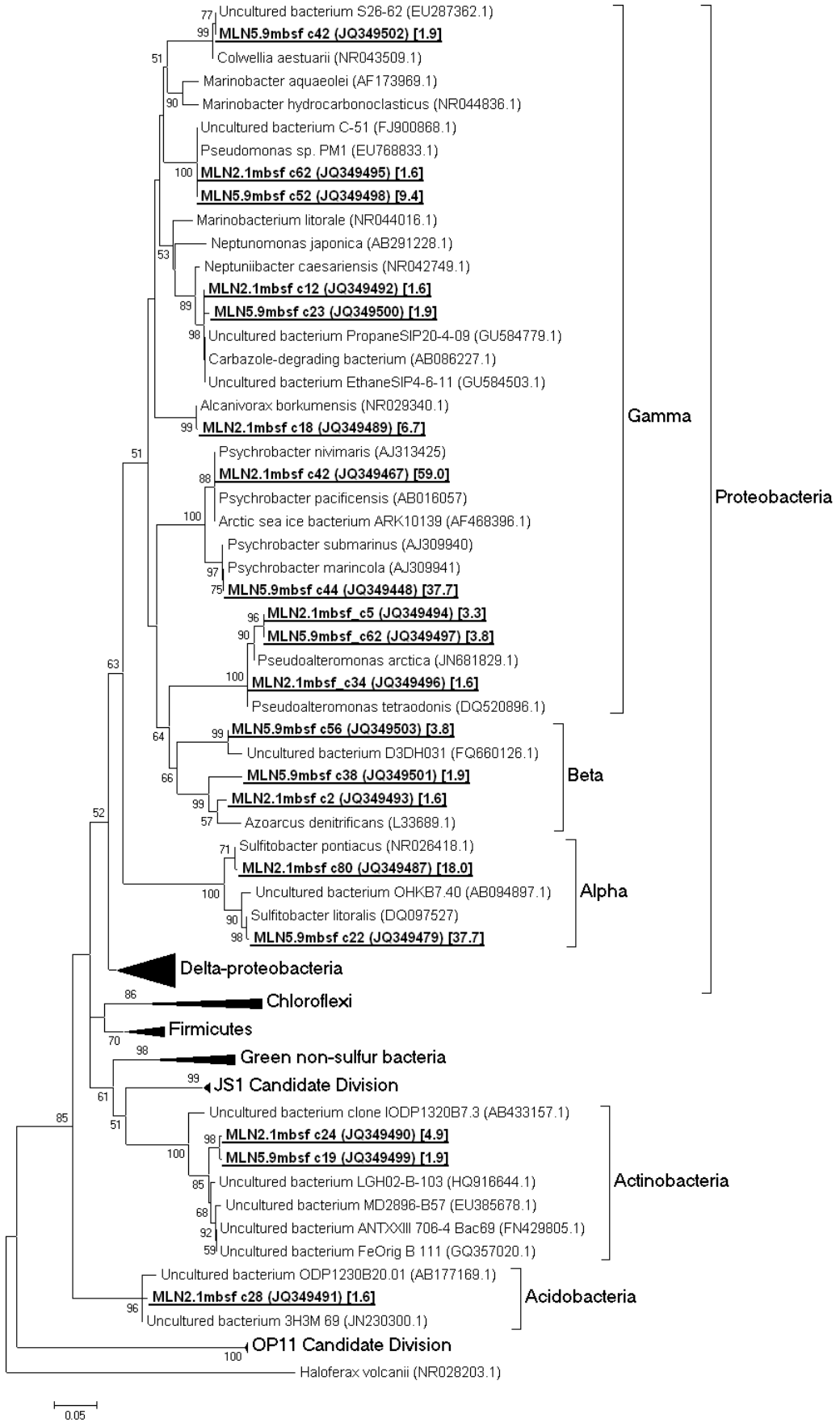
Uncultured bacterium S26-62 (EU287362.1)
MLN5.9mbsf c42 (JQ349502) [1.9]
Colwellia aestuarii (NR043509.1)
Marinobacter aquaeolei (AF173969.1)
Marinobacter hydrocarbonoclasticus (NR044836.1)
Uncultured bacterium C-51 (FJ900868.1)
Pseudomonas sp. PM1 (EU768833.1)
MLN2.1mbsf c62 (JQ349495) [1.6]
MLN5.9mbsf c52 (JQ349498) [9.4]
Marinobacterium litorale (NR044016.1)
Neptunomonas japonica (AB291228.1)
Neptuniibacter caesariensis (NR042749.1)
MLN2.1mbsf c12 (JQ349492) [1.6]
MLN5.9mbsf c23 (JQ349500) [1.9]
Uncultured bacterium PropaneSIP20-4-09 (GU584779.1)
Carbazole-degrading bacterium (AB086227.1)
Uncultured bacterium EthaneSIP4-6-11 (GU584503.1)
Alcanivorax borkumensis (NR029340.1)
MLN2.1mbsf c18 (JQ349489) [6.7]
Psychrobacter nivimaris (AJ313425)
MLN2.1mbsf c42 (JQ349467) [59.0]
Psychrobacter pacificensis (AB016057)
Arctic sea ice bacterium ARK10139 (AF468396.1)
Psychrobacter submarinus (AJ309940)
Psychrobacter marincola (AJ309941)
MLN5.9mbsf c44 (JQ349448) [37.7]
MLN2.1mbsf_c5 (JQ349494) [3.3]
MLN5.9mbsf_c62 (JQ349497) [3.8]
Pseudoalteromonas arctica (JN681829.1)
MLN2.1mbsf_c34 (JQ349496) [1.6]
Pseudoalteromonas tetraodonis (DQ520896.1)
MLN5.9mbsf c56 (JQ349503) [3.8]
Uncultured bacterium D3DH031 (FQ660126.1)
MLN5.9mbsf c38 (JQ349501) [1.9]
MLN2.1mbsf c2 (JQ349493) [1.6]
Azoarcus denitrificans (L33689.1)
Sulfitobacter pontiacus (NR026418.1)
MLN2.1mbsf c80 (JQ349487) [18.0]
Uncultured bacterium OHKB7.40 (AB094897.1)
Sulfitobacter litoralis (DQ097527)
MLN5.9mbsf c22 (JQ349479) [37.7]
Gamma
Beta
Alpha
Proteobacteria
Delta-proteobacteria
Chloroflexi
Firmicutes
Green non-sulfur bacteria
JS1 Candidate Division
Uncultured bacterium clone IODP1320B7.3 (AB433157.1)
MLN2.1mbsf c24 (JQ349490) [4.9]
MLN5.9mbsf c19 (JQ349499) [1.9]
Uncultured bacterium LGH02-B-103 (HQ916644.1)
Uncultured bacterium MD2896-B57 (EU385678.1)
Uncultured bacterium ANTXXIII 706-4 Bac69 (FN429805.1)
Uncultured bacterium FeOrig B 111 (GQ357020.1)
Actinobacteria
Uncultured bacterium ODP1230B20.01 (AB177169.1)
MLN2.1mbsf c28 (JQ349491) [1.6]
Uncultured bacterium 3H3M 69 (JN230300.1)
Acidobacteria
OP11 Candidate Division
Haloferax volcanii (NR028203.1)
0.05

Figure 4.4. Maximum Likelihood phylogenetic tree of bacterial 16S rRNA 2.1mbsf and 5.9 mbsf clone libraries from the Malin pockmark. Selected nucleotide sequences, representing OTU groups from this study are in underlined bold. Accession numbers are in brackets, while values for percentage of total library for each OTU is given in square brackets. The scale bar represents 0.05 base substitutions per site. The tree was subjected to bootstrap analysis (n = 1000) to assess confidence intervals and bootstrap values >50 are reported.

Interestingly a high proportion or dominance of *Psychrobacter* has also been reported in crude oil-contaminated settings (Prabagaran et al., 2007; Radwan et al., 2007; Radwan et al., 2010; Ren et al., 2011) and members of this genus are capable of degradation of aliphatic hydrocarbons (Deppe et al., 2005; Lo Giudice et al., 2010) and certain polyaromatic hydrocarbons (Radwan et al., 2007). *Sulfitobacter* have also also been reported in oil-contaminated settings (Gerdes et al., 2005; Prabagaran et al., 2007; Kostka et al., 2011). Guibert et al. (2012) recently showed that this genus exhibited hydrocarbon-degradation capability in chronically oil-polluted coastal sediments off Argentina, while Roling et al. (2002) showed that *Sulfitobacter* were significant members of artificially contaminated beach sands. Other OTU groups in this study have also been associated with oil and/or polyaromatic hydrocarbon degradation; *Alcanivorax borkumensis* SK2 (Yakimov et al., 1998; Roling et al., 2002). *Pseudoalteromonas* (Hedlund and Staley, 2006; Guibert et al., 2012), *Colwellia* (Redmond and Valentine, 2011), *Variovorax* (Eriksson et al., 2003; Saul et al., 2005) *Pseudomonas* (Ren et al., 2011), and *Thauera* (Heylen et al., 2006; Zhou et al., 1995). In addition OTU group 7 (2.1mbsf) and group 6 (5.9mbsf) are closely related to novel uncultured propane-degrading bacteria (Redmond et al., 2010) associated with known active oil seeps off the coast of Santa Barbara (Hornafius et al., 1999; Kvenvolden and Cooper, 2003). Therefore there is tentative evidence to suggests that the bacterial community is specialized for oil or aromatic compound degradation. Hydrocarbons have been encountered in several of the northwest offshore basins, and Parnell (1992) has suggested that Paleogene reactivation of fractures may have allowed the leakage of reservoir hydrocarbons to the subsurface. However, Szpak et al. (2012) have concluded that this is a gas escape feature, and hence the possibility of the presence of high molecular weight hydrocarbons as a result of seepage is limited. Indeed free hydrocarbon levels or unresolved complex

mixture signatures, typical in areas exposed to oil, were not observed throughout this core (Szpak 2012, personal communication).

4.3.3 Bacterial population microdiversity with sediment depth

Microbial species microdiversity is an important emerging concept in environmental microbiology. Moore et al. (1998) showed that *Prochlorococcus* populations displayed 97% similarity in 16S rRNA genes but exhibited distinct light-dependent physiologies. Field et al. (1997) also demonstrated divergence of the marine planktonic SAR11 cluster, and attributed this divergence to niche specialization in the water column. Thus the environmental conditions appear to be major controls on species microdiversity. The ecotype model (Cohen, 2001) proposes that closely related microbes may be genetically distinct due to adaptation to specific environmental conditions. This study has demonstrated that there is a distinct shift in population abundance and structure of *Psychrobcater* and *Sulfitobacter* with depth (Fig. 4.2 and Table 4.2). Clustering of these populations into distinct sub-groups based on depth is also evident, based on phylogenetic analysis of clones sequences from each clone library (Fig. 4.6). *Psychrobacter* at 2.1 mbsf are most related to *P. nivimaris*, while at 5.9mbsf display greater diversity, with clones closely related to *P. marincola, P. submarinus* and *P. celer.* At 2.1 mbsf the *Sulfitobacter* were most closely matched with *S. pontiacus*, while at 5.9 mbsf was most closely matched with *S. litoralis*. These findings indicate microdiversity among these groups at different sediment depths. *Psychrobacter* are apparently less successful with depth, while the opposite appears to be the case for *Sulfitobacter*. This is supported by PLFA analysis downcore (Fig. 4.2) $C_{18:1\omega9}$ is the major PLFA in known *Psychrobacter* species, accounting for between 41 and 84% (mean 54%, *n*=12) of total PLFA composition (Heuchert et al., 2004), while $C_{18:1\omega7}$ is the major PLFA in *Sulfitobacter*, accounting for between 50 and 91% (mean 78%, *n*=10) of total PLFA composition (Labrenz et al., 2000). The abundances of $C_{18:1\omega9}$ and $C_{18:1\omega7}$ downcore correlate well with the shift in *Psychrobacter* and *Sulfitobacter* 16S rRNA clone distribution with depth. This also supports the results of clone library investigations, as it indicates that these bacteria are among the major bacterial biomass present.

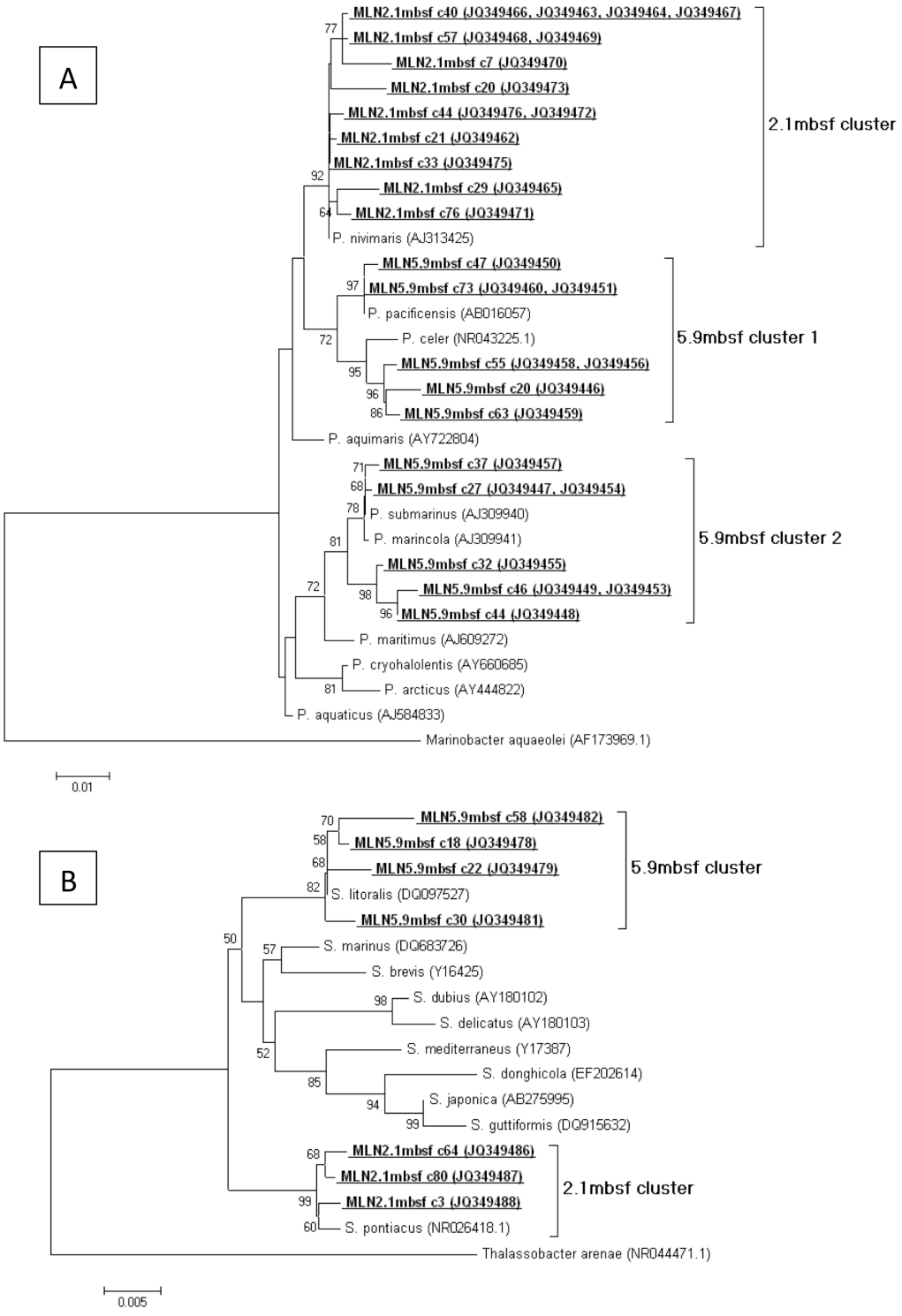
A
MLN2.1mbsf c40 (JQ349466, JQ349463, JQ349464, JQ349467)
MLN2.1mbsf c57 (JQ349468, JQ349469)
MLN2.1mbsf c7 (JQ349470)
MLN2.1mbsf c20 (JQ349473)
MLN2.1mbsf c44 (JQ349476, JQ349472)
MLN2.1mbsf c21 (JQ349462)
MLN2.1mbsf c33 (JQ349475)
MLN2.1mbsf c29 (JQ349465)
MLN2.1mbsf c76 (JQ349471)
P. nivimaris (AJ313425)
2.1mbsf cluster
MLN5.9mbsf c47 (JQ349450)
MLN5.9mbsf c73 (JQ349460, JQ349451)
P. pacificensis (AB016057)
P. celer (NR043225.1)
MLN5.9mbsf c55 (JQ349458, JQ349456)
MLN5.9mbsf c20 (JQ349446)
MLN5.9mbsf c63 (JQ349459)
5.9mbsf cluster 1
P. aquimaris (AY722804)
MLN5.9mbsf c37 (JQ349457)
MLN5.9mbsf c27 (JQ349447, JQ349454)
P. submarinus (AJ309940)
P. marincola (AJ309941)
MLN5.9mbsf c32 (JQ349455)
MLN5.9mbsf c46 (JQ349449, JQ349453)
MLN5.9mbsf c44 (JQ349448)
5.9mbsf cluster 2
P. maritimus (AJ609272)
P. cryohalolentis (AY660685)
P. arcticus (AY444822)
P. aquaticus (AJ584833)
Marinobacter aquaeolei (AF173969.1)
0.01
B
MLN5.9mbsf c58 (JQ349482)
MLN5.9mbsf c18 (JQ349478)
MLN5.9mbsf c22 (JQ349479)
S. litoralis (DQ097527)
MLN5.9mbsf c30 (JQ349481)
5.9mbsf cluster
S. marinus (DQ683726)
S. brevis (Y16425)
S. dubius (AY180102)
S. delicatus (AY180103)
S. mediterraneus (Y17387)
S. donghicola (EF202614)
S. japonica (AB275995)
S. guttiformis (DQ915632)
MLN2.1mbsf c64 (JQ349486)
MLN2.1mbsf c80 (JQ349487)
MLN2.1mbsf c3 (JQ349488)
S. pontiacus (NR026418.1)
2.1mbsf cluster
Thalassobacter arenae (NR044471.1)
0.005

Figure 4.5: Maximum likelihood phylogenetic tree for selected clones from the *Psychrobacter* (A) and *Sulfitobacter* (B) OTU's. Nucleotide sequences from this study are in underlined bold. Accession numbers are in brackets. The scale bars represent the number of base substitutions per site. The tree was subjected to bootstrap analysis (n = 1000) to assess confidence intervals. Bootstrap values >50 are reported. This shows distinct clustering of both bacterial populations between the two depths. At 2.1mbsf *Psychrobacter* clones (n = 14) are phylogenetically most closely related to *P. nivimaris*, while at 5.9mbsf (n = 14) are more diverse and cluster into groups related to *P. celer, P. marincola* and *P. submarinus* (Romanenko et al., 2002). *Sulfitobacter* clones at 2.1mbsf (n = 3) are phylogenetically most closely related to *S. pontiacus*, while at 5.9mbsf (n = 6) are most related to *S. litoralis*.

Sulphate, due to its relatively poor energy yield (-380 kJ mol^{-1}) is utilized as an electron acceptor after depletion of other more favourable electron acceptors (e.g. O_2, NO_3^-). Sulphate is depleted here at about 3.8 mbsf (Szpak et al., 2012) and indicates transition from suboxic to anoxic conditions. Szpak et al. (2012) also noted a decrease in the abundance of labile OM and an accumulation of recalcitrant aliphatic OM downcore. *P. nivimaris* was first isolated associated with organic-rich particulates in seawater, and decreasing availability of labile OM may account for the absence of this group at 5.9 mbsf. *P. celer* is a facultative anaerobe, and clones found associated with this species at 5.9 mbsf may also be capable of anaerobic growth. Interestingly Ettoumi et al. (2010) reported considerable microdiversity between *Psychrobacter* in organic-poor oligotrophic marine sediments. Therefore it is possible that the increase in microdiversity at 5.9 mbsf may reflect community adaptation to conditions of low nutrient and labile OM availability. *S. pontiacus* has a sulfite reductase activity that is close to the activity of autotrophic inorganic sulfur reducers (Gonzalez et al., 1999) and in this setting it is likely that this group is involved in oxidation of reduced sulphur species to sulphate and may be out-competing SRB in the first few metres. The increased abundance of *Sulfitobacter* may be related to increased levels of reduced sulphur below the sulphate depletion zone. *Sulfitobacter* groups at this depth may also be adapted to low nutrient and OM availability. While factors controlling the changes in microdiversity with depth are likely complex, results do suggest that *Psychrobacter* and *Sulfitobacter* in this setting displayed measurable genetic divergence with depth, and may be distinct ecotypes.

4.4 Conclusions

This study has shown that the predominant bacterial populations belong to the Gammaproteobacteria and Alphaproteobacteria. In particular the genera *Psychrobacter* and *Sulfitobacter* appear to be dominant in this setting, based on PLFA analysis of characteristic fatty acids and their major distribution in clone libraries and DGGE profiles. Bacterial communities do not belong to known groups associated with CH_4 seepage, as are found in other active cold seep environments. This supports previous inferences that gas migration to surface sediments and seepage to the water column is occurring. The dominance of *Psychrobacter* and *Sulfitobacter* and the presence of OTUs closely related to *Alcanivorax, Colwellia*, *Pseudoalteromonas*, *Pseudomonas*, *Variovorax* genera, suggests that the bacterial community is specialized for degradation of recalcitrant sedimentary hydrocarbons. Significant variation in population abundance and sub-structure was observed with depth. *Psychrobacter* and *Sulfitobacter* were observed to display distinct clustering based on depth, indicating species microdiversity. These genetically divergent populations could be a result of niche specialisation.

4.5 References

Al Khudary, R., Stober, N.I., Ooura, F., Antranikian, G., 2008. *Pseudoalteromona arctica* sp. nov., an aerobic, psychrotolerant, marine bacterium isolated from Spitzbergen. International Journal of Systematic and Evolutionary Microbiology 58, 2018-2024.

Alongi, D.M., 1992. Vertical profiles of bacterial abundance, productivity and growth rates in coastal sediments of the central Great Barrier Reef lagoon. Marine Biology 112, 657-663.

Ashelford, K.E., Chuzanova, N.A., Fry, J.C., Jones, A.J., Weightman, A.J., 1994. At least 1 in 20 16S rRNA sequence records currently held in public repositories is estimated to contain substantial anomalies. Applied and Environmental Microbiology 71, 7724-7736.

Balkwill, D.L., Leach, F., Wilson, J.T., McNabb, J.F., White, D.C., 1988. Equivalence of microbial biomass measures based on membrane lipid and cell wall components, adenosine triphosphate and direct counts in subsurface aquifer sediments. Microbial Ecology 16, 73-83.

Beal, E.J., House, C.H., Orphan, V.J., 2009. Manganese- and Iron -dependent marine methane oxidation. Science 325, 184-187.

Bernbom, N.E., Yoke Yin, N., Kjelleberg, S., Harder, T., Gram, L., 2011. Marine bacteria from Danish coastal waters show antifouling activity against the marine fouling bacterium *Pseudoalteromonas* sp. strain S91 and Zoospores of the green alga *Ulva australis* independent of bacteriocidal activity. Applied and Environmental Microbiology 77, 8557-8567.

Biddle, J.F., House, C.H., Brenchley, J.E., 2005. Microbial stratification in deeply buried marine sediment reflect changes in sulfate/methane profiles. Geobiology 3, 287-295.

Boetius, A., Ravenschlag, K., Schubert, C.J., Rickert, D., Widdel, F., Gieseke, A., et al., 2000. A marine microbial consortium mediating anaerobic oxidation of methane. Nature 407, 623-626.

Bowman, J.P., Cavanagh, J., Austin, J.J., 1996. Novel *Psychrobacter* species from Antarctic ornithogenic soils. International Journal of Systematic Bacteriology 46, 841-848.

Bowman, J.P., McCammon, S., Brown, M.V., Nichols, D.S., McKeekin, T., 1997. Diversity and association of psychrophilic bacteria in Antarctic sea ice. Applied and Environmental Microbiology 63, 3068-3078.

Bozal, N., Montes, J., Tudela, E., Guinea, J., 2003. Characterization of several Psychrobacter strains isolated from Antarctic environments and description of *Psychrobacter luti* sp. nov. and *Psychrobacter fozii* sp. nov. International Journal of Systematic and Evolutionary Microbiology 53, 1093-1100.

Brakstad, O.G., Lodeng, A.G.G., 2004. Microbial diversity during biodegradation of crude oil in seawater from the North Sea. Microbial Ecology 49, 94-103.

Brinkhoff, T., Sievert, S.M., Kuever, J., Muyzer, G., 1999. Distribution and diversity of sulfur-oxidizing *Thiomicrospira* spp. at a shallow-water hydrothermal vent in the Aegean Sea (Milos, Greece). Applied and Environmental Microbiology 65, 3843-3849.

Cambon-Bonavita, M.A., Nadalig, T., Roussel, E., Delage, E., Duperron, S., Caprais, J.C., et al., 2009. Diversity and distribution of methane-oxidizing communities associated with different faunal assemblages in a giant pockmark of the Gabon continental margin. Deep Sea Research Part II 56, 2248-2258.

Cohan, F.M., 2001. Bacterial species and speciation. Systematic Biology 50, 513-524

Dando, P.R., Austen, M.C., Burke Jr, R.A., Kendall, M.A., Kennicutt II, M.C., Judd, A.G., et al. 1991. Ecology of a North Sea pockmark with an active methane seep. Marine Ecology Progress Series 70, 49-63.

Dang, H., Zhu, H., Wang, J., Li, T., 2009. Extracellular hydrolytic enzyme screening of culturable heterotrophic bacteria from deep-sea sediments of the Southern Okinawa Trough. World Journal of Microbiology and Biotechnology 25, 71-79.

Deppe, U., Richnow, H.H., Michaelis, W., Antranikian, G., 2005. Degradation of crude oil by an arctic microbial consortium. Extremophiles 9, 46-470

Deutzmann, J.S., Worner, S., Schink, B., 2011. Activity and diversity of methanotrophic bacteria at methane seepsin Eastern Lake Constance sediments. Appl Environ Microbiol 77, 2573-2581.

D'Hondt, S., Rutherford, S., 2002. Metabolic activity of subsurface life in deep sea sediments. Science 295, 2067-2070.

Dobson, M.M., Whittington, R.J., 1992. Aspects of the geology of the Malin Sea area. Basins on the Atlantic Seaboard In: Parnell J. (ed) Petroleum Geology,

Sedimentology and Basin Evolution, 1st ed. London Geol Soc Spec Pub p291-311.

Egan, S.T., McCarthy, D.M., Patching, J.W., Fleming, G.T.A., 2012. An investigation of the physiology and potential role of components of the deep ocean bacterial community (of the NE Atlantic) by enrichments carried out under minimal environmental change. Deep-Sea Research Part I 61, 11-20.

Eriksson, M., Sodersten, E., Zhongtang, U., Gunnel, D., Mohn, W.W., 2003. Degradation of aromatic hydrocarbons at low temperature under aerobic and nitrate-reducing conditions in enrichment cultures from northern soils. Applied and Environmental Microbiology 69, 275-284.

Ettoumi, B., Bouhajja, B.S., Daffonchio, D., Boudabous, A., Cherif, A., 2010. *Gammaproteobacteria* occurrence and microdiversity in Tyrrhenian Sea sediments as revealed by cultivation-dependent and –independent approaches. Applied and Systematic Microbiology 33, 222-231.

Felsenstein, J., 1985. Confidence limits on phylogenies: An approach using the Bootstrap. Evolution 39, 783-791.

Field, K.G., Gordon, D., Wright, T., Rappe, M., Urback, E., Vergin, K., Giovannoni, S.J., 1997. Diversity and depth-specific distribution of SAR11 cluster rRNA genes from marine planktonic bacteria. Applied and Environmental Microbiology, 63, 63-70.

Fry, J.C., Parkes, J.R., Cragg, B.A., Weightman, A.J., Webster, G., 2008. Prokaryotic biodiversity and activity in the deep subseafloor biosphere. FEMS Microbiology Ecology 66, 181-196.

Gallagher, J.M., Carton, M.W., Eardly, D.F., Patching, J.W., 2004. Spatio-temporal variability and diversity of water column prokaryotic communities in the eastern North Atlantic. FEMS Microbiology Ecology 47, 249-262.

Gerdes, B., Brinkmeyer, R., Dieckmann, G., Helmke, E., 2005. Influence of crude oil on changes of bacterial communities in Arctic sea-ice. FEMS Microbiology Ecology 53, 129-139.

Guezennec, J., Fiala-Medioni, A., 1996. Bacterial abundance and diversity in the Barbadose Trench determined by phospholipid analysis. FEMS Microbiology Ecology 19, 83-93.

Guibert, L.M., Loviso, C.L., Marcos, M.S., Commendatore, M.G., Dionisi, H.M., Lozada, M., 2012. Alkane biodegradation genes from chronically polluted

subantarctic coastal sediments and their shifts in response to oil exposure. Microbial Ecology 64, 605-616.

Hedlund, B.P., Staley, J.T., 2006. Isolation and characterization of *Pseudoalteromonas* strains with divergent polycyclic aromatic hydrocarbon catabolic properties. Environmental Microbiology 8, 178-182.

Heuchert, A., Glöckner, F.O., Amann, R., Fischer, U., 2004. *Psychrobacter nivimaris* sp. nov., a heterotrophic bacterium attached to organic particles isolated from the South Atlantic (Antarctica). Systematic and Applied Microbiology 27, 399-406.

Heylen, K., Vanparys, B., Wittebolle, L., Verstraete, W., Boon, N., 2006. Cultivation of denitrifying bacteria: optimization of isolation conditions and diversity study. Appied and Environmental Microbiology 72, 2637-2643.

Hiscock, K., 1998. Marine Nature Conservation Review: Benthic marine ecosystems of Great Britain and the north-east Atlantic. Joint Nature Conservation Committee: Peterborough, UK.

Hornafius, J.S., 1999. The world's most spectacular hydrocarbon seeps (Coal Point Seep, Santa Barbara Channel, California): Quantification of emissions. Journal of Geophysical Research 104, 703-711.

Hoshino, T., Morono, Y., Terada, T., Imachi, H., Ferdelman, T.G., Inagaki, F., 2011. Comparative study of subseafloor community structures in deeply buried coral fossils and sediment matrices from the Challenger Mound in the Porcupine Seabight. Frontiers in Microbiology 2, 1-7.

Inagaki, F., Suzuki, M., Takai, K., Oida, H., Sakamoto, T., Aoki, K., Nealson, K.H., Horikoshi, K., 2003. Microbial communities associated with geological horizons in coastal subseafloor sediments from the Sea of Okhotsk. Applied and Environmental Microbiology 69, 7224-7235.

Ivanova, E.P., Romanenko, L.A., Matté, M.H., Matté, G.R., Lysenko, A.M., Simidu, U., Kita-Tsukamoto, K., Sawabe, T., Vysotskii, M.V., Frolova, G.M., Mikhailov, V., Christen, R., Colwell, R.R., 2001. Retrieval of the species *Alteromonas tetraodonis* Simidu et al. 1990 as *Pseudoalteromonas tetraodonis* comb. nov. and emendation of description. International Journal of Systematic and Evolutionary Microbiology 51, 1071-1078.

Jørgensen, B.B., Boetius, A., 2007. Feast or famine - microbial life in the seabed. Nature 5, 770-781.

Judd, A.G., Hovland, M., 2007. Seabed fluid flow: the impact of geology, biology and the marine environment. Cambridge University Press: Cambridge, UK.

Jung, S.Y., Oh, T.K., Yoon, J.H., 2006. *Colwellia aestuarii* sp. nov., isolated from a tidal flat sediment in Korea. International Journal of Systematic and Evolutionary Microbiology 56, 33-37.

Juni, E., Heym, G.A., 1986. *Psychrobacter immobilis* gen. nov., sp. nov.: genospecies composed of gram-negative, aerobic, oxidase positive coccobacilli. International Journal of Systematic Bacteriology 36, 388-391.

Kennedy, J., Baker, B., Piper, C., Cotter, P.D., Walsh, M., Mooij, M.J., et al., 2009. Isolation and analysis of bacteria with antimicrobial activities from the marine sponge *Halicola simulans* collected from Irish waters. Marine Biotechnology 11, 384-396.

King, L.H., MacLean, B., 1970. Pockmarks on the Scotian Shelf. Geological Society of America Bulletin 81, 3141-3148.

Kim, E.H., Cho, K.H., Lee, Y.M., Yim, J.H., Lee, H.K., Cho, J.C., Hong, S.J., 2010. Diversity of cold-active protease-producing bacteria from arctic terrestrial and marine environments revealed by enrichment culture. Journal of Microbiology 48, 426-432.

Kostka, J.E., Prakash, O., Overholt, W.A., Green, S.J., Freyer, G., Canion, A., et al., 2011. Hydrocarbon-degrading bacteria and the bacterial community response in Gulf of Mexico beach sands impacted by the Deepwater Horizon Oil Spill. Applied and Environmental Microbiology 77, 7962-7974.

Kurosawa, N., Sato, S., Kawarabayasi, Y., Imura, S., Naganuma, T., 2010. Archaeal and bacterial community structures in the anoxic sediment of Antarctic meromictic lake Nurume-Ike. Polar Science 4, 421-429.

Kvenvolden, K.A., Cooper, C.K., 2003. Natural seepage of crude oil into the marine environment. Geo-Marine Letters 23, 140-146.

Labrenz, M., Tindall, B.J., Lawson, P.A., Collins, M.D., Schumann, P., Hirsch, P., 2000. *Staleya guttiformis* gen. nov., sp. nov. and *Sulfitobacter brevis* sp. nov., α-Proteobacteria from hypersaline, heliothermal and meromictic antarctic Ekho Lake. International Journal Systematic and Evolutionary Microbiology 50, 303-310.

Lazar, C.S., Dinasquet, J., L'Haridon, S., Pignet, P., Toffin, L., 2011. Distribution of anaerobic methane-oxidizing and sulfatereducing communities in the G11 Nyegga pockmark, Norwegian Sea. Antonie Leeuwenhoek 100, 639-653.

Lo Giudice, A., Brilli, M., Bruni, V., De Domenico, M., Fani, R., Michaud, L., 2007. Bacterium-bacterium inhibitory interactions among psychrotrophic bacteria isolated from Antarctic seawater (Terra Nova Bay, Ross Sea). FEMS Microbiology Ecology 60, 383-396.

Lo Giudice, A., Casella, P., Caruso, C., Mangano, S., Bruni, V., De Domenico, M., et al. 2010. Occurrence and characterization of psychrotolerant hydrocarbon-oxidising bacteria from surface seawater along the Victoria Land coast (Antarctica). Polar Biology 33, 929-943.

Lo Giudice, A., Caruso, C., Mangano, S., Bruno, V., De Dominico, M., Michaud, L., 2012. Marine bacterioplankton diversity and community composition in an antarctic coastal environment. Microbial Ecology 63, 210-223.

Marchesi, J.R., Sato, T., Weightman, A.J., Martin, T.A., Fry, J.C., Hiom, S.J., et al., 1998. Design and evaluation of useful bacterium-specific pcr primers that amplify genes coding for 16S rRNA. Applied and Environmental Microbiology 64, 795-799.

Martin, F., Torelli, S., Le Paslier, D., Barbance, A., Martin-Laurent, F., Bru, D., et al., 2012. Betaproteobacteria dominance and diversity shifts in the bacterial community of PAH-contaminated soil exposed to phenanthrene. Environmental Pollution 162, 345-353.

Maruyama, A., Honda, D., Yamamoto, H., Kitamura, K., Higashihara, T., 2000. Phylogenetic analysis of psychrophilic bacteria isolated from the Japan Trench, including a description of the deep-sea species *Psychrobacter pacificensis* sp. nov. International Journal of Systematic and Evolutionary Microbiology 50, 835-846.

McKew, B., Dumbrell, A.J., Daud, S.D., Hepburn, L., Thorpe, E., Morgensen, L., et al., 2012. Characterization of geographically distinct bacterial communities associated with the coral mucus from *Acropora* spp. and *Porites* spp. Applied and Environmental Microbiology 78, 5229-5237.

Monteys, X., Garcia, X., Szpak, M., Garcia-Gil, S., Kelleher, B., 2008a. Multidisciplinary approach to the study and environmental implications of two

large pockmarks on the Malin Shelf, Ireland. 9th International Conference on Gas in Marine Sediments. ICSG 2008 Abstract Volume. Bremen, Germany.

Monteys, X., Hardy, D., Doyle, E., Garcia-Gil, S., 2008b. Distribution, morphology and acoustic characterisation of a gas pockmark field on the Malin Shelf, NW Ireland. Symposium OSP-01, 33rd International Geological Congress. Oslo, Norway.

Moore, L.R., Rocap, G., Chisholm, S.W., 1998. Physiology and molecular phylogeny of coexisting *Prochlorococcus* ecotypes. Nature 393, 464-467.

Muyzer, G., de Waal, E.C., Uitterlinden, A.G., 1993. Profiling of complex microbial populations by denaturing gradient gel electrophoresis analysis of polymerase chain reaction amplified genes coding for 16S rRNA. Applied and Environmental Microbiology 59, 695-700.

Myers, R.M., Fischer, S.G., Lerman, L.S., Maniatis, T., 1985. Nearly all single base substitutions in DNA fragments joined to a GC-clamp can be detected by denaturing gradient gel electrophoresis. Nucleic Acids Research 13, 3131-3145.

Nichols, P.D., Guckert, J.B., White, D.C., 1986. Determination of monounsaturated fatty acid double-bond position and geometry for microbial monocultures and complex consortia by capillary GC-MS of their dimethyl disulphide adducts. Journal of Microbiological Methods 5, 49-55

Niemann, H., Fischer, D., Graffe, D., Knittel, K., Montiel, A., Heilmayer, O., et al. 2009. Biogeochemistry of a low-activity cold seep in the Larsen B area, western Weddell Sea, Antarctica. Biogeosciences 6, 2383-2395.

Nunoura, T.

Nunoura, T., Inagaki, F., Delwiche, M.E., Colwell, F.S., Takai, K., 2009. Subseafloor microbial communities in methane hydrate-bearing sediment at two distinct locations (ODP Leg 204) in the Cascadia Margin. Microbes in the Environment 23, 317-325.

Olu-Le Roy, K., Caprais, J.C., Fifis, A., Fabri, M.C., Galeron, J., Budzinsky, H., et al. 2007. Cold seep assemblages on a giant pockmark off West Africa: spatial patterns and environmental control. Marine Ecology 28, 115-130.

Omorogie, E.O., Niemann, H., Mastalerz, V., de Lange, G.J., Stadnitskaia, A., Mascle, J., et al., 2009. Microbial methane oxidation and sulfate reduction at

cold seeps of the deep Eastern Mediterranean Sea. Marine Geology 261, 114-127.

Ondreas H, Olu-Le Roy K, Fouquet Y, Charlou JL, Gay A, Dennielou B, et al. (2005) ROV study of a giant pockmark on the Gabon continental margin. Geo-Mar Lett 25:281-292.

Orphan, V.J., House, C.H., Hinrichs, K-U., McKeegan, K.,D., DeLong, E.F., 2001. Methane-consuming archaea revealed by directly coupled isotopic and phylogenetic analysis. Science 293, 484-486.

Park, J.R., Bae, J.W., Nam, Y.D., Chang, H.W., Kwon, H.Y., Quan, Z.X., 2007. *Sulfitobacter litoralis* sp. nov., a marine bacterium isolated from East Sea, Korea. International Journal of Systematic and Evolutionary Microbiology 57, 692-695.

Papaleo, M.C., Fondi, M., Maida, I., Perrin, E., Lo Giudice, A., Michaud, L., et al., 2012. Sponge-associated microbial Antarctic communities exhibiting antimicrobial activity against *Burkholderia cepacia* complex bacteria. Biotechnology Advances 30, 272-293.

Pinkart, H.C., Devereux, R., Chapman, P.J., 1998. Rapid separation of microbial lipids using solid phase extraction columns. Journal of Microbiological Methods 34, 9-15.

Prabagaran, S.R., Manorama, R., Delille, D., Shivaji, S., 2007. Predominance of *Roseobacter, Sulfitobacter, Glaciecola* and *Psychrobacter* in seawater collected off Ushuaia, Argentina, Sub-Antarctica. FEMS Microbiology Ecology 59, 342-355.

Radwan, S.S., Al-Hasan, R.H., Mahmoud, H.M., Eliyas, M., 2007. Oil-utilizing bacteria associated with fish from the Arabian Gulf. Journal of Applied Microbiology 103, 2160-2167.

Radwan, S.S., Mahmoud, H.M., Khanafer, M., Al-Habib, A., Al-Hasan, R.H., 2010. Identities of epilithic hydrocarbon-utilizing diazotrophic bacteria from the Arabian Gulf coasts, and their potential for oil bioremediation without nitrogen supplementation. Microbial Ecology 60, 354-363.

Rajendran, N., Matsuda, O., Urushigawa, Y., Simidu, U., 1994. Characterization of microbial community structure in the surface sediment of Osaka Bay, Japan, by phospholipid fatty acid analysis. Applied and Environmental Microbiology 60, 248-257.

Redmond, M.C., Valentine, D.L., Sessions, A.L., 2010. Identification of novel methane- ethane, and propane-oxidising bacteria at marine hydrocarbon seeps by stable isotope probing. Applied and Environmental Microbiology 76, 6412-6422.

Redmond, M.C., Valentine, D.L., 2011. Natural gas and temperature structured a microbial community response to the Deepwater Horizon oil spill. Proceeding of the National Academy Sciences USA 3, 1-6.

Ren, H.Y., Zhang, X.J., Song, Z.Y., Rupert, W., Gao, G.J., Guo, S.X., et al., 2011. Comparison of microbial community compositions of injection and production well samples in a long-term water-flooded petroleum reservoir. PLoS ONE 6, 1-9.

Ringelberg, D.A., Sutton, S., White, D.C., 1997. Biomass, bioactivity and biodiversity: microbial ecology of the deep subsurface: analysis of ester-linked phospholipid fatty acids. FEMS Microbiology Ecology 20, 371-377.

Roalkvam, I., Jørgensen, S.L., Chen, Y., Stokke, R., Dahle, H., Hocking, WP., 2011. New insight into stratifcation of anaerobic methanotrophs in cold seep sediments. FEMS Microbiology Ecology 78, 233-243.

Roling, W.F.M., Milner, M.G., Jones, D.M., Lee, K., Daniel, F., Swannell, R.J.P., et al., 2002. Robust hydrocarbon degradation and dynamics of bacterial communities during nutrient-enhanced oil spill bioremediation. Applied and Environmental Microbiology 68, 5537-5548.

Romanenko, L.A., Lysenko, A.M., Rohde, M., Mikhailov, V.V., Stackebrandt, E., 2004. *Psychrobacter maritimus* sp. nov. and *Psychrobacter arenosus* sp. nov., isolated from coastal sea ice and sediments of the Sea of Japan. International Journal of Systematic and Evolutionary Microbiology 54, 1741-1745.

Saul, D.J., Aislabie, J.M., Brown, C.E., Harris, L., Foght, J.M., 2005. Hydrocarbon contamination changes the bacterial diversity of soil from around Scott Base, Antarctica. FEMS Microbiology Ecology 53, 141-145.

Scholten, J.C.M., 2000. Isolation and characterisation of acetate-utilising anaerobes from a freshwater sediment. Microbial Ecology 40, 292-299.

Schulz, H.D., 2006. Quantification of early diagenesis: Dissolved constituents in marine pore water. In: Schulz HD & Zabel M (eds.) Marine Geochemistry, 2nd ed. Springer: Germany p124.

Shubenkova, O.V., Likhoshvai, A.V., Kanapatskii, T.A., Pimenov, N.V., 2010. Microbial community of reduced pockmark sediments (Gdansk Deep, Baltic Sea). Microbiology 79, 799-808.

Singleton, D.R., Hu, J., Aitken, M.D., 2012. Heterologous expression of polycyclic aromatic hydrocarbon ring-hydroxylating dioxygenase genes from a novel pyrene-degrading betaproteobacterium. Applied and Environmental Microbiology 78, 3552-3559.

Sorokin, D.Y., 1995. *Sulfitobacter pontiacus* gen. nov., sp. nov. - a new heterotrophic bacterium specialized on sulfite oxidation. Microbiology 64, 295-305.

Stoeck, T., Kröncke, I., Duineveld, G.C.A., Palojärvi, A., 2002. Phospholipid fatty acid profiles at depositional and non-depositional sites in the North Sea. Marine Ecology Progress Series 241, 57-70.

Szpak, M., Monteys, X., O' Reilly, S., Simpson, A., Garcia, X., Evans, R., et al., 2012. Geophysical and geochemical survey of a large pockmark on the Malin Shelf, Ireland. Geochemistry Geophysics Geosystems 13, 1-18.

Tamura, K., Nei, M., 1993. Estimation of the number of nucleotide substitutions in the control region of mitochondrial DNA in humans and chimpanzees. Molecular Biology and Evolution 10, 512-526.

Tamura, K., Peterson, D., Peterson, N., Stecher, G., Nei, M., Kumar, S., 2011. MEGA5: Molecular Evolutionary Genetics Analysis using Maximum Likelihood, Evolutionary Distance, and Maximum Parsimony Methods. Molecular Biology and Evolution 28, 2731-2739.

Thompson, J.D., Higgins, G., Gibson, T.J., 1994. CLUSTAL W: improving the sensitivity of progressive multiple sequence alignment through sequence weighting, position-specific gap penalties and weight matrix choice. Nucleic Acids Research 22, 4673-4680.

Vetriani, C., Jannasch, H.W., MacGregor, B.J., Stahl, D.A., Reysenbach, A.L., 1999. Population structure and phylogenetic characterisation of marine benthic archaea in deep-sea sediments. Applied and Environmental Microbiology 65, 4375-4384.

Wagner-Döbler, I., Biebl, H., 2006. Environmental biology of the marine Roseobacter lineage. Annu Rev Microbiol 60, 255–280.

Wang, Y.P., Gu, J.D., 2006. Degradability of dimethyl terephthalate by *Variovorax paradoxus* T4 and *Sphingomonas yanoikuyae* DOS01 isolated from deep ocean sediments. Ecotoxicology 15, 549-557.

Wegener, G., Shovitri, M., Knittel, K., Niemann, H., Hovland, M., Boetius, A., 2008. Biogeochemical processes and microbial diversity of the Gullfaks and Tommeliten methane seeps (Northern North Sea). Biogeosciences Discussions 5, 971-1015.

White, D.C., Ringelberg, D.B., 1998. Signature lipid biomarker analysis. In: Burlage, R.S., Atlas, R., Stahl, D., Geesey, G., Sayler, G., (eds.). Techniques in Microbial Ecology Oxford University Press:Oxford, UK, p255-288.

Yakimov, M.M., Golyshin, P.N., Lang, S., Moore, E.R.B., Abraham, W.R., Lunsdorf, H., Timmis, K.N., 1998. *Alcanivorax borkumensis* gen. nov., sp. nov., a new hydrocarbon-degrading and surfactant-producing marine bacterium. International Journal of Systematic Bacteriology 48, 339-348.

Yumoto, I., Hirota, K., Sogabe, Y., Nodasaka, Y., Yokota, Y., Hoshino, T., 2003. *Psychrobacter okhotskensis* sp. nov., a lipase-producing facultative psychrophile isolated from the coast of the Okhotsk Sea. International Journal of Systematic and Evolutionary Microbiology 53, 1985-1989.

Zhou, J., Fries, M.R., Chee-Sanford, J.C., Tiedje, J.M., 1995. Phylogenetic analysis of a new group of denitrifiers capable of anaerobic growth of toluene and description of *Azoarcus tolulyticus* sp. nov. Int J Syst Evol Microbiol 45, 500-506.

Zhou, J., Bruns, M.A., Tiedje, J.M., 1996. DNA recovery from soils of diverse composition. Applied and Environmental Microbiology 62, 316-322.

Chapter 5
Multidisciplinary investigation of active shallow pockmarks in Dunmanus Bay, Cork, Ireland

5.1 Introduction

Pockmarks are circular or sub-circular seabed depressions, which may reach diameters of hundreds of metres and depths of tens of metres (Judd and Hovland, 2007). They occur in a variety of settings, which include estuaries (Garcia-Gil et al., 2003; Garcia-Gil 2003) shallow bays (Knebel and Scanlon, 1985; Kelley et al., 1994; Ussler et al., 2003), continental shelves (Nelson et al., 1979;Fader, 1991), continental slopes and rises (Paull et al., 2002; Gay et al., 2006), and lakes (Pickrill, 2006). Sub-seabed fluid escape is usually invoked as the primary formation mechanism for these features, and the current leading formation theory was proposed by Hovland and Judd (1988). This includes three primary stages: (1) the formation of a seabed dome due to excessive fluid pressure underneath the seabed; (2) discharge of the fluid in a single event, expelling the sediment into the water column, winnowing fine-grained sediment and leaving lag deposits; and (3) continuation of pockmark formation due to continual or episodic seepage. Thus lithology is thought to be one of the primary parameters for pockmark occurrence, since fine-grained clay/silt has a lower permeability than coarser grains and hence facilitate gas accumulation and overpressurisation. The main associated fluid is gas, which may be thermogenic or microbial gas from organic-rich sedimentary deposits (Judd and Hovland, 2007). Frequently however, surveyed pockmarks are not associated with evidence, be that geophysical or geochemical, of gas (or other fluids) migration and are deemed inactive or that another formation mechanism may be possible (Paull et al., 2002; Ussler et al., 2003; Rogers et al., 2006). Alternative pockmark formation theories inlcude porewater escape (Harrington, 1985), fresh/groundwater seepage (Whiticar 2002; Christodolou et al., 2003), ice-rafting (Paull et al., 1999), biological activity and meteorite impacts (Judd and Hovland, 2007). Thus significant questions remain regarding pockmark formation, distribution and processes.

To date, there have been few studies of biological productivity associated with pockmarks and most have focused on macrofaunal assemblages present (Dando, 1991; Ondreas et al., 2005; Judd and Hovland, 2007; Webb et al., 2009). In contrast to active deep sea sites, biological productivity at shallow pockmark settings does not seem to be very different from surrounding sediment. Studies of microbial diversity in pockmarks have reported microbes known to be involved in the anaerobic oxidation of methane (AOM), similar to other cold seep features with moderate/high CH_4 flux.

(Wegener et al., 2008; Boulabassi et al., 2009; Cambon-Bonavita et al., 2009; Merkel et al., 2010; Shubenkova et al., 2010; Roalkvam et al., 2011, 2012). However, at present little is known about the effect of pockmark formation and seepage processes on microbial communities, and vice-versa about the role, if any, played by microbes in pockmark formation and seepage.

A pockmark field was discovered in Dunmanus Bay, south west Ireland, in 2007 during multibeam mapping of the bay in shallow water depths of about 40 m. Over 60 pockmarks have been mapped that reach a maximum diameter of 20 m and do not appear to exceed 1 m in depth. These pockmarks occur in clusters, possibly comprising composite features, and also small (1 to 2 m diameter) satellite features. The lithology of the bay is dominated by coarse to medium sand, while mud to fine sand is dominant closer to the mouth of the bay. The Dunmanus Bay pockmark field (DBPF) is coincident with an area of comparatively finer particle size (Szpak, 2012a). Initial surveys have highlighted that acoustic evidence of minor subsurface gas seepage is widespread across the region. However, regions of shallow (< 10 mbsf) acoustic turbidity (AT), indicating gas accumulations, are coincident with fine-grained muddy seabed occurring in the mapped pockmark field. Furthermore, subtle water column acoustic echofacies, have been observed in the DBPF, indicating low to moderate fluid seepage is occurring (Szpak, 2012a). A number of faults bisect and cross the region, and are thought to be likely routes of gas migration to shallow sediments.

However, the exact nature of the seeping fluid, its relationship with seabed lithology and the key biogeochemical processes occurring at this site have not been studied comprehensively and are poorly understood at present. The purpose of this study was to conduct a geochemical and microbiological investigation of pockmarked and non-pockmarked sediment within DBPF, and surrounding sediments in order to elucidate possible distinct chemical and physical processes within the pockmark field.

5.2 Environmental and Geological Setting

Dunmanus Bay is located in southwest Ireland, between the Sheep's Head and Mizen peninsulas (Fig. 5.1). The bay is nearly 7 km wide at its widest point and 25 km long. The Durrus River drains into the bay at Durrus. INFOMAR surveys aboard the RV Celtic Explorer mapped the outer region of Dunmanus Bay in 2006, followed by the intermediate depths in 2007 (RV Celtic Voyager). A Tenix LADS lidar survey was also conducted in 2006 and mapped the nearshore and shallow waters of the bay. Water depths range from 0 to 70 m to the southwest at the mouth of the bay. Dunmanus Bay lies in the South Munster Basin. The Dunmanus Fault runs along the centre of the Bay parallel to the landmass, whereby two minor faults, the Gortavallig Fault and the Letter Fault, occur perpendicular to the Dunmanus Fault in the vicinity of the pockmark field (Szpak, 2012a). Two other notable faults to the north west are the Rossmore Fault and the Glanlough Fault (MacCarthy, 2007). The northern part of the bay is dominated by coarse to medium sand, while mud to fine sand is dominant closer to the mouth of the bay. Localised occurrences of rock outcroppings and gravels also occur, and generally in proximity to the landmasses. Quaternary sediment thickness does not generally exceed 25 m (Monteys et al., 2010). The DBPF consists of an area of seabed of approximately 225000 m^2 and is located in proximity to the landmass (650 m east of Dooneen Point) in about 40 m water depth. Seabed in this area is dominated by mud to fine sand. For an in-depth discussion of the geological and environmental setting of Dunmanus Bay, see Szpak (2012a).

5.3 Materials and Methods

5.3.1 Core sampling

Sediment vibrocores were sampled using a GeoResources Geo-Corer 6000. Cut and capped core sections were split and archive halves photographed and logged. Sediment sub-samples were taken from working sections after gas and porewater sampling (see section 5.3.2), and stored onboard at -20^{o}C, and at -80^{o}C back in the laboratory. Sub-samples for bulk chemical and physical parameters were stored at 4^{o}C.

5.3.2 Gas and porewater analysis

Interstitial gas sampling was carried out immediately upon core retrieval. 10 mL sediment plugs were sampled from windows cut in the core liner, transferred to a 20 mL headspace vial and 1.2 M NaCl solution containing approximately 70 mg L^{-1} thimerosal (Sigma Aldrich, Dorset, UK) was then added to the vial leaving a 3 mL headspace. Sealed vials were stored in the dark at 4°C prior to analysis. CH_4 analysis was performed on an Agilent 7820A GC-FID with a 30 m HP-PLOTQ column (Agilent, Santa Clara, USA). Column conditions were isothermal (50°C). CH_4 was quantified using calibration standards prepared from a 99.995% CH_4 standard (Sigma Aldrich, Dorset, UK). Sediment porewater was sub-sampled from core liner windows using Rhizon samplers (Rhizosphere Research Products, Wageningen, NL). 1 mL aliquots for H_2S analysis were preserved by addition of 400 µL 50 mM zinc acetate. Aliquots for PO_4^{3-} and NH_4^+ analysis were preserved with 1-2 drops of chloroform. Spectrophotometric analysis of H_2S and PO_4^{3-} was performed using leucomethylene blue and phosphomolybdate complexation respectively (Grasshoff et al., 1983). Analysis was conducted on a BIOTEK Powerwave HT plate reader and calibration standards were prepared in artificial seawater prepared from commercially available sea salts (Sigma Aldrich, Dorset, UK). NH_4^+ analysis was performed using a SCHOTT NH1100 ion selective electrode and using NH_3 ISE ion strength adjustment buffer and NH_3 ISE calibration solution (Reagecon, Clare, Ireland). Calibration and quantification was performed according to manufacturer guidelines. SO_4^{2-} and Cl^- anions were determined by suppressed ion chromatography on a DX-120 Dionex Ion Chromatograph with an eluent generator (K_2CO_3) and an anion exchange column (IonPak AS18). The mobile phase was Nanopure grade water (18MΩ), which was automatically amended with hydroxide ions to a preset concentration (15 mM OH^-). The mobile phase flow was set to 1.0 ml min^{-1} and suppressor current was set to 25 mA. Data processing and peaks integration was conducted using the Chromelion software package. See Appendix C for details of gas and porewater analysis and quality control.

5.3.3 Multi sensor core logging

Duplicate cores from each station were scanned using a GEOTEK multi-sensor core logger (MSCL). Cores were scanned in split mode and bulk density, magnetic susceptibility, P-wave velocity, electrical resistivity, fractional porosity and colour

parameters were determined. Scanning was conducted at a resolution of 1 cm^{-1} after calibration according to manufacturer's guidelines (GEOTEK, Daventry, UK). Data was processed using GEOTEK MSCL software (Ver. 7.95.4).

5.3.4 Bulk physical and chemical analysis

Particle size analysis was performed using laser granulometry (Malvern MS2000) for sediment fractions <1000 μm and dry sieving for fractions >1000 μm. Percentage per size class calculated using the MS2000 were converted to total sample percentages and integrated with the >1000 μm data. Total organic carbon and total nitrogen was analysed using an Exeter Analytical CE440 elemental analyser, after oven-drying and removal of inorganic carbonate using 1M HCl. Loss-on-ignition (LOI) was determined in higher resolution by combusting 300 to 500 mg oven-dried sediment to constant weight at 440^{o}C for 8 hr in a muffle furnace.

5.3.5 DNA extraction, PCR and denaturing gradient gel electrophoresis

DNA was extracted using the POWERSOIL DNA isolation kit (MO BIO, Carlsbad, US) according to manufacturer guidelines. Bacterial and archaeal 16S rRNA PCR and DGGE was performed as outlined previously (see Chapter 3).

5.3.6 Lipid biomarker analysis

Freeze-dried powdered samples were extracted by a modified Bligh-Dyer method (White and Ringelberg, 1998) as described previously. Desulfurised TLE's weretionated and phospolipid fatty acids analysed as described previosuly (See Chapter 2 and Appendix A).

5.3.7 Data analysis

Hierarchical cluster analysis of PLFA data was performed using the software PAST (v1.75) (Hammer et al., 2001), using the Bray-Curtis similarity matrix. DGGE gels were digitised and subjected to hierarchical cluster analysis after background subtraction and band matching using the Phoretix 1D gel analysis software (Total Labs Inc., Newcastle, UK)

5.3.8 Sedimentary organic matter composition

Sediment OM was isolated according to previously described methods (Gonçalves et al., 2003; Szpak et al., 2012b). Freeze-dried sediment (~120 g accurately weighed) was extracted with deionised water (x3). OM was concentrated and ferromagnetic minerals removed by shaking samples overnight in 10% 1:1 (v/v) HCl/HF (x2), followed by 10% HF (x8). Concentrated OM was then exhaustively extracted with 0.1 M NaOH. Water and NaOH extracts were centrifuged and supernatants were filtered through 0.22 μm polyvinylidene fluoride membrane filters (Merck Millipore, Billerica, USA). Water extracts were combined and dried by rotary evaporation and stored at -80^{o}C. NaOH extracts were ion-exchanged using AMBERJET 1200H cation exchange resin to remove Na^{+} ions. NaOH extracts were subsequently freeze-dried and all extracts were desiccated for 48 hr prior to further analysis.

Each sample (40 mg) was resuspended in 1 mL of D_2O and titrated to pH 13 using NaOD (40% by wt) to ensure complete solubility. Samples were analysed using a Bruker Avance 500 MHz NMR spectrometer equipped with a $^{1}H–^{19}F–^{13}C–^{15}N$ 5mm, quadrupole resonance inverse probe (QXI) fitted with an actively shielded Z gradient. 1-D solution state ^{1}H NMR experiments were performed at a temperature of 298 K with 128 scans, a recycle delay of 3 s, 16384 time domain points, and an acquisition time of 800 ms. Solvent suppression was achieved by presaturation utilising relaxation gradients and echoes (Simpson and Brown, 2005). Spectra were apodised through multiplication with an exponential decay corresponding to 1-Hz line broadening, and a zero-filling factor of 2. Diffusion-edited (DE) experiments were performed using a bipolar pulse longitudinal encode-decode sequence (Wu et al., 1995). Scans (1024) were collected using a 1.25 ms, 52.5 gauss cm^{-1}, sine-shaped gradient pulse, a diffusion time of 100 ms, 16384 time domain points and 819 ms acquisition time. Spectra were apodised through multiplication with an exponential decay corresponding to 10 Hz line broadening and zero-filling factor of 2.

5.3.9 Porewater dissolved organic matter composition

At least 10 mL aliquots of selected porewater samples were additionally filtered through 0.22 μm PVDF membrane filters and dissolved organic matter (DOM) was subsequently preserved in sodium azide (final concentration of 0.1 %). All NMR experiments were carried out according to Lam and Simpson (2007) on a Bruker Avance 500 MHz equipped with a 5 mm ^{1}H-BB-^{13}C TBI probe with an actively shielded Z-gradient. 1D solution state 1H NMR experiments were acquired with a recycle delay of 2 s, and 32768 time domain points. Spectra were apodized by multiplication with an exponential decay producing a 10 Hz line broadening in the transformed spectrum, and a zero-filling factor of 2. Where appropriate, pre-saturation was applied on resonance generated by a 60 W amplifier attenuated at 50 dB during the relaxation delay. Direct ^{1}H NMR was performed using WATER suppression by GrAdient-Tailored Excitation (WATERGATE) and was carried out using a W5 train and a 125 μs binomial delay such that the 'sidebands' occurred at ca. 12 ppm and 2 ppm and were outside the spectral window. W5-WATERGATE was preceded by a train of selective pulses: 2000, 2 ms, calibrated π (180^{o}) pulses were used, each separated by a 4 μs delay.

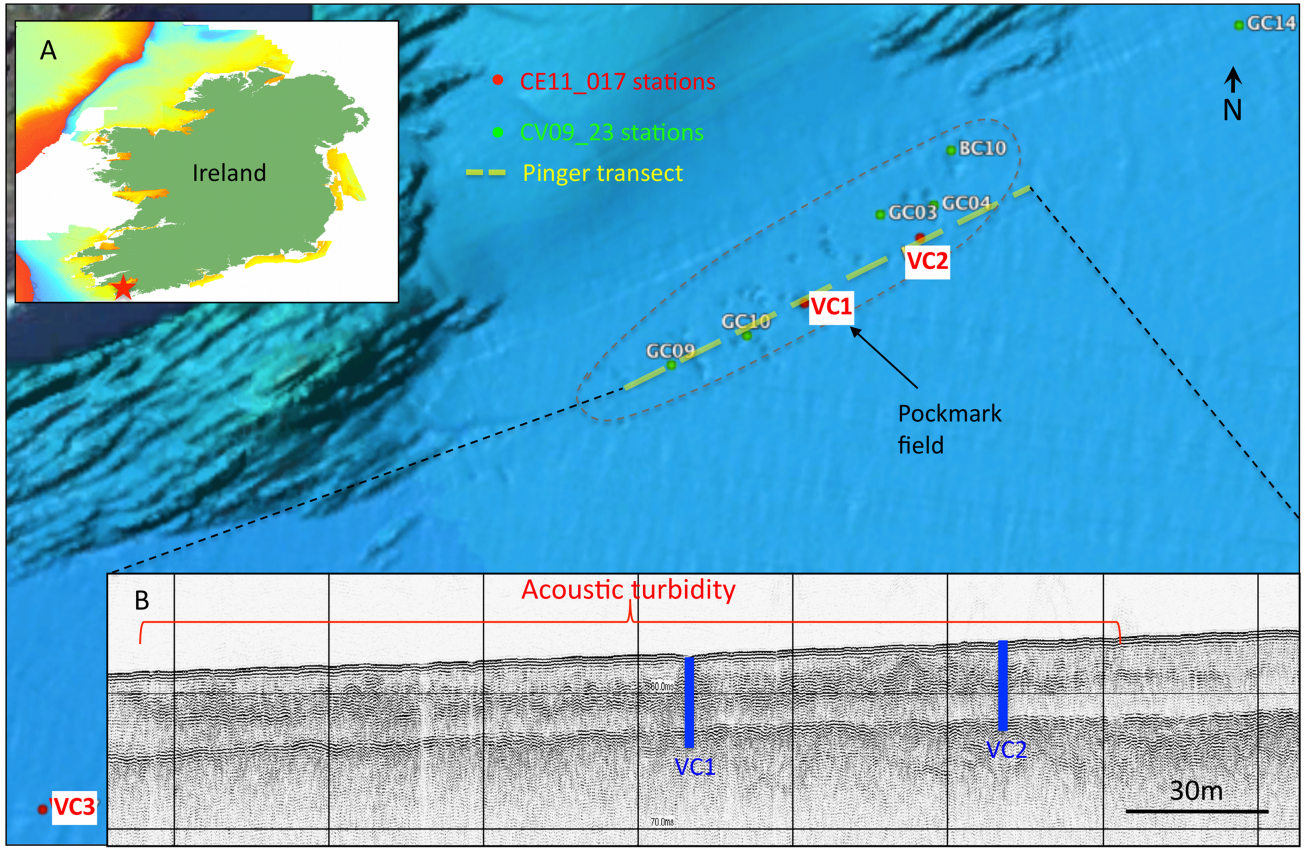

Figure 5.1. Bathymetric map of Dunmanus Bay showing the location and outline of Dunmanus Bay pockmark field. Sampling stations for the 2009 and 2011 surveys are shown. Insets: (A) Geographic location of Dunmanus Bay; (B) Sub-bottom pinger profile showing a transect across the Dunmanus Bay pockmark field (yellow dashed line). Acoustic turbidity, providing indirect evidence of gas accumulations, is evident and coincident with the pockmark field.

5.4 Results and Discussion

5.4.1 Possible lithological control on pockmark formation and geochemical processes

Downcore physical and chemical profiles for cores VC1, VC2 and VC3 are shown in Fig. 5.2, 5.3 and 5.4, respectively. Specifically, sediment class (based on percentage silt, clay and sand composition), bulk organic matter content (expressed as percentage loss-on-ignition), interstitial CH_4, SO_4^{2-}, H_2S, PO_4^{3-}, NH_4^+ and sediment porosity data are provided. Surface sediments in VC1 from 0 to 1.4 mbsf were characterised by poorly sorted mud, with silt and clay averaging 74.2% and 15.7%, respectively. From 1.4 to 1.6 mbsf sediment is characterised by very poorly sorted muddy sand to sandy mud, followed by a transition to poorly sorted/very poorly sorted sandy mud to 3.0 mbsf. Between 3.0 to 3.8 mbsf there is a gradual transition from sandy mud to muddy sand, followed by a sharp contact and a transition from sandy gravel to coarse gravel until about 4.2 mbsf. From 4.2 mbsf until 5.65 mbsf sediment consists of primarily well sorted sand. VC2 exhibits a lower clay content, higher sand content, and overall a more variable lithology in the first 2 mbsf compared to VC1. Below about 1.8 mbsf sediment type is comparable between VC1 and VC2 (Fig. 4). In contrast, the reference core VC3 displays a more homogeneous lithology over the 5.75 metres. Sediment porosity for both VC1 and VC2 was relatively low close to the SWI (~0.4), while the presence of a high porosity layer in the first 12 cm of VC3 was observed (Fig. 5.4). In all 3 cores a distinct gravel stratum was observed at about 4 mbsf. This has been identified as the source of the enhanced reflector in acoustic profiles (Fig. 5.1). Sandy sediments (and indeed gravels) are characterised by a relatively high permeability compared to mud (Wilson et al., 2008). Thus the lithology within DBPF is likely a significant factor controlling the occurrence of pockmarks within this region as opposed to the surrounding coarser-grained sediment types. Gas migration via permeable strata and accumulation in muddy layers and eventual expulsion via fluidisation of gas, water and sediment into the water column, as proposed by Judd and Hovland (1988), is thus a possible formation mechanism for pockmarks in Dunmanus Bay.

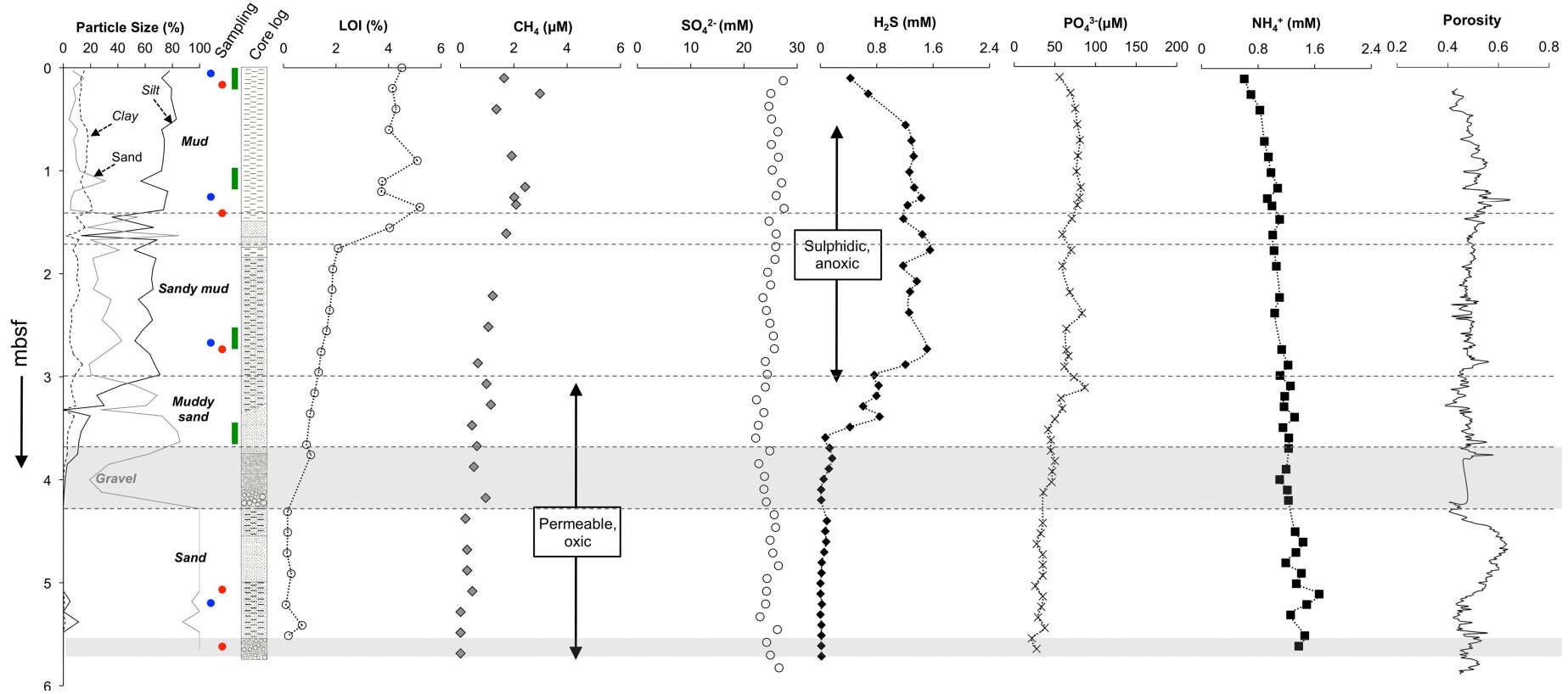

Figure 5.2. Downcore profiles of physical and chemical parameters from core VC1, sampled from within a pockmark cluster. Blue circles – Lipid and DNA sampling, red circles – porewater NMR sampling, green boxes – sedimentary NMR sampling.

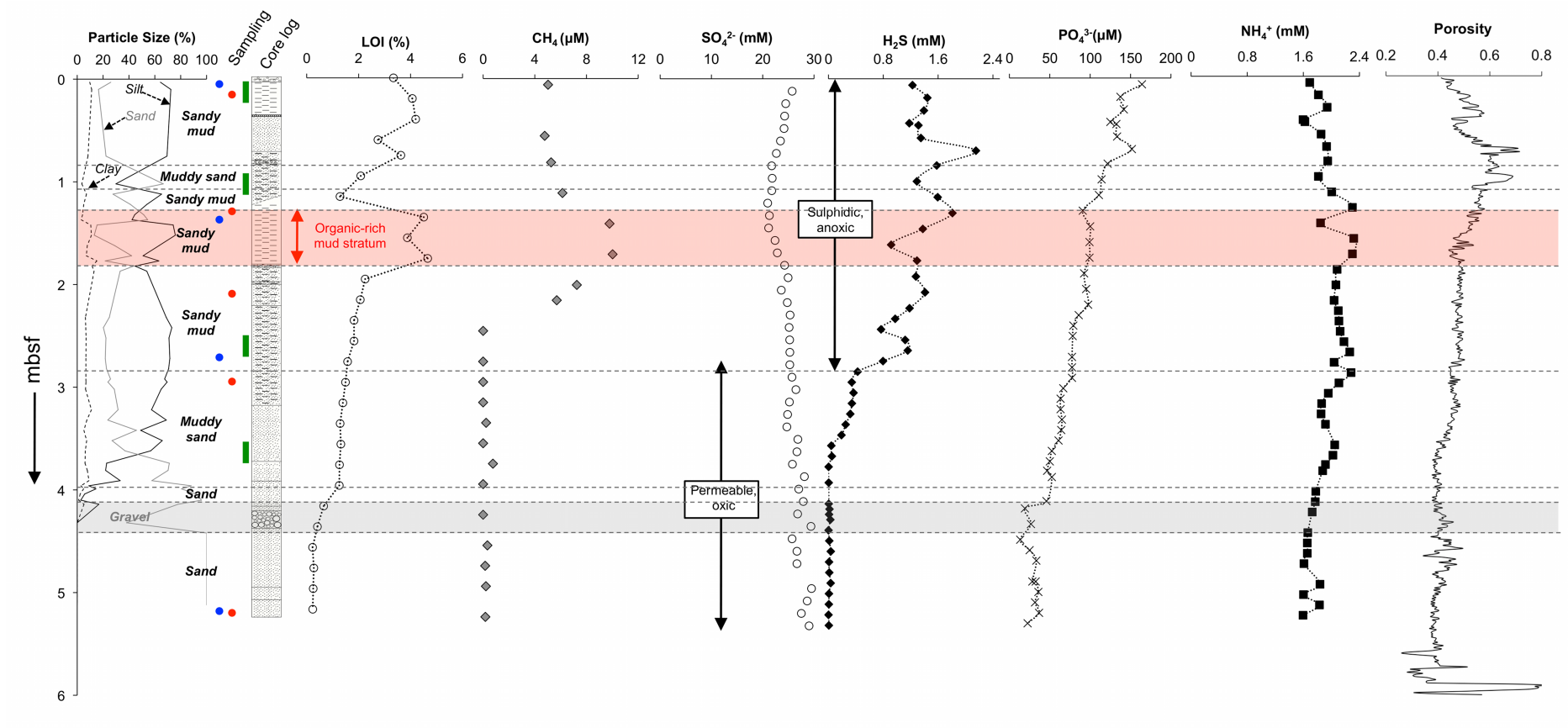

Figure 5.3. Downcore profiles of physical and chemical parameters from core VC2, sampled from acoustically-turbid non-pockmarked sediment within the Dunmanus Bay pockmark field. Blue circles – Lipid and DNA sampling, red circles – porewater NMR sampling, green boxes – sedimentary NMR sampling.

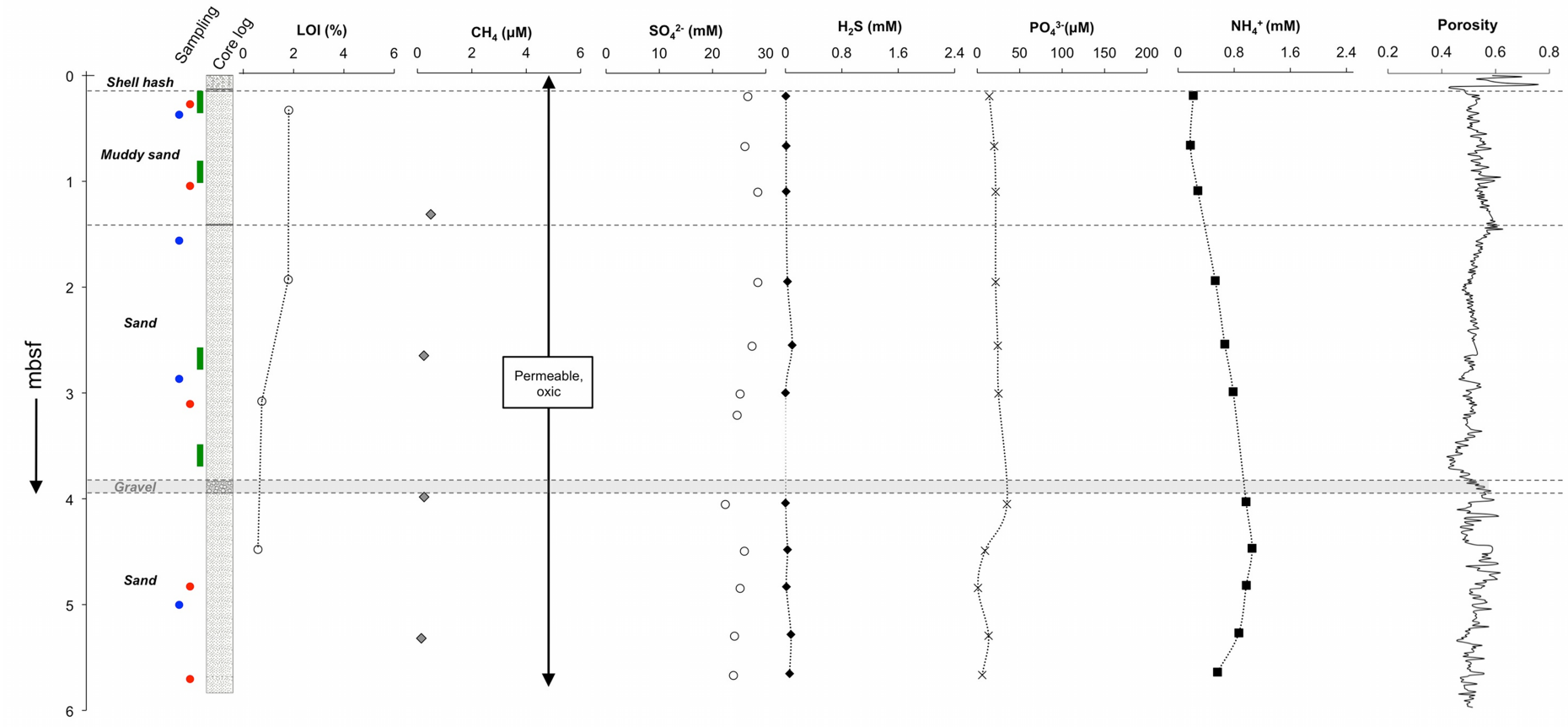

Figure 5.4. Downcore profiles of physical and chemical parameters from core VC3, sampled from representative sandy sediment in Dunmanus Bay. Blue circles – Lipid and DNA sampling, red circles – porewater NMR sampling, green boxes – sedimentary NMR sampling.

Porewater advection through permeable sediments facilitates significant sediment-water exchange of solutes and particles between sediment and the water column (Huettel et al., 1998, 2003; Huettel and Rusch, 2000). In this way permeable sands can be major controlling factors on the biogeochemistry of sediments (Santos et al., 2011, and references therein) and biogeochemical cycling can be as high or even higher than organic-rich muddy sediment types (Boudreau et al., 2001). This appears to be reflected in the porewater geochemistry, whereby H_2S concentrations were high in muddy strata in both VC1 and VC2, but rapidly depleted in deeper sediments with coarser sediment type. Concentrations up to 1.55 and 2.15 mM were measured, respectively in muddy strata. In VC1 H_2S increased linearly from less than 0.3 mM to 1.29 mM at 0.70 mbsf. An approximate plateau follows this until 2.85 mbsf, followed by a sharp decrease to negligible concentrations at 3.55 mbsf. This trend was also observed in VC2, however concentrations close to the surface were much greater (1.22 compared to 0.43 mM at 0.1 mbsf). Low micromolar concentrations of CH_4 were measured throughout the upper 3 m of sediment in upper muddy sediment strata, and were generally negligible below 3 mbsf in the sandy strata, suggesting oxidation in sandy sediments occurred (Fig. 5.2 and 5.3). CH_4 concentrations were typically 2 to 3 times greater in VC2 compared to VC1, and CH_4 was negligible in the sandy reference core (Fig. 5.4). The presence of CH_4 in appreciable levels in VC1 and VC2, while being negligible in VC3, confirms that observed AT in seismic profiles are due to gas and that accumulation in shallow surface sediment in DBPF is occurring. The presence of CH_4 close to the sediment-water interface (SWI) suggests that seepage, albeit in low amounts, is ongoing at DBPF. This is in agreement with previous observations (Szpak, 2012a).

Groundwater discharge has been highlighted as a possible formation mechanism for pockmarks (Whiticar, 2002; Christodolou et al., 2003), in particular in coastal settings. Groundwater discharge in the marine setting is driven by hydraulic gradients from coastal aquifers. In sandy high permeability settings groundwater may occur as submarine springs or seepage at the beach face (Holliday et al., 2007). Christodoulou et al. (2003) observed changes in salinity above pockmarks, together with constant water column methane profiles, to infer that seeping groundwater was the primary formation mechanism for pockmarks in the Corinth Gulf, Greece. A possible conduit for freshwater influx in the DBPF is via permeable sandy strata and gravel deposits that are present in the shallow seabed in the region. However no such

deviation in Cl^- (data not shown) or SO_4^{2-} (Fig. 5.2 to 5.4) was observed. Together with previous water column salinity profiling (Szpak, 2012a), these results support the conclusion that GD is not a formation mechanism for Dunmanus Bay pockmarks. However as found by Szpak (2012a), periodic GD, such as in times of heavy rainfall, cannot be ruled out at present.

In the absence of observable freshwater influence, the rapid depletion of H_2S and CH_4 in sandy sediments (Fig. 5.2 and 5.3) suggests oxic seawater influx may be occurring via permeable sands and gravel layers. This hypothesis is supported by the observation that SO_4^{2-} profiles increase to seawater levels from 1.57 mbsf in VC2 despite the onset of sulfate reduction in the upper metre of sediment. Similar SO_4^{2-} trends were observed in a core from the 2009 survey, whereby SO_4^{2-} reduction was apparent in the first 1 m before increasing (Szpak, 2012a). The presence of permeable sand and gravel layers may provide a conduit for the reintroduction of seawater from depth and oxidation of reduced chemical species. This may also be a possible mechanism for lateral migration of seeping gas from the below DBPF to surrounding sediments. This is one factor that might explain the subtle acoustic gas escape signatures (Szpak 2012a) and the low measured CH_4 concentrations on two surveys (CV09_23 and CE11_017). Based on the multiple analysis performed here, differences in lithology appear to be a key parameter controlling the location of pockmarks in Dunmnaus Bay and the accumulation of gas and geochemical processes at the DBPF. Microbial and geochemical processes are discussed in more details in sections 5.3.2 and 5.3.3.

5.4.2 Microbial activity and overall diversity

5.4.2.1 Porewater geochemistry, PLFAs and DGGE

NH_4^+ in sediment porewaters is derived from the microbial breakdown of marine and terrestrial organic nitrogen and is consumed in the microbial nitrification and denitrification processes that involve reduction of NO_3^- and NO_2^- to N_2. In anoxic, organic-rich marine sediments, the nitrogen transformation reactions cease at the conversion of organic nitrogen to NH_4^+ (Batley and Simpson, 2009). NH_4^+ reaches micromolar concentrations very close to the SWI for VC2, which suggests a net flux to the water column and also significant degradation of N-bearing OM. NH_4^+ displays linearly increasing trends with depth for both VC1 and VC2 (Fig. 5.2 and 5.3). Close to the SWI NH_4^+ is 2.5 times greater at VC2 compared to VC1 (0.60 mM compared to

1.69 mM at 0.1 mbsf, respectively). NH_4^+ levels in VC2 were twice that of VC1 for the first 3 mbsf before approaching comparable levels in deeper sandy sediment strata (Fig. 5.2 and 5.3). VC3 displayed a distinct profile with much lower NH_4^+ concentrations (Fig. 5.4). PO_4^{3-} in porewater reflects the microbial degradation of proteinaceous OM and also from microbial metabolism (released from ATP). PO_4^{3-} profiles for VC1 exhibited maximum concentrations around 0.7 mbsf to 1.25 mbsf, after a comparatively sharp increase from the SWI, while in contrast PO_4^{3-} profiles for VC2 exhibited maximum levels close to the SWI and a clear linear decreasing trend with depth (Fig. 5.3). These profiles indicate higher OM degradation rates and microbial activity in muddy sediments in DBPF, particularly at VC2.

Phospholipid fatty acids (PLFA) are of utility as a measure of viable sedimentary microbial biomass, both eukaryotic and bacterial (Guezennec and Fiala-Medioni, 2006; Mills et al., 2006). PLFA analysis provides broad chemotaxonomic information, for example in determining the relative abundance of algal vs. bacterial biomass or the relative abundance of gram negative vs. gram positive bacteria (White et al., 1997). PLFAs ranged from up 0.80 μg g dw^{-1} at depths close to the surface, to very low concentrations in coarse sands in the deepest section of the cores (Fig. 5.5A). This trend reflects the particle size dependence of microbial biomass in marine sediments (Jackson and Weeks, 2008). PLFA abundance was comparable between all three cores after 2.5 mbsf, but was 1.7 times higher in VC1 than VC2 and 2.7 times higher than VC3. PLFAs ranged from C_{14} to C_{24} carbons and were dominated by $C_{16:0}$ (21.6 and 30.5%). Negligible polyunsaturated fatty acids (PUFA) were observed in samples downcore, indicating a low contribution of viable eukaryotic biomass in these cores. The overall low total PLFA abundance and diversity may correspond to low viable bacterial biomass as a result of H_2S toxicity.

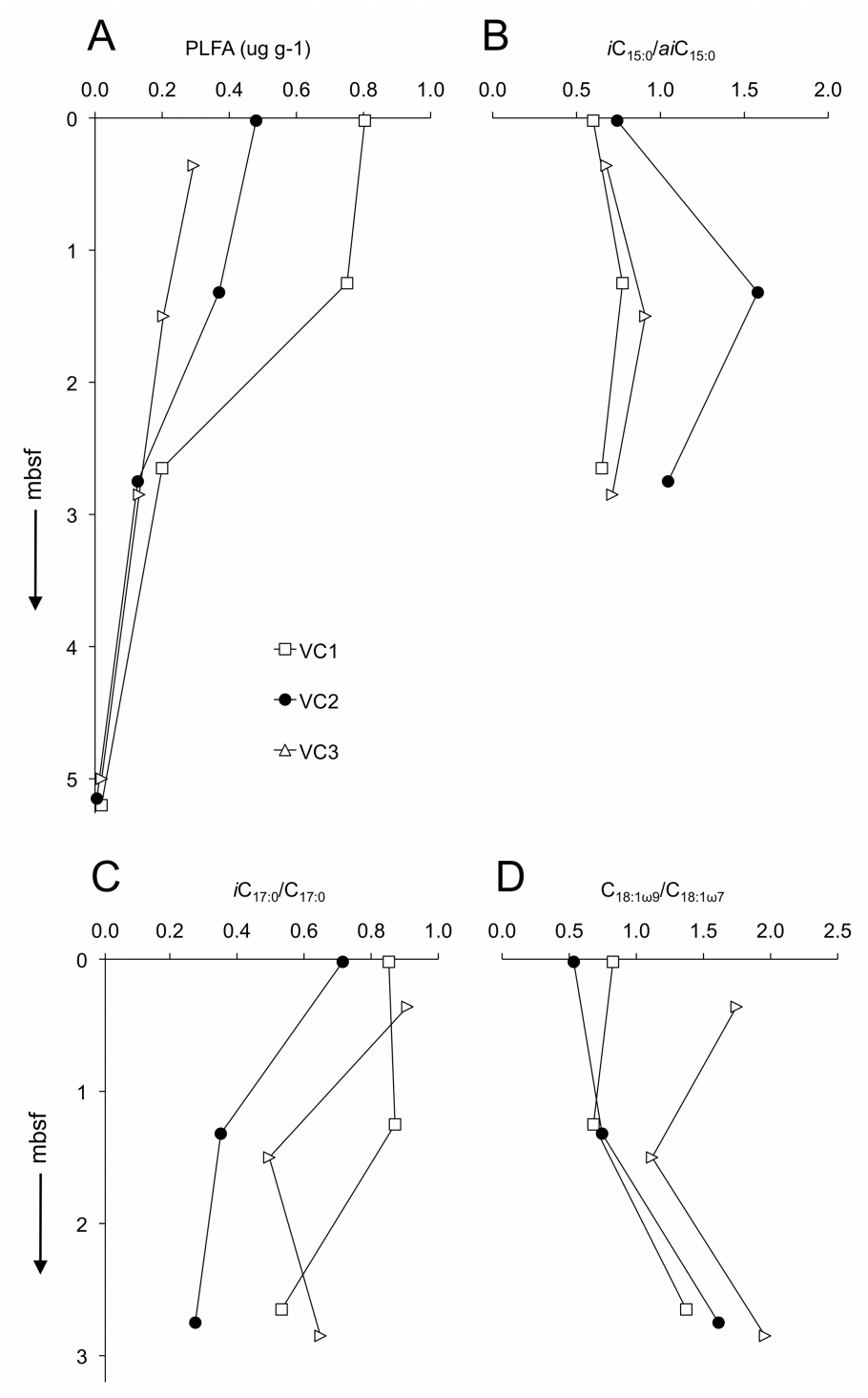

Figure 5.5. Downcore profiles of total phospholipid fatty acid (PLFA) abundances (A) and relevant PLFA ratios (B to D).

Gram-positive and anaerobic gram-negative bacteria primarily synthesise branched saturated fatty acids (brFA) while aerobic gram-negative bacteria are characterised by larger relative abundances of monounsaturated fatty acids (MUFA) (White et al., 1997). The ratio of brFA to MUFA was found to increase with depth initially in all cores, before decreasing again in sandy sediment. Assuming a predominantly bacterial source for MUFA in this setting (in the absence of PUFA), this likely reflects the increased abundance of gram-positive and anaerobic gram-negative bacteria with depth in muddy sulfidic sediments and the increased abundance of aerobic bacteria in sandy oxic sediments below muddy layers (and throughout VC3). Specific changes in relative abundances of populations within these groups are also likely and can be postulated based on relative changes in certain PLFAs. The ratio of $i\mathrm{C}_{15:0}$ to $ai\mathrm{C}_{15:0}$ was consistently higher in VC2 when compared to VC1 and VC3, in particular at 1.32 mbsf (Fig. 5.5B). The ratios of $i\mathrm{C}_{17:0}/\mathrm{C}_{17:0}$ and $\mathrm{C}_{18:1\omega9}/\mathrm{C}_{18:1\omega7}$ were also variable between cores and at different depths (Fig. 5.5C and D).

Sulfate-reducing bacteria (SRB) have consistently higher ratios of $i\mathrm{C}_{15:0}$ to $ai\mathrm{C}_{15:0}$ (Dowling et al., 1986), which suggests that SRB are more prominent in VC2 compared to VC1 and VC3. This correlates with observed SO_4^{2-} reduction in this core (Fig. 5.3). In marine sediments $10\mathrm{MeC}_{16:0}$ has often been used as a diagnostic fatty acid for the *Desulfobacter* genera (Dowling et al., 1986; Rajendran et al., 1993), although its specificity may be questionable (Boschker et al., 2001). This fatty acid did not display comparable trends with $i\mathrm{C}_{15:0}/ai\mathrm{C}_{15:0}$. While being of limited taxonomic use these ratios do provide evidence of relative changes in bacterial populations between cores and with depth in the sediment column. Further evidence for the occurrence of distinct bacterial communities in DBPF was obtained from hierarchical cluster analysis (Fig. 5.6). Two major groupings were produced, whereby populations in muddy sediment strata in VC1 and VC2 clustered together and populations from deeper sandy strata and in VC3 clustered together. Inter-cluster similarity was less than 50%. Sub-groupings were evident also, whereby populations at the surface and 1.3 mbsf in VC1 displayed 92% similarity to each other and the corresponding depths in VC2 were 84% similar.

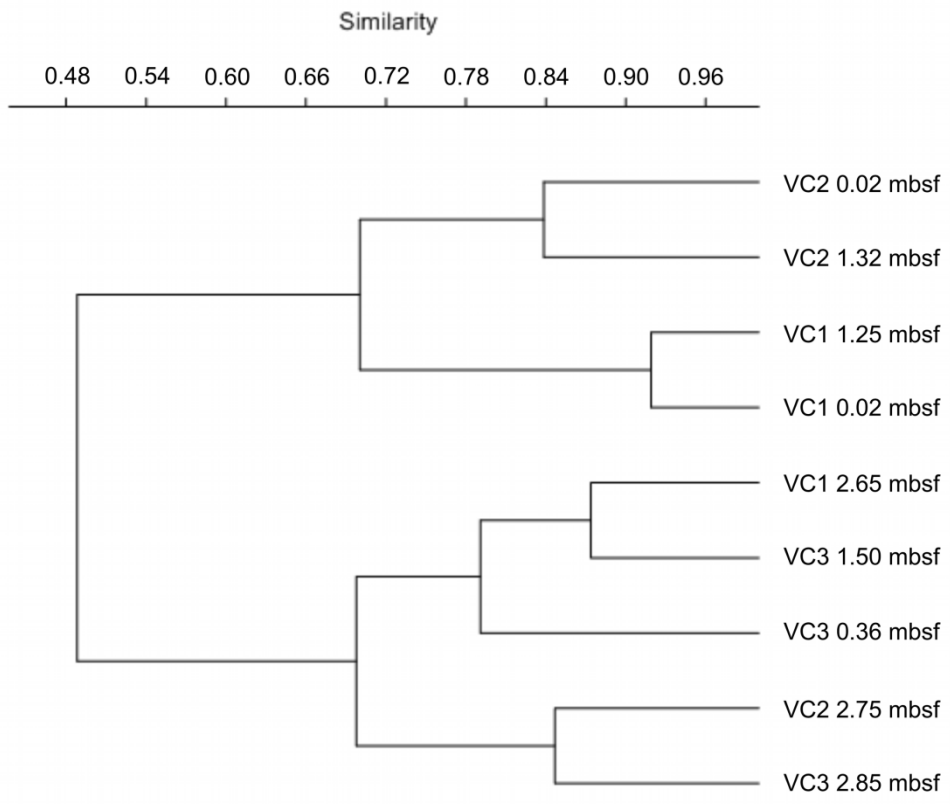

Figure 5.6. Hierarchical cluster analysis of PLFA profiles using the Bray-Curtis similarity matrix.

Cluster analysis of digitised DGGE lanes supports the conclusions drawn from PLFA interpretation. Fig. 5.7 indicates that the bacterial community close to the surface and at about 1 mbsf in VC1 and VC2 display a 75% similarity. The near-surface bacterial population in VC3 displays the highest species richness based on the number of bands present, while in comparison the cores within DBPF exhibit lower richness. The near-surface bacterial community is only 32% similar to all other samples. Whether these observed changes in bacterial biomass abundance and community structure are related primarily to lithological differences, or whether this is a result of seepage activity in the pockmark field cannot be distinguished at present. Population diversity may be expected to decrease in an active seepage setting, in particular with the presence of toxic by-products such as H_2S, such as observed here. Archaeal diversity, based on analysis of samples from 1 mbsf (including a control core GC14, sampled during survey CV09_23 in 2009) is low and indicates a very similar archaeal community structure within DBPF, and one that this is very similar to sediment outside the pockmark field (Fig. 5.8). This suggests that archaea may play a

minor role in ongoing processes at DBPF and that existing populations likely belong to extant groups in this setting rather than distinct seepage-affiliated phylotypes.

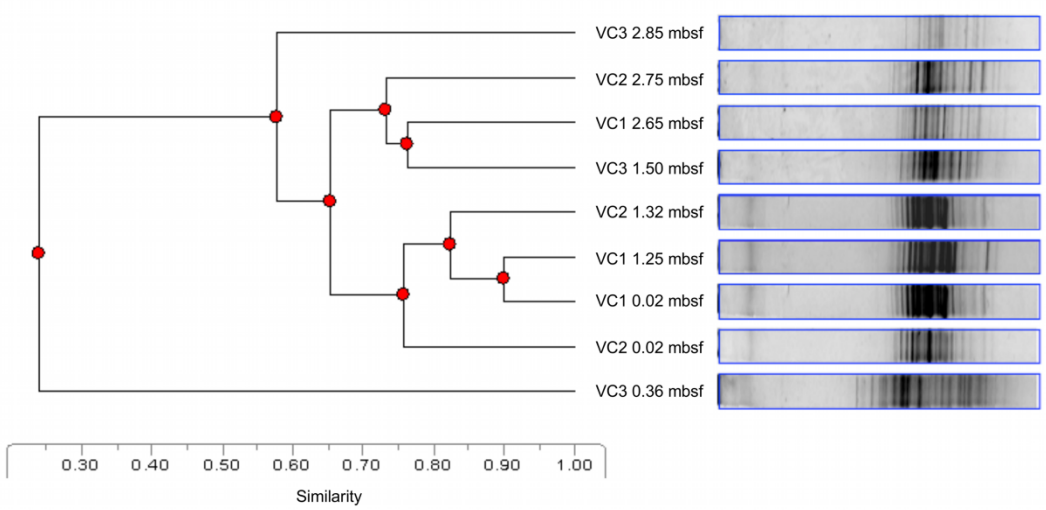

Figure 5.7. 16S rRNA bacterial denaturing gradient gel electrophoresis (DGGE) profiles and hierarchical cluster analysis.

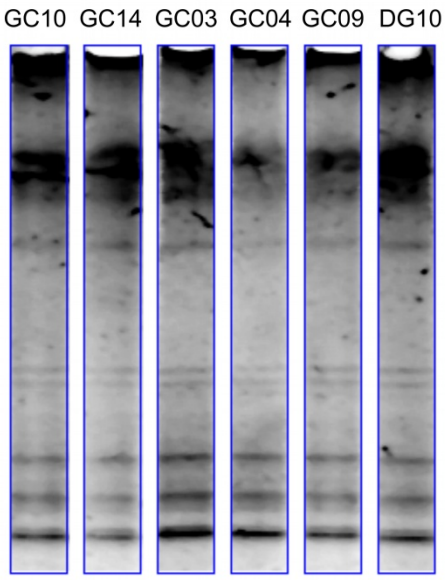

Figure 5.8. 16S rRNA archaeal denaturing gradient gel electrophoresis profiles of samples from the survey in 2009. Sampling depth for DGGE analysis was 1 mbsf. See Fig. 5.1 for locations. GC14 is the control core, taken from outside the pockmark field.

5.4.2.2 Sediment and porewater NMR

1D ^{1}H-NMR analysis of NaOH extracts enabled an overview of total OM composition and specific regions can be assigned to molecular classes in complex environmental samples (Kelleher and Simpson, 2006; Simpson et al., 2007; Simpson et al., 2011; McCaul et al., 2011; Spence et al., 2011; Szpak et al., 2012b). Protons bonding to aliphatic compounds and also signals from some amino acid side chains were identified in the 0.75 to 2.5 ppm region. Protons associated with carbohydrates and O-alkyl groups on amino acids were also identified in the 3.5 to 4.5 ppm region (Fig. 5.9). More specific assignments were protons associated with CH_3 groups in amino acid side chains (3), protons associated with methylene groups in aliphatic compounds (4) and protons associated with N-acetyl functional groups in peptidoglycan (5) (Fig. 5.9). Protons associated with naturally occurring silicates compounds were also observed (*). Based on the broad unresolved peak from 0.8 to 4.4 ppm, OM concentration is greater in VC1 and VC2 in muddy sediment strata, compared to VC3 and in deeper sandy strata. This is also reflected in bulk LOI profiles (Fig. 5.2 to and 5.3). The amount of labile OM, based on the region characteristic of carbohydrates and amino acids, decreases significantly from the surface to ~ 1 mbsf in both VC1 and VC2, while only slight differences were observed for VC3. This may be due to microbial degradation of fresh OM and supports observed porewater profiles of NH_4^+ and PO_4^3.

Protons associated with the *N*-acetylmuramic acid were based on the characteristic resonance peak for the *N*-acetyl functional group at 2.03 ppm, as previously described (Simpson et al., 2007; Szpak et al., 2012b). *N*-acetylmuramic acid is one of the primary constituents of the bacterial cell wall polymer, peptidoglycan. Peptidoglycan is a significant component of sedimentary OM in most samples and indicates a substantial contribution of bacteria-derived OM in these sediments. Peptidoglycan typically represents about 90 % of dry cell weight of Gram-positive bacteria and on average only 10% of dry cell weight of Gram-negative bacteria. However, Gram-negative bacteria are typically most abundant in both oxic (Hagström et al., 2000) and anoxic marine environments (Moriarty and Hayward, 1982). Thus most peptidoglycan in marine settings is probably derived from Gram-negative cell walls (Pedersen et al., 2001). In muddy strata the relative contribution of peptidoglycan appears to be greater in VC2 compared to VC1, while both are higher than VC3. This reflects an increased abundance of bacterial-derived OM in VC2.

Since PLFA analysis has shown that the abundance of viable bacteria, is greater in VC1 compared to VC2 (Fig. 5.5), it is likely that much of the peptidoglycan in VC2 could be derived from microbial necromass. Another possible source is from depositional input rather than *in situ* production as this polymer is chemically recalcitrant and a significant component of soil (Simpson et al., 2007), marine particulate OM (Benner and Kaiser, 2003), refractory dissolved OM (McCarthy et al., 1998; Benner and Kaiser, 2003; McCaul et al., 2011) and marine sedimentary OM (Pedersen et al., 1990; Szpak et al., 2012b).

Direct NMR analysis has, to our knowledge, not been performed on sediment porewaters, and has significant potential for elucidating microbially mediated reactions between sedimentary aqueous and solid phases. 1D water suppressed ^{1}H NMR spectra for selected depths from each core are given in Fig. 5.10. Porewater DOM should include both high and low molecular weight products of depolymerisation of detrital OM (Burdige, 2007). The broad unresolved peak from 0.8 to 4.5 ppm reflects the amount of complex DOM and comparison between the cores indicates the highest relative abundance of total DOM in VC1 and VC2 in the first 1 m approximately. The amount of DOM is comparable between cores in deeper sandy strata. This reflects the increased microbial activity and OM degradation rates observed from porewater NH_4^+ and PO_4^{3-} profiles. A range of volatile organic acids and microbial metabolic end-products were identified in porewater ^{1}H NMR spectra (Fig. 5.10). Specific assignments were leucine (1), ethanol (2), lactic acid (3), acetic acid (4), dimethyl sulphide (5), acetone (6), pyruvic acid (7), methanol (8), glycerol (9), Tyrosine, phenylalanine and formic acid (not shown). Volatile organic acids such as acetic acid, formic acid, lactic acid and pyruvic acid are considered important intermediate products of the anaerobic metabolism of higher molecular weight organics (carbohydrates, fatty acids and proteins) to CH_4 and CO_2 (Sansone and Martens, 1982; Finke et al., 2007a). Acetic acid is thought to be the primary organic substrate for SRB (Sørensen et al., 1981). These volatile organics are significant components of porewater DOM and in highest relative abundance in porewater from muddy strata in VC1 and VC2 and in agreement with porewater geochemistry, indicate significant anaerobic degradation OM in the first 1 m of sediment in both VC1 and VC2. The occurrence of dimethyl sulfide (DMS) and methanol are discussed in detail in section 5.3.3.

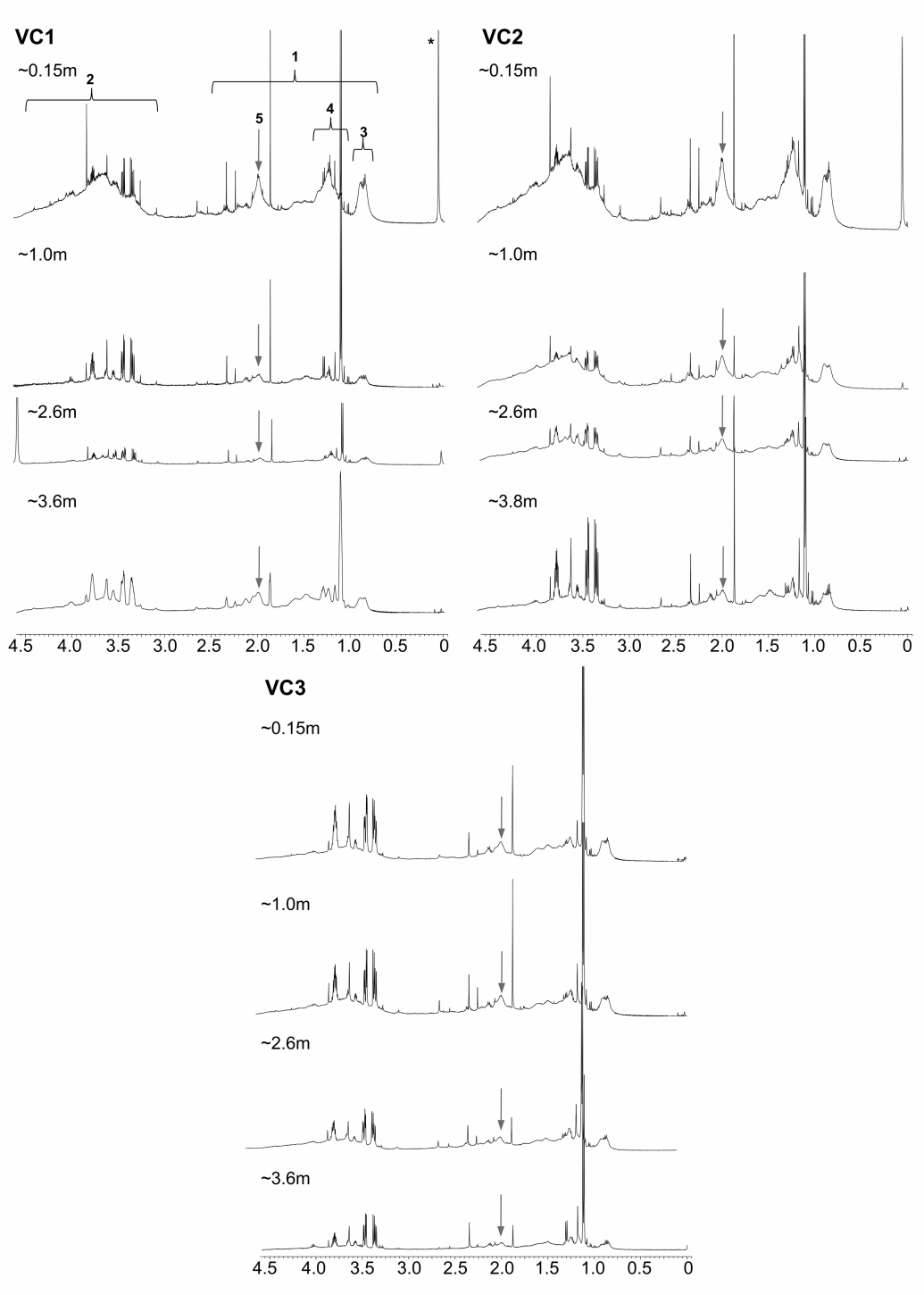

Figure 5.9. Partial 1D ^{1}H NMR spectra from NaOH extracts. General region assignments correspond to aliphatics (1) - signals from various substituted methylenes, and methanes β to a functionality in hydrocarbons (signals from some amino acid side chains will also resonate here), carbohydrates and amino acids (2) – signals from protons α to O-alkyl functional groups. More specific assignments are protons associated with CH_3 groups in amino acid side chains (3), protons associated with methylene groups in aliphatic compounds (4), protons associated with N-acetyl functional groups in peptidoglycan (5) and protons associated with naturally occurring silicates compounds (*). The grey arrow highlights the resonance peak associated with peptidoglycan.

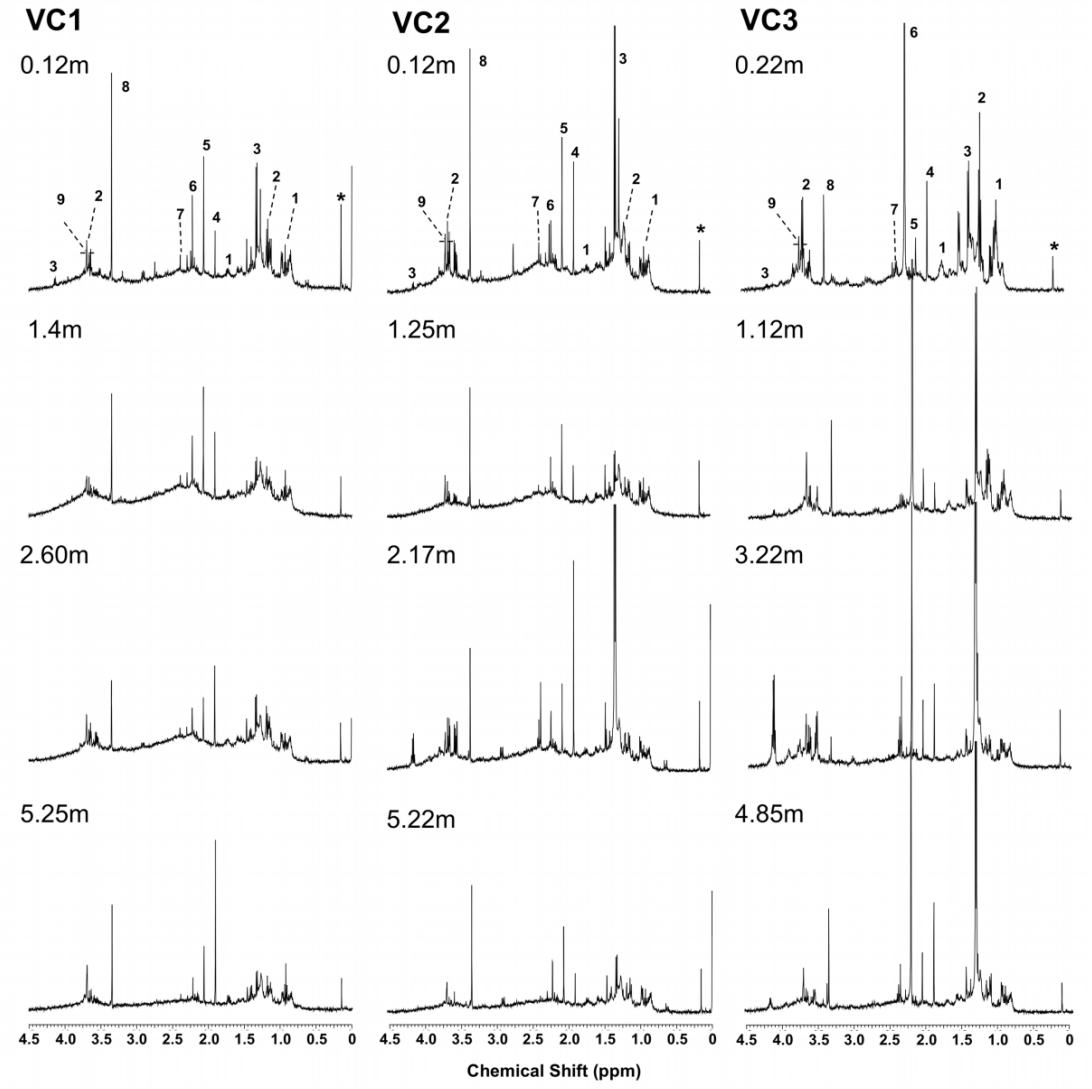

Figure 5.10. 1D water-suppressed ^{1}H NMR spectra of porewater dissolved organic matter from selected depths in VC1, VC2 and VC3. Specific assignments correspond to leucine (1), ethanol (2), lactic acid (3), acetic acid (4), dimethyl sulphide (5), acetone (6), pyruvate (7), methanol (8) and glycerol (9). Tyrosine, phenylalanine and formate were also identified in the 6.8 to 8.5 ppm region but are not included for clarity.

The results presented here suggest that distinct bacterial populations are present in muddy surface layers in acoustically turbid pockmarked and non-pockmarked sediment in DBPF. Variation in overall community composition has been observed based on relative changes in bacterial PLFAs, whereby anaerobic bacteria may be in greater abundance in VC2. The occurrence and increased relative abundance of peptidoglycan in these sediments relative to VC3 indicates an increased contribution of bacterial-derived OM, in particular in VC2. Peptidoglycan signals

most likely reflect significant bacterial necromass and/or depositional input, rather than viable bacterial biomass. Comparison of NH_4^+ and PO_4^{3-} porewater profiles and porewater DOM indicate that microbial activity and OM degradation is enhanced in the muddy sediments in VC1 and VC2, and that this is highest in non-pockmarked gassy sediments in DBPF (VC2).

5.4.3 Possible evidence for alternative sources of gas

SO_4^{2-} reduction and H_2S production in marine sediments is generally linked, whereby the utilisation of SO_4^{2-} as an electron acceptor in OM mineralisation yields reduced H_2S (Jørgensen, 1982). H_2S is typically precipitated as pyrite or else reoxidised to SO_4^{2-}. The presence of significant levels of H_2S in VC1 and VC2 in the absence of SO_4^{2-} depletion (Fig. 5.2 and 5.3) are atypical and indicates that there must be an alternative source of H_2S. In all cores fine-grained muddy strata were dominated by olive-green to grey sediment and did not exhibit highly reduced grey/black sediments typical of pyrite precipitation. Layers with significant high densities of shell hash and organic material were observed throughout the first 2 m of sediment in both VC1 and VC2. These layers were also characterised by horizontal cracking and strong sulfide odours. These coincide in a number of cases with spikes in H_2S levels (Fig. 5.3). Hence these organic-rich shelly layers are a potential source of H_2S. A possible explanation for the presence of mM concentrations of H_2S in the presence of SO_4^{2-} is the anaerobic decomposition of the sulfur-containing proteinaceous OM (Dunnette et al., 1985). In the marine environment algal and macrophyte decomposition is the most common source of proteinaceous OM (Fry, 1987).

There is some evidence that there is considerable input from dead and decaying algal biomass in DBPF. During the CV09_23 survey in 2009 a dark-coloured organic-rich sample was retrieved from a boxcore from within a pockmark cluster in the northeast of the field (Fig. 5.1, BC10). This sample exhibited a distinct putrefying odour. PLFAs were dominated by very high abundances of C_{20}, C_{22} and C_{24} polyunsaturated fatty acids, which are likely derived from eukaryotic biomass such as micro- or macroalgae (Volkman, 2006). Sterol profiles were also distinct, whereby $C_{29}\Delta^{5,24(28)}$ (fucosterol) and its isomers (Δ_5- and Δ_7-avenasterol) were present in much higher abundance compared to commonly major sterols (e.g. $C_{27}\Delta^5$ and $C_{29}\Delta^5$) (Data not shown, see appendix) . $C_{29}\Delta^{5,24(28)}$ is a major sterol in Phaeophyceae (brown algae) (Patterson, 1971). Therefore, the sediment within this pockmark may

have had a significant component of fresh and decaying macroalgal OM, probably kelp or seaweed.

DMS was identified as a major component in porewater DOM in most sub-samples analysed, in particular in the muddy strata in VC1 and VC2 (Fig. 5.10). DMS (along with methanethiol) is an important volatile component of the organic sulfur cycle and one of the most common gaseous compounds emitted from coastal marine environments (Bates et al., 1992). The major source of DMS is from degradation of organo-sulfur compounds such as dimethylsulfoniopropionate (DMSP) or sulfur-containing amino acids (Kiene, 1988; Taylor and Kiene, 1989), or from methylation of H_2S (Finster et al., 1990). DMSP is an osmolyte found in macroalgal (Sørensen, 1988) and halophilic higher plants (Finster et al., 1990). Microbial degradation of DMS and methanethiol produces CO_2 and CH_4, whereby in high concentrations CH_4 is dominant and in low concentrations CO_2 is favoured (Lyimo et al., 2009). It has also been proposed that their degradation in freshwater environments is mediated by methanogenic archaea, and predominantly produces CH_4, while in marine environments both SRB and methanogenic archaea are involved, with CO_2 being the dominant product (Lomans et al., 1997). This provides a potential metabolic route for the *in-situ* production of CH_4 in low amounts, and in the presence of SO_4^{2-}. Further evidence for a source of H_2S, other than from SO_4^{2-} reduction, was obtained from analysis of amplified and sequenced dominant bands from DGGE gels (2009 survey, data not shown). A major band present at 1 mbsf in DBPF, which was not observed in a control core (GC14) was closely related (99%) to *Dethiobacter* sp. The model representative from this genus, *Dethiobacter alkaliphilus*, is an obligately anaerobic non-sulfate reducing representative of the reductive sulfur cycle (Sorokin, 2008).

In the presence of SO_4^{2-}, SRB typically outcompete methanogens for substrates such as acetate or H_2 (Jørgensen, 1982). However, it has been shown that non-competitive substrates may be utilised by methanogens and allow methanogenesis and sulfate reduction simultaneously (Oremland and Polcin, 1982a). This has been demonstrated in a number of settings including anoxic salt marsh sediments (Oremland et al., 1982b), estuarine sediments (Oremland and Polcin, 1982a), in continental margin carbonate sediments (Mitterer et al., 2001) and active mud volcanos (Lazar et al., 2012). In addition, it has been observed that appreciable levels of CH_4 occur in SO_4^{2-} rich sediments in about one sixth of all Deep Sea Drilling Project and Ocean Drilling Project open ocean sites (D'Hondt et al., 2002). The main

non-competitive substrates known are methanol, methylamine and trimethylamine (King et al., 1983; King, 1984; Finke et al., 2007b). Methanol was a major compound in porewater DOM from VC1 and VC2, in particular in the first 1 m of sediment (Fig. 5.9). Therefore there is enough evidence to hypothesise that *in situ* production of CH_4 is occurring in DBPF via non-competitive substrate utilisation.

Assuming that the observed AT in Fig. 5.1 reflects the distribution of gas in the sediment column, it appears that gas is present in a relatively shallow layer in the first 2 m of sediment. No AT or other associated gas signatures were observed below these depths, although overlying gas and the gravel deposits could have caused signal starvation. This AT region correlates well with measured CH_4 concentrations in both VC1 and VC2. Gas is present either as a result of migration from depth or alternatively is produced *in situ*, or it may be a combination of both. The peak in CH_4 between 1.4 and 2.0 mbsf (highlighted in red in Fig. 5.3) suggests that *in situ* production is occurring at these depths. Interestingly, this region correlates well with the observed peak in total OM content, and suggests that OM degradation has a role in CH_4 production. It could be a by-product of OM degradation via DMSP and DMS. DMS is an important gaseous compound in coastal settings and could itself be a source of gas in the DBPF. Microbial production of CH_4 via DMS metabolism is also possible. Thus there appears to be multiple lines of evidence to suggest that *in situ* production of CH_4 is occurring in DBPF. These processes are possible mechanisms for *in situ* gas production and could be a source of gas and observed AT. Therefore these processes could play a role in pockmark formation in this shallow coastal setting.

5.5 Conclusions

Particle size profiles and sediment type within the DBPF exhibited clear stratification with depth, whereby fine-grained sediment is succeeded by progressively coarser strata. The occurrence of fine-grained sandy mud and mud appears to be localised to DBPF and thus this characteristic lithology may be a contributory factor to pockmark formation within DBPF and not in surrounding sediment. The occurrence of low concentrations of CH_4 in sediment strata where SO_4^{2-} was not depleted suggests that CH_4 migration from depth may be occurring. However, evidence presented here also suggests that *in-situ* production of volatile compounds such as DMS, as well as CH_4 are a possible source of gas. CH_4 production via non-competitive substrate utilisation of methanol may be occurring as well as the production of CH_4 (and CO_2) from microbial reduction of volatile sulfur compounds such as DMS. This is supported by the atypical porewater profiles whereby significant concentrations of CH_4 and H_2S are observed in the presence of SO_4^{2-}. A possible source for DMS and H_2S is from putrefactive degradation of proteinaceous macroalgal OM. Microbial activity appears to be higher within the DBPF, and in particular appears to be greater in non-pockmarked acoustically turbid sediment. Higher gas concentrations were also measured here. Thus the contribution of microbial activity to gas and pockmark formation may be underestimated, in particular in small pockmarks in shallow coastal settings.

5.6 References

Bates, T., Lamb, B., Guenther, A., Dignon, J., Stoiber, R., 1992. Sulfur emissions to the atmosphere from natural sources. Journal of Atmospheric Chemistry 1992 14, 315-337.

Batley, G.E., Simpson, S.L., 2009. Development of guidelines for ammonia in estuarine and marine water systems. Marine Pollution Bulletin 58, 1472-1476.

Benner, R., Kaiser, K., 2003. Abundance of amino sugars and peptidoglycan in marine particulate and dissolved organic matter. Limnology and Oceanography 48, 118-128.

Boschker, H., Graaf, W., Köster, M., Meyer Reil, L.A., Cappenberg, T., 2001. Bacterial populations and processes involved in acetate and propionate consumption in anoxic brackish sediment. FEMS Microbiology Ecology 35, 97-103.

Boudreau, B.P., Huettel, M., Forster, S., Jahnke, R.A., McLachlan, A., Middelburg, J.J., et al. 2001. Permeable marine sediments: overturning an old paradigm. Eos Transactions American Geophysical Union 82, 133-136.

Burdige, D.J., 2007 Preservation of organic matter in marine sediments: controls, mechanisms, and an imbalance in sediment organic carbon budgets? Chemical Reviews 107, 467-485.

Christodoulou, D., Papatheodorou, G., Ferentinos, G., Masson, M., 2003. Active seepage in two contrasting pockmark fields in the Patras and Corinth gulfs, Greece. Geo-Marine Letters 23, 194-199.

D'Hondt, S., Rutherford, S., Spivack, A.J., 2002. Metabolic activity of subsurface life in deep-sea sediments. Science 295, 2067-2070.

Dowling, N.J.E., Widdel, F., White, D.C., 1986. Phospholipid ester-linked fatty acid biomarkers of acetate-oxidizing sulphate-reducers and other sulphide-forming bacteria. Journal of General Microbiology 132, 1815-1825.

Dunnette, D.A., Chynoweth, D.P., Mancy, K.H., 1985. The source of hydrogen sulfide in anoxic sediment. Water Research 19, 875-884.

Fader, G.B.J., 1991. Gas-related sedimentary features from the eastern Canadian continental shelf. Continental Shelf Research 11, 1123-1153.

Finke, N., Vandieken, V., Jørgensen, B.B., 2007a. Acetate, lactate, propionate, and isobutyrate as electron donors for iron and sulfate reduction in Arctic marine sediments, Svalbard. FEMS Microbiology Ecology 59, 10-22.

Finke, N., Hoehler, T.M., Jørgensen, B.B., 2007b. Hydrogen 'leakage' during methanogenesis from methanol and methylamine: implications for anaerobic carbon degradation pathways in aquatic sediments. Environmental Microbiology 9, 1060-1071.

Finster, K., King, G.M., Bak, F., 1990. Formation of methylmercaptan and dimethylsulfide from methoxylated aromatic compounds in anoxic marine and fresh water sediments. FEMS Microbiology Letters 74, 295-301.

Fry, J., 1987. Functional roles of major groups of bacteria associated with detritus. In: Moriarty DJW and Pullin RSV (eds.) Detritus and microbial ecology in aquaculture. INCLARM Conference Proceedings: Philippines p83-122.

Garcia-Gil, S., 2003. A natural laboratory for shallow gas: the Rías Baixas (NW Spain). Geo-Marine Letters 23, 215-229.

Garcia-Gil, S., Vilas, F., Garcia-Garcia, A., 2002. Shallow gas features in incised-valley fills (Rıa de Vigo, NW Spain): a case study. Continental Shelf Research 22, 2303-2315.

Gay, A., Lopez, M., Ondreas, H., Charlou, J.L., Sermondadaz, G., Cochonat, P., 2006. Seafloor facies related to upward methane flux within a Giant Pockmark of the Lower Congo Basin. Marine Geology 226, 81-95.

Gonçalves, C.N., Dalmolin, R.S.D., Dick, D.P., Knicker, H., Klamt, E., Kögel-Knabner, I., 2003. The effect of 10% HF treatment on the resolution of CPMAS ^{13}C NMR spectra and on the quality of organic matter in Ferralsols. Geoderma 116, 373-392.

Grasshoff, K., Ehrhardt, M., Kremling, K., Almgren, T., 1983. Methods of seawater analysis. Wiley-VCH: Kiel, Germany

Guezennec, J., Fiala Medioni, A., 2006. Bacterial abundance and diversity in the Barbados Trench determined by phospholipid analysis. FEMS Microbiology Ecology 19, 83-93.

Hagström, Ä., Pinhassi, J., Zweifel, U.L., 2000. Biogeographical diversity among marine bacterioplankton. Aquatic Microbial Ecology 21, 231-244.

Harrington, P., 1985. Formation of pockmarks by pore-water escape. Geo-Marine Letters 5, 193-197.

Holliday, D., Stieglitz, T., Ridd, P., Read, W., 2007. Geological controls and tidal forcing of submarine groundwater discharge from a confined aquifer in a coastal sand dune system. Journal of Geophysical Research: Oceans 112, 1-10.

Hovland, M., Judd, A., 1988. Seabed pockmarks and seepages: impact on geology, biology, and the marine environment. Graham & Trotman: London.

Huettel, M., Røy, H., Precht, E., Ehrenhauss, S., 2003. Hydrodynamical impact on biogeochemical processes in aquatic sediments. Hydrobiologia 494, 231-236.

Huettel, M., Rusch, A., 2000. Transport and degradation of phytoplankton in permeable sediment. Limnology and Oceanography 45, 534-549.

Huettel, M., Ziebis, W., Forster, S., Luther, G., 1998. Advective transport affecting metal and nutrient distributions and interfacial fluxes in permeable sediments. Geochimica et Cosmochimica Acta 62, 613-631.

Jackson, C.R., Weeks, A.Q., 2008. Influence of particle size on bacterial community structure in aquatic sediments as revealed by 16S rRNA gene sequence analysis. Applied and Environmental Microbiology 74, 5237-5240.

Jørgensen, B.B., 1982. Mineralization of organic matter in the sea bed—the role of sulphate reduction. Nature 296, 643-645.

Judd, A., Hovland, M., 2007. Seabed fluid flow: the impact on geology, biology and the marine environment. Cambridge University Press: Cambridge, UK and USA.

Kelleher, B.P., Simpson, A.J., 2006. Humic substances in soils: Are they really chemically distinct? Environmental Science and Technology 40, 4605-4611.

Kelley, J.T., Dickson, S.M., Belknap, D.F., Barnhardt, W.A., Henderson, M., 1994. Giant sea-bed pockmarks: evidence for gas escape from Belfast Bay, Maine. Geology 22, 59-62.

Kiene, R.P., 1988. Dimethyl sulfide metabolism in salt marsh sediments. FEMS Microbiology Letters 53, 71-78.

King, G.M., 1984. Utilization of hydrogen, acetate, and “noncompetitive”; substrates by methanogenic bacteria in marine sediments. Geomicrobiology Journal 3, 275-306.

King, G.M., Klug, M., Lovley, D., 1983. Metabolism of acetate, methanol, and methylated amines in intertidal sediments of Lowes Cove, Maine. Applied and Environmental Microbiology 45, 1848-1853.

Knebel, H.J., Scanlon, K.M., 1985. Sedimentary framework of Penobscot Bay, Maine. Marine Geology 65, 305-324.

Lam, B., Simpson, A.J., 2007. Direct 1H NMR spectroscopy of dissolved organic matter in natural waters. Analyst 133, 263-269.

Lazar, C.S., Parkes J.R., Cragg, B.A., L'Haridon, S., Toffin, L., 2012. Methanogenic activity and diversity in the centre of the Amsterdam Mud Volcano, Eastern Mediterranean Sea. FEMS Microbiology Ecology 81, 243-254

Lomans, B.P., Smolders, A., Intven, L.M., Pol, A., Op, D., Van Der Drift, C., 1997. Formation of dimethyl sulfide and methanethiol in anoxic freshwater sediments. Applied and Environmental Microbiology 63, 4741-4747.

Lyimo, T.J., Pol, A., Harhangi, H.R., Jetten, M.S.M., Op den Camp, H.J.M., 2009. Anaerobic oxidation of dimethylsulfide and methanethiol in mangrove sediments is dominated by sulfate reducing bacteria. FEMS Microbiology Ecology 70, 483-492.

MacCarthy, I.A.J., 2007. The South Munster Basin of southwest Ireland. Journal of Maps 3, 149-172.

McCarthy, M.D., Hedges, J.I., Benner, R., 1998. Major bacterial contribution to marine dissolved organic nitrogen. Science 281, 231-234.

McCaul, M.V., Sutton, D., Simpson, A.J., Spence, A., McNally, D.J., Moran, B.W., et al. 2011. Composition of dissolved organic matter within a lacustrine environment. Environmental Chemistry 8, 146-154.

Mills, C.T., Dias, R.F., Graham, D., Mandernack, K.W., 2006. Determination of phospholipid fatty acid structures and stable carbon isotope compositions of deep-sea sediments of the Northwest Pacific, ODP site 1179. Marine Chemistry 98, 197-209.

Mitterer, R.M., Malone, M.J., Goodfriend, G.A., Swart, P.K., Wortmann, U.G., Logan, G.A., et al. 2001. Co-generation of hydrogen sulfide and methane in marine carbonate sediments. Geophysical Research Letters 28, 3931-3934.

Monteys, X., Bloomer, S., Chapman, R., 2010. Multi-frequency acoustic seabed characterisation in shallow gas-bearing sediments in Dunmanus Bay, SW Ireland. Geophysical Research Abstracts 12, EGU2010-10707-2, EGU General Assembly, Vienna.

Moriarty, D., Hayward, A., 1982. Ultrastructure of bacteria and the proportion of Gram-negative bacteria in marine sediments. Microbial Ecology 8, 1-14.

Nelson, H., Thor, D., Sandstrom, M., Kvenvolden, K., 1979. Modern biogenic gas-generated craters (sea-floor "pockmarks") on the Bering Shelf, Alaska. Geological Society of America Bulletin 90, 1144-1152.

Oremland, R.S., Polcin, S., 1982a. Methanogenesis and sulfate reduction: competitive and noncompetitive substrates in estuarine sediments. Applied and Environmental Microbiology 44, 1270-1276.

Oremland, R.S., Marsh, L.M., Polcin, S., 1982b. Methane production and simultaneous sulphate reduction in anoxic, salt marsh sediments. Nature 296, 143-145.

Patterson, G.W., 1971. The distribution of sterols in algae. Lipids 6, 120-127.

Paull, C., Ussler III, W., Maher, N., Greene, H., Rehder, G., Lorenson, T., et al., 2002. Pockmarks off Big Sur, California. Marine Geology 181, 323-335.

Paull, C., Ussler III, W., Borowski, W., 1999. Freshwater ice rafting: an additional mechanism for the formation of some high-latitude submarine pockmarks. Geo-Marine Letters 19, 164-168.

Pedersen, A.G.U., Thomsen, T.R., Lomstein, B.A., Jorgensen, N.O.G., 2001. Bacterial influence on amino acid enantiomerization in a coastal marine sediment. Limnology and Oceanography 46, 1358-1369.

Pickrill, R., 2006. Shallow seismic stratigraphy and pockmarks of a hydrothermally influenced lake, Lake Rotoiti, New Zealand. Sedimentology 40, 813-828.

Rajendran, N., Suwa, Y., Urushigawa, Y., 1993. Distribution of phospholipid ester-linked fatty acid biomarkers for bacteria in the sediment of Ise Bay, Japan. Marine Chemistry 42, 39-56.

Rogers, J.N., Kelley, J.T., Belknap, D.F., Gontz, A., Barnhardt, W.A., 2006. Shallow-water pockmark formation in temperate estuaries: A consideration of origins in the western gulf of Maine with special focus on Belfast Bay. Marine Geology 225, 45-62.

Sansone, F.J., Martens, C.S., 1982. Volatile fatty acid cycling in organic-rich marine sediments. Geochimica et Cosmochimica Acta 46, 1575-1589.

Santos, I.R., Eyre, B.D., Huettel, M., 2011. The driving forces of porewater and groundwater flow in permeable coastal sediments: A review. Estuarine Coastal andShelf Science 98, 1-15.

Simpson, A.J., Brown, S.A., 2005. Purge NMR: effective and easy solvent suppression. Journal of Magnetic Resonance 175, 340-346.

Simpson, A.J., McNally, D.J., Simpson, M.J., 2011. NMR spectroscopy in environmental research: from molecular interactions to global processes. Progress in Nuclear Magnetic Resonance Spectroscopy 58, 97-175.

Simpson, A.J., Simpson, M.J., Smith, E., Kelleher, B.P., 2007. Microbially derived inputs to soil organic matter: are current estimates too low? Environmental Science and Technology 41, 8070-8076.

Sørensen, J., 1988. Dimethylsulfide and methane thiol in sediment porewater of a Danish estuary. Biogeochemistry 6, 201-210.

Sørensen, J., Christensen, D., Jørgensen, B.B., 1981. Volatile fatty acids and hydrogen as substrates for sulfate-reducing bacteria in anaerobic marine sediment. Applied and Environmental Microbiology 42, 5-11.

Sorokin, D.Y., Tourova, T., Mußmann, M., Muyzer, G., 2008. *Dethiobacter alkaliphilus* gen. nov. sp. nov., and *Desulfurivibrio alkaliphilus* gen. nov. sp. nov.: two novel representatives of reductive sulfur cycle from soda lakes. Extremophiles 12, 431-439.

Spence, A., Simpson, A.J., McNally, D.J., Moran, B.W., McCaul, M.V., Hart, K., et al., 2011. The degradation characteristics of microbial biomass in soil. Geochim Cosmochim Acta 75, 2571-2581.

Szpak, M., 2012a. Chemical and physical dynamics of marine pockmarks with insights into the organic carbon cycling on the Malin Shelf and in the Dunmanus Bay, Ireland. Unpublished Thesis Chapter, accessed online 11/2012 (http://doras.dcu.ie/17524/)

Szpak, M., Monteys, X., O'Reilly, S., Simpson, A., Garcia, X., Evans, R.L., et al. 2012b. Geophysical and geochemical survey of a large marine pockmark on the Malin Shelf, Ireland. Geochemistry Geophyics and Geosystems 13, 1-18.

Taylor, B.F., Kiene, R.P., 1989. Microbial metabolism of dimethyl sulfide. Biogenic sulfur in the environment. American Chemical Society ACS Symposium Series Vol. 393.

Ussler, W., Paull, C.K., Boucher, J., Friederich, G., Thomas, D., 2003. Submarine pockmarks: a case study from Belfast Bay, Maine. Marine Geology 202, 175-192.

Volkman, J.K., 2006. Lipid markers for marine organic matter. In: Volkman, J.K. (Ed.), 2006. Marine Organic Matter: Biomarkers, Isotopes and DNA. Springer-Verlag:Berlin p27-70.

White, D.C., Ringelberg, D.B., 1998. Signature lipid biomarker analysis. In: Burlage, R.A., Atlas, R., Stahl, D., Geesey, G., Sayler, G. (Eds.). Techniques in microbial ecology. Oxford University Press. New York p255-272.

White, D.C., Ringelberg, D.B., Macnaughton, S.J., Srinivas, A., David, S., 1997. Signature Lipid Biomarker Analysis for Quantitative Assessment In Situ of Environmental Microbial Ecology. In: Eganhouse, R.P., (Ed.) Molecular markers in environmental chemistry. American Chemical Society, ACS Symposium Series 671 p22-34.

Whiticar, M.J., 2002. Diagenetic relationships of methanogenesis, nutrients, acoustic turbidity, pockmarks and freshwater seepages in Eckernförde Bay. Marine Geology 182, 29-53.

Wilson, A.M., Huettel, M., Klein, S., 2008. Grain size and depositional environment as predictors of permeability in coastal marine sands. Estuarine Coastal and Shelf Science 80, 193-199.

Wu, D., Chen, A., Johnson, C.S., 1995. An improved diffusion-ordered spectroscopy experiment incorporating bipolar-gradient pulses. Journal of Magnetic Resonance A 115, 260-264.

Chapter 6

Final Conclusions and Future Work

The data presented in this thesis provides a significant advance in knowledge regarding the source and fate of different forms of organic matter in the Irish marine environment, and also provides an important contribution to the field internationally. The scientific output to date, in terms of peer-reviewed publications, reports and presentations at national and international conferences have been significant, and there is potential for a number of additional publications from this thesis. The learning outcomes have also been many, and significant expertise has been obtained in a variety of disciplines, including: marine survey planning, design and implementation; trace organic analysis; chemical instrumentation; compound specific stable isotope analysis; molecular ecological tools (PCR, DGGE, phylogenetic analysis); statistical analysis and geographical mapping of spatial data; and independent research, time management and research collaboration.

To our knowledge, the data presented in Chapter 2 comprises the first report of the sources and distribution of organic matter (OM) in the Irish Sea, as well as the first comprehensive biomarker study in the region. The multi-biomarker approach, combined with mapping and statistical analysis of biomarkers, and bulk physical and chemical parameters, is a powerful approach for studying processes in marine OM cycling. This study highlighted a distinct distribution and relative abundance of a number of key lipid classes both in surface sediments and in the water column. The occurrence and relative abundances of diagnostic phospholipid fatty acids (PLFA), sterols and wax esters indicated that diatom, zooplankton and dinoflagellates are among the major plankton groups present and are an important component of the spring and summer bloom. The distribution and relative abundance of these characteristic biomarkers in sediment and plankton net tows suggests that the distribution of the planktonic species may be controlled by the distinct hydrographic and depositional conditions that exist in the Irish Sea. Lipids derived from terrestrial OM are a significant component of sedimentary organic matter (SOM) and are likely derived from riverine input. These lipids, and hence terrestrial input from major rivers along the coast, may be transported to and preferentially deposited in fine-grained coastal sediments at regions of low tidal energies.

Molecular characterisation of OM in sediment trap studies, over extended time periods, is an attractive avenue for future work and could provide significant information regarding the spatial and temporal cycling of difference compartments of marine OM in the Irish Sea. Additionally, studies of microbial diversity in the Irish

Sea are sparse and have focused on diversity associated with contaminated sites or associated with marine animals. Thus little is known about extant microbial diversity and what roles they may play in the regional ecosystem. Indeed this is a key area of research internationally. It is hypothesized that marine microbial biomass and diversity may also exhibit distinct variability in this setting that may be related to broader hydrographic and depositional conditions. An in-depth analysis of bacterial community structure using phylogenetic analysis of 16S rRNA clone libraries or tagged pyrosequencing is a clear avenue for future

Chapter 3 presented results from one of the few ground-truthing exercises conducted at the Codling Fault Zone (CFZ) mound features in the Irish Sea. This study reported the second documented active seepage from one of the mound features and it appears that the suggestion by Croker et al. (2005) that the CFZ is the most active site of CH_4 seepage in the Irish Designated Seabed Zone of the Irish Sea holds at present. This study also provided a geochemical investigation of recovered hard grounds and confirmation that these extensive mound features are in fact methane-derived authigenic carbonates (MDAC). Underwater towed video (UWTV) ground-truthing suggested that much of these features are buried or only semi-exposed. However, extensive nodules and stacked pavements were recorded as well as numerous patches of anoxic seabed and high densities of fossil tube worms. These tube worms likely belong to opportunistic colonisers of hard grounds, such as *Sabellaria spinulosa*, rather than the more exotic seep-associated *Siboglinid* polychaetes. This stands to reason as these seep-associated fauna have not been found in shallow (shelf and coastal) active cold-seeps, and are largely restricted to deep-sea sites. Investigation of bacterial PLFAs and bound fatty acids associated with retrieved cemented sands indicated that bacterial biomass is largely reliant on detrital input rather than CH_4 supply. This may be expected as this is a productive shallow setting and OM input from photosynthesis likely dilutes input from seabed seepage. This view was supported by the low abundance of neutral archaeal biomarkers, and by the observation that bacterial diversity may be very similar to surrounding surface sands, based on denaturing gradient gel electrophoresis (DGGE) profiling. DGGE did suggest however, that archaeal diversity was enhanced and distinct in the cemented sands.

Microbial populations within active seep settings show considerable variability over the metre or even centimetre spatial scales. Thus, further surveys

utilising a remotely-operated vehicle (ROV) would be particularly important in further ground-truthing and accurately locating sites of active seepage. An in-depth phylogenetic investigation of archaeal and bacterial community diversity from a localized site of active seepage would be a significant step forward to elucidating the key microbial players mediating anaerobic oxidation of methane (AOM). In addition, a more advanced biomarker approach using intact polar lipids (IPLs), such as intact archael glyceryl dialkyl glyceryl tetraethers (GDGTs) could reveal the microbial populations involved in CH_4 cycling at the CFZ MDAC mounds. The setting of these mounds, being approximately 30 km from Dublin Bay and in water depths averaging about 100 m, mean this site holds considerable potential future research opportunities.

Chapter 4 applied molecular ecological tools such as DGGE and phylogenetic analysis of 16S rRNA clone libraries to a core taken from within a pockmark in the Malin Sea, NW Ireland. Previous findings from our research group have indicated that this large composite pockmark is likely dormant in terms of active seepage to the water column. In agreement with these findings, the microbial community was not dominated by known microbes involved in methane cycling. The same conclusion is also suggested based on DGGE sequencing of archaeal 16S sequences. *Psycrobacter* and *Sulfitobacter* genera have been reported regionally and in similar settings and appear to be dominant in this pockmark. The apparent dominance of these genera, as well as the presence of other groups e.g. *Alcanivorax*, suggests that a population suited to aliphatic and aromatic hydrocarbon degradation is present. Previous work has shown that an active fluid system may be present at about 20 metres below the seabed and migration to sediments around the pockmark itself could be occurring. Thus, investigating this phenomenon from a geochemical and microbiological perspective is one avenue of future work. In addition, the Malin Sea is populated by dozens of pockmarks and areas of shallow gas. Besides work from our research group (and collaborators), the region has received little to no attention from the scientific community. Therefore, further exploratory surveys equipped to conduct in-depth gas and pore-water geochemical analysis and microbial analysis would be beneficial.

This project has demonstrated the need for multi-disciplinary and collaborative research in modern marine and environmental studies. The importance of proper design, planning and implementation of marine surveys in order to address relevant and sound scientific hypotheses cannot be overemphasised. Due to the very nature and cost of marine research, errors made at the initial stage can hinder and limit

the quality of scientific outcomes. This has been one of the primary learning outcomes from this project and as can be seen here successive surveys and studies in this project were more ambitious and resulted in research of a high standard. Chapter 5 combined a range of analysis including particle size, porosity, pore water geochemistry, sedimentary and pore water dissolved OM characterisation, phospholipid analysis and DGGE profiling of bacterial 16S rRNA genes in the Dunmanus Bay pockmark field (DBPF) pockmark. Particle size profiles and sediment type within the DBPF are distinct from the surrounding seabed outside the field. Cores from with the pockmark field exhibited clear stratification with depth, whereby fine-grained sediment is succeeded by progressively coarser strata. The occurrence of fine-grained sandy mud and mud appears to be broadly localised to DBPF and thus this characteristic lithology may be a contributory factor to pockmark formation within DBPF and not in surrounding sediment. The occurrence of low concentrations of CH_4 in sediment strata where SO_4^{2-} was not depleted suggests that CH_4 migration from depth may be occurring. However, evidence from a number of techniques presented here also suggests that *in-situ* production of volatile compounds such as dimethyl sulfide (DMS), as well as CH_4 are a possible source of gas. CH_4 production via non-competitive substrate utilisation of methanol was found to be a major component of pore water dissolved OM in muddy strata. The production of CH_4 (and CO_2) from the microbial reduction of volatile sulfur compounds such as DMS is also possible. This hypothesis is supported by the atypical pore water profiles whereby significant concentrations of CH_4 and H_2S are observed in the presence of SO_4^{2-}. A possible source for DMS and H_2S is from putrefactive degradation of proteinaceous macroalgal OM. Sedimentary NMR highlighted the presence of labile OM. Microbial activity appears to be higher within the DBPF, and in particular appears to be greater in non-pockmarked acoustically turbid sediment. Higher gas concentrations were also measured here. Thus the contribution of microbial activity to gas and pockmark formation may be underestimated, in particular in small pockmarks in shallow coastal settings.

This study has produced a significant dataset. The next step would be to conduct an in-depth characterisation of bacterial and archaeal diversity using 16S rRNA clone library construction or pyrosequencing. The analysis of more advanced lipid biomarkers for specific microbial groups i.e. bacteriohopanpolyols (aerobic methane oxidising bacteria) and GDGTs (archaea) inside and outside the DBPF and at

different depths downcore, may also be advantageous. Knowledge regarding what microorganisms are present and dominant in particular physical and geochemical zones may provide information as to what biogeochemical processes are occurring in DBPF. DBPF is an active micro-seepage setting, located less then a kilometre offshore and in water depths not exceeding 40 m. Thus the potential of this site as a 'natural laboratory' is clear. Regular visual monitoring with UWTV or ROV and indeed SCUBA investigation is clearly achievable in this setting. Deployment of seabed, water column and atmospheric sensors to monitor the flux of CH_4 and other chemical species over a range of timescales is one future research direction that could address questions of temporal and spatial variation in gas seepage from pockmarks.

Appendices

Appendix A: GC-MS analyte quantification

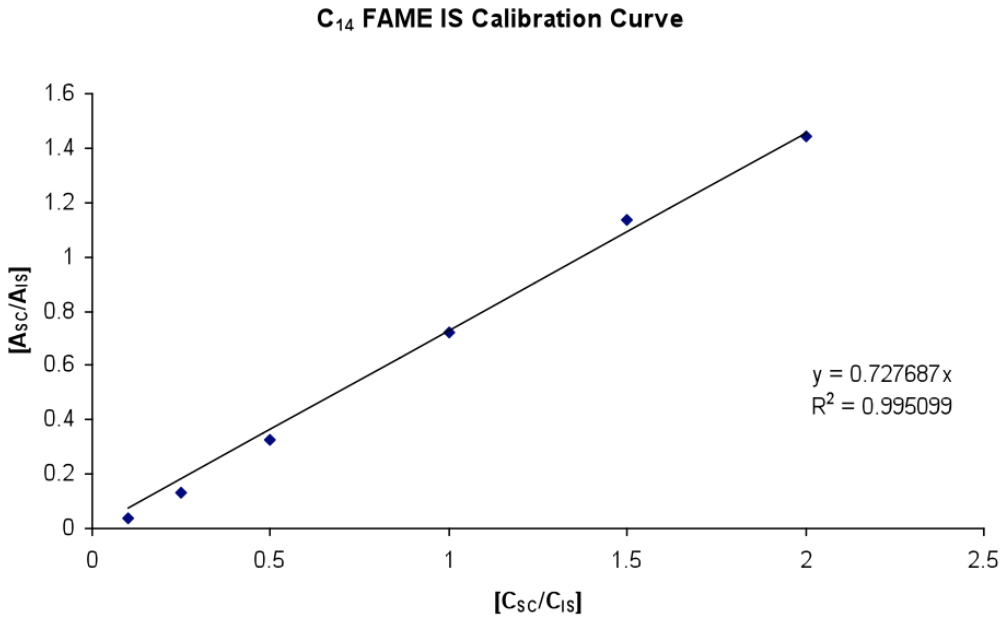

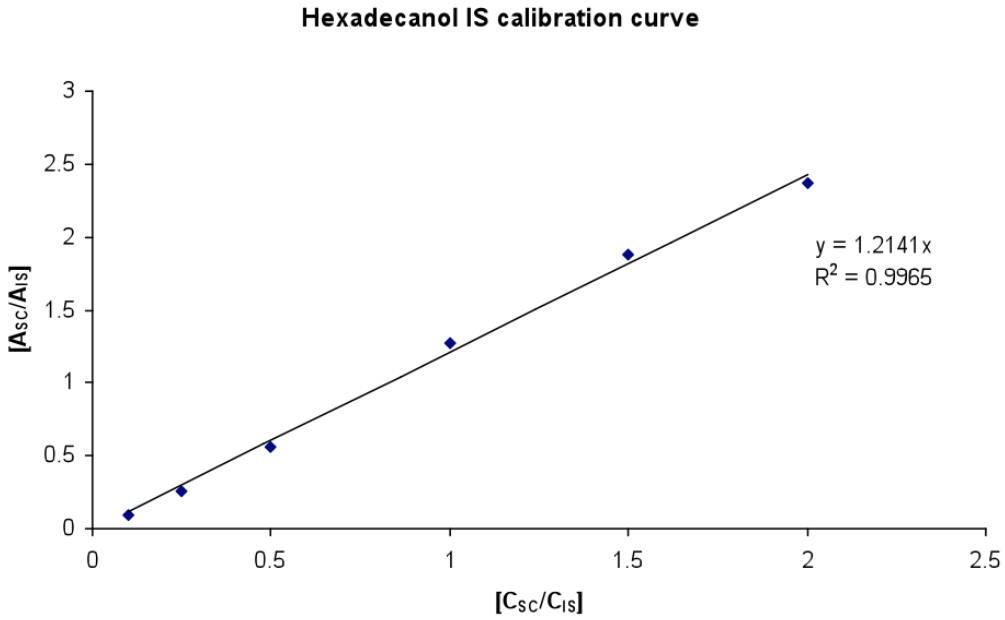

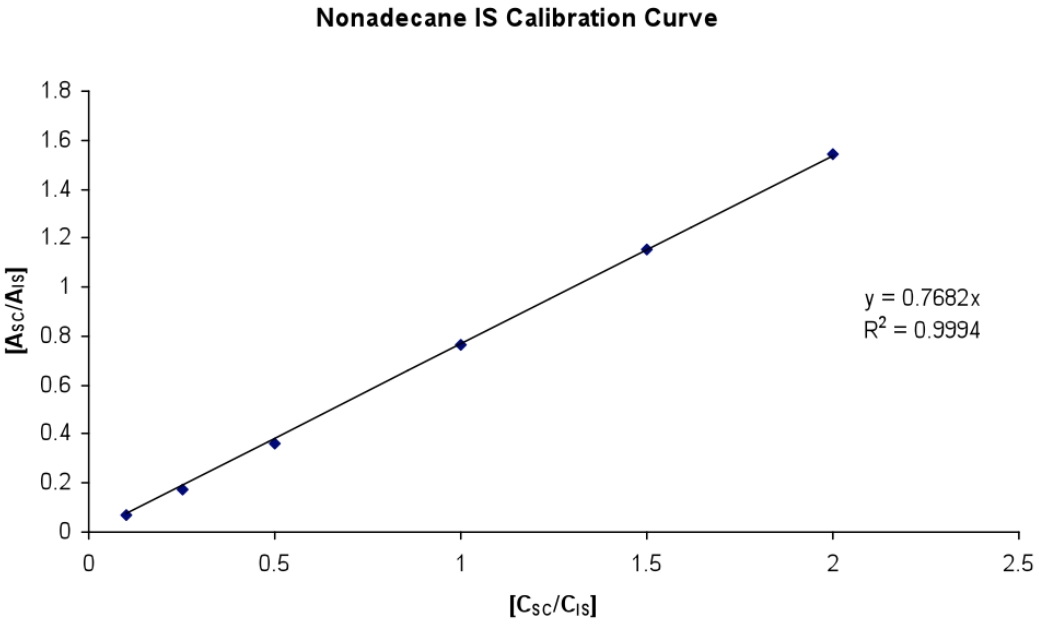
Nonadecane IS Calibration Curve
[ASC/AIS]
[CSC/CIS]
y = 0.7682x
R2 = 0.9994
0
0.2
0.4
0.6
0.8
1
1.2
1.4
1.6
1.8
0
0.5
1
1.5
2
2.5

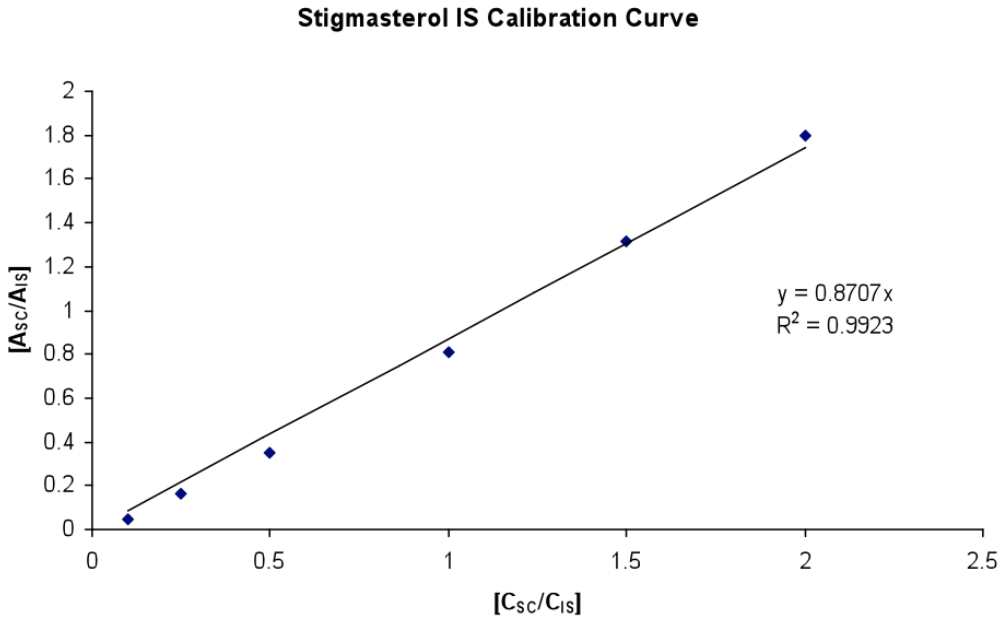
Stigmasterol IS Calibration Curve
[ASC/AIS]
[CSC/CIS]
y = 0.8707x
R2 = 0.9923
0
0.2
0.4
0.6
0.8
1
1.2
1.4
1.6
1.8
2
0
0.5
1
1.5
2
2.5

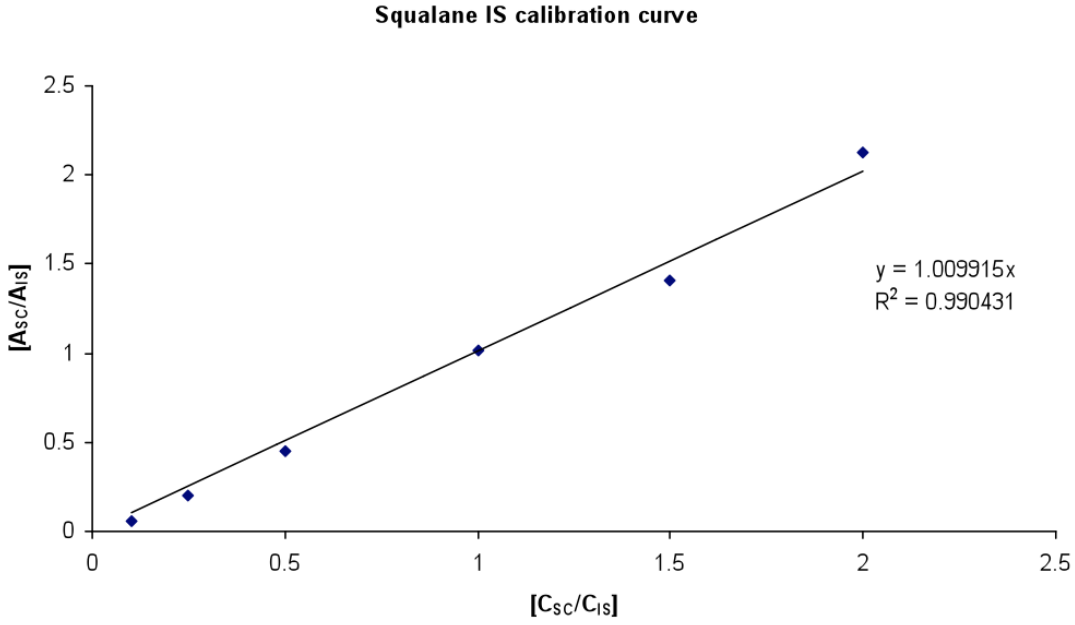
Squalane IS calibration curve
[Asc/Ais]
[Csc/Cis]
y = 1.009915x
R2 = 0.990431
0
0.5
1
1.5
2
2.5

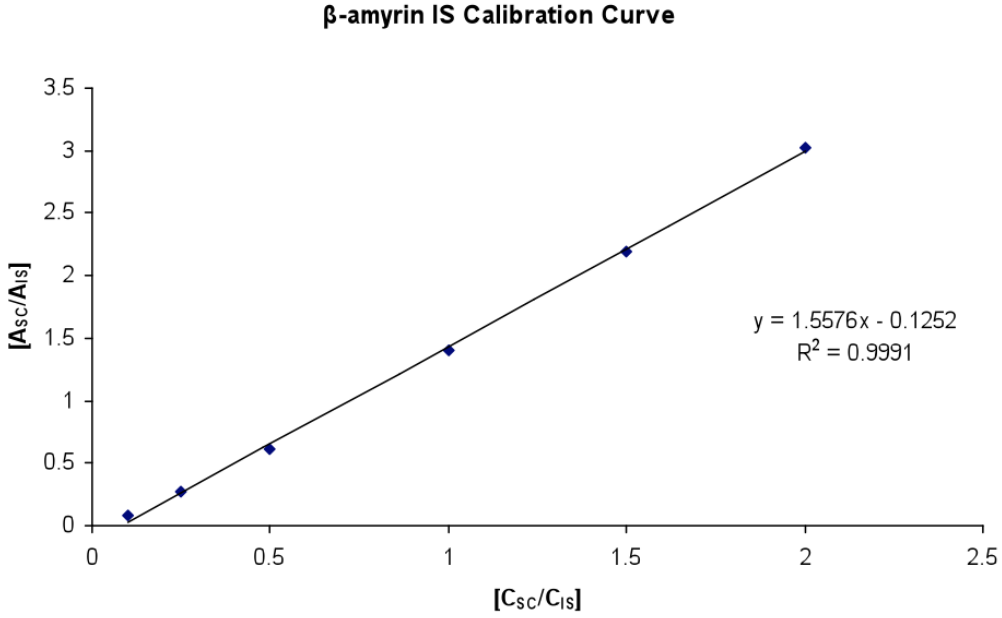
β-amyrin IS Calibration Curve
[Asc/Ais]
[Csc/Cis]
y = 1.5576x - 0.1252
R2 = 0.9991
0
0.5
1
1.5
2
2.5
3
3.5

Appendix B: Isoprime GC-MS/irMS setup and quality control

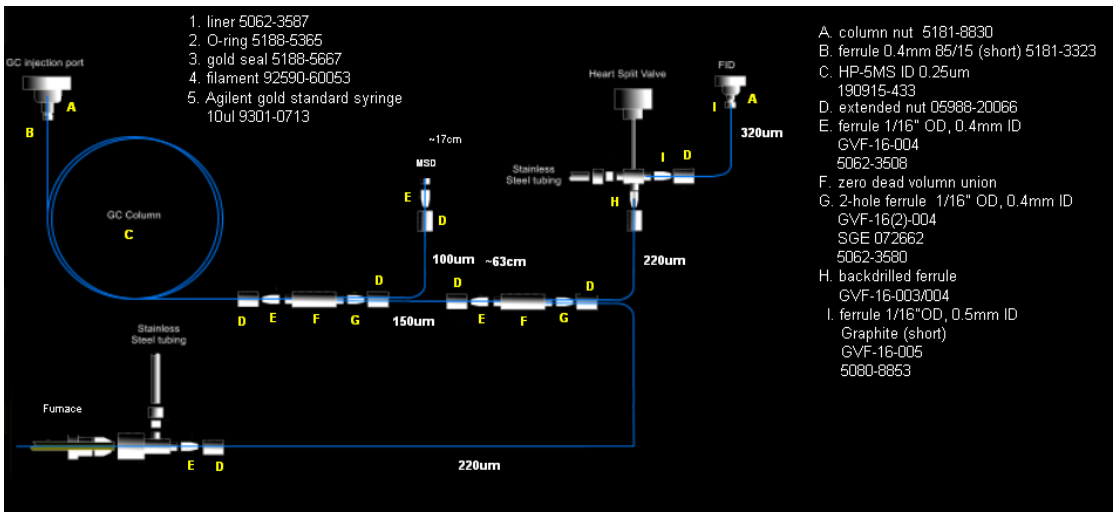

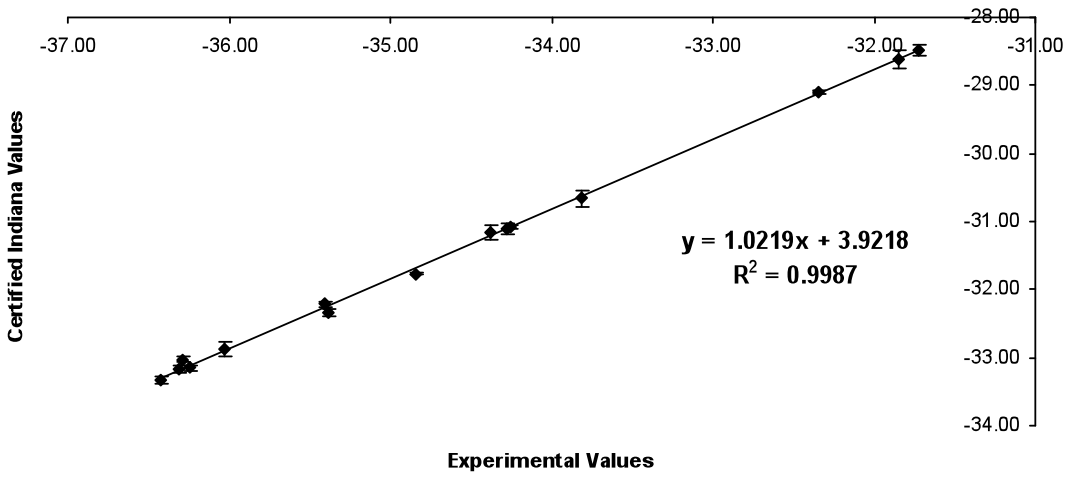

Appendix C: Gas and porewater analysis quality control

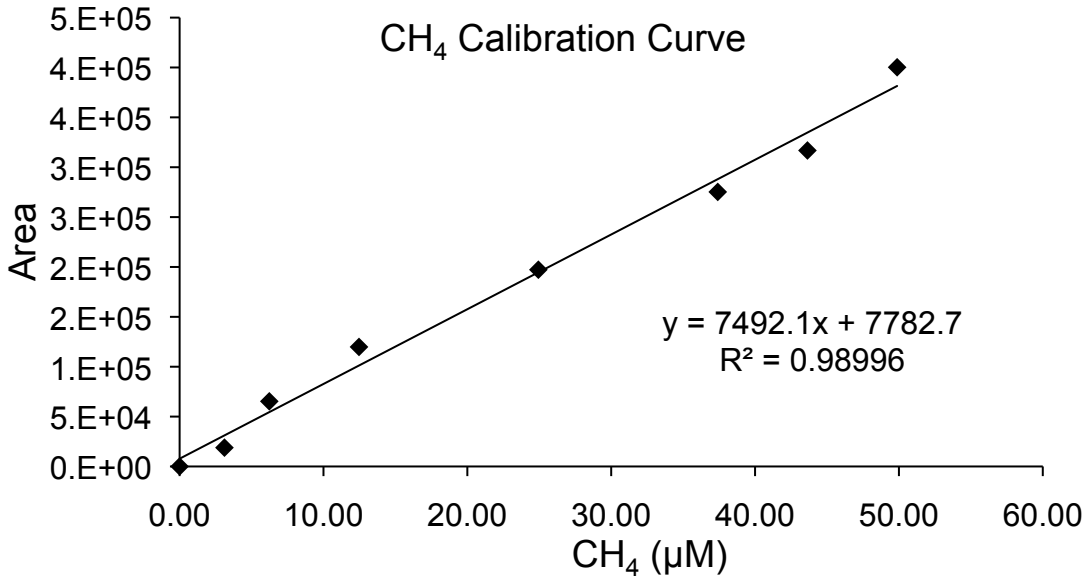

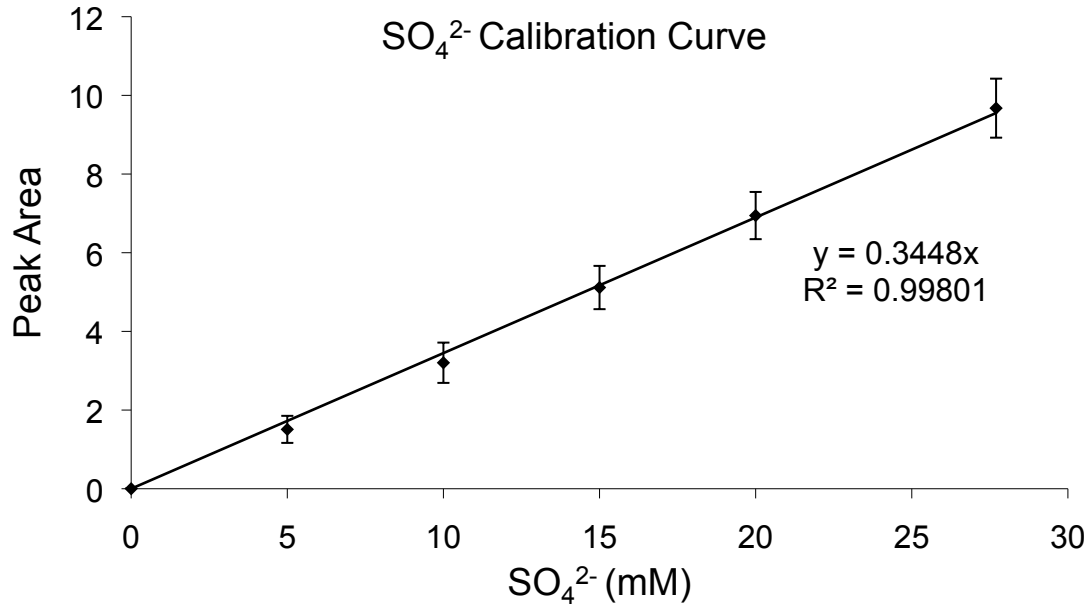

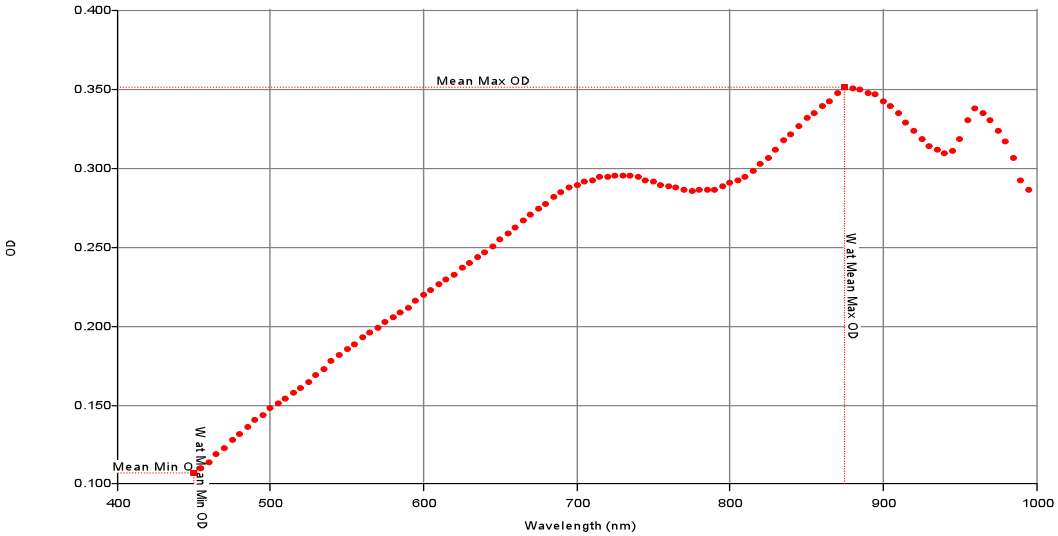
0.400
0.350
0.300
0.250
0.200
0.150
0.100
OD
Mean Max OD
W at Mean Max OD
Mean Min OD
W at Mean Min OD
400
500
600
700
800
900
1000
Wavelength (nm)

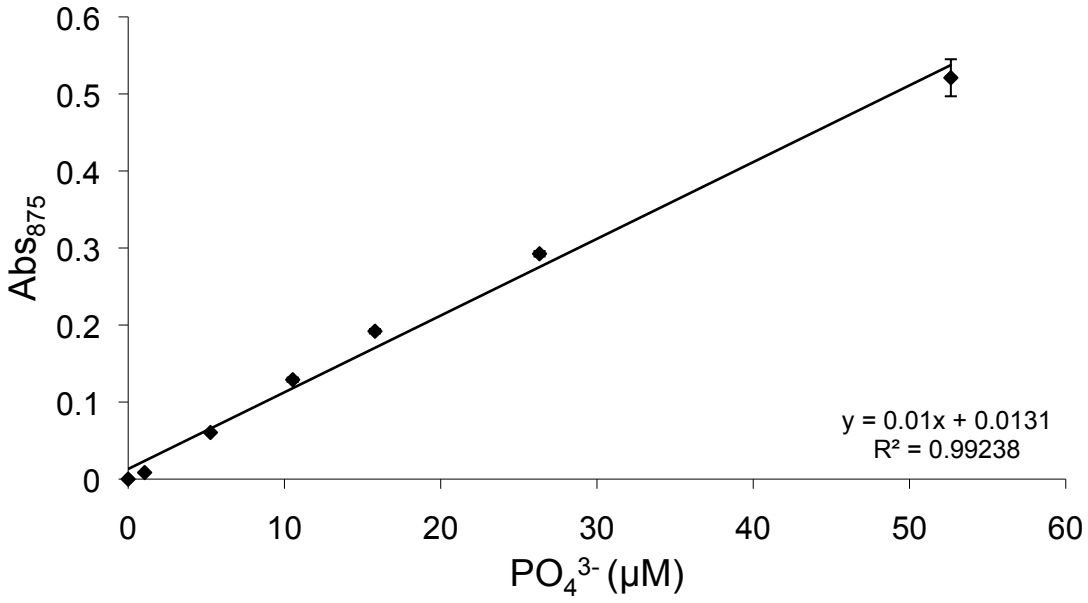
0.6
0.5
0.4
0.3
0.2
0.1
0
Abs875
y = 0.01x + 0.0131
R² = 0.99238
0
10
20
30
40
50
60
PO4 3- (µM)

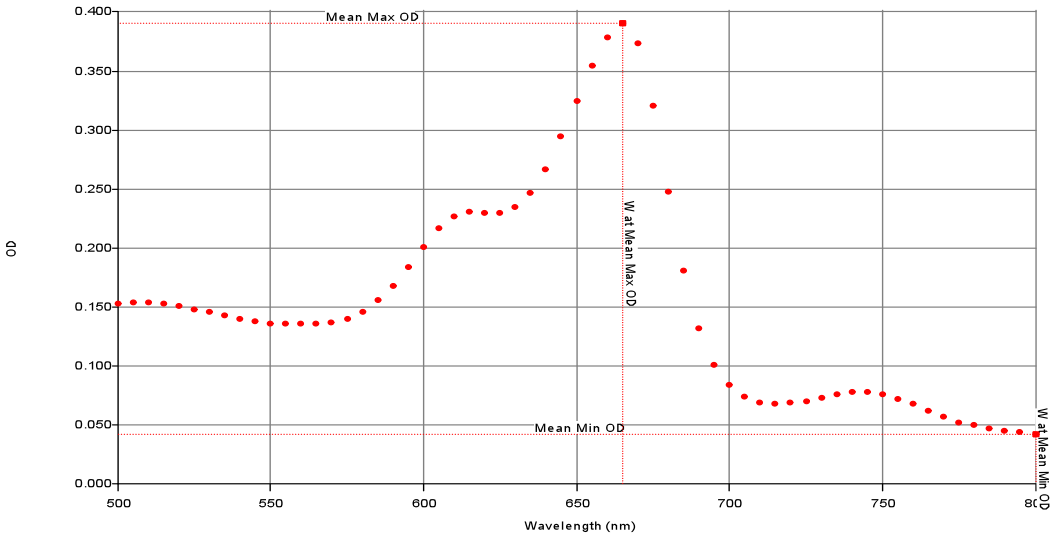
Mean Max OD
Mean Min OD
W at Mean Max OD
W at Mean Min OD
OD
Wavelength (nm)
0.400
0.350
0.300
0.250
0.200
0.150
0.100
0.050
0.000
500
550
600
650
700
750

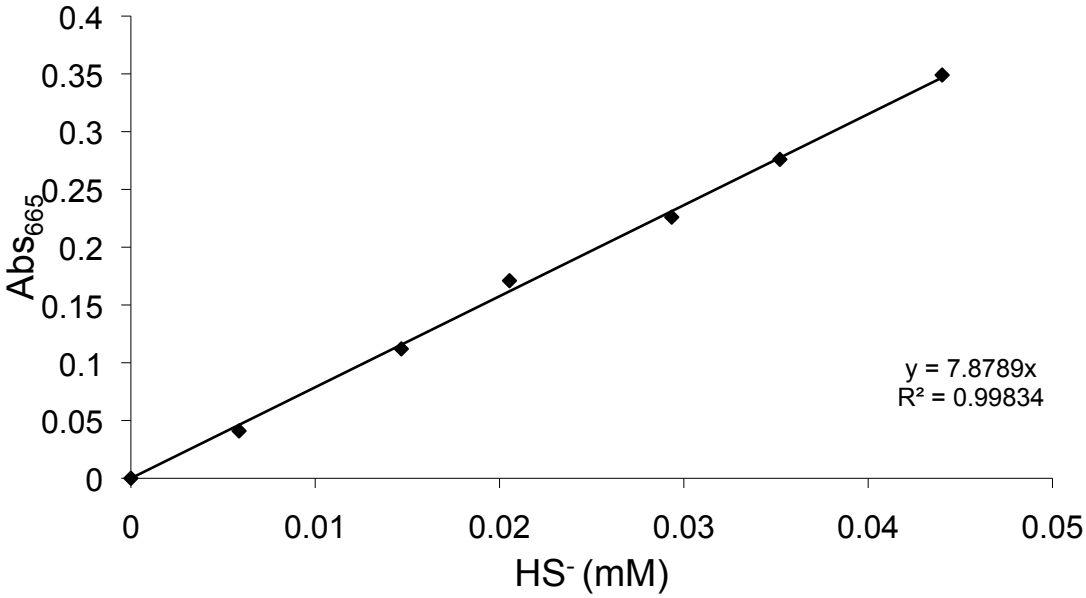
Abs665
HS- (mM)
y = 7.8789x
R² = 0.99834
0.4
0.35
0.3
0.25
0.2
0.15
0.1
0.05
0
0
0.01
0.02
0.03
0.04
0.05

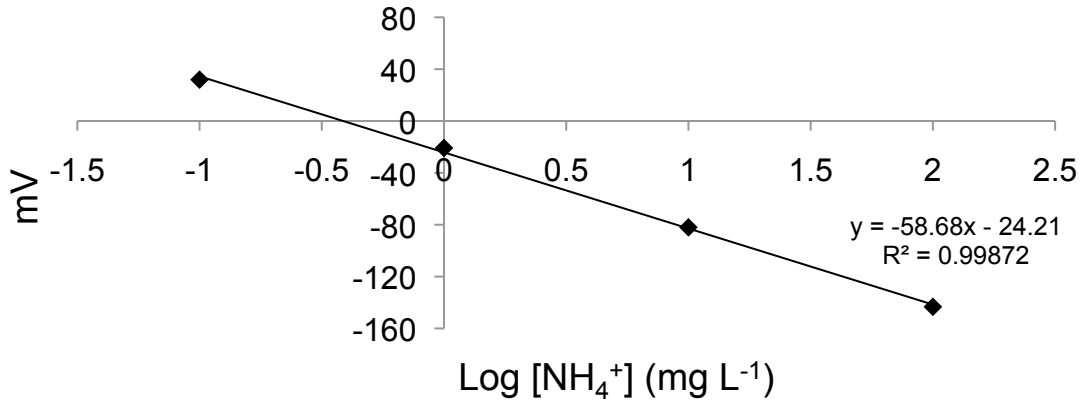
80
40
0
-40
-80
-120
-160
-1.5
-1
-0.5
0
0.5
1
1.5
2
2.5
mV
y = -58.68x - 24.21
R² = 0.99872
Log [NH4+] (mg L-1)

Appendix D: PLFA and neutral lipid total ion chromatograms of BC10 from within a pockmark in Dunmanus Bay